UNIL | Université de Lausanne

UNIVERSIDAD AUTONOMA DE MADRID

Synaptic Plasticity and Sensory Information Processing through the Thalamus and the Cortex of the Rodent Barrel Field

by Natalí Barros Zulaica

Doctoral Thesis in Neuroscience (Universidad Autónoma de Madrid (UAM))

Doctoral Thesis in Information Systems (Université de Lausanne (UNIL))

Departamento de Anatomía, Histología y Neurociencias (UAM)

Département des Systémes d'Information (UNIL)

Supervisors:

Professor Ángel Núñez (UAM)

Professor Alessandro Villa (UNIL)

"Todo hombre puede ser, si se lo propone, escultor de su propio cerebro."

“Every man could be, if he sets his mind to it, the sculptor of his own brain”

Santiago Ramón y Cajal

To my family: mamá, Yuri and David.

You supported me all this hard time.

I love you.

Abstract

Sensory information processing is a key process in the brain because it involves many sensory inputs. Some of them are relevant and should induce a motor or cognitive response. In addition, many irrelevant stimuli reach sensory pathway and should be ignored. Synaptic plasticity in the central nervous system is a general process that enhances or decreases sensory responses according to the temporal pattern of stimuli. My main aim is to study synaptic plasticity in the somatosensory pathway, mainly in the thalamo-cortical loop. Sensory information from rodent whiskers is sent from the whisker follicle to the contralateral area of the thalamus and from the thalamus to the barrel cortex (BC). In this Doctoral Thesis we performed extracellular *in vivo* recordings in the BC and thalamus of urethane anesthetized rats and mice in order to unravel the mechanisms of synaptic plasticity and sensory processing. We observed that repetitive stimulation at frequencies at which the animal explores the environment induced long-term potentiation (LTP). In addition, low frequency stimulation could induce LTP or long-term depression (LTD) depending on the intracellular Ca^{2+} concentration during the stimulation time period. This long-term plasticity depended on NMDA receptors activation and the activation of muscarinic and nicotinic cholinergic receptors. Through an optogenetic study we showed that the basal forebrain (BF), the main source of acetylcholine (Ach) to the neocortex, sent its projections in an organized way. Consequently, the Ach-depending facilitation of cortical responses occurs in a very specific manner. We also found that the postero-medial thalamic nucleus (POM) regulated BC whisker responses through GABAergic (γ-aminobutyric-acid: GABA) neurons located in upper cortical layers.

Key words: Barrel cortex, thalamus, synaptic plasticity, NMDA receptors, acetylcholine

Résumé (French)

Le traitement de l'information sensorielle est un processus clef dans le cerveau parce qu'il reçoit de nombreux inputs sensoriels. Certains d'entre eux sont pertinents et devraient provoquer une réponse motrice ou sensorielle. La plasticité synaptique dans le système nerveux central est un processus général qui améliore ou réduit les réponses sensorielles selon le circuit temporel des stimuli. L'information sensorielle des vibrisses des rongeurs est envoyée depuis le follicule de la vibrisse jusqu'à la zone contralatérale du thalamus et du thalamus jusqu'au cortex somato-sensoriel (BC). Au cours de cette thèse de doctorat nous avons effectué des enregistrements extra-cellulaires *in vivo* dans le BC et le thalamus de rats et souris anesthésiés à l'uréthane afin de découvrir les mécanismes de la plasticité synaptique et du traitement sensoriel. Nous avons observé qu'une stimulation répétée à des fréquences auxquelles l'animal explore son environnement provoquait une potentialisation à long terme (LTP). De plus, une stimulation à basse fréquence peut provoquer une LTP ou une dépression à long terme (LTD) selon la concentration intra-cellulaire de Ca^{2+} pendant la durée de la stimulation. Cette plasticité à long terme dépend de l'activation des récepteurs NMDA et de l'activation des récepteurs cholinergiques muscariniques et nicotiniques. Grâce à une étude optogénétique nous avons pu montrer que le prosencéphale basal (BF), la source principale d'acetylcholine (Ach) vers le cortex, envoyait ses projections de façon organisée. Par conséquent, la facilitation des réponses corticales dépendant de l'Ach se produit de manière très spécifique. Nous avons également découvert que le noyau thalamique postéro-médial (POM) régulait la vibrisse du BC grâce à des neurones GABAergiques situés dans les couches supérieures du cortex.

Mot clefs : cortex somato-sensoriel, thalamus, plasticité synaptique, récepteurs NMDA, acetylcholine

Resumen (Spanish)

El procesamiento de la información sensorial es un proceso clave en el cerebro ya que involucra varios inputs sensoriales. Algunos de ellos son relevantes e inducen respuestas motoras o cognitivas. Además, muchos estímulos irrelevantes alcanzan la via sensorial y deben ser descartados. La plasticidad sináptica en el sistema nervios central es un proceso que aumenta o deprime las respuestas sensoriales según un patrón temporal de estimulación. Mi objetivo principal es estudiar la plasticidad sináptica en la via somatosensorial principalmente en el circuito tálamo-cortex. La información sensorial de las vibrisas de los roedores viaja del folículo de estas a la zona contralateral del tálamo, y desde esta a la corteza de barriles (BC). En esta Tesis Doctoral hicimos registros extracelulares *in vivo* en la BC y el tálamo en ratas y ratones anestesiados con uretano con el objetivo de conocer los mecanismos de la plasticidad sináptica y el procesamiento sensorial en esta vía. Observamos que una estimulación repetitiva a las frecuencias a las cuales el animal explora su entorno, inducen potenciación a largo plazo (LTP). Además, la estimulación a baja frecuencia pudo inducir LTP o depresión a largo plazo (LTD) dependiendo del la concentración de Ca^{2+} intracellular durante el periodo de estimulación. Mediante un estudio de optogenética, observamos que el prosencefalo basal (BF), el núcleo que surte principalmente a la corteza de acetilcolina (Ach) manda proyecciones de forma organizada. Encontramos tambien que el núcleo posterior-medial del talamo (POM) regula la respuesta de la corteza de barriles a traves de las neuronas GABAérgicas de la capa I.

Palabras clave: corteza somatosensorial, tálamo, plasticidad sináptica, receptores NMDA, acetilcolina

Abbreviations

- **A1**: primary auditory cortex
- **Ach**: Acetylcholine
- **AGA**: ω-agatoxin-IVa
- **AMPA**: α-amino-3-hydroxy-5-methyl-4-isoxazole propionic acid
- **AP**: action potential
- **APV or AP5**: (2R)-amino-5-phophono-pentanoate
- **B**: nucleus basalis magnocellularis
- **BC**: barrel cortex
- **BF**: basal forebrain
- **Ca^{2+}**: calcium ion
- **ChAt**: choline-acetyl transferase promoter
- **ChR2-YFP**: channelrhodopsin-2 tagged with a fluorescent protein
- **CNS**: central nervous system
- **EPSC**: excitatory postsynaptic current
- **EPSP**: excitatory postsynaptic potential
- **FB**: fast blue
- **FlGo**: fluoro-gold
- **FS**: fast spiking
- **GABA**: γ-aminobutyric acid
- **Glu**: glutamate
- **HDB**: horizontal limb of the diagonal band of Broca
- **i.p.**: intra peritoneal
- **IB**: intrinsically bursting
- **K^+**: potassium ion
- **LTD**: long term depression
- **LTP**: long term potentiation
- **M1**: primary motor cortex
- **Mg^{2+}**: magnesium ion
- **MK801**: Dizocilpine
- **Na^+**: sodium ion

Abbreviations

- **NMDA**: N-methyl-D-aspartate
- **NT**: neurotransmitter
- **POM**: posterior medial thalamic nucleus
- **PrV**: principal trigeminal nucleus
- **PTX**: pricotoxin
- **PV**: parvalbumin
- **RF**: receptive field
- **RS**: regular spiking
- **S1**: primary somatosensory cortex
- **S2**: secondary somatosensory cortex
- **SI**: substantia innominata
- **SpVi**: spinal trigeminal nucleus
- **STDP**: spike time dependent plasticity
- **VDB**: vertical limb of the diagonal band of Broca
- **VGCC**: voltage gated Ca^{2+} channel
- **VPM**: ventral posterior medial thalamic nucleus

Contents

1 Introduction

1.1. Somatosensory System in Rodents. The Whisker Pathway

The somatosensory system provides the Central Nervous System (CNS) with information that belongs to the corresponding sensory stimulus as: non-discriminative or discriminative touch, vibrations, proprioception (which is the information received from muscles, tendons and joints that allow us to know the body position at any given moment), and nociception which is responsible for the perception of pain [1].

Rodents have a particular area in the somatosensory cortex that processes the information from the whiskers. Whiskers are rigid hairs on the rodent snouts that have a specific tactile function and work in the same way as the human hands. The sensory innervation of each whisker follicle is quite high, reflecting the importance of the information they transmit. Neurons of the trigeminal ganglion innervate whisker follicles in the skin of the rodent's snout and project to the trigeminal complex in the brainstem. The striking characteristic of the whisker somatosensory pathway is that from the periphery to the cortex, these system circuits are topographically organized into the different relay nucleus [2, 3] [Figure 1.1].

1.2. The Somatosensory Thalamus

Sensory information from whiskers is sent from the whisker follicle to the contralateral area of the thalamus through four different and separate pathways: two lemniscal, one extralemniscal and one paralemniscal. The two lemniscal branches innervate different areas of the ventro-postero-medial thalamic nucleus (VPM), one innervates the core region of the barreloids with precise receptive fields from one whisker, while the other projects to the head region of VPM. Neurons in this small area respond to multiple whiskers [4, 5, 6]. In this Doctoral Thesis, we focused our research in the lemniscal pathway that projects to the core of the VPM and the paralemniscal pathway. In the lemniscal pathway, neurons are connected to the sensory principal trigeminal nucleus (PrV) into the brain stem and send projections to the VPM. Neurons from PrV are placed into clusters called barrelettes where each one receives information from only one whisker [7, 3]. In the VPM, neurons are also organized in clusters

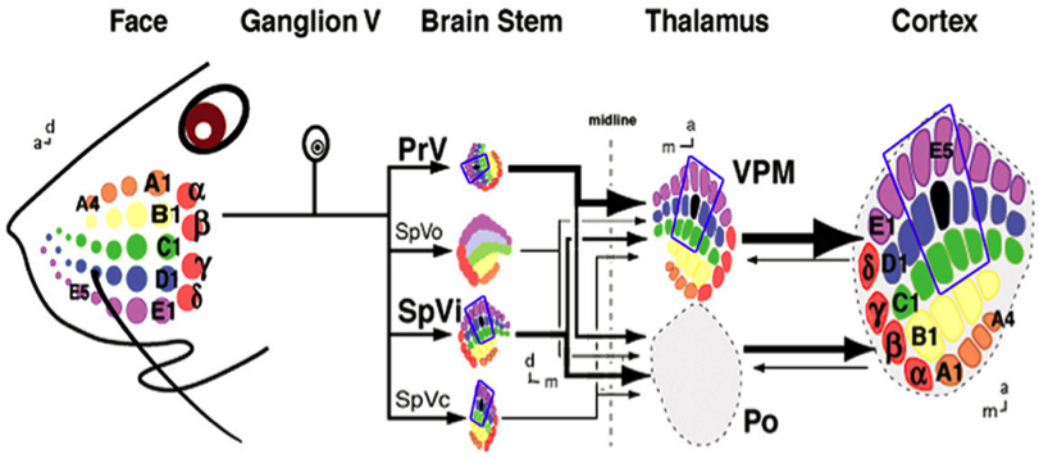

Figure 1.1 – Schematic diagram of the mouse whisker somatosensory system. Whisker rows are labeled A–E along selected whisker arc numbers; whisker straddles are labeled α-δ. The other areas of the pathway: brain stem, thalamus and cerebral cortex are labeled similarly (barrelettes, barreloids and barrels). The black stain in the different nuclei represent the areas related with the whisker activation. (PrV: principal trigeminal nucleus; SpVo: spinal trigeminal subnucleus oralis; SpVi: spinal trigeminal subnucleus interpolaris; SpVc: spinal trigeminal subnucleus caudalis; VPM: ventroposteromedial nucleus of the thalamus; Po: posterior nucleus of the thalamus; a: anterior; d: dorsal; m: medial.) [2]

named barreloids [8]. On the contrary, paralemniscal pathway source from the interpolar section of the rostral area in the spinal trigeminal nucleus (SpVi), at the brain stem level and send projections to the medial area of the posterior thalamic nucleus (POM) and to a little area of the VPM [7, 8]. SpVi relay nucleus is organized topographically in clusters similarly to the POM [8, 3].

Interestingly, the thalamus of rodents has no interneurons in the relay nuclei [9]. The source of GABAergic (γ-aminobutyric-acid: GABA) projections that controls thalamus activity is the reticular thalamic nucleus which receives lateral projections from thalamo-cortical and cortico-thalamic connections [10].

1.2.1. Thalamo-Cortical Projections

All these thalamic projections target the barrel cortex (BC), a topographically organized area where the sensory information from the whiskers arrives (this cortical area will be better introduce in the next point of the Introduction). Although both sensory pathways arrive to the BC, the lemniscal pathway carries precise sensory information from one or two whiskers and mainly target the neurons in the barrel (layer IV of S1), while the paralemniscal pathway is sensitive to simultaneous stimulation of many whiskers and target mainly neurons in the septal area between cortical columns and in layer I and layer Va of S1 [11, 12, 13, 14] .

Between each barrel there is a narrow region called septa, in which neurons are activated by stimuli delivered on several whiskers, probably in order to analyze the background [4]. Thus, the septal regions receive the sensory input from the POM and a thin region of VPM of the paralemniscal pathway [12]. On one hand, barrels in S1 layer IV receive a strong innervation from the sensory input from VPM nuclei of the lemniscal pathway. Although the main targets of VPM neurons are barrels in layer IV, there is also a weak innervation in layer VI [8]. Furthermore, the VPM moderately also sends projections to adjacent regions of the layer VI, Vb and lower portions of the layer III. On the oder hand, the POM thalamic nucleus sends projections to layers I, II, III and Va of S1 [Figure 1.2], and is known to send projections to the secondary somatosensory cortex (S2) and the primary motor cortex (M1) as well [15, 16, 4].

1.2.2. Functional Differences Between VPM and POM

It is possible to find several important differences between both thalamic nuclei in the bibliography. As it was reported in the previous point, VPM is topographically well organized as the POM. However, the spatial resolution of POM neuronal responses is not very accurate [17], mainly because neurons in POM usually respond to multiple whiskers [18]. It is known that the lemniscal pathway through VPM encodes high resolution information [17] and processes temporal characteristics of whisker movements by latency and spike count through thalamo-cortical loops [17, 19]. POM neuron projections target the S1 but are also involved in

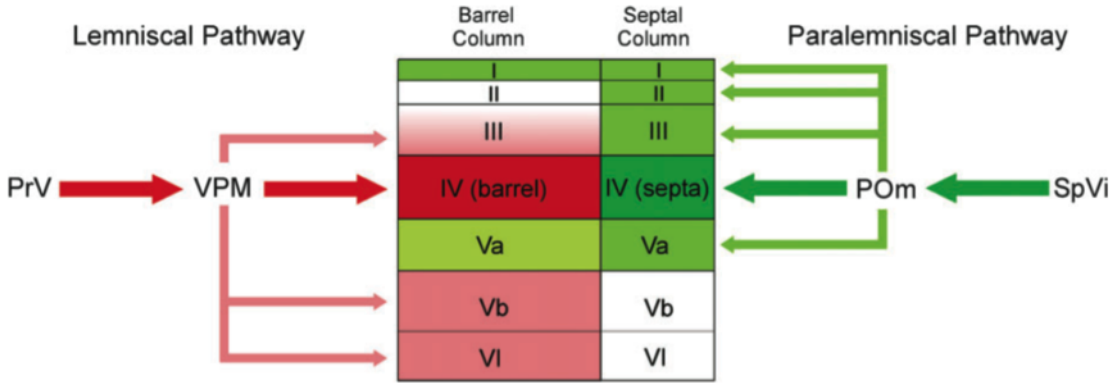

Figure 1.2 – Diagram showing the main connections within the lemniscal and the paralemniscal pathways. [4]

relaying information between cortical areas, mainly projecting to higher order somatosensory cortical regions and motor cortex [20, 21].

It has been suggested that the role of POM could be to modulate BC activity [22]. It has been also proposed that the POM could play the role of a "higher order" thalamic nucleus allowing different cortical areas such S1, S2 and M1 to communicate through corticofugal projections controlling and integrating sensory-motor information [23]. However, the function and the way the POM modulates cortical neuronal processing and what is its function through these trans-thalamic cortico-cortical connections are still under study.

In order to unravel this important issue we recently published an article, which is part of this Doctoral Thesis (***article 4***, Annex). There, we show pieces of evidence of POM cortical regulation through layer I. This regulation was dependent on the time and intensity of POM activation and was mediated by the inhibitory pathway through $GABA_A$ receptors . We also found evidence of POM cortico-cortical control through S2 by cortico-fugal projections through S1 layer V.

1.3. The Barrel Cortex

The BC is a very important structure in sensory perception that belongs to S1. The BC receives and processes somatosensory stimuli belonging to the whiskers and organizes responses depending on these stimuli. This cortex is mainly characterized by its topography, as the rest of the nuclei in the pathway. Each whisker is represented by a cluster of neurons in layer IV that is well delimited and defined as an individual column called barrel [24] [Figure 1.3].

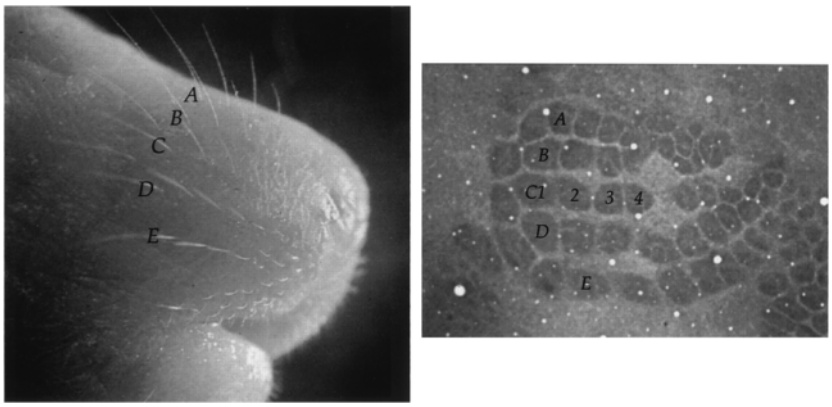

Figure 1.3 – Topography of whisker pad and cortical barrel field. The individual whiskers on the rodent whisker pad are arranged in five rows. This topography arrangement is replicated in layer IV of somatosensory cortex [25].

The somatosensory BC is composed of local circuits heavily interconnected by vertical and horizontal projections [5]. As previously said, sensory information from the whiskers arrives via the brainstem and thalamus to layer IV neurons in BC. Sensory responses are relayed to layer II/III and then to layer V and layer VI, concomitant with feedback from layer V to layer II/III and layer VI to layer IV. This vertical organization is linked horizontally by prominent projections within layer II/III and layer V [26, 27]. This neuronal network allows the cortex to analyze physical characteristics of the stimulus in order to organize a response or to store relevant information in the memory by means of neuronal plasticity.

1.3.1. Anatomical Characteristics of Barrel Cortex

The cytoarchitecture of the BC is characterized by its layer shape. There are three main types of excitatory neurons in the cortex distributed differently according to the layer: spiny stellate, star pyramid and pyramidal cells [28].

Layer I: The superficial layer, it contains a very few neurons. It is basically conformed by the terminals of apical dendrites of pyramidal cells and of a lot of horizontal axons that go in all directions [29]. These horizontal axons connect S1 with other cortical areas such as S2 and M1 [30].

Layers II and III: Layer II is mostly composed by small pyramidal cells while in layer III pyramidal cells are a bit bigger than those in layer II. From these two layers the pyramidal cells send dendrites to layers I and II (from layer III) and axons to layer V. Collaterals of these axons remain in the same layers [31]. Through research performed in mice by Lorente de Nó in 1922 is known there are some projections that target S2 through the white matter from layer III [28].

Layer IV: This layer is mostly composed by spiny stellate cells, the other group that form this layer (23%) are star pyramids cells that are basically placed in the upper part of this layer (layer IVa) [29]. From this layer, it is possible to see projections along all layers, but mainly to layer II/III. There are also loops in layer IV that send projections into the layer and make connections with the adjacent barrels [32]. Due to its cytoarchitecture this layer is also called granular, and consequently the layers above or below are called supra-granular or infra-granular layers respectively.

Layer V: Layer V contains a mixture of all types of cells but is characterized by the presence of large pyramidal cells. It englobes two different areas well defined by the cell density, cell type and connectivity. From layer V, the BC lay down a lot of cortico-cortical connections to different areas such as M1, S2, the ventral area of posterior-parietal-cortex and contralateral barrel cortex through the corpus callosum. It also sends projections to several subcortical structures: neostriatum, upper colliculus, the

thalamus and brain stem [33].

Layer VI: This layer, also called multiform, is formed by several types of neurons. Many of them are pyramidal elongated neurons or fusiform cells that are mostly placed in the deepest part of layer VI [29]. Neurons in this layer also project to the thalamus.

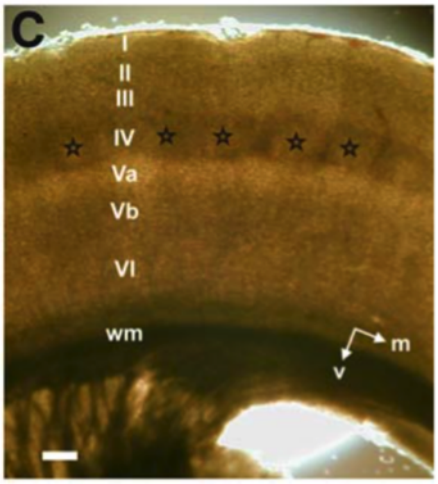

Figure 1.4 – Coronal slice through the BC of a P19 rat illuminated by Dodt gradient contrast. The barrels in layer IV are clearly identifiable (stars) as well as all the cortical layers (vertical roman numerals) [34].

The previous description mainly focuses on the excitatory cells. However, is also known, inhibitory neurons play a fundamental role in cortical computation and behavior, and this is the probable reason why there are inhibitory cells in all cortical layers [35]. For example, approximately 50% of cells in layer IV are inhibitory and they are the main recipient of thalamic input from VPM in the barrel column [36]. For each mayor intrinsic excitatory connection there must probably be another parallel inhibitory connection that provides feed-forward inhibition for this particular pathway [6]. It has been suggested that this feed-forward inhibition onto principal cells limits the integration time window of excitation and therefore confines the rate and timing of action potentials [37, 38].

γ-Aminobutyric acid (GABA) is an important NT in the cerebral cortex and it was known that most cortical inhibitory synapses come from non-pyramidal cells [39]. It has recently been reported that according to their RNA-sequence, it is possible to find around 30 different types of

inhibitory neurons [40]. Beside this, many studies focusing on neocortical inhibitory neurons found at least 10 fundamental types of inhibitory neurons classified by their morphology such as: chandelier cells, basket cells, Martinotti cells, neurogliaform cells, double bouquet cells and others classified according to their axonal and dendritic arborization patterns [6, 39, 41, 42, 43].

The inhibitory GABAergic interneurons expressing calcium-binding protein parvalbumin (PV) constitute the largest subpopulation of interneurons [44, 45]. Most of them are PV-positive cells and are mostly fast spiking (FS) interneurons. These cells mostly inhibit pyramidal and PV-expressing cells [43]. PV-expressing interneurons, basket cells that synapse onto the somata or chandelier cells that target the axon initial segment control the synchrony and the spike firing of large populations of pyramidal cells [46, 47, 48].

1.3.2. Electrophysiological Properties of Barrel Cortex Cells

The mammalian neocortex transforms afferent sensory information into complex spatio-temporal firing patterns, which demonstrate the importance of studying neuronal firing rate and pattern [49]. Classically, it is possible to describe the firing pattern of cortical cells into three principal types [50, 51]: Regular spiking (RS), intrinsically bursting (IB) and fast spiking (FS). RS cells are pyramidal and stellate cells that trigger sodium (Na^+) action potentials (APs) in a sustained manner during the application of a depolarizing current pulse. They are present in all cortical layers except in layer I. Approximately 80% of the synapses received by RS cells in lower layers V and VI are thalamo-cortical fibers and the remaining synapses come from layer IV. On the contrary RS cells from upper layers II and III receive almost no thalamo-cortical connection. IB cells are pyramidal cells principally from layer V that surprisingly do not receive direct thalamo-cortical inputs. They possess unusually thick apical dendrites that rise to layer I. They generate a burst of 3-5 APs riding on a calcium (Ca^{2+}) spike in response to an intracellular depolarization. FS cells are characterized by short duration APs, and the ability to fire tonically at high frequency (>250 Hz) and a relative lack of spike frequency adaptation when long-lasting depolarizing current pulses are applied to these neurons; they are GABAergic interneurons [52]. These cells receive strong innervation from thalamus.

Numerous vertical and horizontal connections must exist within the cortical column . This complexity of connectivity pattern and in the numerous types of neurons that built the somatosensory cortex makes it difficult to study. This is why despite all of the research involved in this issue [50, 8, 34, 6] little is known about how the different spiking types of neurons are distributed according to their firing rate into the BC that probably would help to elucidate how the BC process the afferent sensory information .

In order to shed some light on this issue, we performed a study with a multi-recording electrode to record several layers at the same time (***article 6***, Annex). In this study we wanted to define different neuronal firing patterns in the mouse BC and their distribution in all the recorded volume of the BC. We found four different types of firing patterns that were distributed in a non-homogeneous way, not only within layers, but also antero-posterior and medio-laterally, showing that firing patterns distribution must be important for sensory processing.

1.4. Synaptic Plasticity

One of the main and most interesting characteristic of the mammalian brain is its ability to change the functions and formation of neural circuits through life experiences. This phenomenon is called plasticity. It is believed that these changes are responsible for processes such memory, learning, adaptation and even recovering functions after injury.

Previous works have indicated that long-term cortical synaptic plasticity is a complex multi-component process involving multiple synaptic and cellular mechanisms. In order to study this complex process, it is possible to apply different methods [53]. One is to study changes on a neuronal map through experience: it is possible to teach animals to perform a task and then observe how the synapses in the part of the brain involved in this task change [54]. This process has been well studied in the BC and in other sensory cortical systems [55, 56]. It is also possible to study changes in synapses by blocking or causing injury to a given part of the

studied pathway. Trimming or plucking some whiskers induces S1 neurons to rapidly lose sensory responses to deprived whiskers and to slowly increase responses to spared whiskers, inducing changes whithin the cortical map [57, 58]. A further way of checking this important issue is to perform repetitive sensory stimulations. Repeated activation of a specific sensory input potentiates neural responses to that input. This is usually most robust in young animals [56, 59]. Contrary, 24 hours of continuous whisker deflection weakens the S1 representation of the stimulated whisker [60].

In 1949 Donald Hebb postulated that associative memories should be formed through a process of synaptic modification. These modifications should get strengthened when the activity of the pre-synaptic neuron coincides with the firing in the post-synaptic neuron. He also postulated that if these changes remained over time, some information would be stored [61]. This phenomenon is called synaptic plasticity.

In 1973 the first experimental evidence of Hebb's theory were discovered. Bliss and colleagues established that a repetitive stimulation in the hippocampus of an anesthetized rabbit induced a potentiation in the synaptic strength that could last for days [62]. This phenomenon was called Long-Term Potentiation (LTP). Later, it was also observed that a repetitive stimulation at low frequencies could induce a Long-Term Depression (LTD) [63]. Either LTP or LTD may occur in the same neuron and in the same synaptic pathway. Thus, an important issue is how the mechanism to control balance between LTP or LTD works.

In our laboratory, during our work on this Doctoral Thesis, we observed that a physiological repetitive stimulation to the principal whisker of anesthetized adult rats at frequencies at which the animal explored the environment (4 - 12 Hz) induced LTP (***article 1***; Annex). We also saw that low frequency stimulation could induce LTP or LTD depending on what happened during the stimulation time period (***article 5***; Annex).

Cellular mechanisms for cortical plasticity have been suggested in order to include

changes in physiological mechanisms (functional modification of existing synapses and neurons) and structural mechanisms (physical rewiring of cortical circuits by synapse formation, elimination, and morphological changes) [55]. Both cellular mechanisms involve changes in the glutamatergic neurotransmission.

1.4.1. The Glutamate in Synaptic Plasticity

Glutamate (Glu) is the most abundant neurotransmitter (NT) in the mammalian CNS. Since Glu is the NT used by excitatory cortical neurons, it is involved in learning and memory processes by means of synaptic plasticity. The Glu activity is mediated through the activation of two different types of receptors: ionotropic and metabotropic receptors. Ionotropic receptors are involved in fast neurotransmission in the brain and they can be classified according to the function of the agonist that activates them: N-methyl-D-aspartate (NMDA) receptors, α-amino-3-hydroxy-5-methyl-4-isoxazole propionic acid (AMPA) receptors and kainate receptors. Ionotropic Glu receptors form cationic channels that allow the flux of Na^+, potasium (K^+) and Ca^{2+} ions through them thus producing a depolarization of the neuron [64, 65]. Metabotropic Glu receptors are joined to G-proteins and they regulate the activity of enzymes and ion channels in the membrane in a slower time scale than ionotropic receptors. Through these receptors, Glu mediates fast and slow responses in the CNS [66].

In relation to the ionotropic receptors the process follows the folliwing steps: firstly the activation of AMPA receptors provides sufficient inward current that provides the excitatory postsynaptic potential (EPSP); secondly, the NMDA receptors can be activated depending on the voltage, they get activated at depolarizing membrane potentials. At hyperpolarized membrane potentials these receptors are blocked by extracellular magnesium (Mg^{2+}). Activation of NMDA receptors allows the Ca^{2+} and Na^+ to get into the neuron [64]. It is thought that the entrance of Ca^{2+} detonates the activation of second messengers and the activation of kinase proteins that promotes the addition of AMPA receptors in the postsynaptic neuron.

Cortical LTP is most often mediated by activation of NMDA receptors. In the NMDA-LTP, Ca^{2+} from postsynaptic NMDA receptors and other sources activate kinase proteins, which drive specific AMPA receptor phosphorylation and insertion of AMPA receptors into synapses to increase synaptic responses [67]. A second form of neocortical LTP is expressed presynaptically by increasing Glu release probability, thus facilitating synaptic responses [68]. LTP in adult animals in layers IV and II/III of S1 depends on presynaptic and postsynaptic components [69], indicating that the regulation of synaptic plasticity could be achieved through different complex mechanisms that should be activated, for example, according to the stimulation pattern or the presence of other NTs.

LTD carries on use-dependent, monosynaptic and heterosynaptic weakening and therefore as a response provokes depression to deprived inputs. Multiple forms of LTD exist and possibly play different roles in plasticity [70]. One of the most common LTD is the one depending on NMDA receptor. Ca^{2+} from postsynaptic NMDA receptors activates protein phosphatases leading to internalization of synaptic AMPA receptors.

Learning, memory and sensory processing involve the generation of spike train patterns that trigger experience-dependent plasticity, as shown above. One learning rule that appears to mediate some types of experience-dependent plasticity *in vivo* is spike timing–dependent plasticity (STDP), in which the temporal sequence and interval between pre- and postsynaptic spikes is crucial to evoke synaptic plasticity. In classical STDP if the pre-synaptic spike is closely followed in time (0–20 ms) by the post-synaptic spike, it then becomes possible to induce LTP. If the post-synaptic spike precedes the pre-synaptic spike (0 to 20–50 ms) then LTD will be induced. STDP occurs in many neocortical synapses *in vitro* and can be induced experimentally *in vivo* by pairing sensory stimulation with precisely timed spikes [71]. STDP mechanisms are surprisingly diverse and could involve the activation of NMDA receptors in some synapses [72]. Consequently, STDP has powerful Hebbian-like computational properties that predict development and plasticity of sensory responses [73].

One further study forming a part of this Doctoral Thesis shows that NMDA receptors are essentialin order to generate long-term plasticity induced by a repetitive stimulation. Blocking these receptors resulted in no plasticity at all (***article 1*** and ***5***; Annex). This means that the action of Glu through NMDA receptors is essential for synaptic plasticity processes.

Although plasticity is a property of the entire brain, synaptic plasticity in the neocortex is crucial in sensory processing because one specific area of the cortex processes and combines information from different inputs, and plasticity occurs according to the input pattern. Later, when the plasticity has occurred, the cortical area sends this processed information to other areas for further processing, or it could remain as such as something learned.As far as we know plasticity processes in the sensory cortex depen on the activation of AMPA and NMDA receptors. However, less is known about the participation of metabotropic receptors in cortical sensory plasticity.

1.4.2. The Acetylcholine in Synaptic Plasticity

The Acetylcholine (Ach) is a NT essential for the normal function of the CNS. Ach is involved in several processes such as synaptic plasticity, attention, learning, memory, arousal and reward [74, 75, 76]. Although Ach is a NT that has long been studied, (described by Loewi, Dale and others in 1921-1934) little is known about the neuronal mechanism in which it is implicated. Because of its neuromodulator character it is believed to regulate the overall effectiveness of cortical sensory responses and associative information processing [77].

Ach acts through tow types of receptros: nicotinic and muscarinic. Nicotinic receptors are distributed throughout the whole CNS, they are ionotropic receptors with rapid activation kinetics which causes immediate changes in cortical activity [78]. There are twelve types of subunits of nicotinic receptors, nine of them are located in the cortex and are known to participate in processes of attention and plasticity. But the effect on the cortical activity is not knwon yet [79]. Furthermore, cholinergic nicotinic receptors are placed in the GABAergic inhibitory interneurons, so that Ach plays a role in the modulation of inhibitory cortical circuits

as well. For example, in BC layer V Ach hyperpolarizes FS inhibitory interneurons thus causing a dishinibition of pyramidal cells located in the same cortical layer. This suggests that the cortical cholinergic system reduce inhibition within the column and simultaneously induces a pyramidal cell depolarization increasing the information transfer into cortical columns [80]. Therefore, Ach may regulate cortical network at population level through control of excitation and inhibition.

The other receptors involved in Ach effects are the metabotropic cholinergic muscarinic receptors. They are associated to G-proteins and are slow acting. The cholinergic muscarinic receptors are present in several CNS areas. There are five types of cholinergic muscarinic receptors and although their precise role has not yet been discovered, many studies are conducted to find out how they work [81]. These five types of muscarinic receptors are thought to have different roles. For example, *in vitro* studies in rat showed an increased on the firing rate mediated by m1-cholinergic muscarinic receptors, a decrease of the firing rate mediated by m2-cholinergic muscarinic receptors [82]. They furthermore observed an excitation transmission depression mediated by m4-cholinergic muscarinic receptors [81]. In another example study, Kimura and colleges studied the action of Ach in the visual cortex of rats. They observed a suppression of postsynaptic excitation mediated by m4-cholinergic muscarinic receptors and postsynaptic inhibition suppression mediated by m1-cholinergic muscarinic receptors [83]. The difference may be due to the way of applying Ach, because in one case the experiment was performed in a bath with a small concentration and in the other case Ach was applied at a higher concentration.

The effect of Ach may differ according to activation of nicotinic or muscarinic receptors or if Ach affects local interneurons or pyramidal cells. Accordingly, results *in vitro* and *in vivo* demonstrated that Ach changes the firing pattern of cortical neurons increasing their firing rate and the neuronal response, which is surely a determining point in sensory processes and neuronal plasticity [84, 82].

Because cholinergic receptors are located in a different neuronal position and the Ach concentration is important to start different response mechanisms, the Ach application technic may raise different results. *In vivo*, this means that different concentration of Ach may evoke different effects. The concentration of Ach is not constant, for example, it increases during awake state or REM sleep and decreases during slow wave sleep [85]. Moreover, Ach is locally increased in areas that perform deep information processing. For example, attention tasks induce an increase of Ach in cortical areas involved with these tasks [77, 74, 75, 76].

Experiments performed for this Thesis project showed that Ach increase the number of neurons that performed LTP and this facilitation was mediated through muscarinic receptors (***article 1***;Annex).It is possible to conclude that Ach is a complex neuromodulator, since it has many different effects that still remain unknown, but extremely important for our understanding of the processes of attention and memory. Therefore Ach could enhance sensory detection, processing and plasticity with the intervention of complex synaptic interactions [75, 86, 87].

It is already known since 1983 that the cortical mantle, the amygdaloid complex, the hippocampal formation, the olfactory bulb and the thalamic nuclei receive cholinergic innervation mainly from projections of cholinergic neurons located in the Basal Forebrain (BF) and in the upper brainstem [88]. The BF sends projections to the sensory, motor and prefrontal cortices and the hippocampus from specific areas: the medial septum, horizontal and vertical limbs of the diagonal band of Broca (HDB and VDB), the substantia innominata (SI) and the nucleus basalis magnocelularis (B) [89]. Recent evidences point out that the BF is a very well topographically organized structure [76, 89]. However, there is still a lot of work on in this specific field to unravel how the BF sends its cholinergic projections to help and modulate sensory processing.

In order to achieve one of the objectives of this Doctoral Thesis, we used the optogenetic technic. We performed experiments with mice expressing the light-activated cation channel, channelrhodopsin-2, tagged with a fluorescent protein (ChR2-YFP) under the control of the

choline-acetyl transferase promoter (ChAT) to specifically stimulated cholinergic neurons in different areas of the BF with light, while recordings in S1 and A1 were performed simultaneously. Optogenetical stimulation of HDB/VDB induced larger changes in S1evoked potentials than in A1; while stimulation of B showed similar changes in both cortical areas. This is an evidence that BF is segregated in areas that project to the cortex in a very specific manner (***article 3***; Annex).

Each study described below and performed during my Doctoral Thesis has shown that different stimulation patterns induce synaptic plasticity in S1 cortical neurons by increasing the spike response and the coherence of neuronal firing. These processes were under control of neuro-modulation, such as Ach, and by the action of thalamic neurons. They all together induce very notable changes in thalamo-cortical sensory processing.

2 Hypothesis and Objectives

After the exposition of these pieces of knowledge in the Introduction there still are a lot of crucial points to unravel in the thalamo-cortical pathway involved in synaptic plasticity and sensory information transmission mechanisms. For this main purpose we set the following hypothesis and suggested the subsequent objectives for this Doctoral Thesis.

2.1. Hypothesis

It is known that rodents move their whiskers repetitively to explore the environment. Since we also know that the BC is a structure in which synaptic plasticity processes happen and a repetitive stimulation is one way of developing this process, we hypothesized that: plasticity induced by a repetitive stimulation must change the number of APs fired by a cortical neuron in the BC depending on the frequency of this stimulation. Because the Thalamus is the previous relay nucleus to the cortex it must be involved in information and plasticity processes of the cortex.

2.2. Objectives

1. As a manner of studying synaptic plasticity, we wanted to find out if it was possible to induce long-term changes in the BC of an adult anesthetized rat with a short repetitive stimulation train, performed with an air-puff, to the principal whisker belonging to the barrel. We performed the repetitive stimulation at frequencies that the animal would find in a normal environment. We wanted to test if it was possible to induce different changes dependeding on the frequency of the short train. For this purpose, we performed extracellular recordings with a tungsten electrode.

2. Since it is known that NMDA receptors are involved in synaptic plasticity processes, we wanted to test the relevance of these receptors in the changes produced by the repetitive stimulation. For this purpose we blocked NMDA receptors in two different ways: on one hand with an intraperitoneal (i.p.) injection of MK801, also called dizocilpine, in order to block all these receptors and on the other hand with a local injection of (2R)-amino-5-phophono-pentanoato (APV) intended to only block the receptors in the area that we were recorded.

3. It is also known that the influx of Ca^{2+} in the post-synaptic neuron is important for the system to develop LTP or LTD. In order to unravel this specific point we collaborated with the group of Prof. Fernández de Sevilla. Joining our forces we were able to unravel the mechanisms from two different points of view: *in vitro* and *in vivo*. In this particular case we also studied the neuronal firing changes during the stimulation train.

4. Ach is also known to be involved in synaptic plasticity, for this reason we studied the role of Ach in the possible changes produced by our the repetitive stimulation. To do so we injected eserine (i.p.), a blocker of endogenous acetylcholinesterase enzyme that degrades Ach, in order to increase Ach concentration. To find out if the possible observed changes could be produced through muscarinic receptors, we used atropine as a blocker of these receptors to study this effect.

5. As the behavior of Ach in the brain is such a complex phenomenon, we wanted to study the projection pattern of the BF which is main source of Ach to the cortex. There are some new evidence showing that the BF projections to the cortex could be precisely organized. For this purpose, we performed optogenetics in anesthetized transgenic mice, where we stimulated with blue light HDB/HDV and B nuclei, because it is known that these areas project mainly to S1. These experiments were complemented with anatomical experiments performed by the laboratory group of Prof. Rodrigo-Angulo.

6. Since the thalamus is the previous relay nucleus to the cortex and is known to be involved in cortical processing and cortical synaptic plasticity, we wanted to unravel the influence of VPM and mainly POM thalamic nuclei in cortical sensory processing through *in vivo* recordings in urethane anesthetized rats. We stimulated VPM and POM nuclei electrically and also blocked their activity with muscimol (agonist of $GABA_A$ receptors), to observe the effect in the BC. Since POM has cortico-cortical projections to S2, we studied this issue through electrical stimulation of POM and whisker stimulation with an air-puff while recording in S2.

7. As it is already known, neurons codify sensory information by means of firing in the time scale. It is also known that within the cortex, neurons have some typical firings activities. However, little is known about the distribution of the neurons within the

cortex according to their way of firing. Therefore, we described the distribution of neural firing patterns in the BC. We performed extracellular *in vivo* recordings in anesthetized mice along the whole area with a vertical multi-array electrode in order to capture neural signal from all the layers.

3 Discussion

In this section of this manuscript there is a summary of the results, the discussions and the conclusions of the works, most of them published, which were written during the development of this Doctoral Thesis project. Here I present a list with of the articles ordered chronologically that are attached at the end of the document in the Annex and I add an explanation of my contribution to each work.

- ***article 1***: *"Frequency-specific Response Facilitation of Supra and Infragranular Barrel Cortical Neurons Depends on NMDA Receptor Activation in Rats."* In this publication I designed and performed the experiments as well as the data analysis in collaboration with Mr Castejon.

- ***article 2***: *"Synaptic Plasticity in the Somatosensory Cortex."* This publication is a short review about synaptic plasticity that I also wrote.

- ***article 3***: *"Modulation of Specific Sensory Cortical Areas by Segregated Basal Forebrain Cholinergic Neurons Demonstrated by Neuronal Tracing and Optogenetics Stimulation in Mice."* In this publication which combines anatomy experiments performed by Ms Chaves-Coira with electrophysiology experiments, I performed the optogenetic experiments and I analyzed the electrophysiological data.

- ***article 4***: *"Control of Somatosensory Cortical Processing by Thalamic Medial Nucleus: A New Role of Thalamus in Cortical Function."* In this publication, I performed the data analysis and wrote the paper in collaboration with Mr Castejon.

- ***article 5***: *"Bidirectional Hebbian Plasticity Induced by Low-Frequency Stimulation in Basal Dendrites of Rat Barrel Cortex Layer 5 Pyramidal Neurons."* In this publication which combines *in vitro* experiments performed by Dr Diez-Garcia and *in vivo* experiments performed by me in which I also did the data analysis of these *in vivo* experiments. I have also contributed in the writing of this article.

- ***article 6***: *"Discharge Properties of Neurons Recorded in the Somatosensory Cortex of the Mouse."* In this work not yet published, I performed the experiments, I did the data analysis and also I wrote the manuscript

3.1. Summary of the Results

In our first work (***article 1***), we observed by means of extracellular *in vivo* recordings in anesthetized rats BC that a repetitive stimulation applied to the whisker that belongs to the cortical column at the frequencies to which the animal sweep their whiskers (5 or 8 Hz) induced LTP in supra- and infra-granular layers through the activation of NMDA receptors. We also found that the cortical neurons that achieved LTP did not only fired more APs induced by the stimulus, but also fired them more precisely while the coherence between the neuronal response and the stimulus increased. Furthermore, an increment in the Ach level increased the number of cortical cells that performed LTP after a repetitive stimulation of 5 Hz through the activation of muscarinic receptors. Experiments where supra-granular layer activity was blocked with muscimol while recording VPM thalamic nucleus and infra-granular layer activity simultaneously, showed that the supra-granular layer activity is important for achieving LTP in the infra-granular layer and the VPM.

Article 2 is a small review of synaptic plasticity in the BC. In this bibliographic work, we talk about the already known mechanisms of synaptic plasticity induced by stimulation. We also reported the importance of Glu and Ach as NTs essentials for the proper functionality of synaptic plasticity. Glutamatergic transmission is needed for the correct transmission of sensory information to occur. Glu acts through the activation of AMPA and NMDA receptors. NMDA receptors are the ones involved in synaptic plasticity. The correct function of the cholinergic system is required for several normal live behavior actions involving plasticity processes. Ach acts through the activation of nicotinic and muscarinic receptors that have different subtypes classified according to the time and place of activation, giving the cholinergic system the ability of regulation between excitation an inhibition. It is still unknown how these different receptors work together to give the system this type of regulatory capacity.

Since it is established that Ach is so important for plasticity ***article 3*** describes a study of BF projections to the somatosensory cortex. We saw that the BF projects from its different nuclei, concretely HDB and B, in a very specific and ordered manner. Using optogenetic *in vivo*

stimulation in the target BF nuclei of urethane anesthetized transgenic mice, while recording population activity in S1 and A1 simultaneously, we were able to conclude that the stimulation of B nucleus with a blue light evoked a small facilitation similar in both cortical areas. However, light stimulation of HDB evoked a higher facilitation in S1 than in A1, confirming that the BF projects in a selectively manner to the cortex.

To shed some light on how thalamus activity influences cortical sensory processing we performed the study reported in ***article 4***. In this article we used extracellular *in vivo* recordings combined with pharmacology in order to determine how the activation or the inhibition of VPM or POM affects cortical response in supra- or infra-granular layers. We found that both thalamic nuclei behave in a complementary way. We observed that POM modulated magnitude and duration of BC neuronal response in both cortical layers. We also saw that this modulation was transmitted through S1 layer I by the activation of the GABAergic system. Besides, POM controls sensory processing of S2 trough corticofugal activity of S1 layer V.

Article 5 studies synaptic plasticity mechanisms induced in layer V pyramidal neurons of the rat BC by low frequency stimulation. *In vitro* experiments showed that under blocking inhibition activity, a low-frequency stimulation of the basal dendrites trigger an EPSP followed by an AP burst and a Ca^{2+} spike, mediated by the activation of NMDA receptors that ended in LTP. If the inhibition was active then LTD was achieved, showing the importance of GABAergic system in synaptic plasticity. We also performed *in vivo* extracellular recordings in S1 layer V while a stimulus in the principal whisker at 1 Hz was being performed. We furthermore observed that the neurons that reached LTP had an increment of the second response component during the stimulation train period, thus supporting the fact that NMDA receptors are implicated since the very beginning of the plasticity process.

Moreover, we also wanted to find out more about the functionality of the BC by unraveling the functional map of this area which is a work that we think is extremely important to

untangle somatosensory processing in the BC and which at this time is still under construction. In ***article 6*** we were able to observe, by ,means of extracellular multichannel recordings in urethane anesthetized mice, four different types of firing patterns: regular, irregular, bursting and large bursting. These patterns were all characterized by their autocorrelogram. We saw that the distribution of these firing patterns was not homogeneous.

3.2. Synaptic Plasticity in the Barrel Cortex

Synaptic plasticity is an extremely relevant process involved in memory and learning. It refers to modifications in the strength or efficacy between already existing synapsis through experience, as shown in ***article 2*** and in the Introduction to this document. There are different ways of inducing synaptic plasticity in the somatosensory cortex for example by performing changes in peripheral inputs, through experience in life by learning some specific task or by inflicting a damage in the pathway. In this Doctoral Thesis in particular, we studied synaptic plasticity in rat BC through a sequence of repetitive stimulations.

Given that the experiments performed in this Doctoral Thesis are *in vivo* with the animal under anesthesia, finding an anesthetic allowing us to study plasticity processes and that remaining stable for over 60 minutes was a crucial task. Due to those *sine qua non* conditions, all the experiments performed in the works listed at the beginning of the Discussion were performed under urethane anesthesia conditions. Urethane is an anesthetic that has been used for years due to its minimal effects on the respiratory and cardiovascular systems. Furthermore, urethane affects synaptic transmission in the brain and appears to act on both inhibitory and excitatory transmission [90]. For instance, spontaneous Ach release is lower under the effect of urethane anesthesia than within freely moving animals [91], but is sustained in both conditions [92, 93]. Moreover, a reduction of the receptive field has been reported [94]. Furthermore, urethane is an anesthetic that can last for hours, this being a crucial condition in our experiments. One further important issue is that even though it affects some ion channels, its effect over them is less marked than the effect other anesthetics could induce, thus allowing the nervous system to keep active NMDA and cholinergic channels [90]. For instance, the work of Glazewsky et al. 1998 [95] in which synaptic plasticity remains under urethane conditions

demonstrated that it is possible to achieve LTP in the BC of urethane anesthetized rats through application of an electrical stimulation to layer IV.

In ***article 1*** the main aim was to discover if it was possible to induce a LTP of the neuronal response after a repetitive whisker stimulation train, as well as to find out if the frequency of the stimulation train was relevant in this process. The whisker stimulation train attempted to simulate real natural frequencies that rodents could find in their natural environment or that they could perform in the scope of their normal exploring behavior. Serving this purpose, we performed *in vivo* electrophysiological experiments in urethane anesthetized rats. The stimulus was performed by an air-puff (20 ms duration). We studied the effect of a stimulation train (40 stimuli at frequencies between 0.5 and 8 Hz) was studied over the neuronal response under a continuous stimulation of 0.5 Hz before and 1, 5, 15, 30 and 60 minutes after the stimulation train through whisker-evoked potentials (figure 1A; art1). The continuous stimulation of 0.5 Hz induced a small increase in amplitude in the evoked potential. However, stimulations train at higher frequency such 5 or 8 Hz induced a larger increase of the neuronal response that lasted for at least 60 minutes and reached a stable level at 30 min (figure 1B; art1).

We set the stimulation to be regularly repetitive because we were controlling the air pressure (1-2 kg/cm^2) coming out of the polyethylene tube (1 mm inner diameter with a Picospritzer pneumatic pump). Additionally, we also controlled the direction and the angle ($\approx 15°$) of the whisker deflection with a video-camera and showed that the whisker deflection was the same each time an air-puff was delivered during the time while each experiment was performed. The movement of the whisker occurred in less than 125 mili-seconds that is the maximum interval used in the experiments (frequency of stimulation of 8 Hz).

In order to study the mechanisms of this effect within the BC, we performed extracellular recordings in supra- and infra-granular layers. All recorded neurons displayed a low spontaneous firing rate. Both populations were homogeneous (figure 2; art1) and neurons responded to no more than one or two whiskers. All these pieces if evidence support the idea that we recorded pyramidal cells. Under these conditions LTP was induced with all stimulation train

frequencies. However, for frequencies 0.5, 1 and 2 Hz the increase was modest. The significant LTP was induced at 5 and 8 Hz stimulation train frequencies (figure 3; art1) in the supra-granular layer. In the infra-granular layer the significant LTP was found for frequencies 2, 5 and 8 (figure 4; art1). The largest increment for both layers was found after the stimulation train of 5 Hz. Thus, it is possible to conclude that a short train of whisker stimulation can induce a LTP. The fact that the highest facilitation was found at frequencies 5 and 8 Hz could possibly be explained because rodents move their whiskers while exploring the environment at frequencies comprised between 4 and 12 Hz, as explained in the Introduction. Another reason why 2 Hz also increase the neuronal response in infra-granular layer could possibly be because different layers in the cortex may play different functions in sensory processing. [96].

Once all the aforementioned informations have been given, another important mechanism evoking synaptic plasticity in the brain is through the increase of synchronous neuronal activity to elicit larger synaptic potentials in the postsynaptic neuron than in control condition. In order to study this matter, coherence between the stimulus and the neural response was also computed in ***article 1***. Before applying the stimulation train, we were able to observe some coherence with the control stimulation of 0.5 Hz. However, after the stimulation train of 5 Hz the coherence became stronger showing that an increase in the functional coupling was evoked by the stimulation train (figure 5; art1). The fact that the neurons that showed LTP also showed a stronger coupling between the stimulus and their response occurred in both cortical layers strongly suggest that neuronal coupling play an important role in LTP. It is possible to conclude that this LTP of the neuronal response evoked by a short stimulation train may activate some important mechanisms for processing information in the BC, because not only the neurons fired more, but also induce EPSPs in a narrower time window.

The mechanisms behind this facilitation were also studied in ***article 1***. As I explain in the Introduction and in ***article 2*** review, cortical LTP is mainly due to the activation of Glu NMDA receptors. Consequently, in order to block the NMDA receptors an i.p. injection of MK801, an NMDA receptor antagonist, was applied. Under this condition, the response facilitation after 5 Hz stimulation train was completely blocked in both cortical layers. The NMDA receptor

blocker APV was also locally applied through a cannula placed next to the recording electrode to test if the contribution of NMDA receptors in both layers was similar. Appling APV locally in the supra-granular layer the stimulation train induced an LTD. On the other hand, application of local APV in infra-granular layer did not block facilitation. Although it was not as strong as it was in control conditions this layer was able to perform a LTP (figure 6; art1). This finding supports the hypothesis that cortical layers process information in a different manner. These experiments also show the important implication of NMDA receptors in the generation of this facilitation induced by a short repetitive stimulation of the whisker.

In order to support this idea, we also studied the effect of the repetitive stimulation in the response components in control and 15 minutes after the stimulation train. The early response component is mainly caused by the activation of Glu non-NMDA receptors while the late component is caused by the activation of Glu NMDA receptors. The first component of the response (0 – 20 ms) was only slightly affected in both cortical layers, but there was a significant change in the supra-granular layer with the 5 Hz stimulation train. On the contrary, the second response component was strongly affected by the stimulation train mainly at 5 and 8 Hz in supra-granular layer and at 2, 5 and 8 Hz in infra-granular layer (figure 7; art1), as it was expected from the results shown in figures 3 and 4. These results are consistent with the fact that NMDA receptors are directly implicated with long-term changes in the BC of rodents induced by a repetitive stimulation.

Local injections of muscimol in supra-granular layer blocked LTP in both supra- and infra-granular layers. During muscimol application, the response in the infra-granular layer was reduced but did not was abolished. Thus, sensory inputs from the thalamus to basal dendrites remained. Although this experiment did not clearly establish the origin of the LTP in the BC, data suggest that the supra-granular layer is important in the LTP induced in vivo by repetitive stimulation.

In this first study, ***article 1***, we additionally studied changes in the receptive field (RF) evoked

by a repetitive stimulation. Serving this purpose, we recorded neurons that responded to the principal whisker and to another peripheral whisker with a weaker response. Neurons that showed LTP 15 minutes after 5 Hz stimulation train at the principal whisker, also increase their response to the peripheral whisker stimulation in both layers in a similar fashion (figure 10; art1). Thus, the stimulation of a specific whisker not only facilitated the stimulated whisker but also other whiskers in the receptive field (RF). It is even more interesting to point out that in a few cases, neurons that did not respond at all to the peripheral whisker stimulation, after the stimulation train of 5 Hz to the principal whisker, started to give a weak response to unresponsive whiskers, unmasking lager RFs. This evidence supports the idea that a repetitive whisker stimulation facilitates the principal RF of neurons in the barrel and the adjacent barrels. Possibly this RF enlargement is due to NMDA receptors activation that increase the intracellular concentration of Ca^{2+} that could induce the incorporation of new receptors in dendritic spines, facilitating heterosynaptic inputs.

For further understanding of synaptic plasticity in rodent somatosensory cortex, a study determining the mechanisms that generate LTP or LTD was performed combining experiments *in vitro* and *in vivo*. This study is reported in ***article 5***. With the *in vitro* experiments was possible to induce LTP with a low-frequency stimulation (0.2 Hz) in the basal dendrites of layer V pyramidal neurons. These set of *in vitro* experiments were performed by Dr. Díez-García in the laboratory of Prof. Fernández de Sevilla. Under excitatory conditions, after blocking $GABA_A$ receptors with picrotoxin (PTX), EPSP-Ca^{2+} spikes were evoked without failure. In control conditions with only artificial cerebro-spinal fluid in the bath, Ca^{2+} spikes could not be evoked and excitatory postsynaptic current (EPSC) amplitudes were unaltered. This means that EPSP-Ca^{2+} spikes were dependent on $GABA_A$ inhibition. Repetitive generation of EPSP-Ca^{2+} spikes induced a stable LTP that lasted at least 30 minutes (figure 2D, E; art5).

To better understand Ca^{2+} spike contribution to this type of LTP under PTX condition, Ca^{2+} spikes were inhibited with D-AP5, a NMDA receptor blockade, and with nifedipine which is a L-type voltage gated Ca^{2+} channels (VGCCs) blockade (figure 1F, G; art5). In these conditions, a basal stimulation could not induce LTP. Which means that the Ca^{2+} spike is fundamental for

generating this type of LTP (figure 4B; art5).

As I said earlier, the goal of this study was not only to unravel the mechanisms to the LTP but also to the LTD. What condition is a determining factor for a neuron to select between the one or the other synaptic plasticity? It is thought that the level of Ca^{2+} influx during the dendritic depolarization is crucial for the "decision" between LTP or LTD [96]. Thus, in this work we studied the effect of the membrane hyperpolarization during low-frequency stimulation train, the induction process. A hyperpolarization of -100 mV decreased the amplitude and duration of the EPSP-Ca^{2+} spikes, and after the induction stimulation the result was an LTD. Results showed that cytosolic Ca^{2+} signal was much higher when the neuron was more likely to performed LTP. Thus, it was possible to conclude that the changes in the synaptic plasticity could be regulated by the membrane depolarization and by the cytosolic Ca^{2+} level during the induction stimulation protocol.

In order to support this conclusion, we performed experiments *in vivo* in urethane anesthetized rats. The experimental procedure was the following: extracellular recordings in layer V with a tungsten electrode, while repetitive low-frequency whiskers deflections were applied with an air-puff to the principal whisker. The stimulation protocol was 60 seconds at 0.5 Hz as a control of the neuronal response, then a train of 40 stimuli at 1 Hz to induce long-lasting changes and 1, 5, 15 and 30 minutes later 30 stimuli at 0.5 Hz to observe how the neuronal response had changed. The induced frequency was chosen at 1 Hz, because we considered it to be low enough for an *in vivo* experiment since rats usually move their whiskers at frequencies between 4 – 12 Hz. In these conditions 66% of neurons showed LTP, while 22% showed LTD. The rest did not change their response. A study of the stimulus time histogram during the induction stimulation at 1 Hz was performed and revealed an interesting result: neurons that achieved LTP had their responsiveness increases during the induction train. On the contrary, neurons that achieved LTD saw almost no change during the induction period. As was previously studied in the *in vitro* experiments, the implication of NMDA receptors was tested by a local injection of D-AP5 in anesthetized rats. In this case, neuronal response 30 minutes after the induction stimulation was practically the same as it was in control conditions

before the induction stimulation, suggesting that NMDA receptors play a very important role ruling this bidirectional plasticity (figure 8; art5).

In ***article 1*** we show an LTP that occurs after whisker stimulation at the optimal and physiological frequency of 5 and 8 Hz, both within the range of frequencies in which the rats move their whiskers. However, in ***article 5*** we also show the possibility of achieving an LTP at low frequencies, but only when a synchronous burst of AP occurrs. These findings match with results displayed in ***article 1*** in which coherence of spike responses with the stimulus is relevant to induce LTP. Consequently, the change in the response pattern (from single spikes to burst of spikes) and the increase of temporal coherence with the stimulus may be an important mechanism in sensory plasticity to storage information [97].

3.3. The Importance of Acetylcholine in the Somatosensory System

As it was previously explained in the introduction, Ach is a NT that plays the role of a neuromodulator. As reported in ***article 2*** different extracellular concentrations of Ach can evolve in activation or in inhibition of neuronal activity. Ach is implicated in important processes such synaptic plasticity, attention or control of transitions between awake and sleep, and even more importantly the bad function of the cholinergic system could cause illnesses such as Alzheimer's disease. This means that Ach needs to be at the optimum level of concentration in each important process where it is implicated in order to modulate the process properly.

As it was previously commented and reported in ***article 2***, Ach plays an important role in sensory processes and in the synaptic plasticity of the neocortex. Its implication in cortical plasticity was studied, as we showed in ***article 1*** (figure 11, art1). In this study i.p. injection of eserine, a blocker of endogenous acetylcholinesterase enzyme that degrades Ach, was used to increase the level of Ach in the BC [98, 99]. Under this condition tactile response increased more than two times the standard error of the mean in the supra and infra-granular layers.

After control stimulation, a stimulation train of 40 stimuli at 5 Hz increased the number of neurons showing LTP in the supra-granular layer. However, neurons in the infra-granular layer seem not to be affected. This could be due to a bigger quantity of muscarinic receptors in the supra- than in the infra-granular layer of the BC [100, 101]. It was also interesting to see that although the tactile response increased in control conditions, the percentage of tactile response increment evoked by the repetitive stimulation was not changed by the i.p. injection of eserine. However, a large number of supra-granular cells were facilitated in the presence of eserine whereas infra-granular cells were not affected; this effect was blocked by a previous application of atropine, indicating that the outcome was caused by the activation of cholinergic muscarinic receptors. This result confirms the importance and complexity about the role of Ach. It is reasonable to believe that Ach incremented the number of cells that could be potentiated by repetitive whisker stimulation, changing the firing pattern of synaptic responses, as we demonstrated in *in vitro* experiments in ***article 5***.

This excitatory-inhibitory balance ruled by Ach exogenous concentration is mediated through muscarinic and nicotinic receptors. This evidence is also reported in the review ***article 2*** in which we show, based on previous literature and on our own findings, that the activation of nicotinic and muscarinic receptors enhances synaptic transmission. In pyramidal cortical neurons the activation of cholinergic muscarinic receptors increases excitability that lasts longer than with the activation of nicotinic receptors. If Ach acts over GABAergic interneurons then the inhibition possibly increases. This is one of the reasons why Ach has this role in the control of system excitation, because it can act over a different subtype of cholinergic receptors and over second messengers. These facts were proved by experiments in ***article 1*** and ***5***. In the first study (figure 11, art1) blocking muscarinic receptors with Atropine, injected intraperitoneally 10 minutes before the i.p. injection of eserine, completely blocked the effect of Ach. Even more it blocked the LTP in infra-granular layer, showing that these receptors are fundamental for synaptic plasticity processes in the somatosensory cortex.

Another important issue, which I reviewed in the introduction section of this document and in ***article 2***, is that the transmission of Ach to the somatosensory cortex is mainly caused

by a dense innervation of cholinergic neurons from subcortical regions located in the BF and the pontine-mesencephalic nuclei. Most of the cholinergic innervation to the sensory cortex comes from HDB and VDB, SI and B (Maynert basal magnocellular nucleus in humans). Recently it has been shown that the BF is a nucleus topographically organized that projects to different cortices in a highly structured way. Evidence of this important and relatively new topic can be found in ***article 3***. In this study anatomical evidences of the topological distribution of the BF were found (figures 2, 3 and 4, art3) (these set of anatomical experiments were performed by Ms. Chaves-Coira in the laboratory of Prof. Rodrigo-Angulo). By injecting two different fluorescent retrograde tracers, Fluoro-Gold (FlGo) in S1 and Fast Blue (FB) in A1 it became possible to unravel that HDB is mainly dedicated to modulation of S1 whereas B nucleus projects in a similar way to both sensory cortices. In this study we also tested the specificity of BF cholinergic projections by *in vivo* optogenetic stimulation of BF in transgenic mice expressing the light-activated cation channel, channelrhodopsin-2, tagged with a fluorescent protein (ChR2-YFP) under the control of the choline-acetyl transferase promoter (ChAT). An optrode was used to stimulate them with blue-light and record the unitary activity of the BF; simultaneously the population activity (evoked potentials) of S1 and A1 were also recorded. As a result, a short-lasting blue stimulus induced fast cortical activity in both cortical areas (figure 5, art3).

To quantify this effect, the power spectra before and after the BF light stimulation of both cortical signals was computed (figure 6, art3). Optogenetical stimulation of HDB reduced delta activity in S1 and A1 and increased frequencies over theta frequency band. The same happened when B was stimulated optogenetically. Although apparently nothing changed between the S1 and A1 activity after the stimulation of HDB or B, an important result came out: the blue light stimulation of the BF increased the evoked potential generated by the sensory stimulations. Light stimulation in HDB induced an LTP of the evoked potential (at least 30 minutes) in both cortical areas and the increase was larger for S1 than for A1, as we expected from the anatomical findings (figure 7, art3). On the other hand, optogenetic stimulation of B induced a lower increase of the evoked potentials and did not last more than 5 minutes. Both cortical areas were similarly affected (figure 8, art3). Thus, optogenetic stimulation of these BF

areas confirms anatomical data showing an important modulation of whisker responses in S1 when blue-light stimulation was delivered to HDB. Previous findings and our anatomical studies indicated the existence of a highly structured and topographic organization of BF efferent projections to sensory cortices. Therefore, these results prove the segregation of neuronal population in different BF-cortical networks that may play distinct roles in sensory processing, motor control, or cortical arousal.

We can possibly conclude from these experiments that the Ach is a neuromodulator which capacity of enhancement or depression of sensory responses and that, should be important for processing the information in a very specific manner. Ach regulates neuronal excitability and more concretely synaptic plasticity processes through muscarinic and nicotinic receptors placed in pyramidal and in GABAergic neurons. The main source of Ach to the somatosensory cortex is the BF that is topologically organized and sends cholinergic projections from its nucleus to the cortex in a very specific and sensory-organized manner.

3.4. The Role of the Thalamic Nucleus in Somatosensory Information Processing

As it was reviewed in the Introduction of this Thesis, the thalamus is an important relay station to the cortex in the somatosensory pathway. This means it is important to know the role the thalamus plays to better understand cortical function. In porder to try to unravel this problem, we performed extracellular recordings in VPM and POM nuclei of thalamus in different studies and under different conditions..

In ***article 1***, we wanted to see if the LTP could come from this subcortical nucleus, concretely from the lemniscal pathway. First, we needed to find out if VPM is capable of achieving an LTP. For this purpose, double extracellular unit recordings were performed in the BC and in the VPM. In control conditions, a stimulation train of 5 Hz induced response facilitation in VPM (figure 9A; art1). In order to know if this facilitation came from the cortex or on the contrary if the VPM was the one that transmitted it, the activity of the cortex was blocked with muscimol,

a $GABA_A$ receptor agonist. This cortical inactivation did not affect neuronal responses in VPM to the control stimulation of 0.5 Hz. Under this condition VPM could not achieve facilitation evoked by the stimulation train of 5 Hz (figure 9B; art1). This result suggests that the LTP was generated in the BC.

In ***article 4*** we studied the role of the POM thalamic nucleus to unravel its implication in somatosensory cortical information processing. In order to find this out, we performed experiments in urethane-anesthetized rats brains recording the extracellular activity with a tungstein electrode in the target nuclei. First, we characterized POM neuronal response pattern. The stimulus consisted in air-puffs delivered to one whisker of different durations (20 – 200 ms). Neurons responded to several whiskers and the response was sustained during the stimulus (tonic response; figure 1; art4). In contrast, VPN neurons responded to a single whisker and only at the beginning of the stimulus (phasic response). Neurons recorded in the SpVi trigeminal nucleus showed the same response pattern that POM neurons. These results demonstrate the presence of a sustained response along the paralemniscal pathway.

Second, the influence of POM and VPM in the activity of supra- and infra-granular layers of S1 was studied in two manners: exciting the nuclei with an electric stimulation and inhibiting them with a muscimol injection. By testing the electrical POM or VPM stimulation we were able to conclude that our results were caused by the orthodromic cortical activation of thalamic inputs (figure 2C; art4).

In order to measure the effect of activating POM nucleus in infra- and supra-granular layers two stimulation trains were set (figure 2D; art4). In the first train, 30 pulses (air-puff; 20 ms; 0.5 Hz) were delivered to the principal whisker without the electrical stimulation in POM just to characterize the neuronal response. In the second train, electrical stimulation of POM were delivered 500 mili-seconds before each air-puff. Electrical stimulation of POM elicited orthodromic spikes in the BC that could last up to 50 ms in the supra-granular layer and up to 150 ms in infra-granular layer. The result of the stimulation protocol was that during POM

electric stimulation all cortical response decreased in amplitude and duration. Although no differences were found between both cortical layers, as we knew the importance of NMDA receptors activation in whisker responses of somatosensory cortex (see above), we computed the analysis of different parts of the response (0-20 ms; 20-50 ms) and the effect of POM stimulation on both response components. In the infra-granular layer the first component (mediated by non-NMDA glutamatergic receptors) did not change. However, the second part of the response (mediated by NMDA glutamatergic receptors) decreased 52% in a drastic way. In the supra-granular layer both components were reduced (20% first; 50% second componnets). These reinforce our view of the importance of NMDA receptors in the modulation of the somatosensory cortex function and also show a difference between the layers function.

In order to compare both thalamic nuclei and prove that the electric stimulation was restricted to the target nucleus, VPM was also electrically stimulated with the same stimulation protocol as the POM. VPM electric stimulation caused orthodromic spikes in the cortex with shorter latency than during the POM electric stimulation. VPM electric stimulation increased cortical neuronal responses similarly in both cortical layers. The increment mainly occurred in the second component of the response (figure 3; art4).

These experiments depict different roles between the two thalamic nuclei. It is interesting to notice that the function seems to be complementary because the effect of the electrical stimulation of VPM or POM was just the opposite. Apparently, the VPM nucleus is dedicated to a precise transmission of somatosensory stimuli from the periphery to the cortex. In contrast, POM neurons are dedicated to modulate somatosensory responses according to the stimulation pattern of the environmental conditions.

The effect of POM and VPM over the BC was also measured by blocking the activity with muscimol injections. Inactivation of POM increased sensory responses in both cortical layers; this response increment was remarkable in the second component of the response, while the first component almost did not change. The onset latency was not modified, although the

offset latencies increased differently in the cortical layers (12% infra; 22% supra) (figure 4; art4). The spontaneous firing rate of neurons also increased around 30% in the BC. These pieces of evidence suggest that POM activity regulates cortical excitability of the BC by increasing the response duration and consequently the time window in which temporal and spatial summations may occur. This process is crucial to generate synaptic plasticity. Inactivation of VPM thalamic nucleus reduced sensory responses in both cortical layers and in both response components (figure 5; art4). We found the opposite result again suggesting different roles of these thalamic nuclei processing sensory information.

In order to further understand the role of POM in the influence of cortical sensory processing, we studied changes between the electric stimulus and the air-puff. The magnitude and the response of cortical neurons changed and both layers showed a different behavior. The first response component was not affected in the infra-granular layer. However, in the supra-granular layer the first response component was strongly reduced at all time intervals. Moreover, in the supra-granular layer, no significant changes at intervals larger than 700 miliseconds were found. On the opposite, in infra-granular layer we found significant differences at 1000 ms (figure 6; art4).

The intensity of the electric stimulation was also important. Increasing the intensity of the electric stimulation in POM nucleus caused a decrease in the magnitude and duration of cortical responses (figure 7; art4). The second response component was mainly affected by this intensity effect (figure 8; art4). Taken together these results suggest that the first and the second component of the response codify different type of information [6].

It was discovered that POM sends excitatory connections to the BC. This was in agreement with the orthodromic stimulation, but not with the electric stimulation of POM before the whisker deflection, that suggested that these connections could be inhibitory. It is well known that POM sends numerous projections to layer I and that blocking the activity in this layer increases neuronal responses evoked by whisker deflection. We then hypothesized that

may be the modulatory action of POM was mediated through the layer I.

Since layer I is basically conformed by inhibitory GABAergic neurons, we blocked layer I inhibition with PTX. Under this condition we found a big change in sensory responses in both cortical layers. Spontaneous activity increased around 37%. It is known that parvalbumin (PV) interneurons express Cav2.1 (P/Q-type) voltage-gated Ca^{2+} channels that mediate the liberation of GABA from FS interneurons to pyramidal neurons. In order to study the contribution of PV interneurons we blocked them with w-agatoxin-IVa (AGA). Under this conditions neuronal responses significantly increased. The spontaneous activity of cortical neurons increased 22% in infra-granular and 31% in supra-granular layers (figure 9; art4). The increment in the cortical response magnitude was more obvious in the second response component. Under PTX condition significant changes were observed in the first component of the response. Nevertheless, changes in the second component were larger (figure 10A; art4). The offset latency also increased in both layers, while the onset latency did not change. Under AGA conditions whisker response magnitude increased. However, this time the changes in the first part of the response were not significant, while changes in the second part of the response were significant (figure 10B; art4). After these experiments we were able to confirm that layer I influenced on whisker cortical evoked responses. GABAergic transmission from layer I regulates cortical excitability and magnitude and duration of the sensory response.

In order to confirm that POM regulation acts through layer I, we stimulated electrically POM before (500 ms) each air-puff whisker deflection under conditions of inhibitory inactivation of layer I by PTX. Under these conditions the response magnitude did not decrease significantly (figure 11; art4). The response duration and offset latencies were not affected either (figure 12; art4). When we performed the same experiment but blocked P/Q-type Ca^{2+} channels with AGA, cortical sensory responses changed significantly neither in amplitude nor in latency (figure 13; art4). In order to ensure that POM cortical modulation was mediated through layer I, electric stimulation was applied directly to layer I before sensory stimulus. In this situation, we could find results similar to those from the POM electric stimulation experiment. This evidence suggested that POM modulated effect in sensory cortical responses was mediated by

layer I (figure 14; art4).

As a way to sum up the previous results, we can affirm that layer I is important for the integration of sensory information in the cortex. This makes sense because it receives inputs from other cortical areas and also from the thalamic nucleus. We can also say that the POM probably controls cortical sensory responses through layer I. It is interesting to observe that although there are no so many connections between the infra-granular layer and layer I as occur in the supra-granular layer, the effect of electrically stimulating layer I was similar in both layers. This effect is probably due to the apical dendrites of infra-granular neurons reaching layer I.

Since POM also projects to other cortical areas such as S2, we wanted to find out if this nucleus could also modulate responses in S2 and more interestingly if it modulates the processing of information between both cortical areas. It was known that layer V neurons in S1 project to the POM. At the same time POM neurons project to other cortical areas. We made recordings in the whisker area of S2, while we electrically stimulated S1 layer V . The electric stimulation by itself evoked a strong activity in S2 (figure 15; art4). If S1 was electrically stimulated before each whisker deflection, the response magnitude and latency decreased. The second part of the response was again more affected (figure 16B; art4).

In order to discover if this transmission was mediated by POM, we blocked POM activity with muscimol. Under this condition the electric stimulation of S1 layer V before whisker deflection did not reduce neuronal response of S2, basically neuronal response did not change (figure 16D; art4). Even more so, the response of S2 to the electric stimulation of S1 layer V alone was eliminated when the activity of POM was blocked. This result indicates that POM activity controls sensory processing in S2 that is modulated by corticofugal activity of S1 layer V (figure 17; art4). Since S2 receives projections from the ventrolateral part of the VPM. As this pathway should not be affected by POM inactivation, this first response component could possibly be ruled by VPM-S1-S2 pathway. We also discussed the possibility that layer VI was affected by layer V electric stimulation. However, it is known that electric stimulation of layer VI does not

activate S2, which support the idea that electric stimulation of layer V is being transmitted to S2 through POM.

Thanks to all these set of experiments we can hypothesize that POM plays the role of regulating the gain of the information depending on the relative intensities of the stimulus in a set of whiskers. The POM would integrate the multi-whisker stimulus and would transmit this processed information to the cortex. Also, POM nucleus may contribute to synchronize sensory processing in S1 and S2 cortices. It is also clear that both thalamic nuclei, POM and VPM, play different complementary roles in sensory processing. Lemniscal pathway may process specific sensory information (mono-whisker), while paralemniscal pathway process global information (multi-whisker). An evidence of this hypothesis is that POM can detect changes in sensory activity, by codifying stimulus intensity and duration, and adjusting the gain and timing of cortical response in consequence. Another point is that most of changes in response were found in the second part. As it was proved the second part of the response is regulated by NMDA receptors. This means that these receptors are also implicated not only in plasticity processes that lasted unless for minutes, but also at the first stages of cortical processing information.

Finally, we can affirm that these experiments suggest a new role of POM in cortical processing helping to unravel and better understand the role of thalamo-cortical interactions in sensory processing.

3.5. Functional Organization of the Barrel Cortex

Along the previous subsections it is possible to discern some experiments that expose evidence showing that the cortical layers process sensory information differently. In ***article 1*** some evidence of this interesting point has been proved, as the LTP did not behave equally in supra- and infra-granular layers, suggesting that may be the potentiation was transmitted form supra-granular to the infra-granular layer. In order to study this issue, muscimol was

applied locally in the supra-granular layer and we made extracellular recordings in the infra-granular layer. The spontaneous activity of the infra-granular layer was not affected, but the evoked spikes were reduced in amplitude, probably because the feed forward response from supra-granular layer to the infra-granular layer was almost suppressed. Under this condition a stimulation train of 5 Hz induced a depression in the infra-granular layer (figure 8; art 1). This result suggests that the LTP evoked by a short repetitive stimulation train is transmitted from upper layers to lower layers in the somatosensory cortex. Thus, the supra-granular layer seems to generate the long-lasting facilitation, while the infra-granular layer may possibly contribute to this plasticity procedure by projecting the changes to other cortices and subcortical nuclei.

It is possible to find more evidence about differences in cortical processing in ***article 4***. As extensively explained in the previous subsection electrical stimulation or inhibition of POM caused different effect in the first component of the response that it was significantly affected in the supra-granular but not in the infra-granular layer, as it was demonstrated in the figure 6. More important results come out with the implication of layer I and layer V in the sensory processing mediated by POM activity. Layer I seems to mediate intra-cortical sensory processing by activation of GABAergic interneurons (figure 14; art4), while layer V seems to mediate cortico-cortical processed information through POM (figures 15 and 16; art4).

Consequently, these data suggest that different neuronal populations in S1 also possibly contribute to sensory processing. To study this matter we characterize response properties of S1 neurons by simultaneous recording of neurons in supra- and infra-granular layers of anesthetized mice using multielectrodes in ***article 6***. In this study, still under construction, we found four different types of firing patterns according to their autocorrelograms: irregular (IRR) or type I, bursting cell (BC) or type II, large bursting cell (LBC) or type III and regular (REG) or type IV. Most of the recording cells showed REG activity, which is characterized by a constant probability to spike (figure 2A,B,C,D; art6). We performed a study of the distribution of the firing patterns along all the directions: anteor-posterior, medio-lateral and dorso-ventral (figure 2E,F,G; art6). Mostly significant differences could be found within each layer between the different antero-posterior and medio-lateral areas. Most of the cells with a BC or LBC

firing pattern were placed in more posterior and medial position. IRR cells were placed almost all of them, around the middle of the BC volume, while REG cells are mostly localized in the middle section of the medio-lateral direction with a tendency of being distributed medial and posterior and in addition in the infra-granular layer.

Although ***article 6*** mainly shows mainly preliminary data, we can already conclude that BC functional cell distribution is not homogeneous in the different cortical layers, but is also not uniform allong the atero-posterior and medio-lateral directions. This issue must be important for information processing and should be taken into account when recording the BC.

4 Conclusions

The following conclusions are based on the studies summarized in the Discussion of this Doctoral Thesis that are attached at the end of this document in the Annex.

1. A short train of whisker stimulation can induce a long-lasting facilitation of S1 cortical responses. This facilitation occured at frequencies within the frequency band rodents move their whiskers.

2. Neurons that showed long-lasting facilitation also showed an enhancement in the coherence between their response and the stimulus, meaning that neurons not only fired more but also in a more time-accurate manner.

3. The long-lasting facilitation was generated in the supra-granular layer of the BC and was transmitted to the supra-granular layer and to the VPM nucleus of the thalamus. This LTP depended on the activation of NMDA receptors.

4. Cortical neurons that were facilitated by a short stimulation train of 5 Hz could enlarge their RFs.

5. *In vivo* experiments showed that was possible to induce LTP at low frequencies in layer V of the BC. This process was mediated by the activation of NMDA receptors.

6. High levels of Ach in the extracellular medium of the BC increased the number of neurons that achieved LTP in the supra-granular layer. This effect was mediated by muscarinic and nicotinic receptors.

7. The BF projections to the cortex are topologically distributed. HDB mainly sends projections to S1, while B almost equally projects to S1 and A1. Optogenenic experiments supported this anatomical finding. Light stimulation in HDB induced a long-lasting increase of the sensory evoked potentials larger for S1 than for A1, while optogenetic stimulation of B induced a lower increase of the evoked potentials in both cortical areas.

8. Electric stimulation of POM thalamic nucleus before each whisker deflection decreased the barrel cortical response in amplitude and duration. The same protocol with VPM showed just the opposite. The second part of the response was the most affected showing that NMDA receptors were involved. Inactivation of POM increased sensory responses

in both cortical layers, while inactivation of VPM reduced sensory responses. These pieces of evidence suggest that POM activity regulates cortical excitability in the BC, and that both thalamic nuclei play complementary roles in processing sensory information.

9. POM modulated sensory cortical responses in S1 through layer I activation by GABAergic transmission regulated by PV interneurons.

10. Sensory processing in S2 was modulated by processing in S1 through corticofugal activity of S1 cortex layer V to POM and from this thalamic nucleus to S2 cortex.

11. The fact that different firing patterns cells are not homogeneously distributed in the BC probably means that according to the sensory input, BC uses different neuronal types to process sensory information.

4.1. General Conclusion

The findings presented in this Doctoral Thesis indicate that whisker stimulation induces LTP of cortical responses either at low frequencies that may occur when single stimuli affect the whiskers or at higher frequencies that may occur when the rat is exploring the environment. In both cases, NMDA receptors are involved although the mechanism is different. At low frequencies, NMDA spikes induce a change in the response pattern of cortical neurons (single spikes to burst of spikes). At higher frequencies the stimulus increases the number of evoked spikes and the coherence of responses. Ach, a neurotransmitter that increase its concentration in the cortex during wake states or during attentional processes, also favor LTP at both frequencies. This synaptic plasticity evoked by repetitive whisker stimulation was modulated by thalamic projections (POM nucleus) by activation of GABAergic neurons in upper layers of S1. These processes of synaptic plasticity may have important consequences in attention, learning and memory of a relevant stimulus during periods during which the animal is exploring the environment. Different firing patterns not homogeneously distributed in the BC must have relevant implications in sensory processing and synaptic plasticity.

Conclusiones (Spanish)

Las siguientes conclusiones están basadas en los estudios comentados en la Discusión de esta Tesis Doctoral y que se encuentran adjuntos al final de este documento en el anexo.

1. Una estimulación de corta duración de una vibrisa, puede inducir facilitación a largo plazo de las respuestas corticales de S1. Esta facilitación se observó a las frecuencias dentro de las cuales los roedores baten sus vibrisas para explorar su entorno.

2. Las neuronas que mostraron facilitación a largo plazo, aumentarón la coherencia de sus disparos con la estimulación. Demostrando que no sólo respondian con más APs, sino que también lo hicieron de un modo más preciso con respecto al tiempo.

3. La facilitació a largo plazo se generó en la capa supra-granular de la corteza de barriles y se transmitió a la capa infra-granular y al VPM del tálamo. Esta facilitación a largo plazo fué dependiente de la activación de los receptores NMDA.

4. Las neuronas corticales que facilitaron su respuesta tras un tren corto de estimulación de 5 Hz, pudieron aumentar su campo receptivo.

5. Los experimentos *In vivo* mostraron que era posible inducir LTP con frecuencias bajas en la capa V de la corteza de barriles. Este proceso tabién dependía de la activación de los receptores de NMDA.

6. Niveles altos de Ach en el medio extracelular de la corteza de barriles, aumentaron el número de neuronas que generaron LTP en la capa supra-granular. Este efecto estaba mediado por receptores muscarínicos y nicotínicos.

7. El prosencefalo basal manda proyeciones a la corteza que están organizadas topológicamente. El núcleo HDB proyecta principalmente a S1, mientras que el núcleo B proyecta igualmente a S1 y A1. Experimentos de optogenética demostraron este hecho anatómico. La estimuación de HDB indujo un aumento a largo-plazo del potencial evocado que fue mayor para S1 que para A1. Sin embargo, la estimulación de B indujo un aumento del potencial evocado similar para ambas areas corticales.

8. La estimulación eléctrica en el núcleo talámico POM antes de cada deflexión de la vibrisa deprimió la amplitud y duración de la respuesta cortical. El mismo protocolo de estimulación pero esta vez involucrando el VPM, mostró lo opuesto. La segunda componente de la respuesta fué la más afectada, mostrando que los receptores de NMDA están involucrados. La inactivación del POM aumentó las respuestas sensoriales en ambas capas corticales, mientras que la inactivación del VPM redujo la respuesta sensorial. Estos resultados sugieren que la actividad del POm regula la excitabilidad de la corteza de barriles y que ambos núcleos talámicos tienen papeles complementarios.

9. El POM modula las respuestas corticales sensoriales de S1 a través de la capa I, mediante la activación de la transmisión GABAérgica regulada por interneuronas PV.

10. El procesamiento sensorial en S2 fue modulado mediante el procesamiento en S1 a través de proyeciones corticofugales de la capa V de S1 al POM, y del POm a S2.

11. El hecho de que distintos patrones de disparos neuronales no se encuentren distribuidos uniformemente en la corteza de barriles, probablemente esté relacionado con que la corteza de barriles utiliza distintos tipos neuronales para procesar la información sensorial.

Conclusión General

Los resultados presentados en esta Tesis Doctoral indican que: la estimulación de una vibrisa induce la potenciación a largo plazo de las respuestas corticales tanto a frecuencias bajas, que podría suceder cuando un evento aislado toca la vibrisa, como a frecuencias altas que se pueden dar cuando el animal explora su entorno. En ambos casos, los receptores de NMDA está involucrados, aunque los mecanismos son distintos: a bajas frecuencias las espigas

de NMDA iducen cambios en el patrón de la respuesta neuronal de las neuronas corticales (de espigas simples a bursts); a altas frecuencias el estímulo aumenta el número de espigas evocadas y la coherencia de las respuestas. La Ach, un neurotransmisor que se encuentra en mayor concentración en la corteza durante vigilia a procesos de atención, también favorece la potenciación a largo plazo a ambas frecuencias. Esta plasticidad sináptica evocada por la estimulación repetitva de una vibrisa, fué modulada por las projeciones talámicas (POM) mediante la activación de neuronas GABAérgicas en las capas superiores de S1. Estos procesos de plasticidad sináptica podrían tener importantes consecuencias en procesos como la atención, aprendizaje y memoria de un estímulo relevante durante los momentos en los que el animal está explorando su entorno. Los distintos patrones de descarga, que no se distribuyen de modo homogéneo en la corteza de barriles deben tener importantes implicaciones en el procesamiento sensorial y la plasticidad sináptica.

Bibliography

[1] E Kandel, J Schwartz, T Jessell, S Siegelbaum, and A J Hudspeth. Principles of neural science. *McGraw-Hill Companies*, 2012.

[2] T Mosconi, T A Woolsey, and M F Jacquin. Passive vs. active touch-induced activity in the developing whisker pathway. *Eur J Neurosci*, 32(8):1354–63, Oct 2010.

[3] G Pouchelon, L Frangeul, F M Rijli, and D Jabaudon. Patterning of pre-thalamic somatosensory pathways. *Eur J Neurosci*, 35(10):1533–9, May 2012.

[4] K D Alloway. Information processing streams in rodent barrel cortex: the differential functions of barrel and septal circuits. *Cereb Cortex*, 18(5):979–89, May 2008.

[5] D Feldmeyer. Excitatory neuronal connectivity in the barrel cortex. *Front Neuroanat*, 6:24, 2012.

[6] D Feldmeyer, M Brecht, F Helmchen, C C H Petersen, J F A Poulet, J F Staiger, H J Luhmann, and C Schwarz. Barrel cortex function. *Prog Neurobiol*, 103:3–27, Apr 2013.

[7] P Veinante, P Lavallée, and M Deschênes. Corticothalamic projections from layer 5 of the vibrissal barrel cortex in the rat. *J Comp Neurol*, 424(2):197–204, Aug 2000.

[8] C C H Petersen. The functional organization of the barrel cortex. *Neuron*, 56(2):339–55, Oct 2007.

[9] P Barbaresi, R Spreafico, C Frassoni, and A Rustioni. Gabaergic neurons are present in the dorsal column nuclei but not in the ventroposterior complex of rats. *Brain Res*, 382(2):305–26, Sep 1986.

[10] D Pinault. The thalamic reticular nucleus: structure, function and concept. *Brain Res Brain Res Rev*, 46(1):1–31, Aug 2004.

[11] K A Koralek, K F Jensen, and H P Killackey. Evidence for two complementary patterns of thalamic input to the rat somatosensory cortex. *Brain Res*, 463(2):346–51, Nov 1988.

[12] S M Lu and R C Lin. Thalamic afferents of the rat barrel cortex: a light- and electron-microscopic study using phaseolus vulgaris leucoagglutinin as an anterograde tracer. *Somatosens Mot Res*, 10(1):1–16, 1993.

[13] V C Wimmer, R M Bruno, C P J de Kock, T Kuner, and B Sakmann. Dimensions of a projection column and architecture of vpm and pom axons in rat vibrissal cortex. *Cereb Cortex*, 20(10):2265–76, Oct 2010.

[14] I Bureau, F von Saint Paul, and K Svoboda. Interdigitated paralemniscal and lemniscal pathways in the mouse barrel cortex. *PLoS Biol*, 4(12):e382, Nov 2006.

[15] C Welker. Receptive fields of barrels in the somatosensory neocortex of the rat. *J Comp Neurol*, 166(2):173–89, Mar 1976.

[16] D J Simons. Response properties of vibrissa units in rat si somatosensory neocortex. *J Neurophysiol*, 41(3):798–820, May 1978.

[17] E Ahissar, R Sosnik, and S Haidarliu. Transformation from temporal to rate coding in a somatosensory thalamocortical pathway. *Nature*, 406(6793):302–6, Jul 2000.

[18] M E Diamond, M Armstrong-James, and F F Ebner. Somatic sensory responses in the rostral sector of the posterior group (pom) and in the ventral posterior medial nucleus (vpm) of the rat thalamus. *J Comp Neurol*, 318(4):462–76, Apr 1992.

[19] R Sosnik, S Haidarliu, and E Ahissar. Temporal frequency of whisker movement. i. representations in brain stem and thalamus. *J Neurophysiol*, 86(1):339–53, Jul 2001.

[20] F Clascá, P Rubio-Garrido, and D Jabaudon. Unveiling the diversity of thalamocortical neuron subtypes. *Eur J Neurosci*, 35(10):1524–32, May 2012.

[21] S Ohno, E Kuramoto, T Furuta, H Hioki, Y R Tanaka, F Fujiyama, T Sonomura, M Uemura, K Sugiyama, and T Kaneko. A morphological analysis of thalamocortical axon fibers

of rat posterior thalamic nuclei: a single neuron tracing study with viral vectors. *Cereb Cortex*, 22(12):2840–57, Dec 2012.

[22] A N Viaene, I Petrof, and S M Sherman. Properties of the thalamic projection from the posterior medial nucleus to primary and secondary somatosensory cortices in the mouse. *Proc Natl Acad Sci U S A*, 108(44):18156–61, Nov 2011.

[23] B B Theyel, D A Llano, and S M Sherman. The corticothalamocortical circuit drives higher-order cortex in the mouse. *Nat Neurosci*, 13(1):84–8, Jan 2010.

[24] T A Woolsey and H Van der Loos. The structural organization of layer iv in the somatosensory region (si) of mouse cerebral cortex. the description of a cortical field composed of discrete cytoarchitectonic units. *Brain Res*, 17(2):205–42, Jan 1970.

[25] M A Wilson, M V Johnston, G W Goldstein, and M E Blue. Neonatal lead exposure impairs development of rodent barrel field cortex. *Proc Natl Acad Sci U S A*, 97(10):5540–5, May 2000.

[26] R J Douglas and K A C Martin. Neuronal circuits of the neocortex. *Annu Rev Neurosci*, 27:419–51, 2004.

[27] J C Wester and D Contreras. Columnar interactions determine horizontal propagation of recurrent network activity in neocortex. *J Neurosci*, 32(16):5454–71, Apr 2012.

[28] K Fox. The barrel cortex. *Cambridge University Press*, 2008.

[29] M Abeles. Corticonics. neural circuits of the cerebral cortex. *Cambridge University Press*, 1991.

[30] L J Cauller, B Clancy, and B W Connors. Backward cortical projections to primary somatosensory cortex in rats extend long horizontal axons in layer i. *J Comp Neurol*, 390(2):297–310, Jan 1998.

[31] D Feldmeyer, J Lübke, and B Sakmann. Efficacy and connectivity of intracolumnar pairs of layer 2/3 pyramidal cells in the barrel cortex of juvenile rats. *J Physiol*, 575(Pt 2):583–602, Sep 2006.

[32] K L Bernardo, J S McCasland, and T A Woolsey. Local axonal trajectories in mouse barrel cortex. *Exp Brain Res*, 82(2):247–53, 1990.

[33] A M Hattox and S B Nelson. Layer v neurons in mouse cortex projecting to different targets have distinct physiological properties. *J Neurophysiol*, 98(6):3330–40, Dec 2007.

[34] D Schubert, R Kötter, and J F Staiger. Mapping functional connectivity in barrel-related columns reveals layer- and cell type-specific microcircuits. *Brain Struct Funct*, 212(2):107–19, Sep 2007.

[35] Petilla Interneuron Nomenclature Group, G A Ascoli, L Alonso-Nanclares, S A Anderson, G Barrionuevo, R Benavides-Piccione, A Burkhalter, G Buzsáki, B Cauli, J Defelipe, A Fairén, D Feldmeyer, G Fishell, Y Fregnac, T F Freund, D Gardner, E P Gardner, J H Goldberg, M Helmstaedter, S Hestrin, F Karube, Z F Kisvárday, B Lambolez, D A Lewis, O Marin, H Markram, A Muñoz, A Packer, C C H Petersen, K S Rockland, J Rossier, B Rudy, P Somogyi, J F Staiger, G Tamas, A M Thomson, M Toledo-Rodriguez, Y Wang, D C West, and R Yuste. Petilla terminology: nomenclature of features of gabaergic interneurons of the cerebral cortex. *Nat Rev Neurosci*, 9(7):557–68, Jul 2008.

[36] H Markram, M Toledo-Rodriguez, Y Wang, A Gupta, G Silberberg, and C Wu. Interneurons of the neocortical inhibitory system. *Nat Rev Neurosci*, 5(10):793–807, Oct 2004.

[37] L Gabernet, S P Jadhav, D E Feldman, M Carandini, and M Scanziani. Somatosensory integration controlled by dynamic thalamocortical feed-forward inhibition. *Neuron*, 48(2):315–27, Oct 2005.

[38] S J Cruikshank, T J Lewis, and B W Connors. Synaptic basis for intense thalamocortical activation of feedforward inhibitory cells in neocortex. *Nat Neurosci*, 10(4):462–8, Apr 2007.

[39] Y Kawaguchi and Y Kubota. Gabaergic cell subtypes and their synaptic connections in rat frontal cortex. *Cereb Cortex*, 7(6):476–86, Sep 1997.

[40] A Zeisel, A B Muñoz-Manchado, S Codeluppi, P Lönnerberg, G La Manno, A Juréus, S Marques, H Munguba, L He, C Betsholtz, C Rolny, G Castelo-Branco, J Hjerling-Leffler,

and S Linnarsson. Brain structure. cell types in the mouse cortex and hippocampus revealed by single-cell rna-seq. *Science*, 347(6226):1138–42, Mar 2015.

[41] S Oláh, M Füle, G Komlósi, C Varga, R Báldi, P Barzó, and G Tamás. Regulation of cortical microcircuits by unitary gaba-mediated volume transmission. *Nature*, 461(7268):1278–81, Oct 2009.

[42] D M Gelman and O Marín. Generation of interneuron diversity in the mouse cerebral cortex. *Eur J Neurosci*, 31(12):2136–41, Jun 2010.

[43] Y Kubota. Untangling gabaergic wiring in the cortical microcircuit. *Curr Opin Neurobiol*, 26:7–14, Jun 2014.

[44] B Rudy, G Fishell, S Lee, and J Hjerling-Leffler. Three groups of interneurons account for nearly 100% of neocortical gabaergic neurons. *Dev Neurobiol*, 71(1):45–61, Jan 2011.

[45] X Xu, K D Roby, and E M Callaway. Immunochemical characterization of inhibitory mouse cortical neurons: three chemically distinct classes of inhibitory cells. *J Comp Neurol*, 518(3):389–404, Feb 2010.

[46] B V Atallah, W Bruns, M Carandini, and M Scanziani. Parvalbumin-expressing interneurons linearly transform cortical responses to visual stimuli. *Neuron*, 73(1):159–70, Jan 2012.

[47] N R Wilson, C A Runyan, F L Wang, and M Sur. Division and subtraction by distinct cortical inhibitory networks in vivo. *Nature*, 488(7411):343–8, Aug 2012.

[48] J Courtin, F Chaudun, R R Rozeske, N Karalis, C Gonzalez-Campo, H Wurtz, A Abdi, J Baufreton, T C M Bienvenu, and C Herry. Prefrontal parvalbumin interneurons shape neuronal activity to drive fear expression. *Nature*, 505(7481):92–6, Jan 2014.

[49] A E Villa, I V Tetko, B Hyland, and A Najem. Spatiotemporal activity patterns of rat cortical neurons predict responses in a conditioned task. *Proc Natl Acad Sci U S A*, 96(3):1106–11, Feb 1999.

[50] A Agmon and B W Connors. Correlation between intrinsic firing patterns and thalamocortical synaptic responses of neurons in mouse barrel cortex. *J Neurosci*, 12(1):319–29, Jan 1992.

[51] D A McCormick. Neurotransmitter actions in the thalamus and cerebral cortex and their role in neuromodulation of thalamocortical activity. *Prog Neurobiol*, 39(4):337–88, Oct 1992.

[52] D A McCormick, B W Connors, J W Lighthall, and D A Prince. Comparative electrophysiology of pyramidal and sparsely spiny stellate neurons of the neocortex. *J Neurophysiol*, 54(4):782–806, Oct 1985.

[53] D V Buonomano and M M Merzenich. Cortical plasticity: from synapses to maps. *Annu Rev Neurosci*, 21:149–86, 1998.

[54] K Lebida and J W Mozrzymas. Spike timing-dependent plasticity in the mouse barrel cortex is strongly modulated by sensory learning and depends on activity of matrix metalloproteinase 9. *Mol Neurobiol*, Oct 2016.

[55] D E Feldman. Synaptic mechanisms for plasticity in neocortex. *Annu Rev Neurosci*, 32:33–55, 2009.

[56] M E Diamond, M Armstrong-James, and F F Ebner. Experience-dependent plasticity in adult rat barrel cortex. *Proc Natl Acad Sci U S A*, 90(5):2082–6, Mar 1993.

[57] S Glazewski and K Fox. Time course of experience-dependent synaptic potentiation and depression in barrel cortex of adolescent rats. *J Neurophysiol*, 75(4):1714–29, Apr 1996.

[58] V Jacob, A Mitani, T Toyoizumi, and K Fox. Whisker row deprivation affects the flow of sensory information through rat barrel cortex. *J Neurophysiol*, 117(1):4–17, Jan 2017.

[59] Y Han, M Huang, M Sun, S Duan, and Y Yu. Long-term synaptic plasticity in rat barrel cortex. *Cereb Cortex*, 25(9):2741–51, Sep 2015.

[60] G W Knott, C Quairiaux, C Genoud, and E Welker. Formation of dendritic spines with gabaergic synapses induced by whisker stimulation in adult mice. *Neuron*, 34(2):265–73, Apr 2002.

[61] D Hebb. The organization of behavior. a neuropsychological theory. *New York: John Wiley and Sons*, 1949.

[62] T V Bliss and T Lomo. Long-lasting potentiation of synaptic transmission in the dentate area of the anaesthetized rabbit following stimulation of the perforant path. *J Physiol*, 232(2):331–56, Jul 1973.

[63] R M Mulkey and R C Malenka. Mechanisms underlying induction of homosynaptic long-term depression in area ca1 of the hippocampus. *Neuron*, 9(5):967–75, Nov 1992.

[64] R Dingledine, K Borges, D Bowie, and S F Traynelis. The glutamate receptor ion channels. *Pharmacol Rev*, 51(1):7–61, Mar 1999.

[65] V M Storozhuk, V I Khorevin, N N Razumna, I V Tetko, and A P Villa. [activation of glutamate ionotropic connections of sensorimotor cortex neurons during conditioning]. *Zh Vyssh Nerv Deiat Im I P Pavlova*, 52(3):292–301, 2002.

[66] P J Conn and J P Pin. Pharmacology and functions of metabotropic glutamate receptors. *Annu Rev Pharmacol Toxicol*, 37:205–37, 1997.

[67] R Malinow and R C Malenka. Ampa receptor trafficking and synaptic plasticity. *Annu Rev Neurosci*, 25:103–26, 2002.

[68] D V Buonomano. Distinct functional types of associative long-term potentiation in neocortical and hippocampal pyramidal neurons. *J Neurosci*, 19(16):6748–54, Aug 1999.

[69] N Hardingham, S Glazewski, P Pakhotin, K Mizuno, P F Chapman, K P Giese, and K Fox. Neocortical long-term potentiation and experience-dependent synaptic plasticity require alpha-calcium/calmodulin-dependent protein kinase ii autophosphorylation. *J Neurosci*, 23(11):4428–36, Jun 2003.

[70] R C Malenka and M F Bear. Ltp and ltd: an embarrassment of riches. *Neuron*, 44(1):5–21, Sep 2004.

[71] C D Meliza and Y Dan. Receptive-field modification in rat visual cortex induced by paired visual stimulation and single-cell spiking. *Neuron*, 49(2):183–9, Jan 2006.

[72] R C Froemke, M Poo, and Y Dan. Spike-timing-dependent synaptic plasticity depends on dendritic location. *Nature*, 434(7030):221–5, Mar 2005.

[73] N Caporale and Y Dan. Spike timing-dependent plasticity: a hebbian learning rule. *Annu Rev Neurosci*, 31:25–46, 2008.

[74] B J Everitt and T W Robbins. Central cholinergic systems and cognition. *Annu Rev Psychol*, 48:649–84, 1997.

[75] M Sarter and J P Bruno. Cortical cholinergic inputs mediating arousal, attentional processing and dreaming: differential afferent regulation of the basal forebrain by telencephalic and brainstem afferents. *Neuroscience*, 95(4):933–52, 2000.

[76] L Golmayo, A Nuñez, and L Zaborszky. Electrophysiological evidence for the existence of a posterior cortical-prefrontal-basal forebrain circuitry in modulating sensory responses in visual and somatosensory rat cortical areas. *Neuroscience*, 119(2):597–609, 2003.

[77] M Sarter and J P Bruno. Cognitive functions of cortical acetylcholine: toward a unifying hypothesis. *Brain Res Brain Res Rev*, 23(1-2):28–46, Feb 1997.

[78] R B Poorthuis and H D Mansvelder. Nicotinic acetylcholine receptors controlling attention: behavior, circuits and sensitivity to disruption by nicotine. *Biochem Pharmacol*, 86(8):1089–98, Oct 2013.

[79] G Zolles, E Wagner, A Lampert, and B Sutor. Functional expression of nicotinic acetylcholine receptors in rat neocortical layer 5 pyramidal cells. *Cereb Cortex*, 19(5):1079–91, May 2009.

[80] Z Xiang, J R Huguenard, and D A Prince. Cholinergic switching within neocortical inhibitory networks. *Science*, 281(5379):985–8, Aug 1998.

[81] S Gigout, G A Jones, S Wierschke, C H Davies, J M Watson, and R A Deisz. Distinct muscarinic acetylcholine receptor subtypes mediate pre- and postsynaptic effects in rat neocortex. *BMC Neurosci*, 13:42, Apr 2012.

[82] A Nuñez, S Domínguez, W Buño, and D Fernández de Sevilla. Cholinergic-mediated response enhancement in barrel cortex layer v pyramidal neurons. *J Neurophysiol*, 108(6):1656–68, Sep 2012.

[83] F Kimura and R W Baughman. Distinct muscarinic receptor subtypes suppress excitatory and inhibitory synaptic responses in cortical neurons. *J Neurophysiol*, 77(2):709–16, Feb 1997.

[84] E Oldford and M A Castro-Alamancos. Input-specific effects of acetylcholine on sensory and intracortical evoked responses in the "barrel cortex" in vivo. *Neuroscience*, 117(3):769–78, 2003.

[85] H H Jasper and J Tessier. Acetylcholine liberation from cerebral cortex during paradoxical (rem) sleep. *Science*, 172(3983):601–2, May 1971.

[86] M E Hasselmo and L M Giocomo. Cholinergic modulation of cortical function. *J Mol Neurosci*, 30(1-2):133–5, 2006.

[87] M A Castro-Alamancos. Cortical up and activated states: implications for sensory information processing. *Neuroscientist*, 15(6):625–34, Dec 2009.

[88] M M Mesulam, E J Mufson, B H Wainer, and A I Levey. Central cholinergic pathways in the rat: an overview based on an alternative nomenclature (ch1-ch6). *Neuroscience*, 10(4):1185–201, Dec 1983.

[89] L Zaborszky, A Csordas, K Mosca, J Kim, M R Gielow, C Vadasz, and Z Nadasdy. Neurons in the basal forebrain project to the cortex in a complex topographic organization that reflects corticocortical connectivity patterns: an experimental study based on retrograde tracing and 3d reconstruction. *Cereb Cortex*, 25(1):118–37, Jan 2015.

[90] Koji Hara and R Adron Harris. The anesthetic mechanism of urethane: the effects on neurotransmitter-gated ion channels. *Anesth Analg*, 94(2):313–8, table of contents, Feb 2002.

[91] R Bertorelli, G Forloni, and S Consolo. Modulation of cortical in vivo acetylcholine release by the basal nuclear complex: role of the pontomesencephalic tegmental area. *Brain Res*, 563(1-2):353–6, Nov 1991.

[92] D D Rasmusson, K Clow, and J C Szerb. Frequency-dependent increase in cortical acetylcholine release evoked by stimulation of the nucleus basalis magnocellularis in the rat. *Brain Res*, 594(1):150–4, Oct 1992.

[93] M E Jiménez-Capdeville, R W Dykes, and A A Myasnikov. Differential control of cortical activity by the basal forebrain in rats: a role for both cholinergic and inhibitory influences. *J Comp Neurol*, 381(1):53–67, Apr 1997.

[94] Irina A Erchova, Mikhail A Lebedev, and Mathew E Diamond. Somatosensory cortical neuronal population activity across states of anaesthesia. *Eur J Neurosci*, 15(4):744–52, Feb 2002.

[95] S Glazewski. Experience-dependent changes in vibrissae evoked responses in the rodent barrel cortex. *Acta Neurobiol Exp (Wars)*, 58(4):309–20, 1998.

[96] D E Feldman and M Brecht. Map plasticity in somatosensory cortex. *Science*, 310(5749):810–5, Nov 2005.

[97] C I Moore. Frequency-dependent processing in the vibrissa sensory system. *J Neurophysiol*, 91(6):2390–9, Jun 2004.

[98] J Crossland and P Slater. The effect of some drugs on the "free" and "bound" acetylcholine content of rat brain. *Br J Pharmacol Chemother*, 33(1):42–7, May 1968.

[99] B Karlén, G Lundgren, J Lundin, and B Holmstedt. Effect of physostigmine and atropine on acetylcholine turnover in mouse brain. *Naunyn Schmiedebergs Arch Pharmacol*, 308(1):61–5, Jul 1979.

[100] A I Levey, C A Kitt, W F Simonds, D L Price, and M R Brann. Identification and localization of muscarinic acetylcholine receptor proteins in brain with subtype-specific antibodies. *J Neurosci*, 11(10):3218–26, Oct 1991.

[101] M Yamasaki, M Matsui, and M Watanabe. Preferential localization of muscarinic m1 receptor on dendritic shaft and spine of cortical pyramidal cells and its anatomical evidence for volume transmission. *J Neurosci*, 30(12):4408–18, Mar 2010.

A Annex

A.1. Article 1 (published)

FREQUENCY-SPECIFIC RESPONSE FACILITATION OF SUPRA AND INFRAGRANULAR BARREL CORTICAL NEURONS DEPENDS ON NMDA RECEPTOR ACTIVATION IN RATS

Neuroscience 281 (2014) 178–194

FREQUENCY-SPECIFIC RESPONSE FACILITATION OF SUPRA AND INFRAGRANULAR BARREL CORTICAL NEURONS DEPENDS ON NMDA RECEPTOR ACTIVATION IN RATS

N. BARROS-ZULAICA, C. CASTEJON AND A. NUÑEZ*

Departamento de Anatomía, Histología y Neurociencia, Facultad de Medicina, Universidad Autónoma de Madrid, 28029 Madrid, Spain

Abstract—Sensory experience has a profound effect on neocortical neurons. Passive stimulation of whiskers or sensory deprivation from whiskers can induce long-lasting changes in neuronal responses or modify the receptive field in adult animals. We recorded barrel cortical neurons in urethane-anesthetized rats in layers 2/3 or 5/6 to determine if repetitive stimulation would induce long-lasting response facilitation. Air-puff stimulation (20-ms duration, 40 pulses at 0.5–8 Hz) was applied to a single whisker. This repetitive stimulation increased tactile responses in layers 2/3 and 5/6 for 60 min. Moreover, the functional coupling (coherence) between the sensory stimulus and the neural response also increased after the repetitive stimulation in neurons showing response facilitation. The long-lasting response facilitation was due to activation of N-methyl-D-aspartate (NMDA) receptors because it was reduced by APV ((2*R*)-amino-5-phosphonovaleric acid, (2*R*)-amino-5-phosphonopentanoate) and MK801 application. Inactivation of layer 2/3 also blocked response facilitation in layer 5/6, suggesting that layer 2/3 may be fundamental in this synaptic plasticity processes. Moreover, i.p. injection of eserine augmented the number of layer 2/3 neurons expressing long-lasting response facilitation; this effect was blocked by atropine, suggesting that muscarinic receptor activation favors the induction of the response facilitation. Our data indicate that physiologically repetitive stimulation of a single whisker at the frequency at which rats move their whiskers during exploration of the environment induces long-lasting response facilitation improving sensory processing.
© 2014 IBRO. Published by Elsevier Ltd. All rights reserved.

Key words: wavelet coherence, LTP, sensory plasticity, somatosensory system, thalamocortical network.

INTRODUCTION

The somatosensory barrel cortex is composed of local circuits heavily interconnected by vertical and horizontal projections (Feldmeyer, 2012; Feldmeyer et al., 2013). Sensory information from the whiskers passes via the brain stem and thalamus to layer 4 neurons in the barrel cortex. Sensory responses are relayed to layer 2/3 and then to layer 5 and layer 6, concomitant with feedback from layer 5 to layer 2/3 and layer 6 to layer 4. This vertical organization is linked horizontally by prominent projections within layer 2/3 and layer 5 (Douglas and Martin, 2004; Wester and Contreras, 2012). Distinct synaptic and intrinsic properties of these neurons may be involved in different sensory plasticity responses observed in the barrel cortex. Recently, it has been demonstrated that ''N-methyl-D-aspartate (NMDA) spikes'' and L-type voltage-gated Ca^{2+} channel activation increase the excitability of layer 5 neurons, thereby possibly mediating neuronal plasticity (Nuñez et al., 2012).

The barrel cortex of rodents is a remarkable structure that is capable of fine tactile discrimination based on whisker movements across objects or surfaces in repeated rhythmic sweeps at frequencies between 4 and 12 Hz (Carvell and Simons, 1990; Fanselow and Nicolelis, 1999), see for review (Moore, 2004). Sensory experience induces neuronal plasticity and has profound effects on synaptic responses in the neocortex. Long-term potentiation (LTP) of cortical synaptic potentials in response to repetitive stimulation is involved in sensory experience effects. For example, tetanic stimuli applied in layer 4 can induce LTP lasting several hours in layer 2/3 neurons (Glazewski et al., 1998). Repetitive whisker stimulation also induces a long-lasting increase in the amplitude of somatosensory-evoked potentials in layers 2/3 and 4 of the barrel cortex of neonatal rats or mice (Borgdorff et al., 2007; An et al., 2012), suggesting that it may participate in the activity-dependent wiring of the cortex during development. Moreover, multiwhisker stimulation at 2 or 8 Hz induces LTP in layers 2/3 and 4 of barrel cortical neurons of mature mice (Megevand et al., 2009), suggesting that sensory plasticity may contribute to information processing in adult animals.

Experiments on the possibility of inducing LTP in sensorially deprived barrel cortex provide further evidence on the role of LTP in cortical experience-dependent plasticity. In young adult rats with intact whiskers the incidence of LTP is relatively low,

*Corresponding author. Address: Departamento de Anatomía, Histología y Neurociencia, Facultad de Medicina, Universidad Autónoma de Madrid, c/ Arzobispo Morcillo 4, 28029 Madrid, Spain. Tel: +34-91-207-3755; fax: +34-91-397-5338.
E-mail address: angel.nunez@uam.es (A. Nuñez).
Abbreviations: Ach, acetylcholine; APV, (2*R*)-amino-5-phosphonovaleric acid, (2*R*)-amino-5-phosphonopentanoate; LTP, long-term potentiation; MK801, dizocilpine; NMDA, N-methyl-D-aspartate receptor; PSTH, peristimulus time histogram; RF, receptive field; SEM, standard errors of the mean; VPM, ventral posteromedial thalamic.

http://dx.doi.org/10.1016/j.neuroscience.2014.09.057
0306-4522/© 2014 IBRO. Published by Elsevier Ltd. All rights reserved.

approximately 35% of neurons. However, this values rises to 70% following whisker deprivation (Hardingham et al., 2007), indicating also that LTP may contribute to sensory plasticity in adults.

In addition, several studies have shown that acetylcholine (Ach) regulates thalamocortical network synaptic plasticity in many important brain functions, such as arousal, attention, learning and memory (e.g. Celesia and Jasper, 1966; Sarter and Bruno, 2000; Oldford and Castro-Alamancos, 2003; Sarter et al., 2003; Hasselmo and Giocomo, 2006). Moreover, it has been demonstrated that Ach enhances synaptic plasticity in the hippocampus (e.g. Doralp and Leung, 2008; Fernandez de Sevilla et al., 2008; Navarrete et al., 2012) and neocortex (e.g. Metherate and Ashe, 1993; Kuo et al., 2009; Bueno-Junior et al., 2012; Nuñez et al., 2012) and may modulate tactile response facilitation. Here, we show that a brief period of repetitive whisker stimulation in anesthetized adult rats induces a frequency-specific long-lasting facilitation of tactile responses in layer 2/3 and layer 5/6 neurons. For this purpose we used single-unit recordings of rat barrel cortical neurons and analyzed tactile responses to whisker stimulation consisting of 20-ms air puffs at 1–8 Hz. Also, unit recordings were performed in the ventral posteromedial thalamic (VPM) nucleus to demonstrate that response facilitation was originated in the barrel cortex.

EXPERIMENTAL PROCEDURES

Animals

All animal procedures were performed in accordance with the Ethics Committee of the Universidad Autonoma de Madrid, and with Council Directive 86/609/EEC of the European Community. Rats were group housed with a 12-h light/dark cycle and had free access to food and water. Every effort was made to minimize the number, and suffering, of the animals used.

Electrophysiological recordings

Experiments were performed on 122 urethane-anesthetized (1.6 g/kg i.p.) adult Sprague–Dawley rats weighing 200–250 g. Animals were placed in a Kopf stereotaxic device in which surgical procedures and recordings were performed. The body temperature was maintained at 37 °C; the end-tidal CO_2 and heart rate were monitorized. Local anesthetic (lidocaine 1%) was applied to all skin incisions and supplemental doses of anesthetic were given to maintain areflexia. An incision was made exposing the skull and a small hole was drilled in the bone over the barrel cortex. Single-unit recordings in the barrel cortex (*A* 1–3 mm, *L* 5–7 mm from bregma) were made 200–1500 μm below the surface with tungsten microelectrodes (2–5 MΩ) placed in both hemispheres. Units were recorded at different levels of the same track to ensure that we were moving along a single cortical column due to its response to specific whisker stimulation. After that, the stimulation train protocol was applied to that whisker (Fig. 1A). This recording protocol was repeated in different columns of the barrel cortex, applying the stimulation protocol to different whiskers. Also, unit recordings were performed in the VPM nucleus (*A* 3.2–3.8 mm, *L* 2.5 mm from bregma, *D* 6.5–7 mm from the surface) with tungsten microelectrodes. Unit firing was filtered (0.3–3 kHz), amplified via an AC preamplifier (DAM80; World Precision Instruments, Sarasota, USA), and fed into a personal computer (sample rate 10 kHz) with the temporal references of the stimuli for off-line analysis with Spike 2 software (Cambridge Electronic Design, Cambridge, UK). In some experiments (18 rats) the field potential was recorded through tungsten macroelectrodes (<1 MΩ). The activity was filtered between 0.3 and 100 Hz, amplified and sampled at 500 Hz.

Sensory stimulation

Whisker deflections were performed by brief air puffs using a pneumatic pressure pump (Picospritzer) that delivers an air pulse through a 1-mm-inner diameter polyethylene tube (20-ms duration). To avoid complex responses due to deflections of multiple whiskers, all whiskers were trimmed to 5 mm in length, so that reproducible responses were evoked from a single, targeted, whisker. The pressure was set at 1–2 kg/cm^2, resulting in whisker deflections of ≈15°. When a single neuron was isolated, its cutaneous receptive field (RF) was carefully mapped with a small hand-held brush. RFs were monitored by listening to the audio conversion of the amplified activity signal. Thus, we could identify the whiskers belonging to the recorded neuron's RF. In this study two air tubes were used: one to stimulate the whisker that gave the highest spike response, called the principal whisker; the other to stimulate another whisker that gave a smaller response, called the peripheral whisker.

Pharmacological study

Drugs were injected (0.1 or 1 μl) through a cannula connected to a Hamilton syringe and targeted to layer 2/3 or 5/6. The complete experimental protocol began 5 min after the injection (see below; Fig. 1A).

The following drugs were used: (2*R*)-amino-5-phosphonovaleric acid, (2*R*)-amino-5-phosphono-pentanoate (APV; 50 μM), which is a selective NMDA receptor antagonist, and Muscimol (5-(aminomethyl)-isoxazol-3-ol) (8 mM), which is a selective agonist for $GABA_A$ receptors, were locally applied. Dizocilpine, also known as MK801 (0.5 mg/kg), which is a non-competitive antagonist of the NMDA receptor, eserine also known as physostigmine (0.1 mg/kg) and is an acetylcholinesterase inhibitor, and atropine sulfate (5 mg/kg), which is an antagonist of muscarinic receptors, were intraperitoneally (i.p.) injected.

Experimental protocol

The experimental protocol consisted of 30 pulses delivered to the principal or peripheral whiskers at 0.5 Hz (control period) followed by a train of 40 pulses at 0.5–8 Hz (stimulation train) delivered only to the

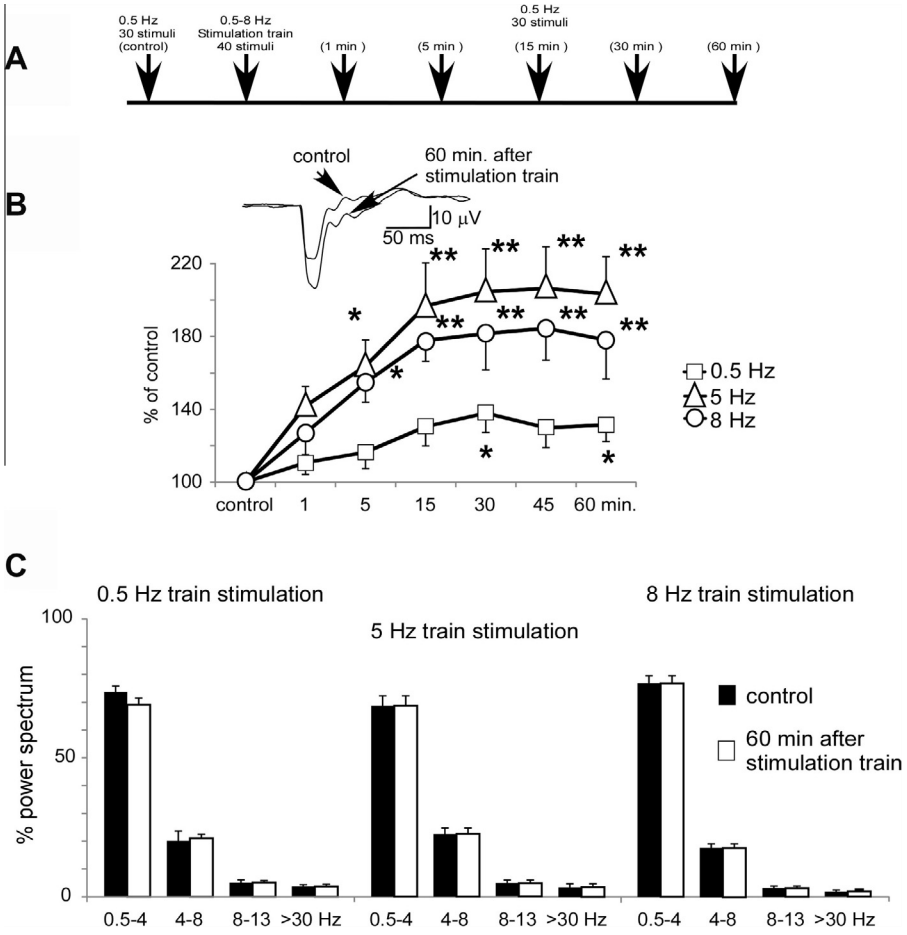

Fig. 1. Field potential analysis indicated that tactile response facilitation lasted at least 60 min. (A) Experimental protocol of whisker stimulation. The effect of a stimulation train (40 stimuli at 0.5–8 Hz) was studied on tactile responses to 0.5 Hz stimuli delivered at the whisker. (B) Plot of the evoked potential amplitude elicited by whisker stimulation; the control response is considered 100%. A stimulation train at 0.5 Hz ($n = 8$) induced a slight amplitude increase in the evoked response. This response increase was larger when the frequency of the stimulation train was 5 ($n = 13$) or 8 Hz ($n = 10$). In all cases the response facilitation stabilized after 30 min. Inset shows an example in control conditions and 60 min after a stimulation train at 5 Hz. (C) Plot of the percentage of the frequency bands in the cortical field potential recorded before (control) or 60 min after stimulus train application at 0.5, 5 or 8 Hz. The proportion of delta waves and faster activities was equal in all cases, indicating that the level of cortical activation remained equal during the experiment. In this and in the following figures: $^{*}P < 0.05$; $^{**}P < 0.01$. Asterisks in B indicate statistical differences obtained by the Wilcoxon-matched pairs post hoc analysis with respect to control values of each frequency.

principal whisker. Thirty air pulses at 0.5 Hz were delivered again to both whisker types at specific intervals of 1, 5, 15, 30 or 60 min after the stimulation train (see Fig. 1A, upper trace).

Experiment 1: This experiment consisted of application of the above experimental protocol with different stimulation train frequencies (0.5–8 Hz) to study the frequency-specific response facilitation.

Experiment 2: APV (cortical) or MK-801 (i.p.) was injected before beginning the experimental protocol application to study the mechanisms of response facilitation.

Experiment 3: Muscimol was applied locally in layer 2/3 before beginning the experimental protocol application to study the origin of the response facilitation.

Experiment 4: Simultaneous unit recordings in the barrel cortex and VPM thalamic nuclei were performed during the application of the experimental protocol to establish the cortical origin of the frequency-specific response facilitation. Muscimol was also injected into the barrel cortex to study the thalamic or cortical contribution to response facilitation.

Experiment 5: Eserine was i.p. injected to study the cholinergic modulation of the response facilitation. Atropine (i.p.) was injected 10 min before eserine injection in another set of experiments designed to reveal the participation of muscarinic receptors.

Data analysis

The mean tactile response was measured from the peristimulus time histogram (PSTH; 1-ms binwidth; 30 stimuli) as the number of spikes evoked in the 0–50-ms time window after the stimulus onset divided by the number of stimuli. Neuronal responses larger/smaller than two times the mean tactile response plus/minus two standard errors of the mean (SEM) were considered statistically significant to detect changes in tactile responses. We also measured response latencies as

the time elapsed between stimulus onset and the highest peak in the PSTH.

The power spectrum (to detect general changes of cortical excitability) and the evoked potential elicited by tactile stimuli (30 stimuli) were calculated from the field potential. The amplitude of the evoked potential was measured from the baseline to the first negative peak.

To quantify the time–frequency functional association between the stimulus and the neural spike responses we used wavelet coherence (Goelz et al., 2000; Lachaux et al., 2002; Castellanos et al., 2007). Because we were interested in studying the coherence level (or functional coupling) between the stimulus events and neural responses, we focused on the frequency band corresponding to the stimulus frequency (0.5 Hz) and used a 10-ms time bin. Although large coherence amplitude usually indicates the presence of a consistent functional coupling between neuronal responses and the stimulus, it is also possible that it could be due to a random variation in the spike trains. Thus, the statistical significance of the observed coherence should be cross-checked. Consequently, a coherence level of 1 means a perfect synchrony between neurons while 0 means a random time-relationship. To evaluate the significance level for the wavelet coherence we used the surrogate data test with the Monte Carlo simulation to establish a 95% confidence interval.

Statistical analysis was performed using GraphPad Prism 5 software (San Diego, CA, USA). We used Wilcoxon-matched pairs test to compare data from neurons in different conditions. In order to evaluate drug effects we used Chi-square test to compare response differences from neurons recorded in control conditions (application of saline solution) with respect to neurons recorded after drug application. For multiple comparisons we used Kruskal–Wallis analysis of variance plus Wilcoxon-matched pairs test as post hoc test. The threshold level of significance was set at $P < 0.05$. Data are presented as mean ± SEM.

Histological analysis

Upon completion of the experiments, animals were deeply anesthetized with sodium-pentobarbital (50 mg/kg) and then perfused transcardially with saline followed by formalin (4% in saline). The brain was removed, stored in 20% sucrose saline and cut on a freezing microtome. Coronal sections 50 μm thick were stained with the Nissl method to locate the recording track.

RESULTS

Long-lasting tactile response increase by repetitive stimulation

The field potential was recorded in layer 2/3 of the barrel cortex to study the time course of the response variations after application of a stimulation train. The evoked potential amplitude elicited by displacements of one whisker (20-ms duration; 30 stimuli) was measured in 31 cases from 18 animals. A continuous stimulation at 0.5 Hz induced a slight increase of amplitude (Kruskal–Wallis analysis: $P = 0.029$; Table 1). However, Kruskal–Wallis analysis showed that a 5- and 8-Hz stimulation train induced a larger increase of the response during at least 60 min, reaching a stable level 30 min after the stimulus train ($P < 0.0001$ and $P = 0.003$, respectively; Fig. 1B). These stimulation frequencies were selected because they are the frequency used by rodents to explore the environment.

It is possible that a repetitive stimulation of the whisker at high frequencies could induce a general activation process in the cortex that might be responsible for the response facilitation described above. Cortical field potentials showed a dominance of slow delta waves elicited by urethane anesthesia. The power spectrum of the field potential recorded in control condition and 60 min after repetitive stimulation at 0.5, 5 or 8 Hz did not reveal a change in frequency band proportions (Fig. 1C), indicating that the long-lasting response facilitation evoked by a stimulation train was not due to a general change in the cortical excitability.

To study the mechanisms of this long-lasting facilitation evoked by a repetitive stimulation, barrel cortical neurons were recorded in layer 2/3 (200–600 μm) or 5/6 (900–1200 μm) in 48 urethane-anesthetized rats. Neurons were silent or displayed a low firing rate (0.1–2 spikes/s) in spontaneous conditions. All neurons displayed a response to contralateral displacements of one to two whiskers. In control conditions tactile responses had on average 1.7 ± 0.5 spikes/stimulus at 16 ± 0.3-ms latency in layer 2/3 ($n = 197$) or 1.8 ± 0.4 spikes/stimulus at 16 ± 0.5 ms in layer 5/6 ($n = 191$). Linear regression analysis of response latency vs. spikes per stimulus from layer 2/3 and layer 5/6 neurons indicated that both neuronal populations were homogeneous ($R^2 = 0.0069$ and $R^2 = 0.011$, respectively; Fig. 2). The low spontaneous firing rate and the reduced tactile response to the deflection of one-two whiskers provide strong support to the notion that recordings were obtained from pyramidal cells in the barrel cortex, as it was reported previously (Manns et al., 2004; Melzer et al., 2006; de Kock et al., 2007; de Kock and Sakmann, 2008; Chakrabarti and Alloway, 2009; Wright and Fox, 2010).

We have investigated changes in tactile responses (stimuli delivered at 0.5 Hz; control period) following a stimulation train of 40 tactile stimuli at 0.5, 1, 2, 5 or 8 Hz. Note that a stimulation train at 0.5 Hz was similar to the control period and tactile stimulation applied after the stimulation train. Thus, this protocol represents a period of continuous stimulation at 0.5 Hz lasting 30 min, to be compared with the effect of stimulation trains of higher frequencies. Fig. 3 shows tactile responses of layer 2/3 neurons in control conditions and after application of a stimulation train at 0.5 Hz ($n = 30$), 1 Hz ($n = 28$), 2 Hz ($n = 56$), 5 Hz ($n = 57$) or 8 Hz ($n = 26$). The Kruskal–Wallis analysis showed that a long-lasting response facilitation occurred significantly at 5 Hz ($P < 0.0001$) and 8 Hz stimulation frequencies ($P = 0.0007$). The percentage of increment with respect to control values reached 177% and 171% for those stimulation train frequencies, respectively (Fig. 3;

Table 1. Evoked potential amplitude (μV) after the stimulus train

Stimulation train frequency	Control	1 min	5 min	15 min	30 min	45 min	60 min
0.5 Hz	20.1	21.7	23.4	25.6	26.6*	25.1	26.4*
5 Hz	16.5	22	25.3*	28.6**	29.7**	30.0**	29.8**
8 Hz	18.7	24.0	29.7*	33.0**	34.1**	35.2**	33.0**

P indicates the statistical significance respect to control values. $P < 0.05$ (*); $P < 0.01$ (**); Wilcoxon-matched pairs test.

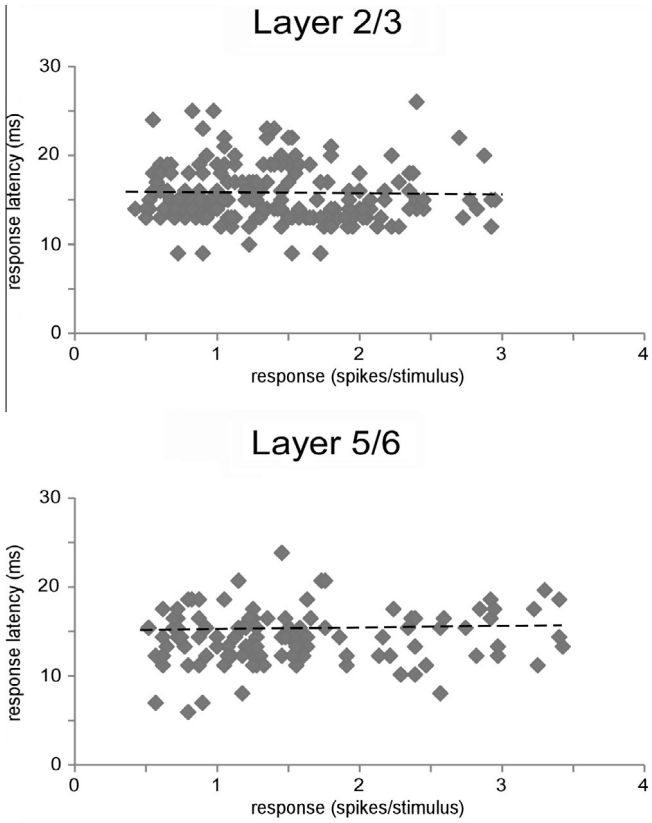

Fig. 2. Response characteristics of layer 2/3 and 5/6 neurons. Data points represent the relationship between response latency and spikes/stimulus and showed a homogeneous neuronal population. Dash line indicates linear regression. R^2 values were calculated collapsing across both latency and spikes (see text).

Percentage). Also, layer 5/6 neurons increased their tactile response after the stimulation train at 0.5 Hz ($n = 27$), 1 Hz ($n = 28$), 2 Hz ($n = 56$), 5 Hz ($n = 40$) or 8 Hz ($n = 40$; Fig. 4), reaching statistical significance at 2, 5 and 8 Hz (Kruskal–Wallis analysis: $P = 0.0054$, $P < 0.0001$ and $P < 0.0001$, respectively). The largest increment occurred after a stimulation train of 5 Hz (188%; Fig. 4, Percentage). Thus, data indicated that a short train of whisker repetitive stimulation induced a long-lasting facilitation of tactile responses depending on the stimulation frequency.

Coherence analysis of cortical neuronal responses

The stimulation time-pattern is important in the generation of synaptic plasticity since a high frequency stimuli train may induce a large postsynaptic response. For this purpose we evaluated wavelet coherence between unit responses and the onset of tactile stimuli for 71 cortical neurons. Fig. 5 illustrates the wavelet coherence of the tactile stimulus events and the evoked neural response. To analyze response coherence we shall measure only the stimulation frequency (0.5 Hz in control and after the stimulation train). Fig. 5A shows an example in a representative layer 2/3 neuron; coherence is indicated in a color scale. During the control stimulation period we observed only a small island of significant coherence in the stimulus frequency band (Fig. 5A, control). This demonstrates the presence of a low stimulus–response association. The stimulus coherence of the neural response became stronger after the repetitive stimulation of the principal whisker at 5 Hz (Fig. 5A, lower plots). Thus, the wavelet coherence confirmed the presence of a strong functional coupling between the neural responses and stimulus events at the stimulus frequency band. Fig. 5B shows the mean wavelet coherence between firing responses and tactile stimuli in layer 2/3 ($n = 45$) and layer 5/6 ($n = 26$) neurons for the control tactile stimulation and after the repetitive stimulation of the principal whisker at 5 Hz. Neurons that

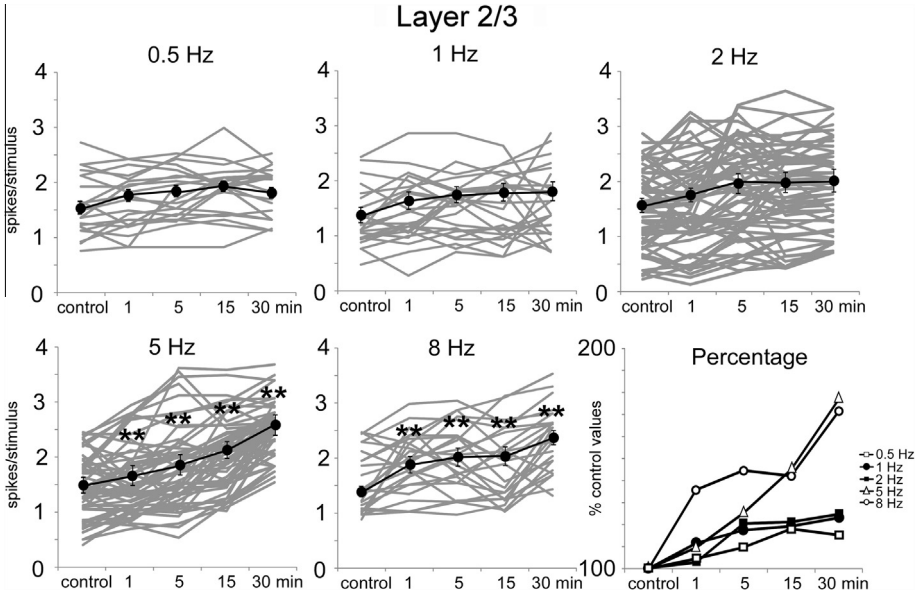

Fig. 3. Tactile response facilitation evoked by repetitive stimulation of a single whisker in layer 2/3. Plots of layer 2/3 neuronal responses in control and after a stimulation train at different frequencies. The stimulus test consisted of whisker stimuli (20-ms duration) delivered at 0.5 Hz before and after a stimulus train of 40 tactile stimuli at 0.5–8 Hz stimulation frequency. Note that long-lasting response facilitation was evoked at higher stimulation frequencies. Percentage plot shows differences with respect to control values. Asterisks indicate statistical differences obtained by the Wilcoxon-matched pairs post hoc analysis with respect to control values of each frequency.

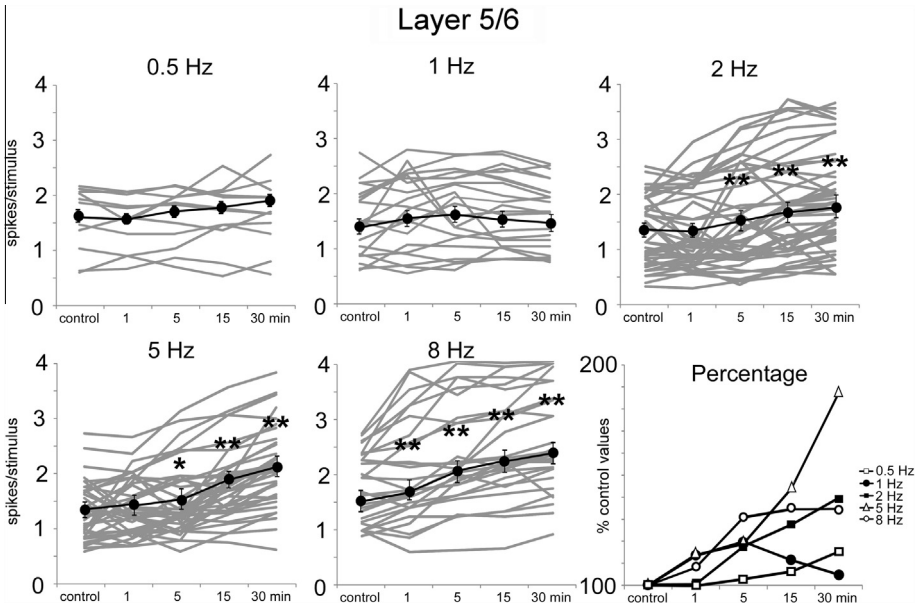

Fig. 4. Tactile response facilitation evoked by repetitive stimulation of a single whisker in layer 5/6. Plots of tactile responses in control and after a stimulation train at different frequencies. Note that long-lasting response facilitation was evoked at higher stimulation frequencies. Percentage plot shows differences with respect to control values. Differences were larger when a 5-Hz stimulation train was applied. Asterisks indicate statistical differences obtained by the Wilcoxon-matched pairs post hoc analysis with respect to control values of each frequency.

showed a facilitation of their response after the 5-Hz stimulation train (tactile responses increased at least two times the SEM of control values) showed that the strength of the functional stimulus–neural response coupling increased by the repetitive stimulation either in layer 2/3 (31 out of 45 neurons; 69%; Kruskal–Wallis analysis: $P < 0.0001$,) or in layer 5/6 (17 out of 26 neurons; 65%; Kruskal–Wallis analysis: $P = 0.0035$; Fig. 5B, upper plot). In contrast, neurons that were not affected or decreased (at least two times the SEM of control values) their stimulus response after 5 Hz repetitive stimulation also showed a decreased wavelet coherence in layer 2/3 (14 out of 45 neurons; 31%; Kruskal–Wallis analysis: $P = 0.0001$) but it was not-significant in layer 5/6 (9 out of 26 neurons; 35%; Kruskal–Wallis analysis: $P = 0.1394$, Fig. 5B, lower

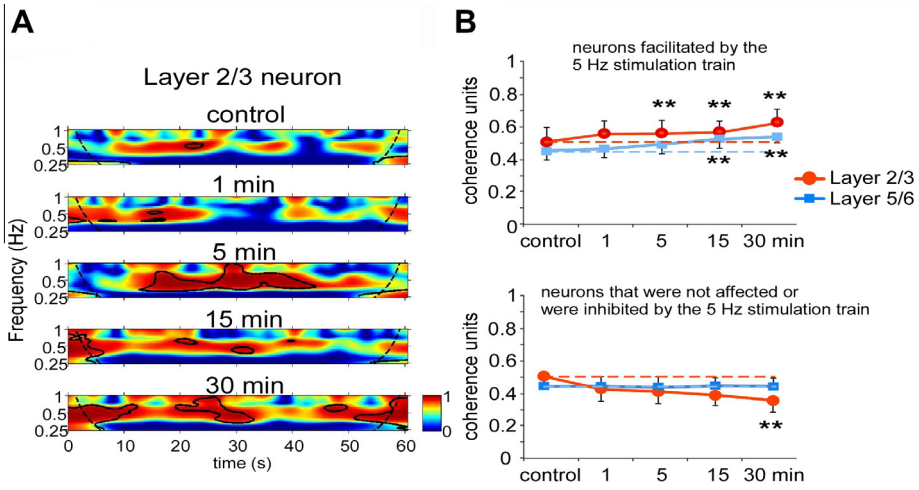

Fig. 5. Repetitive stimulation increased the functional coupling between the neural responses and stimuli. (A) Wavelet coherence of the spike response to tactile stimuli for a control epoch and after a stimulation train of the whisker at 5 Hz (1–30 min). Coherence increased after a stimulation train. Solid black lines delimit islands of statistically significant coherence. (B) Plots of the mean firing coherence between layer 2/3 (n = 8) and layer 5/6 (n = 8) neurons with the stimuli for the control tactile stimulation and after the repetitive stimulation of the principal whisker. Note that neurons showing long-lasting facilitation displayed increased wavelet coherence (upper plot) while neurons that were not affected or decreased their stimulus response after the repetitive stimulation also showed decreased wavelet coherence. Asterisks indicate statistical differences obtained by the Wilcoxon-matched pairs post hoc analysis with respect to control values of each frequency.

plot). Note that the wavelet coherence changes were larger in layer 5/6 neurons than in layer 2/3 neurons.

Mechanisms of long-lasting tactile response increase

The above results indicate that a train of stimulus may induce a long-lasting increment in tactile responses similar to those that occur during cortical LTP. Cortical LTP is mainly due to the activation of NMDA receptors (e.g. Daw et al., 2006; Remy and Spruston, 2007). To establish if the mechanisms behind the tactile response facilitation evoked by repetitive stimulation are similar to cortical LTP, the NMDA receptor blocker APV was applied through a cannula located next to the recording electrode in the same layer (layer 2/3 or layer 5/6) of 10 rats. Application of APV (50 μM; 0.1 μl) into layer 2/3 decreased tactile responses (1.8 ± 0.33 spikes/stimulus vs. 1.4 ± 0.26 spikes/stimulus; Chi-square test; P < 0.001; n = 28; Fig. 6A, left PSTHs). APV injection into layer 5/6 also induced a decrease of tactile responses (1.9 ± 0.39 spikes/stimulus vs. 1.3 ± 0.3 spikes/stimulus; Chi-square test; P < 0.001; n = 19). The spontaneous activity did not change after APV application in cortical neurons (0.8 ± 0.42 spikes/s vs. 0.6 ± 0.31 spikes/s; Chi-square test; P = 0.135; n = 47).

In control conditions (after application of 0.1-μl saline solution) a train of 40 stimuli at 5 Hz induced a long-lasting increase of response in either layer 2/3 neurons (48% of increment; n = 20; Kruskal–Wallis analysis: P < 0.0001) or in layer 5/6 neurons (42% of increment; n = 20; Kruskal–Wallis analysis: P < 0.0001) when measured 15 min after the stimulation train (Fig. 6B, C). The response increase evoked by the 5-Hz stimulation train was reduced if the stimulation train was applied after APV cortical administration (50 μM; 0.1 μl) into layer 2/3 (n = 25; Kruskal–Wallis analysis: P = 0.0058) or layer 5/6 (n = 19; Kruskal–Wallis analysis: P = 0.0019) neurons (Fig. 6B, C). Indeed, in this condition the stimulation train induced response depression in layer 2/3 and reduced the response facilitation in layer 5/6. Thus, data suggest that the activation of NMDA receptors in layer 2/3 plays a fundamental role in the generation of the response facilitation evoked by the 5-Hz stimulation train.

Additionally, we also used the NMDA receptor antagonist MK801 injected intraperitoneally in nine rats to establish if NMDA responses of other neurons located in the somatosensory pathway were involved in cortical facilitation. Intraperitoneal injection of MK801 (0.5 mg/kg) reduced tactile responses in layer 2/3 neurons (0.6 ± 0.15 spikes/stimulus; Chi-square test; P < 0.001; n = 24; Fig. 6A, right PSTHs) or in layer 5/6 neurons (0.3 ± 0.06 spikes/stimulus; Chi-square test; P < 0.001; n = 20) with respect to control conditions. In contrast, MK801 did not modify the spontaneous activity of cortical neurons (from 0.8 ± 0.26 to 1.0 ± 0.18 spikes/s, respectively; Chi-square test; P = 0.256; n = 44). After MK801 administration a 5-Hz stimulus train did not induce a long-lasting increase of tactile responses in layer 2/3 neurons or in layer 5/6 neurons (Kruskal–Wallis analysis: P = 0.079 or P = 0.088, respectively; Fig. 6B, C).

The above results suggest that the NMDA-mediated component of the tactile response is relevant for the tactile response plasticity observed in barrel cortical neurons. A previous study by our laboratory in layer 5 cortical neurons reported that the second component of the tactile response (20–50-ms-response latency) was mainly due to the activation of NMDA receptors while the first response component (0–20 ms) was not affected by NMDA receptor antagonists (Nuñez et al., 2012). The separation into two components was based

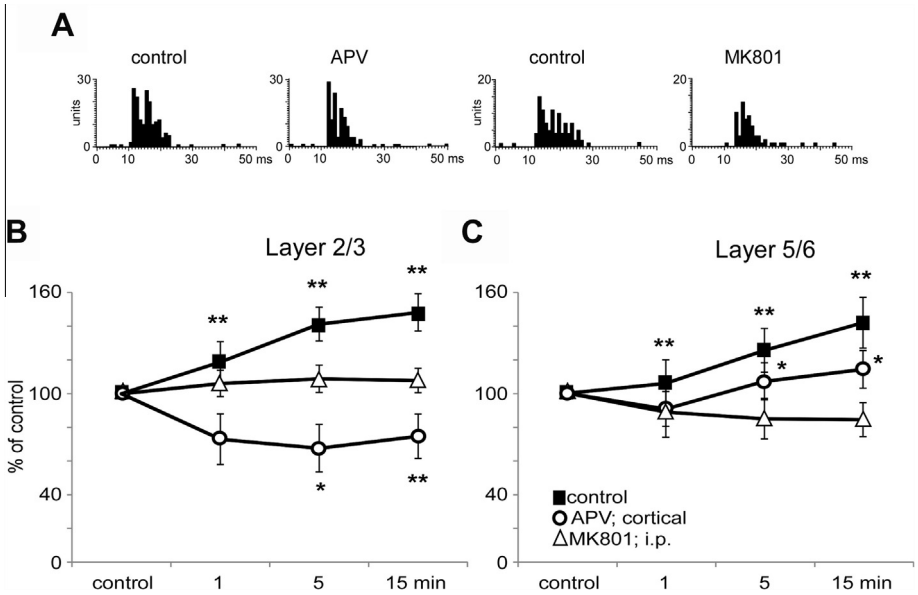

Fig. 6. The long-lasting response facilitation was mediated by activation of NMDA receptors. (A) Representative PSTHs of layer 2/3 neurons in control conditions and after cortical application of APV (50 μM; 0.1 μl; layer 2/3; left histograms) or intraperitoneal injection of MK801 (0.5 mg/kg; right histograms). Note that both NMDA blockers decreased tactile responses. (B) Plot of layer 2/3 neuronal response percentages with respect to control values (100%). In control conditions (0.1-μl saline solution) layer 2/3 neurons were facilitated by a 5-Hz stimulation train (n = 20). APV application (50 μM; 0.1 μl) into layer 2/3 (n = 25) abolished response facilitation. The same effect was evoked by intraperitoneal injection of MK801 (n = 24). (C) Same plot as in B from layer 5/6 neurons. Note that APV application in layer 5/6 (n = 19) decreased the response facilitation with respect to control. However, intraperitoneal MK801 injection abolished the response facilitation (n = 20). Asterisks indicate statistical differences obtained by the Wilcoxon-matched pairs post hoc analysis with respect to control values of each frequency.

on estimated response pattern and because of the marked inhibition, mainly of the second component, by NMDA receptor antagonists (MK-801 or APV), which suggested that both components were elicited by the activation of different glutamatergic receptors. In agreement with these data, application of NMDA antagonists (APV or MK801) reduced the second component in both layer 2/3 and layer 5/6 neurons (see Fig. 6A).

Consequently, we studied the effect of repetitive whisker stimulation on those response components in control and 15 min after the application of the stimulation train at different frequencies (Fig. 7A). As shown in Fig. 7, the first component of the response (0–20 ms) was slightly affected by the increased stimulus train frequency in layer 2/3 (n = 32) and layer 5/6 (n = 32) neurons, reaching statistical significance for 5 Hz stimulation in layer 2/3 (Kruskal–Wallis analysis: P = 0.024). In contrast, the second response component (20–50 ms) was clearly affected by stimulation train frequency, especially in layer 2/3 at 1 and 5 Hz stimulation trains (Kruskal–Wallis analysis: P = 0.03 and P = 0.0028) and in layer 5/6 at 2- and 5-Hz stimulation trains (Kruskal–Wallis analysis: P = 0.0093 and P = 0.012; Fig. 7B, C, respectively). Results indicated that both components of the glutamatergic response (mediated by non-NMDA and NMDA receptors) were affected by the frequency of the stimulation train. However, the second component presents larger changes than the first component, suggesting that the NMDA component is more important in the generation of the long-lasting response facilitation than the non-NMDA component.

Tactile response facilitation was due to the activation of layer 2/3 neurons

The above results suggest that the long-lasting increase of tactile responses in layer 5/6 neurons may be a reflection of feed forward transmission of the response increase in layer 2/3 neurons. To elucidate this point, the $GABA_A$ receptor agonist muscimol was applied to layer 2/3 through a cannula (0.1 μl; 8 mM) in eight rats. Ten minutes later we studied the effect of a 5-Hz stimulus train on layer 5/6 neurons. The spontaneous activity of layer 5/6 neurons was not significantly modified (Chi-square test; P = 0.367; n = 22 cells; Fig. 8A, left histogram). Nevertheless, the evoked spikes in response to whisker stimulation were reduced by muscimol in layer 5/6 (Chi-square test; P = 0.0015; n = 22 cells; Fig. 8A, right histogram), suggesting that the feed forward response transmission from layer 2/3 to layer 5/6 was reduced. As it is stated in the Introduction, sensory responses are relayed to layer 2/3 and then to layer 5 and layer 6; although direct synaptic inputs from VPM also reach layers 5B and 6A (Feldmeyer, 2012). Application of a 5-Hz stimulation train induced a response depression after inhibition of layer 2/3 activity by muscimol (0.1 μl; 8 mM; Kruskal–Wallis analysis: P < 0.0001) while in control conditions (0.1-μl saline solution) the stimulation evoked a response facilitation of tactile responses in layer 5/6 (Kruskal–Wallis analysis: P < 0.0001; Fig. 8B). Thus, results strongly suggest that the long-lasting facilitation evoked by repetitive stimulation may be generated in layer 2/3 and transmitted to layer 5/6.

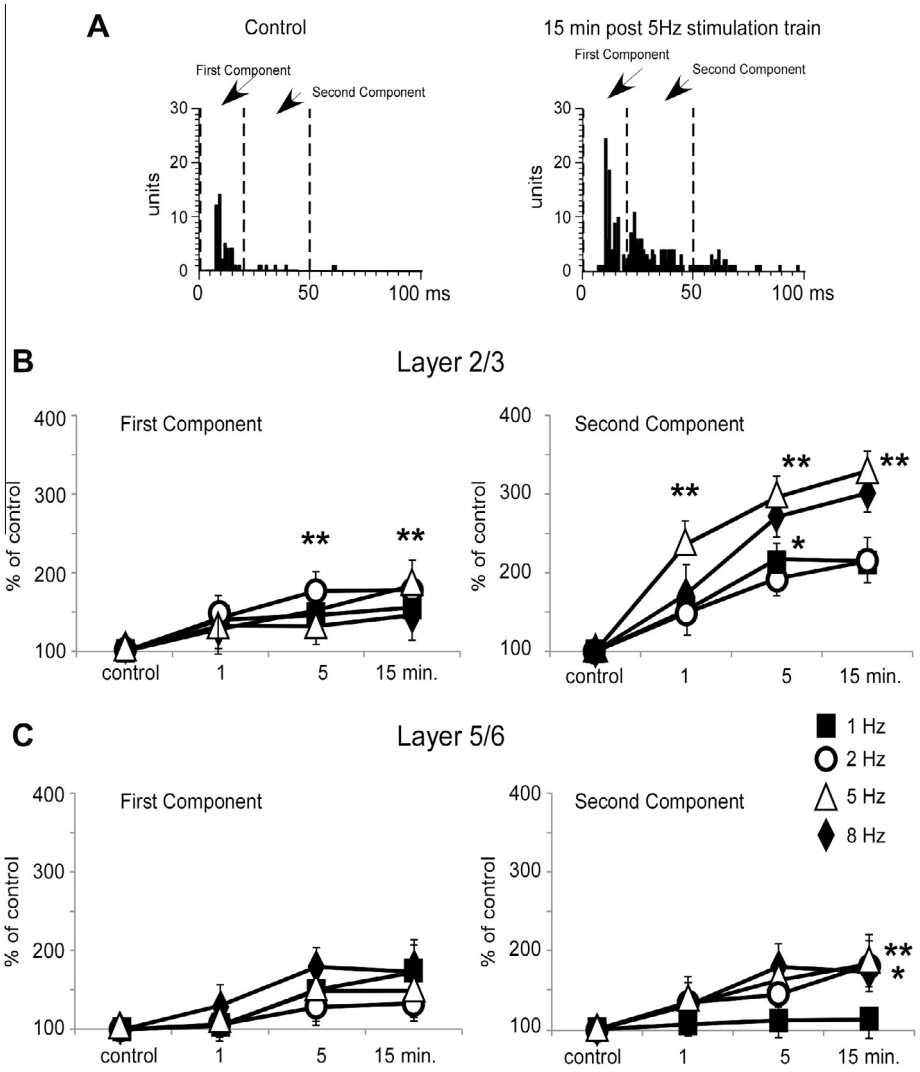

Fig. 7. The second component of tactile response was the main response component affected by repetitive whisker stimulation. (A) PSTHs of a representative case in a layer 2/3 neuron in which the second response component (20–50 ms) was mainly affected 15 min after a 5-Hz stimulation train. (B) Plots of the changes in the first and second component of the PSTH in layer 2/3 neurons (n = 32) after a stimulation train in the principal whisker. Note that the second component was more affected by the stimulation train than the first component, especially at higher stimulation frequencies. (C) Same plots as in B with values from layer 5/6 neurons (n = 32). Repetitive stimulation of the whisker induced smaller response changes than in layer 2/3 neurons. Asterisks indicate statistical differences obtained by the Wilcoxon-matched pairs post hoc analysis with respect to control values of each frequency.

Corticothalamic temporal course of the response facilitation

Simultaneous double unit recordings in the barrel cortex and in the VPM nucleus were performed to determine if a 5-Hz stimulation train could evoke response facilitation in thalamic neurons. Twenty-four double recordings of layer 2/3 neurons and VPM neurons and another 12 double recordings of layer 5/6 and VPM neurons from nine rats were selected for analysis because they revealed an overlapping RF. On average, the VPM thalamic neurons had 1.4 ± 0.2 spikes/stimulus with a mean latency of 11 ± 0.28 ms (n = 36). In control conditions a 5-Hz stimulation train induced response facilitation in layer 2/3 (Kruskal–Wallis analysis: $P < 0.0001$), layer 5/6 (Kruskal–Wallis analysis: $P = 0.0005$) as well as in VPM neurons (Kruskal–Wallis analysis: $P = 0.0004$; Fig. 9A). The time course of response facilitation was similar in the barrel cortex and in VPM nucleus.

To elucidate if the response facilitation observed in the VPM nucleus was due to cortical mechanisms we applied the $GABA_A$ receptor agonist muscimol into the barrel cortex through a cannula located in layer 2/3. We applied large doses of muscimol (1 μl; 8 mM; four rats) to decrease neuronal activity in all cortical layers. To confirm the effect of muscimol we performed unit recordings in layer 5/6. Responses decreased in layer 5/6 20 min after muscimol injection (from 1.9 ± 0.18 spikes/stimulus to 1.0 ± 0.21 spikes/stimulus; Wilcoxon-matched pairs test; $P < 0.001$; n = 12;). In this moment, we analyzed the simultaneous unit recordings in VPM. Cortical inactivation did not affect the tactile

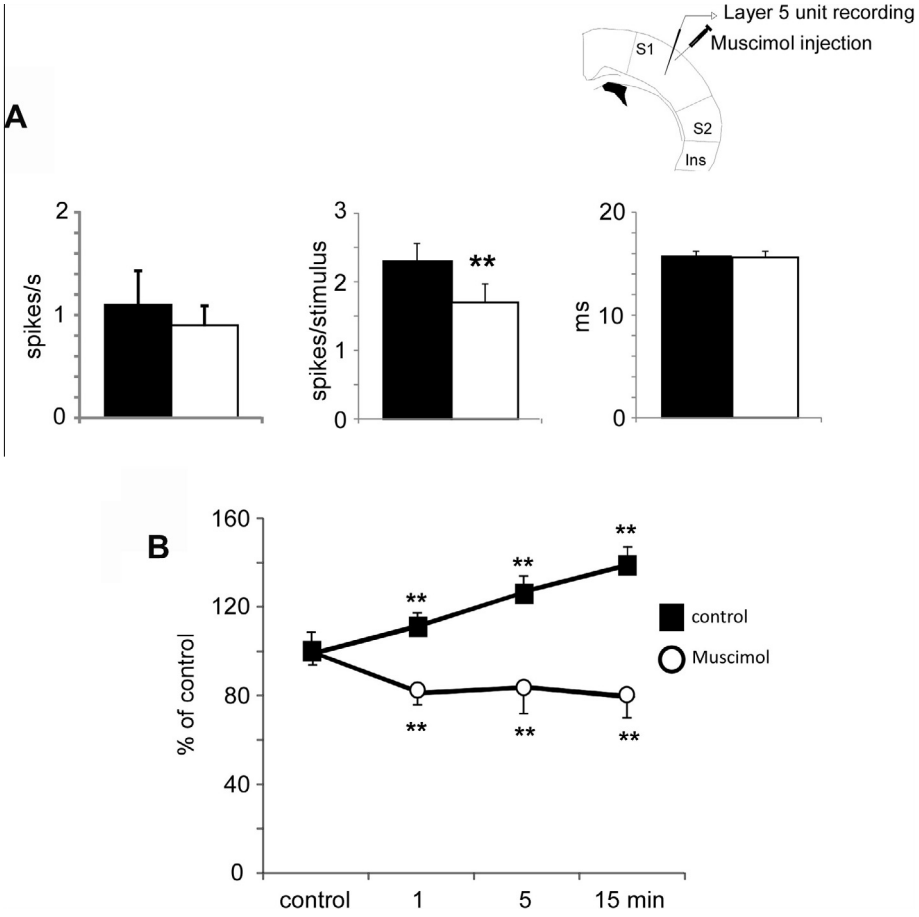

Fig. 8. Layer 2/3 neurons were responsible for response facilitation evoked by repetitive stimulation. (A) Plots of spontaneous activity (left plot), tactile response (middle plot) and response latency (right plot) of layer 5/6 neurons in control (n = 18) and after muscimol (0.1 μl; 8 mM) injection in layer 2/3 (n = 22). Muscimol in layer 2/3 only decreased tactile responses in layer 5/6. (B) Percentage of responses in layer 5/6 neurons in comparison with control values (100%) after a 5-Hz stimulation train in control condition (n = 18) and in the presence of muscimol in layer 2/3 (n = 22). In the presence of muscimol a response depression was observed. Asterisks in B indicate statistical differences obtained by the Wilcoxon-matched pairs post hoc analysis with respect to control values of each frequency.

responses of VPM neurons (2.1 ± 0.16 spikes/stimulus vs. 1.9 ± 0.14 spikes/stimulus; Wilcoxon-matched pairs test; P = 0.79; n = 12). In this condition, a 5-Hz stimulation train did not evoke long-lasting facilitation of tactile responses in either VPM (Kruskal–Wallis analysis: P = 0.126) or layer 5/6 neurons (Kruskal–Wallis analysis: P = 0.092; Fig. 9B), suggesting that the response facilitation evoked by 5 Hz tactile stimulation in thalamic neurons was generated in the barrel cortex.

Effect of repetitive stimulation on the RF

In order to study RF changes evoked by repetitive stimulation of the principal whisker, we analyzed 43 neurons from RFs in which it was possible to stimulate a principal whisker and another peripheral whisker with a weaker response. Layer 2/3 (n = 25) showed a mean response to the principal whisker stimulation of 1.6 ± 0.19 spikes/stimulus and a mean latency of 15.1 ± 0.1 ms. The response was lower when tactile stimulation was applied to the peripheral whisker (1.1 ± 0.19 spikes/stimulus; Wilcoxon-matched pairs test; P = 0.005; latency of 16.5 ± 0.1 ms; P = 0.003;). Layer 2/3 neurons showed a long-lasting increase of tactile responses from the principal whisker after a 5-Hz stimulus train applied to this whisker as well as tactile responses from the peripheral whisker (172% and 196%, respectively; Kruskal–Wallis analysis: P < 0.0001 and P < 0.0001, respectively; Fig. 10A). The response increased to 2.8 ± 0.2 spikes/stimulus for the principal whisker (Wilcoxon-matched pairs test; P < 0.001) and to 2.1 ± 0.29 spikes/stimulus for the peripheral whisker (Wilcoxon-matched pairs test; P < 0.001). However, the response latency was not modified (15.1 ± 0.1 ms or 17.4 ± 0.1 ms for the peripheral whisker, respectively, 15 min after the stimulation train; Wilcoxon-matched pairs test; P = 0.113 or P = 0.406, respectively).

Layer 5/6 (n = 18) showed a mean response to the principal whisker stimulation of 1.7 ± 0.4 spikes/stimulus and a mean latency of 16.0 ± 0.1 ms. Equally, response was lower when tactile stimulation was applied to the peripheral whisker (0.98 ± 0.38 spikes/stimulus; Wilcoxon-matched pairs test; P = 0.005) although the latency was 18.5 ± 0.3 ms; Wilcoxon-matched pairs

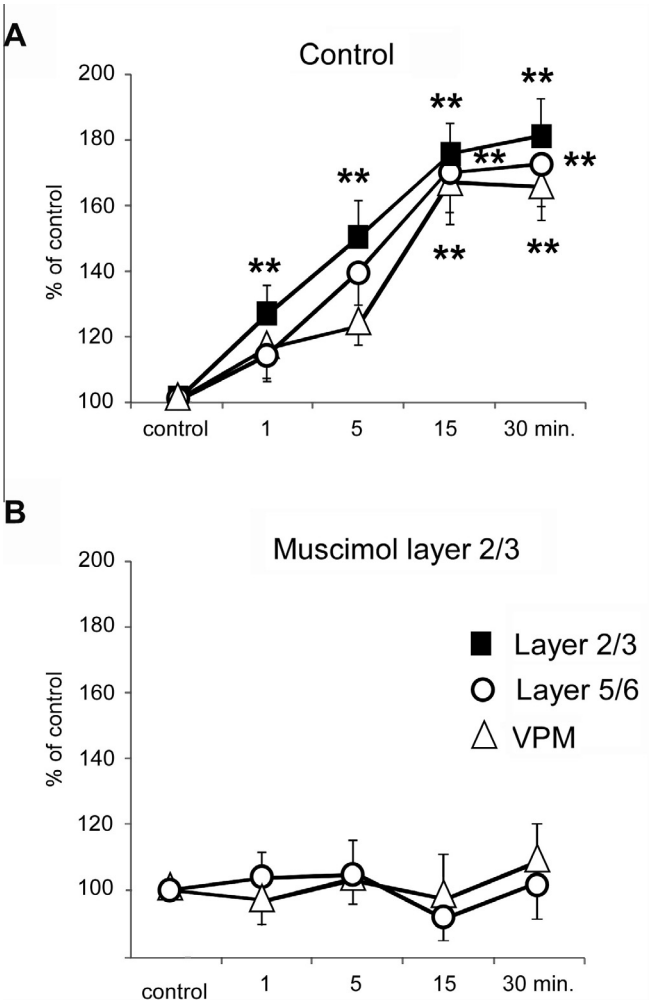

Fig. 9. Thalamic VPM response facilitation was blocked by cortical inactivation. (A) Percentage of tactile responses in comparison with control values (100%) after a repetitive stimulation of the whisker at 5 Hz. Responses of cortical (n = 18 layer 2/3 and n = 8 layer 5/6 neurons) and thalamic neurons (n = 11 VPM neurons) were facilitated. (B) Muscimol application (1 µl; 8 mM) in layer 2/3 to reduce cortical activity blocked response facilitation in either layer 5/6 neurons (n = 12) or thalamic VPM neurons (n = 12). Asterisks in A indicate statistical differences obtained by the Wilcoxon-matched pairs post hoc analysis with respect to control values of each frequency.

test; P = 0.133). Tactile responses in layer 5/6 neurons from the principal or peripheral whiskers increased after application of a 5-Hz stimulation train in the principal whisker (Kruskal–Wallis analysis: $P < 0.0001$ and $P = 0.008$; 1.7 ± 0.4 vs. 2.8 ± 0.9 spikes/stimulus; $P = 0.01$, or 0.98 ± 0.38 vs. 1.5 ± 0.65 spikes/stimulus; Wilcoxon-matched pairs test; $P = 0.02$, respectively; Fig. 10B) as well as for response latency (16.0 ± 0.1 vs. 14.8 ± 0.3 ms for the principal whisker; Wilcoxon-matched pairs test; $P = 0.136$ or 18.5 ± 0.3 ms vs. 16.2 ± 0.2 ms for the peripheral whisker; $P = 0.059$).

Moreover, in a few cases, layer 2/3 (4 out of 18 neurons; 22%) or layer 5/6 (2 out of 14; 14%) neurons expanded their RFs to adjacent areas. In these cases, tactile stimulation of the adjacent whisker to the principal one did not evoke any response in control conditions but, after a 5-Hz stimulus train at the principal whisker, a weaker response appeared among layer 2/3 neurons (0.3 ± 0.05 spikes/stimulus) and layer 5/6 neurons (0.2 ± 0.08 spikes/stimulus), unmasking a large RF.

Effects of Ach on the tactile response increase

Ach has been proposed to participate in cortical synaptic plasticity (see Introduction). Acetylcholinesterase is an endogenous enzyme that degrades Ach released into the synaptic cleft. We used the inhibition of this enzyme through intraperitoneal injection of eserine to evoke an accumulation of Ach in the cortex and to study its participation in the response facilitation evoked by repetitive whisker stimulation. Intraperitoneal injection of eserine (0.1 mg/kg; 11 rats) increased spontaneous activity and tactile responses in layer 2/3 and layer 5/6 neurons (Table 2). The response enhancement was characterized by an important increase of the second response component that is mainly mediated by activation of NMDA receptors (Fig. 11A, arrow), as indicated above and in a previous publication (Nuñez et al., 2012).

In the presence of eserine repetitive 5-Hz stimulation induced an increase in the number of neurons showing long-lasting tactile response facilitation (tactile

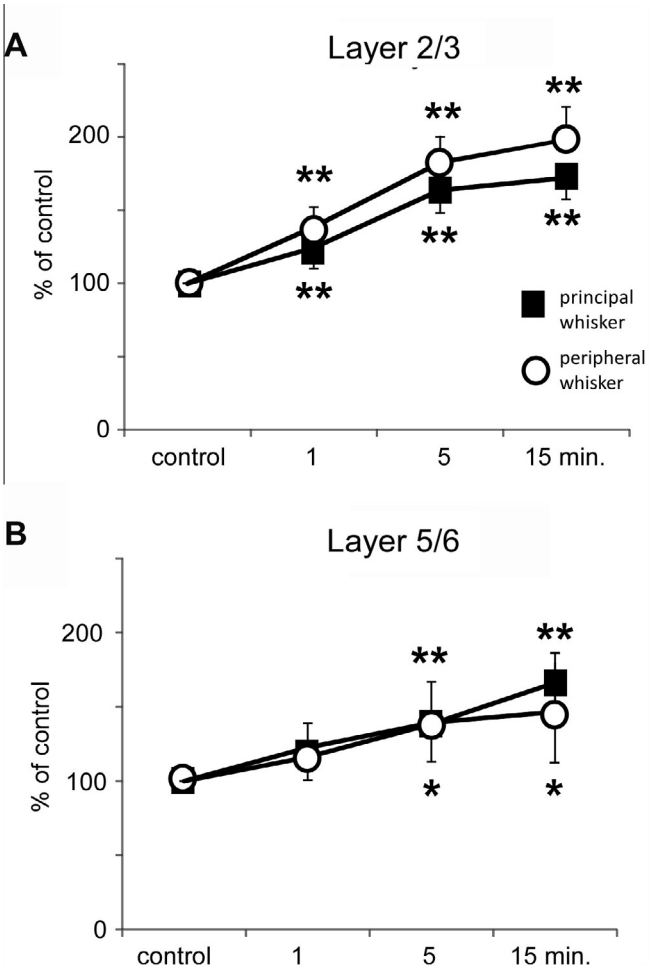

Fig. 10. Repetitive whisker stimulation increased tactile responses from both principal and peripheral whiskers. (A and B) Percentage of responses with respect to control values (100%) in layer 2/3 neurons (n = 25) or layer 5/6 neurons (n = 18) for the principal and peripheral whisker stimulation after a repetitive stimulation at 5 Hz of the principal whisker. The peripheral RF was more affected than the center of the RF in layer 2/3 neurons. Asterisks in A and B indicate statistical differences obtained by the Wilcoxon-matched pairs post hoc analysis with respect to control values.

Table 2. Effect of eserine intraperitoneal injection on cortical neurons. The effect was blocked by atropine

	Layer 2/3		Layer 5/6	
	Spontaneous activity (spikes/s)	Tactile responses (spikes/stimulus)	Spontaneous activity	Tactile responses
Control	0.6 ± 0.2 (n = 22)	1.2 ± 0.21 (n = 22)	0.4 ± 0.2 (n = 18)	1.2 ± 0.19 (n = 18)
Eserine i.p.	3.5 ± 0.7 (p < 0.001; n = 42)	1.6 ± 0.15 (p = 0.005; n = 42)	2.8 ± 0.2 (p < 0.001; n = 36)	1.6 ± 0.3 (p = 0.006; n = 36)
Atropine + eserine i.p.	0.7 ± 0.32 (p > 0.05; n = 15)	0.9 ± 0.28 (p > 0.05; n = 15)	0.5 ± 0.25 (p > 0.05; n = 14)	1.0 ± 0.25 (p > 0.05; n = 14)

P indicates the statistical significance respect to control values obtained by Wilcoxon-matched pairs test.

responses increased more than two times the SEM) in layer 2/3 while layer 5/6 neurons were not affected (Fig. 11C). Layer 2/3 (n = 22) or layer 5/6 (n = 18) neurons showed response facilitation in control conditions (155% or 148% of increment from control values, respectively, 30 min after stimulation train; Kruskal–Wallis analysis: P < 0.0001 and P = 0.0007, respectively) and after eserine injection (152% or 145%; Kruskal–Wallis analysis: P = 0.0005 and P = 0.048, respectively). Note that the percentage of tactile response increment evoked by the repetitive stimulation was not affected by intraperitoneal injection of eserine (Fig. 11B). The increment of neurons facilitated by eserine was reduced by atropine (5 mg/kg; i.p. injected 10 min before eserine application; five rats) and therefore this effect was attributed to muscarinic receptor activation (Fig. 11C). In this condition, 5-Hz stimulation train only facilitates layer 2/3 neurons

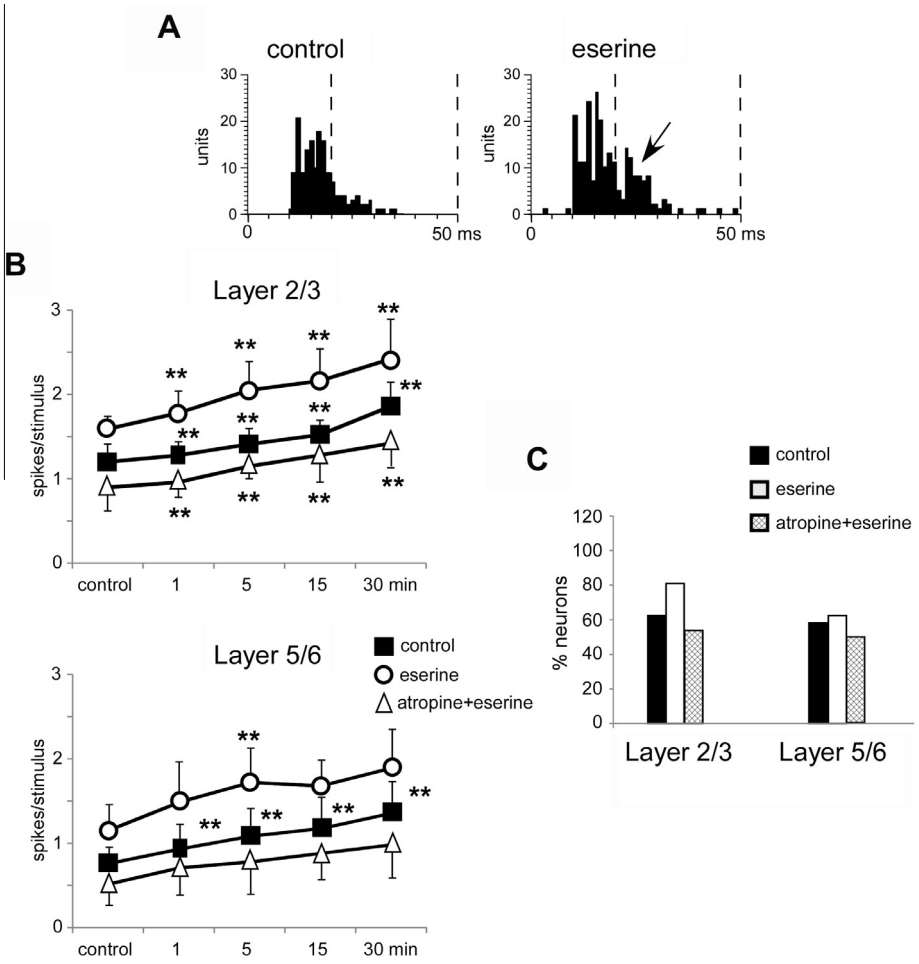

Fig. 11. Accumulation of cortical Ach increased the number of cells that showed long-lasting tactile response facilitation. (A) PSTHs of a representative case in a layer 2/3 neuron in which eserine (i.p. 0.1 mg/kg) increased tactile responses. (B) Plots of the layer 2/3 cell (n = 42) or layer 5/6 cell (n = 36) responses showing long-lasting response facilitation after a 5-Hz stimulation train. Eserine increased tactile responses in layer 2/3 and layer 5/6 neurons. In contrast, i.p. injection of atropine (5 mg/kg; i.p. injected 10 min before eserine) decreased tactile responses. (C) Plots of the percentage of neurons that were facilitated by the 5-Hz stimulation train. A large number of 2/3 cells were facilitated in the presence of eserine; this effect was blocked by a previous application of atropine. Asterisks in B indicate statistical differences obtained by the Wilcoxon-matched pairs post hoc analysis with respect to control values.

(Kruskal–Wallis analysis: P = 0.0023) while layer 5/6 neurons were not affected (Kruskal–Wallis analysis: P = 0.61).

DISCUSSION

Rats actively explore their environment by repetitively sweeping their whiskers through their surroundings (whisking behavior). Our data show that repetitive stimulation of one whisker at the frequency used to explore the environment (5–8 Hz) induces a long-lasting response facilitation of layer 2/3 and 5/6 neurons by activation of NMDA receptors. Response facilitation increased synaptic efficacy in cortical neurons because the coherence between neuronal responses and stimuli increased, which it may have important consequences in sensory processing. Moreover, strengthening Ach activity by i.p. eserine injection increased the number of response-facilitated cells by repetitive stimulation through activation of muscarinic receptors. Results also suggest that layer 2/3 neurons are involved in the generation of this long-lasting response facilitation and that it is transferred to layer 5/6 neurons in order to facilitate sensory processing during active exploration.

Analyses of whisking behavior have shown that adult rats actively sweep their whiskers over objects and surfaces rhythmically at frequencies of 4–15 whisker movements per second to explore their environment (Carvell and Simons, 1990; Moore, 2004; Melzer et al., 2006). In the present study, we used a train of short-lasting air pulses at frequencies of 0.5–8 Hz to specifically examine the effects of stimulus frequency on the response facilitation generation at cortical layers 2/3 and 5/6. Trigeminal ganglion cells show spike firing during whisking through air, although at rates that are approximately an order of magnitude lower than those associated with direct object contact (Leiser and Moxon, 2007). Thus, rhythmic inputs at different frequencies may reach cortical neurons in different conditions, modulating cortical sensory responses. Neurons included in our study are probably located in the barrel because these neurons showed small RFs and a short response latency. Moreover, the

response efficacy of our neuronal population was similar to previously reported data for barrel neurons and efficacy was distant from neurons recorded in the septa (Melzer et al., 2006). Anatomical analysis of the electrode locations also indicated that the electrode was moved along the barrel.

This study used a stimulation train of 0.5 Hz as a control. Continuous stimulation at this frequency induced a modest increase of the response when it was applied for up to 1 h. At 1-Hz stimulation frequency the increase in tactile responses was modest, as well. However, this change was very small in comparison with the changes observed after the application of a 2–8-Hz stimulation train. Single-unit results suggested that response was facilitated beyond 30 min for 5- or 8-Hz stimulation frequencies (Figs. 4 and 5). However, studying the neuronal population by means of evoked potential analysis (Fig. 1B) indicated that the response reached a plateau 30 min after the stimulation train and remained elevated at least 60 min. As noted above, these frequencies are behaviorally relevant frequencies. The analysis of the power spectrum indicated that the level of anesthesia or the cortical activity did not change during the experiment. Thus, a short repetitive stimulation period was able to induce changes in cortical response that may facilitate sensory processing during active exploration. Garabedian et al. (2003) observed that the spike response in S1 cortex was higher at a stimulation range from 5 to 12 Hz than at lower and higher stimulation frequencies. Also, the frequency of whisker stimulation modulates the horizontal extent of the activated cortex by stimulation of the whisker (the cortical "point spread" function). In anesthetized rats, stimulation of a whisker at 1 Hz evokes a significantly broader point spread than stimulation at 5 or 10 Hz, suggesting more precise sensory processing (Sheth et al., 1998). In agreement with previous results, we found that stimulation frequencies of 2–8 Hz induced long-lasting sensory response facilitation.

Results suggest that the whisker sensory system enhances sensory stimuli after a repetitive stimulation at frequencies that correspond to the rhythmic whisker movement during active exploration (4–15 Hz). We have recently reported that layer 5 cortical neurons fire Ca^{2+} spikes mediated by activation of NMDA receptors and L-type voltage-gated Ca^{2+} channels facilitating synaptic responses to low frequency stimuli at the basal dendrites (Nuñez et al., 2012). This mechanism may enhance the detection of a single whisker contact while present results suggest the existence of a cortical mechanism that would facilitate behaviorally relevant stimuli at 2–8 Hz in adult animals. Consequently, the number of neurons that express response facilitation increased in the presence of Ach, suggesting that this process may be enhanced during wakefulness or paradoxical sleep.

We used wavelet coherence analysis to quantify the time–frequency functional association between the stimulus and the neural spike responses (Castellanos et al., 2007; Malmierca et al., 2009). This analysis revealed a large coherence enhancement after repetitive stimulation in neurons that showed response facilitation. Their synchronized stimulus-driven discharges will induce excitatory postsynaptic potentials within a narrow temporal window in the postsynaptic neuron, increasing the chances of generating spikes in those neurons. Repetitive stimulation causes a potent and sustained response enhancement that may increase the contrast between activated neurons by rhythmic whisker movements during active exploration and neurons activated by random stimuli. Consequently, the long-lasting facilitation described here may have fundamental consequences for the signal processing capacity in the barrel cortex.

It is well known that LTP in the sensory cortex is mainly due to the activation of NMDA receptors that induce a long-lasting enhancement of the response; the insertions of AMPA receptors in the membrane also contribute to LTP generation (Daw et al., 2006; Remy and Spruston, 2007). This process might be implicated in sensory plasticity in the cortex (e.g. Daw et al., 2007; Nuñez et al., 2012). Earlier findings have indicated that theta-burst stimulation produces NMDA receptor-dependent LTP in the layer 4 to 2/3 pathway in the barrel cortex *in vivo* (Hardingham et al., 2003) and between different barrels *in vitro* (Urban et al., 2002). Antagonists of NMDA receptors also block cortical plasticity after electrical thalamic stimulation (Heynen and Bear, 2001). Our results indicate that the long-lasting response facilitation has similar characteristics to the previously described cortical LTP. It lasts at least 60 min and was blocked by antagonists of the NMDA receptors like APV or MK801. APV affected response facilitation when it was applied in the superficial layers. However, APV application in layer 5/6 had lower effect on the long-lasting facilitation, suggesting that facilitation was generated in the layer 2/3 cells, as has been suggested previously (Huang et al., 1998). Furthermore, systemically injected MK801 (intraperitoneal) blocked long-lasting facilitation in both layer 2/3 and layer 5/6 cells.

It is interesting to note that a 5-Hz stimulation train induced response depression in layer 5/6 after local application of muscimol in layer 2/3. In contrast, the same stimulation protocol evoked response facilitation without muscimol. It is possible that the reduction of the excitatory input from layer 2/3 to layer 5/6 neurons change the balance excitation/inhibition, facilitating long-lasting depression. In fact, it has been described that sensory use, disuse, and training induce LTP or depression in the cortex by intrinsic or synaptic mechanisms (see for review Feldman, 2009). It seems that NMDA receptor activation in layer 2/3 by repetitive stimuli induces long-lasting changes in the synaptic efficacy that spread to other layers along the cortical column such as layer 5/6 neurons.

It is possible that layer 4 neurons might generate the long-lasting response facilitation evoked by repetitive stimulation because they innervate layer 2/3, layer 5A–B, and layer 6A pyramidal cells (Feldmeyer et al., 2005, 2013; Petreanu et al., 2009). If layer 4 is responsible for response facilitation in all cortical layers, response facilitation in layer 5/6 should continue even after layer 2/3 inactivation because of the direct projections to these layers. Consequently, although we cannot exclude the

participation of layer 4 neurons in the response facilitation, data strongly suggest that layer 2/3 neurons are involved in synaptic plasticity generation.

Furthermore, tactile responses of VPM neurons were also facilitated after repetitive stimulation of the whisker at 5 Hz. However, thalamic response facilitation was blocked by cortical inactivation elicited by application of muscimol into the barrel cortex, indicating that the barrel cortex is the origin of the response facilitation and this facilitation is transmitted to the thalamus by corticofugal projections (for review see Nuñez and Malmierca, 2007).

Appropriate patterns of sensory inputs are particularly important during early postnatal development, when cortical maturation is highly dependent on incoming sensory stimuli, to induce experience-dependent plasticity. However, a significant amount of evidence demonstrates that sensory cortices, including the primary somatosensory cortex, maintain a significant capacity for synaptic plasticity beyond early development. Repetitive visual or auditory stimulation can induce synaptic plasticity including LTP of cortical responses evoked by sensory inputs in humans and adult animals (Clapp et al., 2005, 2006; Teyler et al., 2005; Kuo and Dringenberg, 2012). Moreover, Megevand et al. (2009) induced a long-term response facilitation by 10 min of 8-Hz multiwhisker stimulation in the granular and supragranular layers of the barrel cortex that lasted over 90 min. Similarly, it has been reported that electrical stimulation of layer 4 induces LTP in layer 2/3 neurons of adult rats recorded *in vivo* (Glazewski et al., 1998) or in adult mice recorded *in vitro* (Banerjee et al., 2009). The present findings demonstrate that 40 stimuli to one whisker in anesthetized adult animals are enough to induce response facilitation in layer 2/3 and 5/6 cortical neurons. Either the first or the second component of the tactile response, probably mediated by AMPA and NMDA receptors, was increased, as occurs in cortical LTP.

The Ach has a complex effect on the cortex due to the activation of presynaptic and postsynaptic receptors located in pyramidal neurons and in local interneurons. Thus, the level of Ach in the cortex can enhance or depress sensory responses (Oldford and Castro-Alamancos, 2003; Noori et al., 2012). Based on microdialysis studies, spontaneous Ach release is lower under urethane anesthesia than in freely moving animals (Bertorelli et al., 1991), but the basal release of ACh is sustained in both conditions (Rasmusson et al., 1992; Jimenez-Capdeville et al., 1997). These data suggest that urethane-anesthetized rats provide a suitable model to study the importance of the cholinergic system in sensory processing. Our data showed that the number of cell that displayed long-lasting response facilitation increased in the presence of eserine in layer 2/3 and remained equal in layer 5/6. This specific effect may be due to a large number of muscarinic receptors in layer 2/3 (Levey et al., 1991; Yamasaki et al., 2010). In agreement with previous results (Nuñez et al., 2012), Ach mainly increased the second response component through an indirect activation of NMDA receptors, improving the generation of long-lasting response facilitation by repetitive whisker stimulation. This result may have relevant behavioral consequences because rats actively sweep their whiskers during behavioral states in which cortical Ach is increased such as wakefulness, REM sleep, or during attention tasks (e.g. Sarter and Bruno, 2000).

Experience dramatically changes sensory maps in the primary somatosensory cortex (see for review Kaas, 1991; Buonomano and Merzenich, 1998). Our findings indicate that the long-lasting facilitation evoked by repetitive stimulation of a single whisker also facilitated other whisker responses (from the RF periphery), even unmasking larger RFs. The larger increase in peripheral whiskers as compared to principal whiskers cannot be the result of saturation of the neuronal responses for the principal whisker because cortical neurons may respond even more in the presence of eserine. Therefore repetitive whisker stimulation facilitates a principal RF, formed by the principal neurons in the barrel, and a surrounding field, formed by inputs from neighboring barrels. However, LTP expression was recently reported to be mostly restricted to the activated barrel column in the neonatal rat barrel cortex (An et al., 2012). This discrepancy may be due to the different ages of the rats (adult rats in our study and P0–P14 rats in An's study) since the synaptic connections between barrels may not have developed yet in those young animals (see for review Erzurumlu and Gaspar, 2012). It is possible that the mechanisms of response facilitation are a result of NMDA receptor activation increasing the intracellular Ca^{2+} concentration which would induce the incorporation of new receptors in the dendritic spine. Intracellular Ca^{2+} may facilitate the principal input from the stimulated whisker as well as synaptic inputs from whiskers from the RF periphery.

CONCLUSION

These data are consistent with the notion that experience-dependent plasticity occurs in adult rats through changes in the behaviorally relevant sensory responses such as repetitive stimulation at a behavioral relevant frequency. Layer 2/3 neurons seem to be the major factor in generating the long-lasting facilitation evoked by repetitive stimulation while layer 5/6 neurons could contribute to cortical plasticity by projecting the changes in sensory response to other cortical and subcortical areas.

CONTRIBUTIONS

NBZ, CC and AN designed the experiments. NBZ and CC conducted the experiments and analyzed the data. AN wrote the paper.

Acknowledgments—We thank N. Castellanos for comments on the manuscript, M. Callejo for technical assistance and C.F. Warren for revision of English language usage. This work was supported by a grant from Ministerio de Economia y Competitividad (BFU2012-36107).

The authors declare no conflicts of interest.

REFERENCES

An S, Yang JW, Sun H, Kilb W, Luhmann HJ (2012) Long-term potentiation in the neonatal rat barrel cortex in vivo. J Neurosci 32:9511–9516.

Banerjee A, Meredith RM, Rodriguez-Moreno A, Mierau SB, Auberson YP, Paulsen O (2009) Double dissociation of spike timing-dependent potentiation and depression by subunit-preferring NMDA receptor antagonists in mouse barrel cortex. Cereb Cortex 19:2959–2969.

Bertorelli R, Forloni G, Consolo S (1991) Modulation of cortical in vivo acetylcholine release by the basal nuclear complex: role of the pontomesencephalic tegmental area. Brain Res 563:353–356.

Borgdorff AJ, Poulet JF, Petersen CC (2007) Facilitating sensory responses in developing mouse somatosensory barrel cortex. J Neurophysiol 97:2992–3003.

Bueno-Junior LS, Lopes-Aguiar C, Ruggiero RN, Romcy-Pereira RN, Leite JP (2012) Muscarinic and nicotinic modulation of thalamo-prefrontal cortex synaptic plasticity [corrected] in vivo. PLoS One 7:e47484.

Buonomano DV, Merzenich MM (1998) Cortical plasticity: from synapses to maps. Annu Rev Neurosci 21:149–186.

Carvell GE, Simons DJ (1990) Biometric analyses of vibrissal tactile discrimination in the rat. J Neurosci 10:2638–2648.

Castellanos NP, Malmierca E, Nunez A, Makarov VA (2007) Corticofugal modulation of the tactile response coherence of projecting neurons in the gracilis nucleus. J Neurophysiol 98:2537–2549.

Celesia GG, Jasper HH (1966) Acetylcholine released from cerebral cortex in relation to state of activation. Neurology 16:1053–1063.

Chakrabarti S, Alloway KD (2009) Differential response patterns in the SI barrel and septal compartments during mechanical whisker stimulation. J Neurophysiol 102:1632–1646.

Clapp WC, Kirk IJ, Hamm JP, Shepherd D, Teyler TJ (2005) Induction of LTP in the human auditory cortex by sensory stimulation. Eur J Neurosci 22:1135–1140.

Clapp WC, Eckert MJ, Teyler TJ, Abraham WC (2006) Rapid visual stimulation induces N-methyl-D-aspartate receptor-dependent sensory long-term potentiation in the rat cortex. Neuroreport 17:511–515.

Daw MI, Bannister NV, Isaac JT (2006) Rapid, activity-dependent plasticity in timing precision in neonatal barrel cortex. J Neurosci 26:4178–4187.

Daw MI, Scott HL, Isaac JT (2007) Developmental synaptic plasticity at the thalamocortical input to barrel cortex: mechanisms and roles. Mol Cell Neurosci 34:493–502.

de Kock CP, Sakmann B (2008) High frequency action potential bursts (> or = 100 Hz) in L2/3 and L5B thick tufted neurons in anaesthetized and awake rat primary somatosensory cortex. J Physiol 586:3353–3364.

de Kock CP, Bruno RM, Spors H, Sakmann B (2007) Layer- and cell-type-specific suprathreshold stimulus representation in rat primary somatosensory cortex. J Physiol 581:139–154.

Doralp S, Leung LS (2008) Cholinergic modulation of hippocampal CA1 basal-dendritic long-term potentiation. Neurobiol Learn Mem 90:382–388.

Douglas RJ, Martin KA (2004) Neuronal circuits of the neocortex. Annu Rev Neurosci 27:419–451.

Erzurumlu RS, Gaspar P (2012) 9 Development and critical plasticity of the barrel cortex. Eur J Neurosci 35:1540–1553.

Fanselow EE, Nicolelis M (1999) Behavioral modulation of tactile responses in the rat somatosensory system. J Neurosci 19:7603–7616.

Feldman DE (2009) Synaptic mechanisms for plasticity in neocortex. Ann Rev Neurosci 32:33–55.

Feldmeyer D (2012) Excitatory neuronal connectivity in the barrel cortex. Front Neuroanat 6:24.

Feldmeyer D, Roth A, Sakmann B (2005) Monosynaptic connections between pairs of spiny stellate cells in layer 4 and pyramidal cells in layer 5A indicate that lemniscal and paralemniscal afferent pathways converge in the infragranular somatosensory cortex. J Neurosci 25:3423–3431.

Feldmeyer D, Brecht M, Helmchen F, Petersen CC, Poulet JF, Staiger JF, Luhmann HJ, Schwarz C (2013) Barrel cortex function. Prog Neurobiol 103:3–27.

Fernandez de Sevilla D, Nunez A, Borde M, Malinow R, Buno W (2008) Cholinergic-mediated IP3-receptor activation induces long-lasting synaptic enhancement in CA1 pyramidal neurons. J Neurosci 28:1469–1478.

Garabedian CE, Jones SR, Merzenich MM, Dale A, Moore CI (2003) Band-pass response properties of rat SI neurons. J Neurophysiol 90:1379–1391.

Glazewski S, Herman C, McKenna M, Chapman PF, Fox K (1998) Long-term potentiation in vivo in layers II/III of rat barrel cortex. Neuropharmacology 37:581–592.

Goelz H, Jones RD, Bones PJ (2000) Wavelet analysis of transient biomedical signals and its application to detection of epileptiform activity in the EEG. Clin EEG 31:181–191.

Hardingham N, Glazewsk S, Pakhotin P, Mizuno K, Chapman PF, Giese KP, Fox K (2003) Neocortical long-term potentiation and experience-dependent synaptic plasticity require alpha-calcium/calmodulin-dependent protein kinase II autophosphorylation. J Neurosci 23:4428–4436.

Hardingham NR, Hardingham GE, Fox KD, Jack JJ (2007) Presynaptic efficacy directs normalization of synaptic strength in layer 2/3 rat neocortex after paired activity. J Neurophysiol 97:2965–2975.

Hasselmo ME, Giocomo LM (2006) Cholinergic modulation of cortical function. J Mol Neurosci 30:133–135.

Heynen AJ, Bear MF (2001) Long-term potentiation of thalamocortical transmission in the visual cortex in vivo. J Neurosci 21:9801–9813.

Huang W, Armstrong-James M, Rema V, Diamond ME, Ebner FF (1998) Contribution of supragranular layers to sensory processing and plasticity in adult rat barrel cortex. J Neurophysiol 80:3261–3271.

Jimenez-Capdeville ME, Dykes RW, Myasnikov AA (1997) Differential control of cortical activity by the basal forebrain in rats: a role for both cholinergic and inhibitory influences. J Comp Neurol 381:53–67.

Kaas JH (1991) Plasticity of sensory and motor maps in adult mammals. Annu Rev Neurosci 14:137–167.

Kuo MC, Dringenberg HC (2012) Comparison of long-term potentiation (LTP) in the medial (monocular) and lateral (binocular) rat primary visual cortex. Brain Res 1488:51–59.

Kuo MC, Rasmusson DD, Dringenberg HC (2009) Input-selective potentiation and rebalancing of primary sensory cortex afferents by endogenous acetylcholine. Neuroscience 163:430–441.

Lachaux JP, Lutz A, Rudrauf D, Cosmelli D, Le Van Quyen M, Martinerie J, Varela F (2002) Estimating the time-course of coherence between single-trial brain signals: an introduction to wavelet coherence. Neurophysiol Clin 32:157–174.

Leiser SC, Moxon KA (2007) Responses of trigeminal ganglion neurons during natural whisking behaviors in the awake rat. Neuron 53:117–133.

Levey AI, Kitt CA, Simonds WF, Price DL, Brann MR (1991) Identification and localization of muscarinic acetylcholine receptor proteins in brain with subtype-specific antibodies. J Neurosci 11:3218–3226.

Malmierca E, Castellanos NP, Nuñez-Medina A, Makarov VA, Nuñez A (2009) Neuron synchronization in the rat gracilis nucleus facilitates sensory transmission in the somatosensory pathway. Eur J Neurosci 30:593–601.

Manns ID, Sakmann B, Brecht M (2004) Sub- and suprathreshold receptive field properties of pyramidal neurons in layers 5A and 5B of rat somatosensory barrel cortex. J Physiol (London) 556:601–622.

Megevand P, Troncoso E, Quairiaux C, Muller D, Michel CM, Kiss JZ (2009) Long-term plasticity in mouse sensorimotor circuits after rhythmic whisker stimulation. J Neurosci 29:5326–5335.

Melzer P, Sachdev RN, Jenkinson N, Ebner FF (2006) Stimulus frequency processing in awake rat barrel cortex. J Neurosci 26:12198–12205.
Metherate R, Ashe JH (1993) Nucleus basalis stimulation facilitates thalamocortical synaptic transmission in the rat auditory cortex. Synapse 14:132–143.
Moore CI (2004) Frequency-dependent processing in the vibrissa sensory system. J Neurophysiol 91:2390–2399.
Navarrete M, Perea G, Fernandez de Sevilla D, Gomez-Gonzalo M, Nuñez A, Martin ED, Araque A (2012) Astrocytes mediate in vivo cholinergic-induced synaptic plasticity. PLoS Biol 10:e1001259.
Noori HR, Fliegel S, Brand I, Spanagel R (2012) The impact of acetylcholinesterase inhibitors on the extracellular acetylcholine concentrations in the adult rat brain: a meta-analysis. Synapse 66:893–901.
Nuñez A, Malmierca E (2007) Corticofugal modulation of sensory information. Adv Anat Embryol Cell Biol 187:1–74.
Nuñez A, Dominguez S, Buño W, Fernandez de Sevilla D (2012) Cholinergic-mediated response enhancement in barrel cortex layer V pyramidal neurons. J Neurophysiol 108:1656–1668.
Oldford E, Castro-Alamancos MA (2003) Input-specific effects of acetylcholine on sensory and intracortical evoked responses in the ''barrel cortex'' in vivo. Neuroscience 117:769–778.
Petreanu L, Mao T, Sternson SM, Svoboda K (2009) The subcellular organization of neocortical excitatory connections. Nature 457:1142–1145.
Rasmusson DD, Clow K, Szerb JC (1992) Frequency-dependent increase in cortical acetylcholine release evoked by stimulation of the nucleus basalis magnocellularis in the rat. Brain Res 594:150–154.
Remy S, Spruston N (2007) Dendritic spikes induce single-burst long-term potentiation. Proc Natl Acad Sci USA 104:17192–17197.
Sarter M, Bruno JP (2000) Cortical cholinergic inputs mediating arousal, attentional processing and dreaming: differential afferent regulation of the basal forebrain by telencephalic and brainstem afferents. Neuroscience 95:933–952.
Sarter M, Bruno JP, Givens B (2003) Attentional functions of cortical cholinergic inputs: what does it mean for learning and memory? Neurobiol Learn Mem 80:245–256.
Sheth BR, Moore CI, Sur M (1998) Temporal modulation of spatial borders in rat barrel cortex. J Neurophysiol 79:464–470.
Teyler TJ, Hamm JP, Clapp WC, Johnson BW, Corballis MC, Kirk IJ (2005) Long-term potentiation of human visual evoked responses. Eur J Neurosci 21:2045–2050.
Urban J, Kossut M, Hess G (2002) Long-term depression and long-term potentiation in horizontal connections of the barrel cortex. Eur J Neurosci 16:1772–1776.
Wester JC, Contreras D (2012) Columnar interactions determine horizontal propagation of recurrent network activity in neocortex. J Neurosci 32:5454–5471.
Wright N, Fox K (2010) Origins of cortical layer V surround receptive fields in the rat barrel cortex. J Neurophysiol 103:709–724.
Yamasaki M, Matsui M, Watanabe M (2010) Preferential localization of muscarinic M1 receptor on dendritic shaft and spine of cortical pyramidal cells and its anatomical evidence for volume transmission. J Neurosci 30:4408–4418.

(Accepted 26 September 2014)
(Available online 2 October 2014)

A.2. Article 2 (published)

SYNAPTIC PLASTICITY IN THE SOMATOSENSORY CORTEX

Neurotransmitter 2015; 2: e588. doi: 10.14800/nt.588; © 2015 by *Natali Barros-Zulaica, et al.*
http://www.smartscitech.com/index.php/nt

REVIEW

Synaptic Plasticity in the Somatosensory Cortex

Natali Barros-Zulaica[1,2], Angel Nuñez[1]

[1]*Departamento de Anatomía, Histología y Neurociencia, Facultad de Medicina, Universidad Autónoma de Madrid, 28029 Madrid, Spain*
[2]*Département des Systèmes d'Information; Faculté des Hautes Etudes Commerciales, Université de Lausanne, Lausanne, Switzerland*

Correspondence: Angel Nuñez
E-mail: angel.nunez@uam.es
Received: February 02, 2015
Published online: February 22, 2015

The term synaptic plasticity implies modification in the strength or efficacy of synaptic transmission between pre-existing synapses. Long-term changes in synaptic efficacy have been widely proposed as the cellular mechanism of the learning and memory machineries of the brain. However both the induction and expression mechanisms of synaptic plasticity processes remain elusive and more diverse than formerly though. In this review we show the principal mechanisms of experience-dependent plasticity in the somatosensory barrel cortex. The somatosensory barrel cortex is composed of local circuits interconnected by vertical and horizontal projections. Sensory information from the whiskers is transmitted through the brain stem and thalamus to layer 4 neurons in the barrel cortex. Sensory responses are relayed from layer 4 to layer 2/3 and then to layer 5 and layer 6. At the same time, there is feedback from layer 5 to layer 2/3 and layer 6 to layer 4. This vertical organization is linked horizontally by strong projections between barrels. Distinct synaptic and intrinsic properties of these neurons are involved in different sensory plasticity responses observed in the barrel cortex.

Keywords: LTP; STDP; NMDA; acetylcholine; whisker response; barrel cortex; sensory plasticity

To cite this article: Natali Barros-Zulaica, *et al*. Synaptic Plasticity In The Somatosensory Cortex. Neurotransmitter 2015; 2: e588. doi: 10.14800/nt.588.

Introduction

One of the most important objectives in Neuroscience has been to unravel the synaptic plasticity mechanisms that build up memory, learning and adaptive behavior processes. In this review we will perform a summary of the principal mechanisms of experience-dependent plasticity in the somatosensory barrel cortex that have been studied.

Plasticity is one of the most fascinating properties of the mammalian brain that has the ability to modify, through experience, the functions and formation of neural circuits and consequently thoughts, feelings and actions. Thus, plasticity is an adaptive capacity that allows the brain to learn and memorize sensory experiences, to improve movements and to recover functions after injury. This is a relatively new concept that was discovered in 1949 by Donald Hebb, who proposed the idea that these important modifications were consequences of several synaptic changes and that if these changes between synapsis remained in time, then some information had been stored in the circuit in which the synapsis was embedded.

This phenomenon was called synaptic plasticity and refers to the modification in the strength or efficacy of synaptic transmission between pre-existing synapses. Synaptic plasticity is a crucial process for a healthy brain, and is thought to play an important role in the development of neural circuits. In fact, dysfunctional plasticity processes reveal serious neuropsychiatric disorders[1].

There are three main paradigms for studying sensory

plasticity: one of these is experience-dependent map plasticity. In all species there is a broadly somatotopic representation of the body in the primary somatosensory cortex (S1) as well as in other subcortical relay stations. Similarly, auditory and visual cortices have a topographical map of the cochlea and retina, respectively. These sensory maps may change in adults as a result of modifications of peripheral inputs or behaviorally important experience throughout life [2, 3]. There are several works in which rats or mice were taught to explore their environment using their whiskers. What these researchers observed was that, as rats and mice learned, the S1 cortex generated qualitatively different neuronal responses, reorganizing the somatosensory functional map[4]. Another way of studying plasticity is by blocking or causing an injury in nuclei or any small part of the studied pathway. Many studies have been performed in which changes in the functional map could be seen after inflicting damage along the studied pathway. For example, removing several whisker follicles eliminates completely the whisker sensory input resulting in major changes in somatosensory functional maps [2, 3].A further way of seeing changes in neural maps is to make sensory stimulations and observe how the neural response and its connections have changed. Accordingly, there are studies where a repetitive stimulation was performed in order to study synaptic plasticity processes [5, 6]. This is the method we followed in our laboratory where we observed that a repetitive whisker stimulation at different frequencies in an anesthetized rat resulted in a frequency-specific, long-lasting increase in neuronal responses in the S1 barrel cortex. The stimulation frequencies used in the experiments were selected from the range of frequencies that rats use to explore the environment. Overall, our results suggested that natural, rhythmic stimulation of whiskers can modify sensory processing, providing a possible mechanism for learning during sensory perception [5].

Consequently, synaptic plasticity may be the neurobiological foundation for processing and storing sensory information, because synaptic transmission can be increased or depressed according to sensory experience and these changes can remain from milliseconds to hours, days or even longer [7]. In the early 1970s Bliss and colleagues established that repetitive stimulation of excitatory synapses in the hippocampus caused a potentiation of synaptic strength that could last for minutes or days [8]. This phenomenon was called Long-Term Potentiation [LTP]; many studies have been performed in order to learn how this process works for achieving the storage of information into a neuronal circuit by the repetitive stimulation of the synapses. In addition, prolonged repetitive stimulation at low frequencies [0.5-5 Hz] may induce a Long-Term Depression [LTD] [9]. The balance between LTP and LTD processes in the cortex probably modulates sensory responses and may be the main candidate that rules many forms of experience-dependent plasticity.

Synaptic Plasticity In Glutamatergic Pathways

Glutamate is a neurotransmitter normally involved in learning and memory processes since the modulation of glutamate receptors contributes to synaptic plasticity. The postsynaptic cell has two major ionotropic glutamate receptors, namely α-amino-3-hydroxy-5-methyl-4-isoxazole propionic acid receptor [AMPAR] and N-methyl-D-aspartate receptor [NMDAR], which bind to the glutamate and are activated. The next steps in the process are as follows: firstly, the AMPAR provides most of the inward current that generates the excitatory postsynaptic potential (EPSP) through a channel that is permeable to monovalent cations (Na^+ and K^+). Secondly, the NMDARs can be activated, depending on the voltage, due to the blocking of their channel at negative membrane potentials by extracellular magnesium [Mg^{2+}]. Through NMDARs, Ca^{2+} and Na^+ ions can pass into the postsynaptic neuron. LTP takes place at glutamatergic synapses in many brain areas such as the hippocampus and the neocortex[10, 11].

How a long-lasting plasticity process such as LTP can be maintained over an extended period is still partially unknown. However, there is a hypothesis in this regard: the increase in Ca^{2+} concentration leads to activation of intracellular second messengers involving a number of protein kinases, mainly calcium/calmodulin-dependent protein kinase II (CaMKII)[12, 13]. This promotes the addition of AMPRs into the post-synaptic density. At the same time some structural changes occur within the synapsis, for example the size of the post-synaptic density and dendritic spines increase. Further post-synapsis changes drive an enhancement of the pre-synaptic size, indicating that the synapsis has been potentiated and strengthened. If this increment in the synaptic weight should be maintained for hours or days, the processes described must remain active for a certain time in order to maintain the synaptic strength [7].

Plasticity processes in the sensory cortex are mainly due to the activation of NMDARs that induce a long-lasting enhancement or depression of the response to a stimulus[14]. In the neocortex, repetitive stimulation of excitatory synapses produces in most cases a classic NMDA-LTP. This experience may contribute to the correct formation and refinement of the receptive fields in the barrel cortex and hence, on the sensory cortical maps [2, 3]. However, animals in which the barrel cortex is chronically treated with the NMDAR antagonist, AP5, during the first postnatal week, fail to develop the topographical representational map of the

whiskers in S1 [2, 15]. In adults, many studies have concluded, by blocking NMDAR activation with AP5 or MK801 that the cortical LTP process performed within the cortex is mediated by NMDAR activation [5, 16].

Insertions of AMPA receptors in the membrane also contribute to the generation of these plasticity processes that can remain over time [17, 18]. Several studies were able to induce long-term plasticity processes in the cortex, between layers [12] and between different barrels [19], after repetitive stimulation.

Although plasticity is a property of the entire brain, the neocortex is a particularly relevant region for plasticity because it performs sensory, motor and cognitive tasks with strong learning components[3]. As examples, Mégevand and colleagues [6] induced a long-term response facilitation through 10 minutes of 8 Hz whisker stimulation in the granular and supragranular layers of the barrel cortex that lasted for over 90 minutes. Similarly, it has been reported that electrical stimulation of layer 4 induces LTP in layers 2/3 of rat neurons recorded *in vivo*[20] or in mice recorded *in vitro*[21].

Many studies have been conducted which conclude, by blocking NMDAR activation with APV or MK801, that the LTP process performed in the cortex is mediated by NMDAR [5, 22, 23]. Concretely, the somatosensory pathway belonging to the whiskers has proven to be a powerful system for studying somatosensory plasticity in many researchers [5, 10, 24, 25]. Whiskers are active tactile detectors represented by a cluster of neurons called barrels in layer 4 [26]. Many studies show that repetitive whisker stimulation at a frequency of around 5 Hz generates an enhancement of the recorded neuronal response, which means a LTP process.

Another surprising property of synaptic plasticity is that it is considered to be crucial during development. Repetitive whisker stimulation induces a long-lasting increase in the evoked potential amplitude in layers 2/3 and 4 of the barrel cortex of neonatal rats or mice [27, 28], suggesting that it may participate in the activity-dependent wiring of the cortex during development. Furthermore, recent studies confirm the existence of plasticity in mature mammalians showing that repetitive stimulation can induce synaptic plasticity including LTP of cortical responses evoked by sensory inputs in humans and adult animals[6, 29, 30]. It is well known that this type of plasticity can also occur in other cortical areas, such as the visual or auditory cortex, in which the principal mechanisms are common. This is not really surprising because plasticity relies on properties at cellular level that are similar in these systems. However, the type of basal activity that drives plasticity may be different in each cortical area, and as this issue has not yet been studied in depth it may well give us some surprises in future researches [10]. For example, stimulation frequencies between 4-12 Hz that are typically used for studying the whisker somatosensory system [rhythmic movements of the whiskers used by rodents during active exploration] induce LTP in the S1 cortex [5].

Traditionally, LTP is induced by short bursts of high-frequency stimulation or by pairing low-frequency stimulation with postsynaptic depolarization. Moreover, it has been establish that temporal stimulation pattern is important to induce LTP. For example, Levy and Steward [31] demonstrated that when a weak and a strong input from the entorhinal cortex to the dentate gyrus were activated together, the temporal order of activation was crucial. LTP of the weak input was induced when the strong input was activated concurrently with the weak input or following it by as much as 20 ms. However, LTD was induced when the temporal order was reversed. Later studies have further addressed the importance of the temporal order of pre- and postsynaptic spiking in long-term modification of a variety of glutamatergic synapses and have defined the "critical windows" for spike timing [1]. This form of activity-dependent LTP/LTD is now referred to as spike timing-dependent plasticity (STDP) [32]. Consequently, synaptic modifications depend on the temporal order of the pre- and postsynaptic activation, which allow the Ca^{2+} to enter the cell through NMDARs and to induce synaptic plasticity. The classic LTP and STDP obey the "Hebbian" rule. Thus, repetition of temporally correlated pre- and postsynaptic activity is required to induce synaptic plasticity.

Despite the importance of STDP in the creation of LTP, some studies have stated that this process might not be as important as we thought regarding *in vivo* brain, because the intact brain must be governed by much more complex rules [33].

Effect Of Acetylcholine In Synaptic Plasticity

Acetylcholine (ACh) has a variety of effects as a neuromodulator upon synaptic plasticity, attention, learning, memory, arousal and reward [34-38]. The basal forebrain is the major source of cholinergic afferents to the neocortex [39-41]. In Alzheimer's and related neurodegenerative diseases, there is an important loss of cholinergic system. Thus, ACh is essential to normal CNS function, modulating the activity of the cortex and subcortical regions, regulating networks activity in many important brain functions during arousal and, probably, during paradoxical sleep [42-45]. It is well known that ACh enhances synaptic plasticity in the hippocampus and neocortex [23, 46-49].

ACh modifies brain activity through nicotinic and muscarinic receptors that have several presynaptic and postsynaptic effects on neurons. Activation of nicotinic cholinergic receptors enhances synaptic transmission [50]. Activation of muscarinic cholinergic receptors also increases neuronal excitability and responsiveness for a longer lasting period than nicotinic receptors in pyramidal cortical neurons [51, 52]. Contrariwise, under different conditions, such as high ACh exogenous concentration, it is possible to observe a decrease of the activity in the cortex [52]. It has been studied that this can happen whenever there is a suitable extracellular concentration of ACh. Insufficient or excessive levels of ACh prevent the plasticity process from taking place, promoting inhibition[53]. This means that ACh has to be at the optimum concentration for each important process it is involved in, which is why is called a neuromodulator. Thus Ach regulates both activation and inhibition.

ACh regulates inhibition because it also activates muscarinic receptors placed in GABAergic interneurons [50]. This is one of the reasons why ACh has such different effect in the cortex. It is thought that this complex behavior is due to the effect of ACh on a different subtype of cholinergic receptors and over second messengers [23, 53, 54]. Furthermore, cholinergic mechanisms have been implicated as a necessary substrate for the reorganization of cortical maps following manipulations of peripheral inputs[55, 56]. Importantly, ACh exerts highly selective, input-specific effects in the visual, pyriform and S1 cortex, with a facilitatory effect on thalamocortical inputs and a profound suppression of intracortical connections[47, 52, 57, 58].

Microiontophoresis of ACh induces a long-lasting increase of sensory responses, including uncovering new receptive fields and increasing receptive field size in the somatosensory [59], visual [60] or auditory cortex [51]. Electrical stimulation of the basal forebrain (the main source of ACh in the cortex)induces a potent enhancement of the responses evoked by whisker deflections in barrel cortical neurons [5, 23, 52, 61]. The response enhancement induced by basal forebrain stimulation is reduced by the muscarinic AChR antagonist atropine. Also, the response enhancement is largely caused by an increased late response that roughly corresponds to the timing of the NMDA-spike and action potential burst evoked by thalamocortical synaptic inputs. Consequently, mAChR-induced and NMDAR-mediated mechanisms are responsible for the long-lasting increase of sensory responses evoked by basal forebrain stimulation.

According to the above results, ACh has a complex effect in the modulation of cortical sensory response [62, 63]. This circumstance has an important role in sensory processing because the level of ACh is higher in wakefulness and REM sleep than during slow sleep stages [42, 64]. Moreover, the basal forebrain has been implicated in a variety of behavioral functions, including learning, memory and attention, increasing the level of ACh in the cortex [34-38]. Consequently, the neuronal response to identical sensory stimuli changes during the sleep-wakefulness cycle or according to attention.

ACh has a significant effect on the plasticity of cortical excitability because ACh can change the response pattern to glutamatergic inputs, usually by facilitating responses to glutamatergic inputs and reinforcement of the synchronous activity between cortical pyramidal neurons. Moreover, it has been described that ACh increases excitability and synaptic excitation by membrane depolarization, raising the input resistance, and reducing local GABAergic inhibition [23]. These changes result in the generation of all-or-none Ca^{2+} spikes, displaying properties of NMDA-spikes. Therefore, cholinergic activity can switch the output of cortical pyramidal neurons from single spikes to a bursting spike mode that could have fundamental consequences in the processing of sensory information in the barrel cortex [65-67].

Conclusions

The results shown above demonstrate that glutamatergic transmission is fundamental in sensory pathways to transmit stimuli from peripheral receptors to the cortex. The AMPA-component of the EPSP, precisely transmits information from one neuron to others. The NMDA-dependent component of the EPSP has more plastic properties: it increases the amplitude and duration of the evoked EPSPs at depolarized membrane potentials or during repetitive stimulation, thus enhancing the possibility of synaptic interactions by temporal summation between successive EPSPs. Moreover, Ca^{2+} flowing through NMDARs may trigger different forms of synaptic plasticity as has been shown in different systems [14, 22].

The response pattern evoked by a single stimulus is crucial to evoke synaptic plasticity. For example, short spike bursts at ≥100 Hz may induce dendritic Ca^{2+}electrogenesis in distal compartments of cortical neurons, which in turn determines dendritic plasticity mechanisms [68, 69]. Hence, the activation of NMDA receptors in cortical neurons causes a potent and sustained response enhancement with possible consequences in plastic properties and sensory processing that are present during natural whisking [5, 6, 70, 71].

Moreover, the interaction between NMDAR and ACh may have important roles in sensory processing, as has been indicated previously. For instance, it is established that ACh is related to attention, and is thought to be delivered when a

stimulus must be processed in a specific and precise manner. This concept can explain how the barrel cortex could enhance the detection of a single whisker contact and process only the information belonging to this whisker in a very specific way while the other whiskers are transmitting information at the same time but are ignored, as may also occur with synaptic inputs from other sensory systems [36, 38].

Although glutamate and ACh are the main neurotransmitters involved in synaptic plasticity process, it is known that others such as serotonin or dopamine are involved in this important issue. However, little is known about the importance of these neurotransmitters. In conclusion we must say that, despite all the work conducted striving to unravel synaptic-plasticity processes, more research is necessary for understanding this important process that is so relevant for life.

Conflict

No conflicts of interest, financial or otherwise, are declared by the authors.

Acknowledgements

This research was supported by a grant from Ministerio de Economia y Competitividad [BFU2012-36107].

References

1. Piochon C, Kloth AD, Grasselli G, Titley HK, Nakayama H, Hashimoto K, *et al*. Cerebellar plasticity and motor learning deficits in a copy-number variation mouse model of autism. Nat Commun 2014;5:5586.
2. Buonomano DV, Merzenich MM. Cortical plasticity: From synapses to maps. Annu Rev Neurosci 1998;21:149-186.
3. Kaas JH. Neurobiology: How cortex reorganizes. Nature 1995;375:735-736.
4. Wiest MC, Thomson E, Pantoja J, Nicolelis MA. Changes in S1 neural responses during tactile discrimination learning. J Neurophysiol 2010;104:300-312.
5. Barros-Zulaica N, Castejon C, Nuñez A. Frequency-specific response facilitation of supra and infragranular barrel cortical neurons depends on NMDA receptor activation in rats. Neuroscience 2014;281C:178-194.
6. Megevand P, Troncoso E, Quairiaux C, Muller D, Michel CM, Kiss JZ. Long-term plasticity in mouse sensorimotor circuits after rhythmic whisker stimulation. J Neurosci 2009;29:5326-5335.
7. Citri A, Malenka RC. Synaptic plasticity: multiple forms, functions, and mechanisms. Neuropsychopharmacology 2008;33:18-41.
8. Bliss TV, Lomo T. Long-lasting potentiation of synaptic transmission in the dentate area of the anaesthetized rabbit following stimulation of the perforant path. J Physiol 1973;232:331-356.
9. Mulkey RM, Malenka RC. Mechanisms underlying induction of homosynaptic long-term depression in area CA1 of the hippocampus. Neuron 1992;9:967-975.
10. Feldman DE. Synaptic mechanisms for plasticity in neocortex. Annu Rev Neurosci 2009;32:33-55.
11. Malenka RC, Bear MF. LTP and LTD: an embarrassment of riches. Neuron 2004;44:5-21.
12. Hardingham N, Glazewski S, Pakhotin P, Mizuno K, Chapman PF, Giese KP, *et al*. Neocortical long-term potentiation and experience-dependent synaptic plasticity require alpha-calcium/calmodulin-dependent protein kinase II autophosphorylation. J Neurosci2003;23:4428-4436.
13. Reymann KG, Frey JU. The late maintenance of hippocampal LTP: requirements, phases, 'synaptic tagging', 'late-associativity' and implications. Neuropharmacology 2007;52:24-40.
14. Thomson AM. Facilitation, augmentation and potentiation at central synapses. Trends Neurosci 2000;23:305-312.
15. Fox K, Glazewski S, Chen CM, Silva A, Li X. Mechanisms underlying experience-dependent potentiation and depression of vibrissae responses in barrel cortex. J Physiol Paris 1996;90:263-269.
16. Rema V, Armstrong-James M, Ebner FF. Experience-dependent plasticity of adult rat S1 cortex requires local NMDA receptor activation. The Journal of neuroscience J Neurosci1998;18:10196-10206.
17. Daw MI, Bannister NV, Isaac JT. Rapid, activity-dependent plasticity in timing precision in neonatal barrel cortex. J Neurosci 2006;26:4178-4187.
18. Remy S, Spruston N. Dendritic spikes induce single-burst long-term potentiation. Proc Natl Acad Sci U S A 2007;104:17192-17197.
19. Urban J, Kossut M, Hess G. Long-term depression and long-term potentiation in horizontal connections of the barrel cortex. Eur J Neurosci 2002;16:1772-1776.
20. Glazewski S, Herman C, McKenna M, Chapman PF, Fox K. Long-term potentiation in vivo in layers II/III of rat barrel cortex. Neuropharmacology 1998;37:581-592.
21. Banerjee A, Meredith RM, Rodriguez-Moreno A, Mierau SB, Auberson YP, Paulsen O. Double dissociation of spike timing-dependent potentiation and depression by subunit-preferring NMDA receptor antagonists in mouse barrel cortex. Cereb Cortex 2009;19:2959-2969.
22. Malenka RC, Nicoll RA. NMDA-receptor-dependent synaptic plasticity: multile forms and mechanisms. Trends Neurosci 1993;16:521-526.
23. Nuñez A, Dominguez S, Buño W, Fernandez de Sevilla D. Cholinergic-mediated response enhancement in barrel cortex layer V pyramidal neurons. J Neurophysiol 2012;108:1656-1668.
24. Hogsden JL, Dringenberg HC. Decline of long-term potentiation [LTP] in the rat auditory cortex in vivo during postnatal life: involvement of NR2B subunits. Brain Res 2009;1283:25-33.
25. Pais-Vieira M, Lebedev MA, Wiest MC, Nicolelis MA. Simultaneous top-down modulation of the primary somatosensory cortex and thalamic nuclei during active tactile discrimination. J Neurosci2013;33:4076-4093.

26. Woolsey TA, Van der Loos H. The structural organization of layer IV in the somatosensory region [SI] of mouse cerebral cortex. The description of a cortical field composed of discrete cytoarchitectonic units. Brain Res 1970;17:205-242.

27. An S, Yang JW, Sun H, Kilb W, Luhmann HJ. Long-term potentiation in the neonatal rat barrel cortex in vivo. J Neurosci 2012;32:9511-9516.

28. Borgdorff AJ, Poulet JF, Petersen CC. Facilitating sensory responses in developing mouse somatosensory barrel cortex. J Neurophysiol 2007;97:2992-3003.

29. Clapp WC, Kirk IJ, Hamm JP, Shepherd D, Teyler TJ. Induction of LTP in the human auditory cortex by sensory stimulation. Eur J Neurosci 2005;22:1135-1140.

30. Clapp WC, Muthukumaraswamy SD, Hamm JP, Teyler TJ, Kirk IJ. Long-term enhanced desynchronization of the alpha rhythm following tetanic stimulation of human visual cortex. Neurosci Lett 2006;398:220-223.

31. Levy WB, Steward O. Synapses as associative memory elements in the hippocampal formation. Brain Res 1979;175:233-245.

32. Dan Y, Poo MM. Spike timing-dependent plasticity of neural circuits. Neuron 2004;44:23-30.

33. Schulz J. Synaptic plasticity in vivo: more than just spike-timing? Front Synaptic Neurosci 2010;2:150.

34. Alenda A, Nuñez A. Cholinergic modulation of sensory interference in rat primary somatosensory cortical neurons. Brain Res 2007;1133:158-167.

35. Everitt BJ, Robbins TW. Central cholinergic systems and cognition. Annu Rev Psychol 1997;48:649-684.

36. Golmayo L, Nuñez A, Zaborszky L. Electrophysiological evidence for the existence of a posterior cortical-prefrontal-basal forebrain circuitry in modulating sensory responses in visual and somatosensory rat cortical areas. Neuroscience 2003;119:597-609.

37. Rasmusson DD. The role of acetylcholine in cortical synaptic plasticity. Behav Brain Res 2000;115:205-218.

38. Sarter M, Bruno JP. Cortical cholinergic inputs mediating arousal, attentional processing and dreaming: Differential afferent regulation of the basal forebrain by telencephalic and brainstem afferents. Neuroscience 2000;95:933-952.

39. Mesulam M-M, Mufson EJ, Wainer BH, Levey AI. Central cholinergic pathways in the rat: an overview based on an alternative nomenclature (Ch1-Ch6). Neuroscience 1983;10:1185-1201.

40. Semba K. Multiple output pathways of the basal forebrain: organization, chemical heterogeneity, and roles in vigilance. Behav Brain Res 2000;115:117-141.

41. Zaborszky L, Buhl DL, Pobalashingham S, Bjaalie JG, Nadasdy Z. Three-dimensional chemoarchitecture of the basal forebrain: spatially specific association of cholinergic and calcium binding protein-containing neurons. Neuroscience2005;136:697-713.

42. Buzsaki G, Bickford RG, Ponomareff G, Yhal LJ, Mandel R, Gage FH. Nucleus basalis and thalamic control of neocortical activity in the freely moving rat. Neuroscience 1988;8:4007-4026.

43. Hasselmo ME, Sarter M. Modes and models of forebrain cholinergic neuromodulation of cognition. Neuropsychopharmacology 2011;36[1]:52-73.

44. Nuñez A. Unit activity of rat basal forebrain neurons: Relationship to cortical activity. Neuroscience 1996;72:757-766.

45. Szymusiak R, Alam N, McGinty D. Discharge patterns of neurons in cholinergic regions of the basal forebrain during waking and sleep. Behav Brain Res 2000;115:171-182.

46. Fernandez de Sevilla D, Nuñez A, Borde M, Malinow R, Buño W. Cholinergic-mediated IP3-receptor activation induces long-lasting synaptic enhancement in CA1 pyramidal neurons. J Neurosci 2008;28:1469-1478.

47. Kuo MC, Rasmusson DD, Dringenberg HC. Input-selective potentiation and rebalancing of primary sensory cortex afferents by endogenous acetylcholine. Neuroscience 2009;163:430-441.

48. Metherate R, Ashe JH. Nucleus basalis stimulation facilitates thalamocortical synaptic transmission in the rat auditory cortex. Synapse 1993;14:132-143.

49. Bueno-Junior LS, Lopes-Aguiar C, Ruggiero RN, Romcy-Pereira RN, Leite JP. Muscarinic and nicotinic modulation of thalamo-prefrontal cortex synaptic plasticity [corrected] in vivo. PloS one 2012;7:e47484.

50. Xiang Z, Huguenard JR, Prince DA. Cholinergic switching within neocortical inhibitory networks. Science 1998;281:985-988.

51. Metherate R, Weinberger NM. Cholinergic modulation of responses to single tones produces tone-specific receptive field alterations in cat auditory cortex. Synapse 1990;6:133-145.

52. Oldford E, Castro-Alamancos MA. Input-specific effects of acetylcholine on sensory and intracortical evoked responses in the "barrel cortex" in vivo. Neuroscience 2003;117:769-778.

53. Shulz DE, Ego-Stengel V, Ahissar E. Acetylcholine-dependent potentiation of temporal frequency representation in the barrel cortex does not depend on response magnitude during conditioning. J Physiol Paris 2003;97:431-439.

54. Miranda MI, Ramirez-Lugo L, Bermudez-Rattoni F. Cortical cholinergic activity is related to the novelty of the stimulus. Brain Res 2000;882:230-235.

55. Juliano SL, Ma W, Eslin D. Cholinergic depletion prevents expansion of topographic maps in somatosensory cortex. Proc Natl Acad Sci U S A 1991;88:780-784.

56. Sachdev R, Lu SM, Wiley RG, Ebner FF. Role of the basal forebrain cholinergic projection in somatosensory cortical plasticity. J Neurophysiol 1998;79:3216-3228.

57. Hasselmo ME, Bower JM. Cholinergic suppression specific to intrinsic not afferent fiber synapses in rat piriform [olfactory] cortex. J Neurophysiol1992;67:1222-1229.

58. Kimura F, Fukuda M, Tsumoto T. Acetylcholine suppresses the spread of excitation in the visual cortex revealed by optical recording: possible differential effect depending on the source of input. Eur J Neurosci 1999;11:3597-3609.

59. Donoghue JP, Carroll KL. Cholinergic modulation of sensory responses in rat primary somatic sensory cortex. Brain Res 1987;408:367-371.

60. Sillito AM, Kemp JA. Cholinergic modulation of the functional organization of the cat visual cortex. Brain Res

1983;280:299-307.

61. Webster HH, Rasmusson DD, Dykes RW, Schliebs R, Schober W, Bruckner G, *et al*. Long-term enhancement of evoked potentials in raccoon somatosensory cortex following co-activation of the nucleus basalis of Meynert complex and cutaneous receptors. Brain Res 1991;545:292-296.
62. Castro-Alamancos MA. Cortical up and activated states: implications for sensory information processing. Neuroscientist 2009;15:625-634.
63. Noori HR, Fliegel S, Brand I, Spanagel R. The impact of acetylcholinesterase inhibitors on the extracellular acetylcholine concentrations in the adult rat brain: a meta-analysis. Synapse 2012;66:893-901.
64. Steriade M. Acetylcholine systems and rhythmic activities during the waking--sleep cycle. Prog Brain Res 2004;145:179-196.
65. Giocomo LM, Hasselmo ME. Neuromodulation by glutamate and acetylcholine can change circuit dynamics by regulating the relative influence of afferent input and excitatory feedback. Mol Neurobiol 2007;36:184-200.
66. Major G, Polsky A, Denk W, Schiller J, Tank DW. Spatiotemporally graded NMDA spike/plateau potentials in basal dendrites of neocortical pyramidal neurons. J Neurophysiol 2008;99:2584-2601.
67. Yuste R, Tank DW. Dendritic integration in mammalian neurons, a century after Cajal. Neuron 1996;16:701-716.
68. Larkum ME, Waters J, Sakmann B, Helmchen F. Dendritic spikes in apical dendrites of neocortical layer 2/3 pyramidal neurons. J Neurosci 2007;27:8999-89008.
69. Stuart GJ, Sakmann B. Active propagation of somatic action potentials into neocortical pyramidal cell dendrites. Nature 1994;367:69-72.
70. de Kock CP, Sakmann B. Spiking in primary somatosensory cortex during natural whisking in awake head-restrained rats is cell-type specific. Proc Natl Acad Sci U S A 2009;106:16446-16450.
71. Gambino F, Pages S, Kehayas V, Baptista D, Tatti R, Carleton A, *et al*. Sensory-evoked LTP driven by dendritic plateau potentials in vivo. Nature 2014;515:116-119.

A.3. Article 3 (published)

MODULATION OF SPECIFIC SENSORY CORTICAL AREAS BY SEGREGATED BASAL FOREBRAIN CHOLINERGIC NEURONS DEMONSTRATED BY NEURONAL TRACING AND OPTOGENETIC STIMULATION IN MICE

frontiers in Neural Circuits

ORIGINAL RESEARCH
published: 20 April 2016
doi: 10.3389/fncir.2016.00028

Modulation of Specific Sensory Cortical Areas by Segregated Basal Forebrain Cholinergic Neurons Demonstrated by Neuronal Tracing and Optogenetic Stimulation in Mice

*Irene Chaves-Coira†, Natali Barros-Zulaica†, Margarita Rodrigo-Angulo and Ángel Núñez**

Departamento de Anatomía, Histología y Neurociencia, Facultad de Medicina, Universidad Autónoma de Madrid, Madrid, Spain

Neocortical cholinergic activity plays a fundamental role in sensory processing and cognitive functions. Previous results have suggested a refined anatomical and functional topographical organization of basal forebrain (BF) projections that may control cortical sensory processing in a specific manner. We have used retrograde anatomical procedures to demonstrate the existence of specific neuronal groups in the BF involved in the control of specific sensory cortices. Fluoro-Gold (FlGo) and Fast Blue (FB) fluorescent retrograde tracers were deposited into the primary somatosensory (S1) and primary auditory (A1) cortices in mice. Our results revealed that the BF is a heterogeneous area in which neurons projecting to different cortical areas are segregated into different neuronal groups. Most of the neurons located in the horizontal limb of the diagonal band of Broca (HDB) projected to the S1 cortex, indicating that this area is specialized in the sensory processing of tactile stimuli. However, the nucleus basalis magnocellularis (B) nucleus shows a similar number of cells projecting to the S1 as to the A1 cortices. In addition, we analyzed the cholinergic effects on the S1 and A1 cortical sensory responses by optogenetic stimulation of the BF neurons in urethane-anesthetized transgenic mice. We used transgenic mice expressing the light-activated cation channel, channelrhodopsin-2, tagged with a fluorescent protein (ChR2-YFP) under the control of the choline-acetyl transferase promoter (ChAT). Cortical evoked potentials were induced by whisker deflections or by auditory clicks. According to the anatomical results, optogenetic HDB stimulation induced more extensive facilitation of tactile evoked potentials in S1 than auditory evoked potentials in A1, while optogenetic stimulation of the B nucleus facilitated either tactile or auditory evoked potentials equally. Consequently, our results suggest that cholinergic projections to the cortex are organized into segregated pools of neurons that may modulate specific cortical areas.

Keywords: diagonal band of Broca, nucleus basalis magnocellularis, cholinergic projections, cholinergic facilitation, cortical evoked potentials, transgenic mice

OPEN ACCESS

Edited by:
Edward S. Ruthazer, McGill University, Canada

Reviewed by:
Dirk Feldmeyer, Rheinisch-Westfälische Technische Hochschule (RWTH) Aachen University, Germany
Gertrudis Perea, Instituto Cajal, Spain

****Correspondence:***
Ángel Núñez
angel.nunez@uam.es

†These authors have contributed equally to this work.

Received: *11 January 2016*
Accepted: *29 March 2016*
Published: *20 April 2016*

Citation:
Chaves-Coira I, Barros-Zulaica N, Rodrigo-Angulo M and Núñez Á (2016) Modulation of Specific Sensory Cortical Areas by Segregated Basal Forebrain Cholinergic Neurons Demonstrated by Neuronal Tracing and Optogenetic Stimulation in Mice. Front. Neural Circuits 10:28. doi: 10.3389/fncir.2016.00028

INTRODUCTION

Acetylcholine (ACh) is essential to normal central nervous system (CNS) function, modulating the activity of the thalamocortical network in many important brain functions, such as arousal (e.g., Buzsáki et al., 1988; Détári, 2000; Szymusiak et al., 2000; Lee et al., 2004; Goard and Dan, 2009), attention (Chiba et al., 1999; Sarter et al., 2003), learning (Wilson and Rolls, 1990a,b; Mayse et al., 2015) and memory (Pauli and O'Reilly, 2008; Hasselmo and Sarter, 2011; Luchicchi et al., 2014; Sarter et al., 2014). Moreover, ACh enhances synaptic plasticity in the hippocampus (Doralp and Leung, 2008; Fernández de Sevilla et al., 2008; Navarrete et al., 2012) and neocortex (Metherate and Ashe, 1993; Kuo et al., 2009; Bueno-Junior et al., 2012; Núñez et al., 2012; Barros-Zulaica et al., 2014; Martin-Cortecero and Núñez, 2014).

In the CNS, ACh transmission is mainly guaranteed by dense innervation of cortical and subcortical regions from disperse groups of cholinergic neurons within the basal forebrain (BF) and the pontine-mesencephalic nuclei. The BF contains a diverse population of neurons, including cortically-projecting cholinergic and noncholinergic neurons as well as various interneurons (Zaborszky et al., 2012). The BF includes the medial septum, horizontal and vertical limbs of the diagonal band of Broca (HDB and VDB, respectively), the substantia innominata (SI), and the nucleus basalis magnocellularis (B), which provide the majority of the cholinergic innervation to the sensory, motor and prefrontal cortices and hippocampus (Semba and Fibiger, 1989; Semba, 2000; Zaborszky et al., 2012, 2015).

Early anatomical descriptions of cholinergic projections were consistent with the notion of a diffuse pathway from the BF to the cortex (Saper, 1987). Nearly all cortical areas and regions are innervated by BF cholinergic neurons (Eckenstein et al., 1988; Lysakowski et al., 1989; Callaway and Henriksen, 1992; Golmayo et al., 2003). However, newer evidence concerning the BF system indicates the existence of a highly structured and topographic organization of efferent projections to sensory cortices (Zaborszky, 2002; Golmayo et al., 2003; Zaborszky et al., 2005, 2015). The above mentioned authors propose that cholinergic and noncholinergic projections to the neocortex are not diffuse but instead are organized into segregated or overlapping neuronal groups (Zaborszky et al., 2015).

Studies measuring cortical ACh level have demonstrated that visual stimulation causes much greater ACh release in visual cortex than in non-visual cortical areas (Collier and Mitchell, 1966; Fournier et al., 2004; Laplante et al., 2005). However, anatomical tracing methods have not revealed any extensive projections from sensory relay nuclei to the BF (Semba et al., 1988; Zaborszky et al., 1991). Thus, it has been proposed that sensory information arrives at the BF through cortico-cortical projections from primary cortical sensory areas via the prefrontal cortex (Zaborszky et al., 1997). Results from both electrophysiological recordings (Golmayo et al., 2003) and inactivation of the prefrontal cortex (Rasmusson et al., 2007) have demonstrated that the prefrontal cortex is necessary for sensory-evoked cortical ACh release. These results strongly support the proposed specific pathway –sensory cortex to prefrontal cortex to BF– for each sensory modality.

In this study, we used retrograde anatomical procedures to demonstrate the existence of specific neuronal groups in the BF involved in the control of specific sensory cortices. Fluoro-Gold (FlGo) and Fast Blue (FB) fluorescent retrograde tracers were deposited into the primary somatosensory (S1) and primary auditory (A1) cortices in mice. In addition, we used an optogenetic method for selective stimulation of cholinergic neurons in the BF of transgenic mice to study the effect of selective stimulation of BF cholinergic neurons on cortical activity. Our studies suggest that cholinergic projections to the cortex are organized into segregated and overlapping pools of neurons that may modulate specific cortical areas.

MATERIALS AND METHODS

All animal procedures were approved by the Ethical Committee of the Autonomous University of Madrid, in accordance with European Community Council Directive 2010/63/UE. Efforts were made to minimize animal suffering as well as to reduce the number of animals used. Animals were housed in groups of two to four per cage in a temperature-controlled room with a 14/10 light/dark cycle. Food and water were provided *ad libitum*.

Anatomical Procedures

The anatomical pathways linking BF with cortical areas were studied by injecting or depositing the neuroanatomical fluorescent retrograde tracers (FlGo; Fluorochromes, Llc. Denver, CO, USA) and (FB; Polysciences, Inc. Warrington, PA, USA) in 18 B6.Cg-Tg (Chat-COP$_4$*H$_{134}$R/EYFP, Slc$_1$8a$_3$)5^{Gfng}/J mice. For a better understanding of the characteristics of the cortical afferent connections from BF, FlGo injections were made in the S1 cortex and FB deposits in the A1 cortex of the animals.

The mice were anesthetized with an intraperitoneal injection of a mixture of ketamine (70mg/kg) and xylazine (5 mg/kg) maintained with inhalation anesthetic Isofluorane (0.5%, maintenance doses) and placed in the stereotaxic frame. After appropriate craniotomy, 200 nl of a 4% saline dilution of FlGo was injected in the corresponding cortices of the animals by means of a 10 μl Hamilton syringe at stereotaxic coordinates: for S1 (AP −1.46 mm, L 3 mm, DV 1.5 mm) and A1 (AP −2.46 mm, L 4 mm, DV 2.2 mm), according to the Paxinos and Franklin (2003). Deposits of 0.5–1 mm^2 pieces of absorbable gelatin "Spongostan" soaked in a 1% saline solution of FB were placed on the appropriate cortex in the animals, for 15 min. Animals were treated with the longer-lasting analgesic buprex (0.075 mg/kg) at the end of the experiment. After a survival period of 1 week, animals were anesthetized with an overdose of the same anesthesia and perfused transcardially with 4% paraformaldehyde in 0.1 M phosphate buffer at pH 7.3 followed by increasing concentrations of sucrose solutions (5%, 10%, and 20%) in the same buffer. Brains were stored in 30% sucrose for at least 5 days for tissue cryopreservation and frozen sectioned

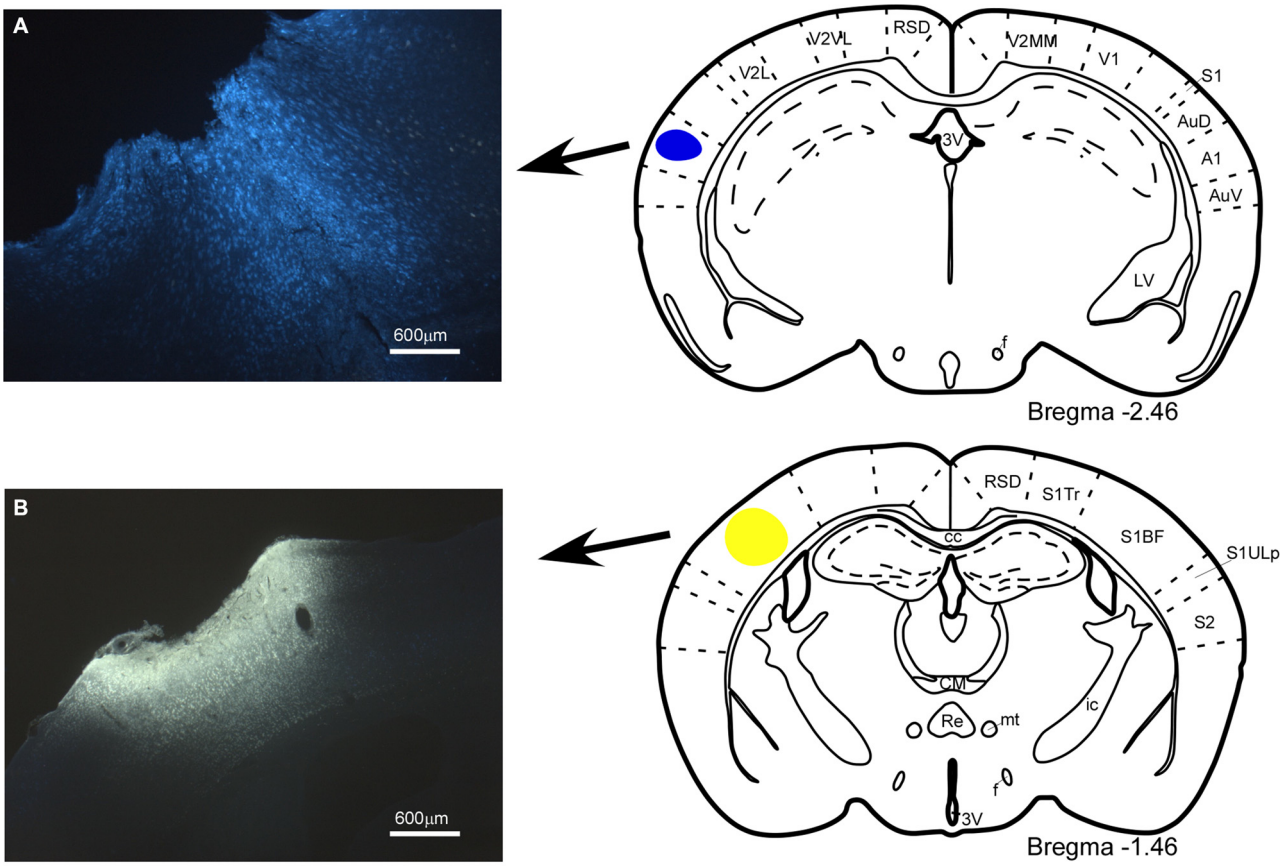

FIGURE 1 | Location of the injection and deposit of fluorescent retrograde tracers. Microphotographs of coronal brain sections and schematic drawings showing the injection sites of the retrograde tracers. **(A)** Fast Blue (FB), deposit in the A1 cortex; **(B)** Fluoro-Gold (FlGo), injection in the S1 cortex. In this and in the following figures, abbreviations are: 3V, 3rd ventricle; A1, primary auditory cortex; AuD, secondary auditory cortex, dorsal area; AuV, secondary auditory cortex, ventral area; cc, corpus callosum; CM, central medial thalamic nucleus; f, fornix; ic, internal capsule; LV, lateral ventricle; mt, mamillothalamic tract; Re, reuniens thalamic nucleus; RSD, retrosplenial dysgranular cortex; S1, primary somatosensory cortex; S1BF, primary somatosensory cortex, barrel field; S1Tr, primary somatosensory cortex, trunk region; S1ULp, primary somatosensory cortex, upper lip region; S2, secondary somatosensory cortex; V1, primary visual cortex; V2L, secondary visual cortex, lateral area; V2MM, secondary visual cortex, mediomedial area; V2MM, secondary visual cortex, mediomedial area. Calibration toolbar 600 μm.

on the coronal plane at 40 μm; sections were collected in three consecutive ordered series devoted to Nissl staining, fluorescent visualization and ChAT immunocytochemistry.

Series processed for Nissl staining were used for delimiting structures. Sections containing the cerebral cortex of the fluorescent visualization series were studied under a Nikon Axioskop fluorescent microscope. Sections for ChAT immunostaining were incubated with 1:100 goat anti-ChAT primary antibody (Chemicon AB144P) in a solution containing 20% normal rabbit serum, 5% bovine serum albumin (BSA), and 0.5% Triton X-100 in phosphate-buffered saline (PBS) for 36 h. Incubation in the secondary antibody was carried out with 1:200 biotinylated rabbit anti-goat (Chemicon) in the same solution for 2 h and in Elite ABC kit (Vector Laboratories Inc., Burlingame, CA, USA) for 1.5 h before development with 0.05% 3–3′DAB and 0.003% H_2O_2. These sections were studied under an optical/fluorescent microscope, so both ChAT positive neurons and fluorochrome labeled cells could be observed.

For a quantitative study, selected sections were analyzed under a confocal microscope (Leica TCSSP5), using the LASAF Software TileScan tool; samples were analyzed using bio-mapping (maximal projections) under both lin405 mm UV and linAr488 mm using a 10x objective for the quantification of neurons in each channel. Images were a stack of sections in maximal projection, but neurons were counted in each individual layer. Maximal projections of the images were analyzed in two channels (UV and green) and the merged image was also studied. The following procedure was used: (1) For neuronal counting in each channel we selected labeled neurons in each section of the region of interest (ROI). We eliminated the nonspecific background, moved the images to eight bits and then smoothed them with the filter to apply the previous segmentation particle analyzer. In some cases it was necessary to use the ROI from the BG subtraction plugin tool and Watershed tool to separate and count labeled neurons correctly. In cases where the particle analyzer results were entirely satisfactory they were

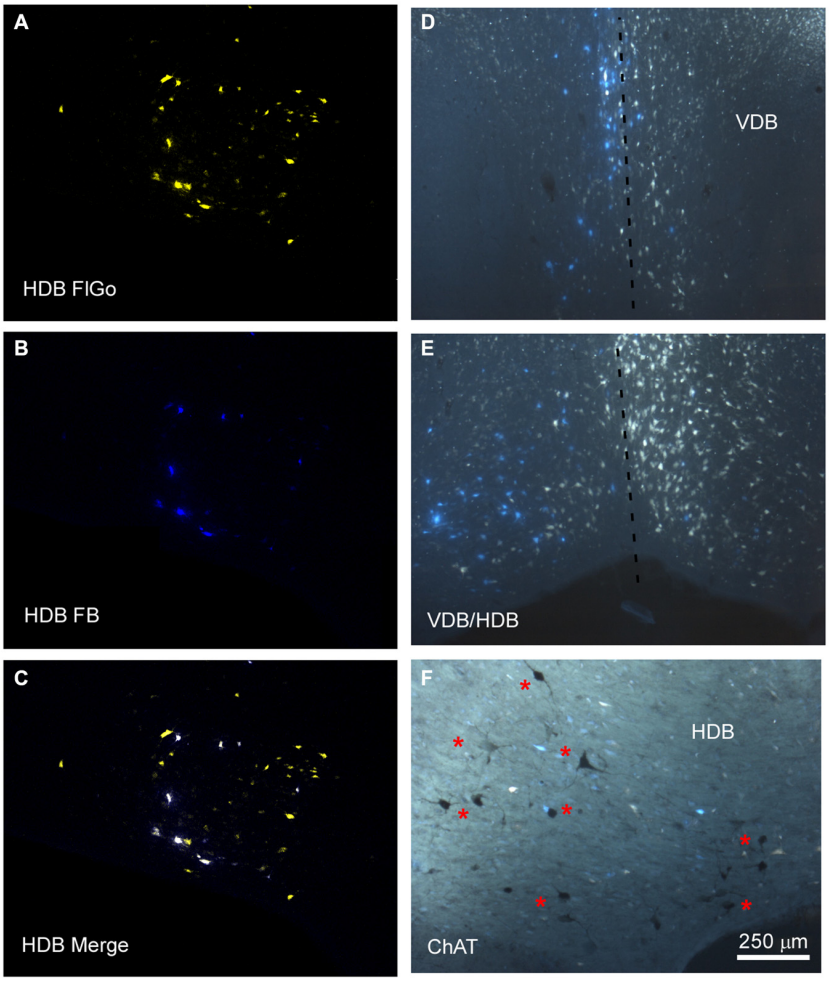

FIGURE 2 | Distribution of labeled neurons in the VDB/HDB. (A–C) Confocal microscope images of retrogradely FlGo (S1 injection) and FB (A1 injection) labeled neurons in the VDB/HDB; **(D,E)** fluorescence microscope images of both Fluoro Gold and Fast Blue labeled neurons in the VDB and HDB. Note that some neurons project to both cortical areas. Dashed line indicates the medial hemispheric line. **(F)** Image combining fluorescent microscopy with acetylcholine transferase (ChAT) immunocytochemistry techniques in HDB. Asterisks indicates cholinergic neurons. HDB, nucleus of the horizontal limb of the diagonal band; VDB, nucleus of the vertical limb of the diagonal band. Calibration toolbar for **(A–F)** 250 μm.

then manually reviewed in the Cell Counter plugin; and (2) for the proportion of double labeled neurons, a manual multipoint tool was used on the merged image and separate channels were also used to corroborate the results. In cases of doubt, possible co-localization of channels was assessed in a merged image combining images of the resulting ROIs in the previous section, in both color channels.

Electrophysiological Recordings

We have used transgenic B6.Cg-Tg (Chat-COP$_4$*H$_{134}$R/EYFP, Slc$_1$8a$_3$)5^{Gfng}/J mice; The Jackson Laboratory) mice expressing the light-activated cation channel, channelrhodopsin-2, tagged with a fluorescent protein (ChR2-YFP) under the control of the choline-acetyl transferase promoter (ChAT). Thus, all cholinergic neurons in CNS express the channelrhodopsin-2 and could be stimulated by blue light and were used for optogenetic stimulation of the BF. Young adult mice (3–6 months old) were anesthetized with urethane (1.5 g/kg, i/p). Depth of anesthesia was sufficient to eliminate pinch withdrawal, palpebral reflex and whisker movement and was assessed periodically during the experiment. Local anesthetic (Lidocaine 1%) was applied to all skin incisions and supplemental doses of urethane were given to maintain areflexia. Animals were placed in a Kopf stereotaxic device (David Kopf Instruments, Tujunga, CA, USA) in which surgical procedures and recordings were performed. The body temperature was maintained at 37°C. An incision was made exposing the skull and small holes were drilled in the bone over the barrel and auditory cortices (AP 1–3 mm, L 5–7 mm, DV 0.2–1 mm, and AP −2.5 mm, L 4 mm, DV 2.5 mm from Bregma, respectively) as well as on the BF, HDB (AP 0.14 mm, L 2 mm, DV 4 mm) and B nucleus (AP −0.7, L 2, DV 4).

Single-unit recordings were performed with tungsten microelectrodes (2–5 MΩ, World Precision Instruments, WPI,

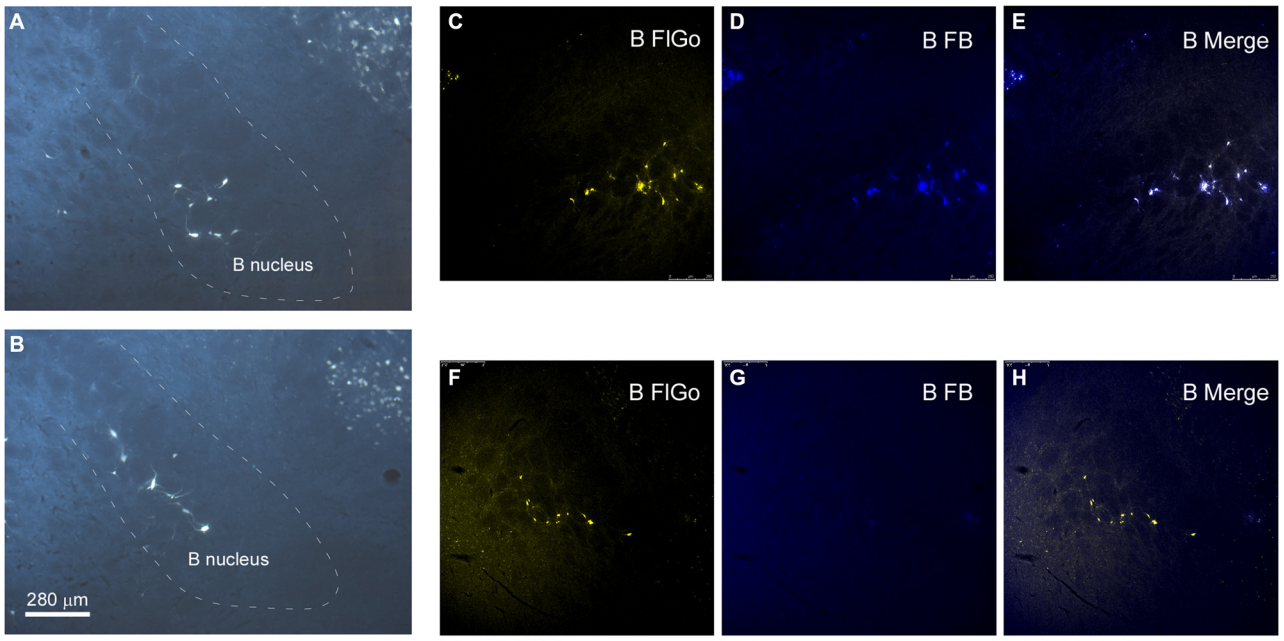

FIGURE 3 | Distribution of labeled neurons in B nucleus. (A,B) Microphotographs of coronal sections showing retrogradely-labeled neurons located in B nucleus at two different antero-posterior coordinates. Dashed lines delimitate the B nucleus. **(C–H)** Confocal microscope detail of FIGo (S1 injection) and FB (A1 injection) labeled neurons in B nucleus. Note that some neurons project to both cortical areas. Calibration toolbar for **(A–H)** 280 μm.

Sarasota, FL, USA) and the cortical field potential was recorded through tungsten macroelectrodes (<1 MΩ). Unit recordings in BF were also performed by an optrode (see below). Unit firing was filtered (0.3–3 kHz), amplified via an AC preamplifier (P15, Grass Instruments) and sampled at 10 KHz while field potentials were filtered between 0.3–100 Hz, amplified and sampled at 500 Hz.

Signals were fed into a personal computer with the temporal references of the stimuli for off-line analysis with Spike 2 Software (Cambridge Electronic Design, Cambridge, UK). We used Spike 2 Software for the offline spike sorting. The algorithm first performs crude spike detection by capturing windows around events defined by the voltage crossing of a user-defined threshold. Then, spike sorting is performed with a combination of template matching and a principal component analysis-based cluster cutting.

Sensory Stimulation

Whisker deflections were performed by brief air puffs using a pneumatic pressure pump (Picospritzer) that delivers an air pulse through a 1 mm inner diameter polyethylene tube (1–2 kg/cm^2, 20 ms duration, resulting in whisker deflections of ≈15°). To avoid complex responses due to deflections of multiple whiskers, these were trimmed to 5 mm in length, so that reproducible responses were evoked. The experimental protocol consisted of 30 pulses delivered to the principal whisker (whisker that gives the highest spike response) at 0.5 Hz (control period). Whisker stimulation was also applied after blue light stimulation of the BF during 30 min. Auditory click stimulation was performed by application of a brief (1 ms duration) square voltage pulse to Sony earphones. The stimuli were presented at a rate of 0.5 Hz at the level 30 dB. Following the baseline recording, stimulation was also applied after blue light stimulation of the BF during 30 min.

Optogenetic Stimulation

Optical stimulation of ChR2-expressing neurons was achieved with light-emitting diodes (LED; 473 nm; Thomas Recording, Germany) delivered from an optical fiber (core diameter 120 μm) or through an optrode (microelectrode 1–2 MΩ; core diameter 80 μm + optical fiber; core diameter 120 μm) positioned directly above BF area. The LED was triggered with a square-step voltage command. Stimulation was applied by 20 ms pulse trains of 473 nm light at 5 Hz or by a single long-lasting pulse (200 ms). Illumination intensity was <30 mW/mm^2 at the BF, which is below the damage threshold of ∼100 mW/mm^2 for blue light (Cardin et al., 2010). The stimulation area was very restricted since total transmitted light power was reduced by 50%, after passing through 100 μm of neuronal tissue, and by 90% at 1 mm (Aravanis et al., 2007).

Data Analysis

The somatosensory or auditory evoked potentials were calculated every 1 min (30 stimuli). The amplitude of the evoked potential was measured from the baseline to the first negative peak. The mean tactile response was measured from the peristimulus time histogram (PSTH) as the number of spikes evoked in the 0–50 ms time window after the onset of the stimulus divided by the number of stimuli. The power spectrum and wavelet transform

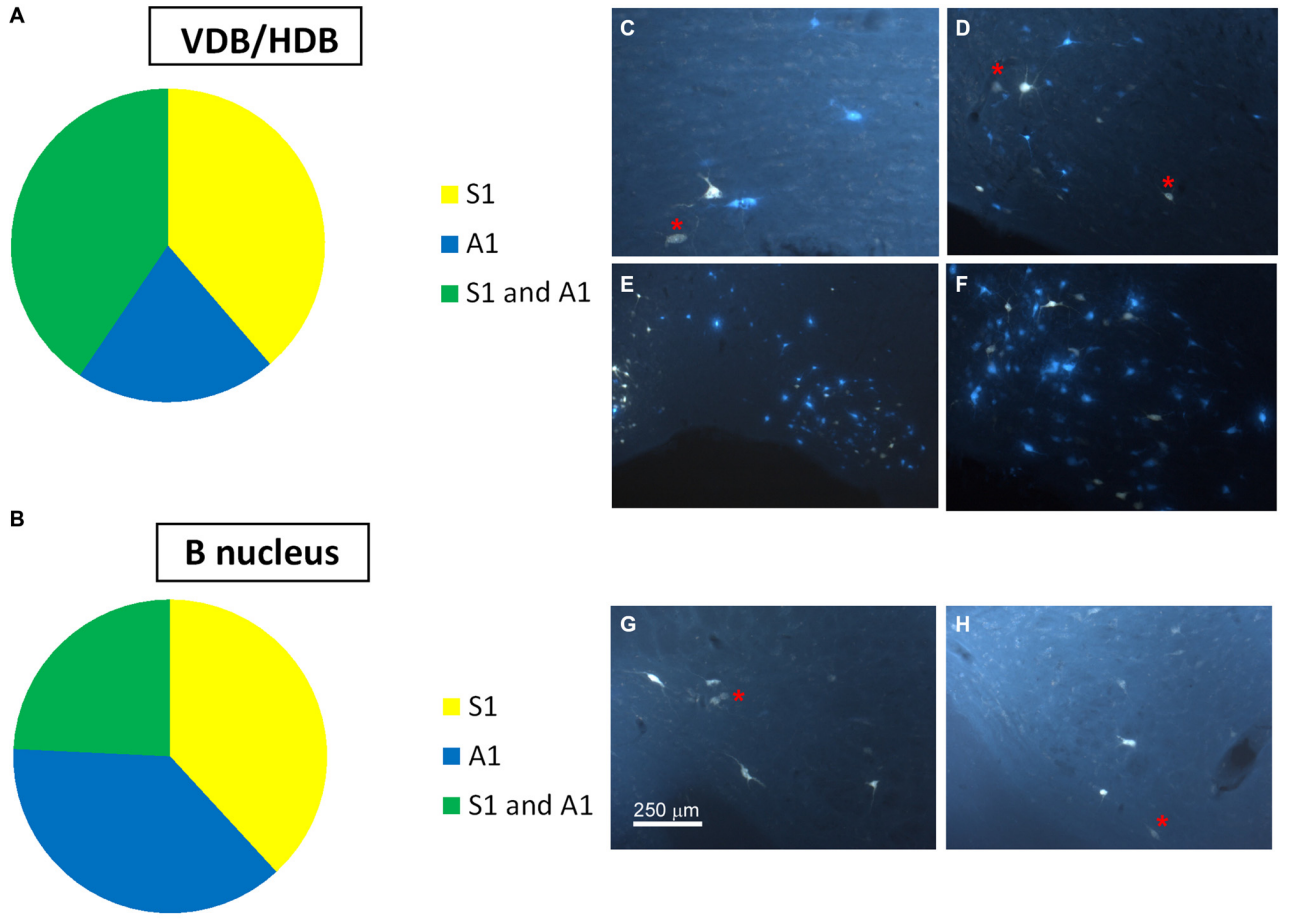

FIGURE 4 | Distribution of labeled neurons in the VDB/HDB and B nuclei. (A) Graphic representation of number of labeled neurons in the VDB/HDB after deposit in the S1 and A1 cortices. Note that this BF area mainly project to the S1 cortex. **(B)** Graphic representation of the number of labeled neurons in the B nucleus after deposits in the S1 and A1 cortices. Note that this BF area project to the S1 and A1 cortices in a similar proportion. **(C–F)** Samples of fluorescent microscope images of single- and double-labeled neurons in HDB. **(G,H)** Samples of fluorescent microscope images of single- and double-labeled neurons in SI/B nucleus. Red asterisks indicate double-labeled neurons. Calibration toolbars **(C,D,F–H)** 230 μm, **(E)** 530 μm.

were also calculated from cortical field potentials. Field potential periods of 30 s were analyzed by Spike 2 Software, using the fast Fourier transform algorithm to obtain the power spectra. The mean power density was calculated for three different frequency bands: δ-band (0.3–4 Hz), θ-band (4–10 Hz), and β-band (10–30 Hz). Every 30 s the percentage contribution of each band to the global wavelength of the EEG (band power × 100/total band powers) was calculated and normalized against the control value (calculated as the mean value of the 30 s before the blue light stimulation).

Statistical analysis was performed using GraphPad Prism 5 Software (San Diego, CA, USA). Statistical analyses consisted of paired comparisons between the same cells before and after BF optogenetic stimulation. If the data were considered normally distributed, according to the Shapiro–Wilk normality test, we used parametric statistics. For two groups, the *t* test (paired) was used. For multiple comparisons the one-way ANOVA analysis of variance followed by Bonferroni *post hoc* test was used. Data are presented as mean ± standard error of the mean (SEM). The threshold level of significance was set at $^{*}P < 0.05$ and $^{**}P < 0.01$ are indicated in figures.

RESULTS

Different Neuronal Groups in Basal Forebrain Display Specific Anatomical Pathways to Sensory Cortices

The anatomical study of the BF efferent connections to the somatosensory and auditory cortices was performed on 18 cases. The locations of the FlGo injection site in the cortices as well as the FB deposit were confirmed using the sections reserved for fluorescence and Nissl studies (**Figure 1**). Both injections and deposits were confined to the desired site without signals of diffusion in any case. In all 18 cases the study of the fluorescence series allowed us to detect numerous fluorescent retrogradely single- or double-labeled neurons in the HDB, VDB (**Figure 2**) or in the SI and B nuclei (**Figure 3**). The mean number of total

labeled neurons in each animal was 1758 ± 234 in VDB/HDB and 56 ± 6 in B nuclei (n = 10 mice).

Neurons in the SI and B nuclei were considered together because the two nuclei were difficult to distinguish at caudal levels. Two tracers were deposited in the two different sensory cortices (S1/A1) of the same hemisphere (n = 10 mice). This experimental approach allowed us to establish whether the pathway of the BF cortical projecting neurons reaches A1, S1 or both cortices. The microscopy study of VDB/HDB revealed numerous intermingled neurons in these nuclei labeled by FlGo, FB or both tracers (**Figures 4C–F**). The study of the distribution and percentages of these neurons showed that 34 ± 1.1% of the neurons located in the VDB/HDB were labeled by both fluorescent tracers (neurons projecting to both the S1 and A1 cortices), while most of the VDB/HDB neurons (44.2 ± 7.4%) were single-labeled by FlGo injected into S1 cortex; only 21.8 ± 2.4% of neurons were labeled by FB injected into A1 cortex (**Figure 4A**). Conversely, the percentage of double-labeled neurons in B nucleus was lower than in VDB/HDB (22 ± 2.1%; **Figure 4B**), while the percentage of B neurons single-labeled by either one or other tracer was roughly the same (40.6 ± 2.7% from S1 and 37.4 ± 3.1% from A1; **Figures 4B,G,H**). In addition, the immunochemical study revealed that fluorescent labeled neurons appeared to be scattered among the characteristic cholinergic neurons of the different BF nuclei and some of them were also positive for ChAT immunocytochemistry (**Figure 2F**).

Optogenetic Stimulation of Cholinergic Neurons Evokes Different Sensory Cortical Responses

The above results indicate that neurons in HDB mainly projected to the S1 (78.2%; corresponding to 44.2% single labeled neurons and 34% double labeled neurons) whereas B neurons similarly projected to the S1 (62.6%; corresponding to 40.6% single labeled neurons and 22% double labeled neurons) and A1 (59.4%; corresponding to 37.4% single labeled neurons and 22% double labeled neurons) cortices. We used optogenetic methods for selective stimulation of cholinergic neurons in specific BF areas. To verify that blue LED stimuli induced spike firing of cholinergic neurons, we used an optrode to perform unit recordings in the BF simultaneously with optical stimulation in the same place. Short-lasting blue LED stimuli applied to the BF (HDB or B nucleus) induced spike firing in the BF neurons of ChAT-ChR2-YFP mice with a mean latency of 6.2 ± 1.1 ms (**Figure 5A**). All light-responsive cells (n = 12 cells) had slow spontaneous firing rates (0.5 ± 0.3 spikes/s). Also, a train of stimuli (20 ms pulse duration; 5 Hz) or a single pulse lasting 200 ms induced spike firing of BF neurons and a desynchronization of the cortical field potential (**Figure 5B**). During control conditions, the cortical field potential produced spontaneous slow oscillations reflecting a synchronized state induced by the anesthetic, which was reduced by blue light stimulation. Wavelet analysis showed that light stimulation induced an increase of fast cortical activity (>4 Hz; **Figure 5C**). The desynchronization in response to light stimulation lasted for only a few seconds, and could be evoked repeatedly.

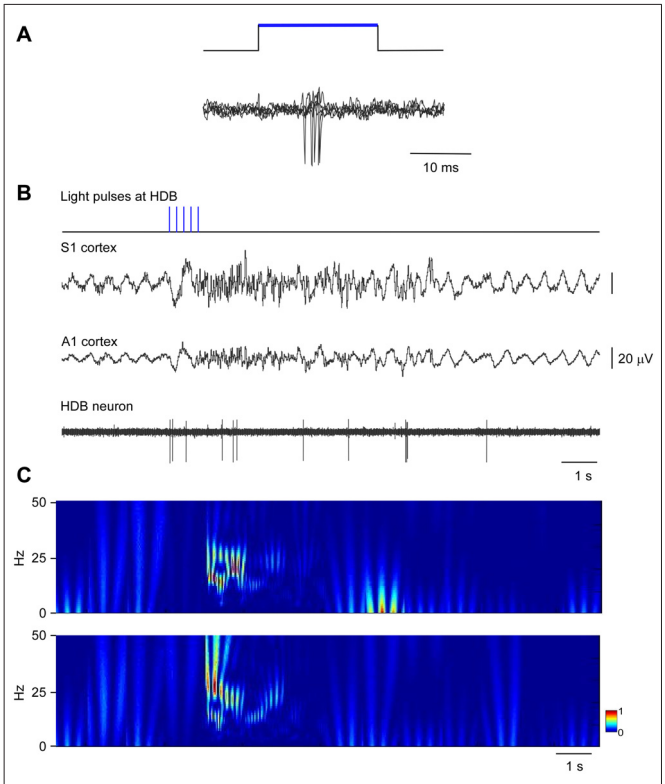

FIGURE 5 | Blue light stimulation of BF neurons induces spike firing in the BF and desynchronization of the somatosensory and auditory field potentials. (A) A short-lasting blue LED stimuli induced spike firing in a representative B neuron (three superimposed traces are shown). **(B)** A train of stimuli (20 ms pulse duration, 5 Hz) evokes spike firing in an HDB neuron simultaneously to a desynchronization of cortical field potentials (S1 and A1 cortices). The effect lasted less than 10 s. **(C)** Wavelet analysis of the same trace shown in (**B**; S1 upper trace; A1 lower trace). Fast activity increases in both cortical field potentials after the blue light stimulation of the HDB area.

To quantify desynchronization, we compared the power spectra of the cortical field potential before (30 s; control) and after the onset of blue light stimulation (a single pulse of 200 ms duration; 30 s). **Figure 6** shows the percentage change with respect to the control values (100%) in the delta frequency band (0.5–4 Hz), in the theta frequency band (4–10 Hz) and in a faster frequency band (10–30 Hz) that mainly correspond to beta frequencies. Data were calculated from six recordings in the S1 cortex and from six recordings in the A1 cortex). Blue light stimulation to the HDB reduced delta activity in the S1 and A1 cortices and increased theta frequencies and faster activities in the S1 and A1 cortices (**Figure 6**). The same result occurred when the blue light was applied to the B area. Although the differences were not statistically significant, HDB stimulation increased more theta frequencies in the S1 and A1 cortices than B stimulation. By contrast, B stimulation increased more beta frequencies in both cortices than HDB stimulation.

Blue light stimulation at the BF also increased the evoked potential amplitude elicited by whisker stimulation (somatosensory evoked potential) or by the application of clicks (auditory evoked potential). HDB optogenetic stimulation

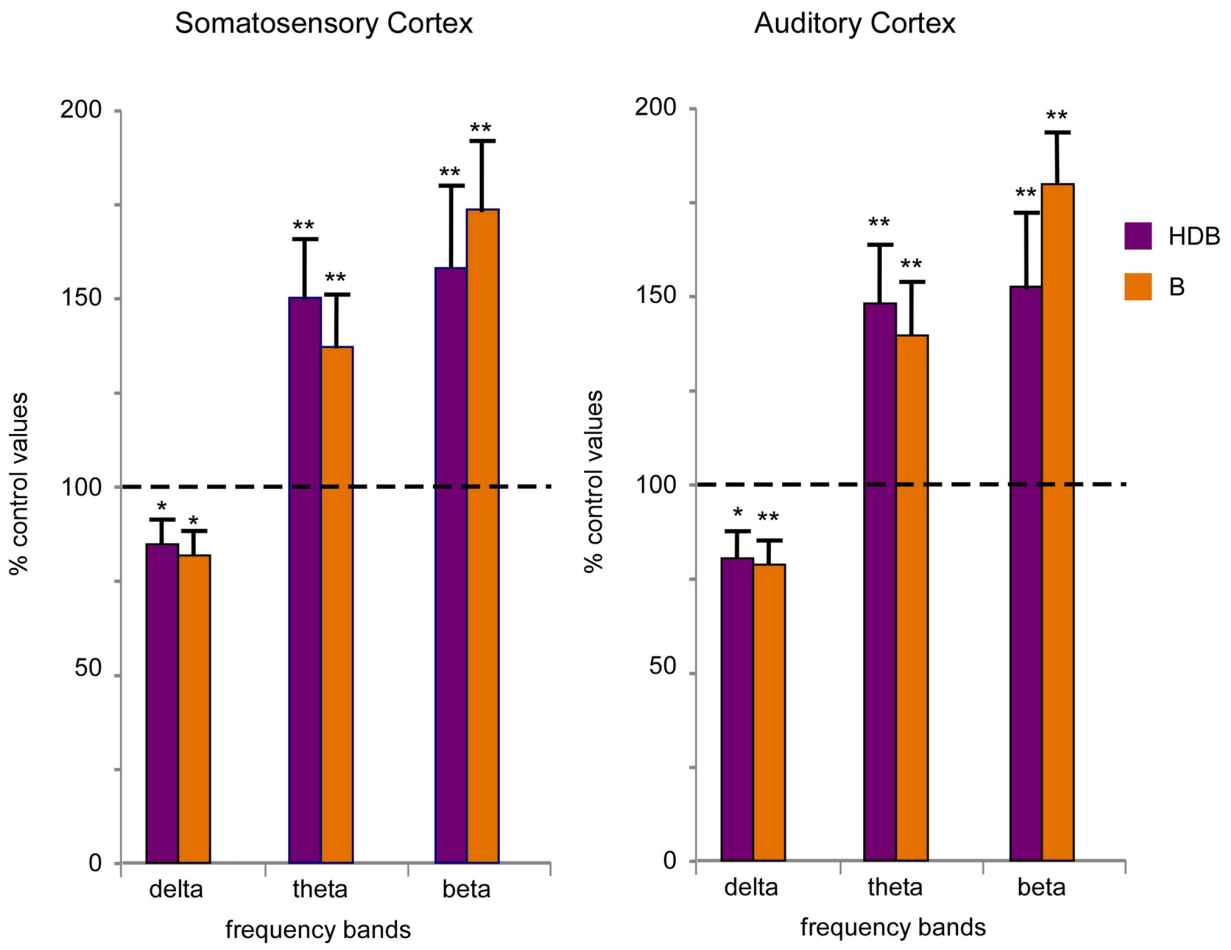

FIGURE 6 | Blue light stimulation of BF neurons induces fast activity in the cortical field potentials. Plots of the percentage of change in the frequency band of 30 s of EEG recording respect to 30 s of a control period (100%) in the S1 and A1 cortices (left and right plots, respectively). Blue light stimulation of the HDB or B nuclei reduced the percentage of delta activity (0.5–4 Hz) and increased theta (4–10 Hz) and beta (10–30 Hz) activity during 30 s after light stimulation.

induced a long-lasting increase in either the somatosensory or auditory evoked potentials (**Figure 7A**). The effect lasted at least 30 min and was larger for the somatosensory evoked potentials than the auditory evoked potentials (**Figure 7B**). The mean amplitude increased rapidly from 6.6 ± 1.3 μV in the control conditions to 11.4 ± 2.0 μV, 5 min after optogenetic stimulation (ANOVA analysis, $P = 0.002$; $n = 12$) and remained 10.5 ± 1.9 μV, 30 min after stimulation (ANOVA analysis, $P = 0.0016$; $n = 12$; **Figure 7C**). Auditory evoked potentials were less affected by the blue light when it was directed at the HDB. The mean amplitude changed from 3.9 ± 0.6 μV in the control to 4.8 ± 1.1 μV 5 min after optogenetic stimulation (ANOVA analysis, $P = 0.101$; $n = 12$). The increase reached statistical significance 10 min after blue light stimulation (6.0 ± 1.6 μV; ANOVA analysis, $P = 0.0109$; $n = 12$) and remained facilitated 30 min after stimulation (5.2 ± 0.8 μV; ANOVA analysis, $P = 0.0207$; $n = 12$; **Figure 7C**).

In contrast to the HDB stimulation, B optogenetic stimulation induced a lower increase of somatosensory evoked potentials at 5 min after the application of blue light in comparison with HDB stimulation (**Figures 8A,B**). The mean amplitude of the somatosensory evoked potential increased from 5.5 ± 0.5 μV in the control conditions to 8.6 ± 0.9 μV, 5 min after optogenetic stimulation (ANOVA analysis, $P = 0.0217$; $n = 12$) and 7.9 ± 1.0 μV, at 30 min after stimulation (ANOVA analysis, $P = 0.072$; $n = 12$; **Figure 8C**). Auditory evoked potentials were also less affected by the blue light in comparison with the effect on the somatosensory evoked potentials. The mean amplitude changed from 3.7 ± 1.0 μV in the control to 4.4 ± 1.2 μV, 5 min after blue light stimulation (ANOVA analysis, $P = 0.1338$; $n = 12$), reaching statistical significance 10 min after blue light stimulation (5.2 ± 1.4 μV; ANOVA analysis, $P = 0.0109$; $n = 12$). However, the stimulation effect vanished 30 min after optogenetic stimulation (4.2 ± 1.2 μV; ANOVA analysis, $P = 0.072$; $n = 12$; **Figures 8B,C**).

DISCUSSION

A fundamental question in the present study, concerns whether the BF neuronal population operates more as a unified group,

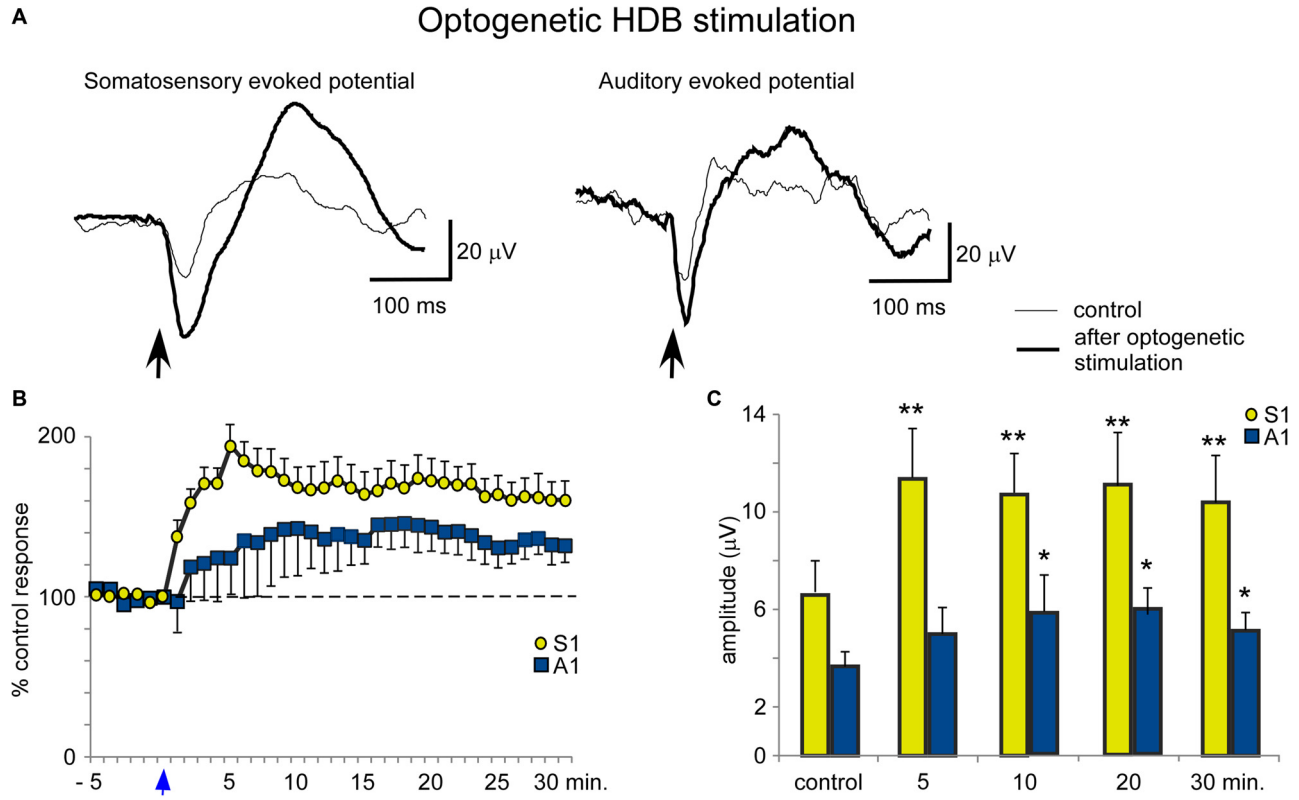

FIGURE 7 | Blue light stimulation of HDB nucleus induces an increase of somatosensory and auditory evoked potentials. (A) Raw data shows an important increase of the somatosensory evoked potentials and a modest increase of the auditory evoked potentials (control and 5 min after blue light stimulation; thin and thick traces, respectively). **(B)** Plot shows the time course of evoked potential amplitude in 12 cases. The 100% represent the mean amplitude during the control period. Note the greater increase in somatosensory evoked potentials (S1) than in auditory evoked potentials (A1) by HDB stimulation (reference 0 s; vertical blue arrow). **(C)** Plot of the mean amplitude measured in control and at 5, 10, 20 or 30 min after blue light stimulation at HDB area. The amplitude increase was larger for somatosensory than auditory evoked potentials.

simultaneously activating all cortical areas, or as a set of distinct neuronal groups that differentially activate specific cortical regions. Our results support the latter possibility because they reveal that the BF is a heterogeneous area in which neurons projecting to different cortical areas are segregated into different neuronal groups. Most of the HDB has a large number of neurons that project to the S1 cortex (considering single and double labeled neurons), indicating that this area is specialized in sensory processing of somatosensory stimuli. By contrast, the B nucleus shows a similar number of cells projecting to the S1 and A1 cortices. Accordingly, optogenetic HDB stimulation induced more extensive facilitation of tactile evoked potentials than auditory evoked potentials. Cortical response facilitation evoked by the B nucleus stimulation was lower in both cortices and appeared more slowly in A1 than by HDB stimulation. This finding may be due to the neuronal density of the cortical projecting neurons, which is higher in the HDB area than in the B nucleus (see below).

The topography of BF projections to the cortex is an important issue because it may indicate the manner in which the cholinergic BF system participates in cortical sensory processing. The use of retrograde fluorescent neuroanatomical tracing allow us to suggest that the HDB neurons give rise to fairly widespread cortical projections but with high-density innervation focused on the S1 cortex although neurons projecting to the A1 cortex were also observed. However, we did not find a selective BF area projecting to the A1 cortex. This finding is probably due to the importance of the whisker sensory system in rodents, giving greater evidence for the existence of neuronal clusters involved in the information processing of somatosensory stimuli; this pattern of projection was also found in other sensory systems although it was less evident. In fact, the cholinergic neurons that project to V1 are located in the BF, particularly the ventral pallidum, SI and the HDB (Gaykema et al., 1990; Laplante et al., 2005). In this regard, Zaborszky et al. (2015) have demonstrated that the cholinergic and non-cholinergic pathways to the cortex are organized into segregated or overlapping pools of projection neurons. The extent of the overlap between the BF populations projecting to the cortex depends on the degree of connectivity between the cortical targets of these projection populations. By contrast, the B nucleus displayed a non-selective projection to the S1 and A1 cortices.

Previous reports have indicated regional differences in the regulation of cortical ACh release (Fournier et al., 2004;

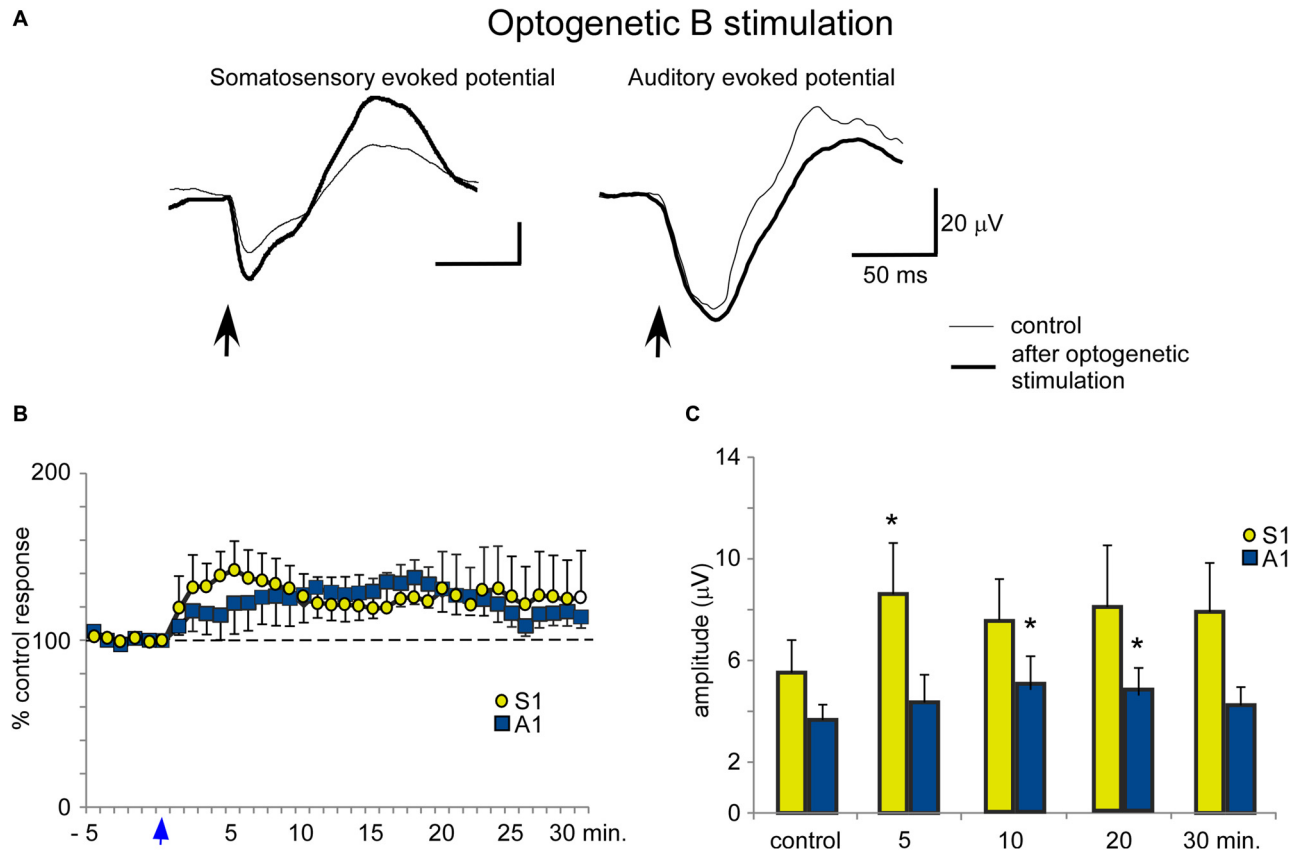

FIGURE 8 | Blue light stimulation of B nucleus induces an increase of somatosensory and auditory evoked potentials. (A) Raw data shows that only somatosensory evoked potentials were affected by blue light stimulation at the B nucleus (control and 5 min after stimulation; thin and thick traces, respectively). **(B)** Plot shows the time course of evoked potential amplitude in 12 cases (light stimulation occurs at reference 0 s; vertical blue arrow). The 100% represent the mean amplitude during the control period. **(C)** Plot of the mean amplitude measured in control and 5, 10, 20 or 30 min after blue light stimulation at the B nucleus. The effect was smaller than after HDB stimulation.

Laplante et al., 2005). This has been demonstrated in a neurophysiological experiment wherein differential modulation of somatosensory and visual cortices to tactile and visual stimuli, respectively, resulted from the activation of neighboring BF neurons (Golmayo et al., 2003). Moreover, those investigators proposed that the BF could be an anatomical and functional relay between the prefrontal cortex and sensory cortical areas. Regionally-specific activation of ACh release has also been demonstrated in visual and somatosensory cortices following the presentation of either visual or somatosensory stimuli (Fournier et al., 2004; Laplante et al., 2005). This modality-specific activation is supported by the topographical projections from the BF to sensory cortices (Zaborszky, 2002; Zaborszky et al., 2005, 2015). Taken together these results and our results suggest that cortical ACh release is increased with regional specificity in response to a specific sensory stimulus. Anatomical specificity has also been observed in the activation of prefrontal cortex-projecting vs. motor cortex-projecting BF cholinergic neurons during task performance (Parikh et al., 2007). These findings suggest the existence of different subpopulations of BF neurons involved in the modulation of specific tasks. Accordingly, clustering techniques applied to unit recordings of BF neurons during different attentional tasks have revealed a large number of distinct categories of task-phase-specific activity patterns in these BF neurons (Tingley et al., 2014). Consequently, anatomical and optogenetic results strongly suggest the existence of cholinergic neuronal populations in the BF that are involved in the modulation of sensory cortical response, as has been published recently in the somatosensory cortex (Barros-Zulaica et al., 2014; Martin-Cortecero and Núñez, 2014).

Cortically projecting neurons in the BF were characterized as cholinergic, GABAergic or peptidergic (Fisher et al., 1988; Zaborszky and Duque, 2000; Zaborszky et al., 2005; Mascagnis and McDonald, 2009). Because cholinergic neurons in the BF are scattered among neurons with different neurochemical identities, we used optogenetic stimulation of cholinergic neurons to study the specific cholinergic effects on sensory cortical responses. The optogenetic stimulation of these cholinergic

HDB neurons mostly facilitated tactile evoked potentials in the S1 rather than auditory-evoked potentials in the A1 cortex. Therefore, our results support a localized cortical effect of cholinergic projections. In agreement with our data, optogenetic activation of BF cholinergic axons in the visual cortex enhances performance of a visual discrimination task, while silencing the BF cholinergic cells impaired performance (Pinto et al., 2013). However, optogenetic stimulation of cholinergic B neurons only facilitated tactile responses in the S1 while auditory-evoked potentials in the A1 cortex were less and more slowly affected. It seems that the small density of cholinergic projections from the B area to the cortex is not enough to evoke a long-lasting facilitation of sensory responses. The different result observed in the S1 and the A1 may be because the tactile stimulus was more precise (only one whisker) than the auditory stimulus (a click stimulating the entire cochlea).

In contrast to the specific long-lasting facilitation of sensory responses, blue light stimulation of either HDB or the B nucleus caused similar desynchronization of the S1 or A1 field potential during a short time period. Likewise, the illumination of neocortex desynchronizes the local field potential in the same anesthetized transgenic mice, indicating that light evoked the release of ACh in the cortex (Kalmbach et al., 2012). These findings suggest that a large network of synaptically-related cholinergic BF neurons is involved in cortical activation which is probably caused by reductions in potassium conductances (McCormick, 1992; Oldford and Castro-Alamancos, 2003). However, cholinergic modulation of precise sensory responses may be controlled by specific groups of neurons through modulation of glutamatergic cortical receptors (Carr and Surmeier, 2007; Núñez et al., 2012; Barros-Zulaica et al., 2014). In agreement with the existence of two functional roles for cholinergic BF pathways, microdialysis studies in the medial prefrontal cortex have reported a tonic ACh increase during attention-related performance tasks (Passetti et al., 2000) that may promote a general state of cortical arousal (EEG desynchronization). Moreover, ACh can also be released briefly (phasic release) in concert with cue detection in a cued appetitive response task to facilitate specific information processing (Parikh et al., 2007). Thus, phasic release of ACh would support more rapid transitions of cortical states, consistent with cholinergic regulation of attention to relevant stimuli, while a sustained ACh release could promote a general state of cortical activation (see Luchicchi et al., 2014; Sarter et al., 2014). Our results support these findings and suggest that different BF cholinergic neurons may be involved in these different roles.

AUTHOR CONTRIBUTIONS

MR-A and ÁN conceived and supervised all aspects of the study. IC-C and NB-Z collected all data. IC-C analyzed anatomical aspects of the data. NB-Z analyzed electrophysiological aspects of the data.

FUNDING

This work was supported by a Grant from Ministerio de Economia y Competitividad (BFU2012–36107).

ACKNOWLEDGMENTS

We would like to acknowledge L. Zaborszky for his collaboration and comments in the first stage of the project. The first experiments were done in Zaborszky's laboratory and supported the initial phase of the project (NIH/NINDS NS023945). Also, M. Callejo and G. de la Fuente for their technical assistance.

REFERENCES

Aravanis, A. M., Wang, L.-P., Zhang, F., Meltzer, L. A., Mogri, M. Z., Schneider, M. B. M., et al. (2007). An optical neural interface: *in vivo* control of rodent motor cortex with integrated fiberoptic and optogenetic technology. *J. Neural. Eng.* 4, S143–S156. doi: 10.1088/1741-2560/4/3/s02

Barros-Zulaica, N., Castejon, C., and Núñez, Á. (2014). Frequency-specific response facilitation of supra and infragranular barrel cortical neurons depends on NMDA receptor activation in rats. *Neuroscience* 281, 178–194. doi: 10.1016/j.neuroscience.2014.09.057

Bueno-Junior, L. S., Lopes-Aguiar, C., Ruggiero, R. N., Romcy-Pereira, R. N., and Leite, J. P. (2012). Muscarinic and nicotinic modulation of thalamo-prefrontal cortex synaptic plasticity [corrected] *in vivo*. *PLoS One* 7:e47484. doi: 10.1371/journal.pone.0047484

Buzsáki, G., Bickford, R. G., Ponomareff, G., Thal, L. J., Mandel, R., and Gage, F. H. (1988). Nucleus basalis and thalamic control of neocortical activity in the freely moving rat. *Neuroscience* 8, 4007–4026.

Callaway, C. W., and Henriksen, S. J. (1992). Neuronal firing in the nucleus accumbens is associated with the level of cortical arousal. *Neuroscience* 51, 547–553. doi: 10.1016/0306-4522(92)90294-c

Cardin, J. A., Carlén, M., Meletis, K., Knoblich, U., Zhang, F., Deisseroth, K., et al. (2010). Targeted optogenetic stimulation and recording of neurons *in vivo* using cell-type-specific expression of Channelrhodopsin-2. *Nat. Protoc.* 5, 247–254. doi: 10.1038/nprot.2009.228

Carr, D. B., and Surmeier, D. J. (2007). M1 muscarinic receptor modulation of Kir2 channels enhances temporal summation of excitatory synaptic potentials in prefrontal cortex pyramidal neurons. *J. Neurophysiol.* 97, 3432–3438. doi: 10.1152/jn.00828.2006

Chiba, A. A., Bushnell, P. J., Oshiro, W. M., and Gallagher, M. (1999). Selective removal of cholinergic neurons in the basal forebrain alters cued target detection. *Neuroreport* 10, 3119–3123. doi: 10.1097/00001756-199909290-00044

Collier, B., and Mitchell, J. F. (1966). The central release of acetylcholine during stimulation of the visual pathway. *J. Physiol.* 184, 239–254. doi: 10.1113/jphysiol.1966.sp007913

Détári, L. (2000). Tonic and phasic influence of basal forebrain unit activity on the cortical EEG. *Behav. Brain Res.* 115, 159–170. doi: 10.1016/s0166-4328(00)00256-4

Doralp, S., and Leung, L. S. (2008). Cholinergic modulation of hippocampal CA1 basal-dendritic long-term potentiation. *Neurobiol. Learn. Mem.* 90, 382–388. doi: 10.1016/j.nlm.2008.05.013

Eckenstein, F. P., Baughman, R. W., and Quinn, J. (1988). An anatomical study of cholinergic innervation in rat cerebral cortex. *Neuroscience* 25, 457–474. doi: 10.1016/0306-4522(88)90251-5

Fernández de Sevilla, D., Núñez, Á., Borde, M., Malinow, R., and Buño, W. (2008). Cholinergic-mediated IP3-receptor activation induces long-lasting synaptic enhancement in CA1 pyramidal neurons. *J. Neurosci.* 28, 1469–1478. doi: 10.1523/JNEUROSCI.2723-07.2008

Fisher, R. S., Buchwald, N. A., Hull, C. D., and Levine, M. S. (1988). GABAergic basal forebrain neurons project to the neocortex: the localization of glutamic acid decarboxylase and choline acetyltransferase in feline corticopectal neurons. *J. Comp. Neurol.* 272, 489–502. doi: 10.1002/cne.902720404

Fournier, G. N., Semba, K., and Rasmusson, D. D. (2004). Modality- and region-specific acetylcholine release in the rat neocortex. *Neuroscience* 126, 257–262. doi: 10.1016/j.neuroscience.2004.04.002

Gaykema, R. P., Luiten, P. G., Nyakas, C., and Traber, J. (1990). Cortical projection patterns of the medial septum-diagonal band complex. *J. Comp. Neurol.* 293, 103–124. doi: 10.1002/cne.902930109

Goard, M., and Dan, Y. (2009). Basal forebrain activation enhances cortical coding of natural scenes. *Nat. Neurosci.* 12, 1444–1449. doi: 10.1038/nn.2402

Golmayo, L., Núñez, Á., and Zaborszky, L. (2003). Electrophysiological evidence for the existence of a posterior cortical-prefrontal-basal forebrain circuitry in modulating sensory responses in visual and somatosensory rat cortical areas. *Neuroscience* 119, 597–609. doi: 10.1016/s0306-4522(03)00031-9

Hasselmo, M. E., and Sarter, M. (2011). Modes and models of forebrain cholinergic neuromodulation of cognition. *Neuropsychopharmacology* 36, 52–73. doi: 10.1038/npp.2010.104

Kalmbach, A., Hedrick, T., and Waters, J. (2012). Selective optogenetic stimulation of cholinergic axons in neocortex. *J. Neurophysiol.* 107, 2008–2019. doi: 10.1152/jn.00870.2011

Kuo, M. C., Rasmusson, D. D., and Dringenberg, H. C. (2009). Input-selective potentiation and rebalancing of primary sensory cortex afferents by endogenous acetylcholine. *Neuroscience* 163, 430–441. doi: 10.1016/j.neuroscience.2009.06.026

Laplante, F., Morin, Y., Quirion, R., and Vaucher, E. (2005). Acetylcholine release is elicited in the visual cortex, but not in the prefrontal cortex, by patterned visual stimulation: a dual *in vivo* microdialysis study with functional correlates in the rat brain. *Neuroscience* 132, 501–510. doi: 10.1016/j.neuroscience.2004.11.059

Lee, M. G., Manns, I. D., Alonso, A., and Jones, B. E. (2004). Sleep-wake related discharge properties of basal forebrain neurons recorded with micropipettes in head-fixed rats. *J. Neurophysiol.* 92, 1182–1198. doi: 10.1152/jn.01003.2003

Luchicchi, A., Bloem, B., Viaña, J. N., Mansvelder, H. D., and Role, L. W. (2014). Illuminating the role of cholinergic signaling in circuits of attention and emotionally salient behaviors. *Front. Synaptic Neurosci.* 6:24. doi: 10.3389/fnsyn.2014.00024

Lysakowski, A., Wainer, B. H., Bruce, G., and Hersh, L. B. (1989). An atlas of the regional and laminar distribution of choline acetyltransferase immunoreactivity in rat cerebral cortex. *Neuroscience* 28, 291–336. doi: 10.1016/0306-4522(89)90180-2

Martin-Cortecero, J., and Núñez, Á. (2014). Tactile response adaptation to whisker stimulation in the lemniscal somatosensory pathway of rats. *Brain Res.* 1591, 27–37. doi: 10.1016/j.brainres.2014.10.002

Mascagnis, F., and McDonald, A. J. (2009). Parvalbumin-immunoreactive neurons and GABAergic neurons of the basal forebrain project to the rat basolateral amygdala. *Neuroscience* 160, 805–812. doi: 10.1016/j.neuroscience.2009.02.077

Mayse, J. D., Nelson, G. M., Avila, I., Gallagher, M., and Lin, S. C. (2015). Basal forebrain neuronal inhibition enables rapid behavioral stopping. *Nat. Neurosci.* 18, 1501–1508. doi: 10.1038/nn.4110

McCormick, D. A. (1992). Neurotransmitter actions in the thalamus and cerebral cortex and their role in neuromodulation of thalamocortical activity. *Prog. Neurobiol.* 39, 337–388. doi: 10.1016/0301-0082(92)90012-4

Metherate, R., and Ashe, J. H. (1993). Nucleus basalis stimulation facilitates thalamocortical synaptic transmission in the rat auditory cortex. *Synapse* 14, 132–143. doi: 10.1002/syn.890140206

Navarrete, M., Perea, G., Fernandez de Sevilla, D., Gómez-Gonzalo, M., Núñez, Á., Martín, E. D., et al. (2012). Astrocytes mediate *in vivo* cholinergic-induced synaptic plasticity. *PLoS Biol.* 10:e1001259. doi: 10.1371/journal.pbio.1001259

Núñez, Á., Domínguez, S., Buño, W., and Fernández de Sevilla, D. (2012). Cholinergic-mediated response enhancement in barrel cortex layer V pyramidal neurons. *J. Neurophysiol.* 108, 1656–1668. doi: 10.1152/jn.00156.2012

Oldford, E., and Castro-Alamancos, M. A. (2003). Input-specific effects of acetylcholine on sensory and intracortical evoked responses in the "barrel cortex" *in vivo*. *Neuroscience* 117, 769–778. doi: 10.1016/s0306-4522(02)00663-2

Parikh, V., Kozak, R., Martinez, V., and Sarter, M. (2007). Prefrontal acetylcholine release controls cue detection on multiple timescales. *Neuron* 56, 141–154. doi: 10.1016/j.neuron.2007.08.025

Passetti, F., Dalley, J. W., O'Connell, M. T., Everitt, B. J., and Robbins, T. W. (2000). Increased acetylcholine release in the rat medial prefrontal cortex during performance of a visual attentional task. *Eur. J. Neurosci.* 12, 3051–3058. doi: 10.1046/j.1460-9568.2000.00183.x

Pauli, W. M., and O'Reilly, R. C. (2008). Attentional control of associative learning—a possible role of the central cholinergic system. *Brain Res.* 1202, 43–53. doi: 10.1016/j.brainres.2007.06.097

Paxinos, G., and Franklin, K. B. J. (2003). *The Mouse Brain in Stereotaxic Coordinates*. San Diego, CA: Academic Press.

Pinto, L., Goard, M. J., Estandian, D., Xu, M., Kwan, A. C., Lee, S. H., et al. (2013). Fast modulation of visual perception by basal forebrain cholinergic neurons. *Nat. Neurosci.* 16, 1857–1863. doi: 10.1038/nn.3552

Rasmusson, D. D., Smith, S. A., and Semba, K. (2007). Inactivation of prefrontal cortex abolishes cortical acetylcholine release evoked by sensory or sensory pathway stimulation in the rat. *Neuroscience* 149, 232–241. doi: 10.1016/j.neuroscience.2007.06.057

Saper, C. B. (1987). "Diffuse cortical projection systems: anatomical organization and role in cortical function," in *Handbook of Physiology: The Nervous System*, eds V. B. Mountcastle and F. Plum (Bethesda, MD: American Physiological Society), 169–210.

Sarter, M., Bruno, J. P., and Givens, B. (2003). Attentional functions of cortical cholinergic inputs: what does it mean for learning and memory? *Neurobiol. Learn. Mem.* 80, 245–256. doi: 10.1016/s1074-7427(03)00070-4

Sarter, M., Lustig, C., Howe, W. M., Gritton, H., and Berry, A. S. (2014). Deterministic functions of cortical acetylcholine. *Eur. J. Neurosci.* 39, 1912–1920. doi: 10.1111/ejn.12515

Semba, K. (2000). Multiple output pathways of the basal forebrain: organization, chemical heterogeneity and roles in vigilance. *Behav. Brain Res.* 115, 117–141. doi: 10.1016/s0166-4328(00)00254-0

Semba, K., and Fibiger, H. C. (1989). Organization of central cholinergic systems. *Prog. Brain Res.* 79, 37–63. doi: 10.1016/s0079-6123(08)62464-4

Semba, K., Reiner, P. B., McGeer, E. G., and Fibiger, H. C. (1988). Brainstem afferents to magnocellular basal forebrain studied by axonal transport, immunohistochemistry and electrophysiology in the rat. *J. Comp. Neurol.* 267, 433–453. doi: 10.1002/cne.902670311

Szymusiak, R., Alam, N., and McGinty, D. (2000). Discharge patterns of neurons in cholinergic regions of the basal forebrain during waking and sleep. *Behav. Brain Res.* 115, 171–182. doi: 10.1016/s0166-4328(00)00257-6

Tingley, D., Alexander, A. S., Kolbu, S., de Sa, V. R., Chiba, A. A., and Nitz, D. A. (2014). Task-phase-specific dynamics of basal forebrain neuronal ensembles. *Front. Syst. Neurosci.* 8:174. doi: 10.3389/fnsys.2014.00174

Wilson, F. A., and Rolls, E. T. (1990a). Learning and memory is reflected in the responses of reinforcement-related neurons in the primate basal forebrain. *J. Neurosci.* 10, 1254–1267.

Wilson, F. A., and Rolls, E. T. (1990b). Neuronal responses related to reinforcement in the primate basal forebrain. *Brain Res.* 509, 213–231. doi: 10.1016/0006-8993(90)90546-n

Zaborszky, L. (2002). The modular organization of brain systems. Basal forebrain: the last frontier. *Prog. Brain Res.* 136, 359–372. doi: 10.1016/s0079-6123(02)36030-8

Zaborszky, L., Buhlm, D. L., Pobalashinghamm, S., Bjaaliem, J. G., and Nadasdym, Z. (2005). Three-dimensional chemoarchitecture of the basal forebrain: spatially specific association of cholinergic and calcium binding

protein-containing neurons. *Neuroscience* 136, 697–713. doi: 10.1016/j.neuroscience.2005.05.019

Zaborszky, L., Csordas, A., Mosca, K., Kim, J., Gielow, M. R., Vadasz, C., et al. (2015). Neurons in the basal forebrain project to the cortex in a complex topographic organization that reflects corticocortical connectivity patterns: an experimental study based on retrograde tracing and 3D Reconstruction. *Cereb. Cortex* 25, 118–137. doi: 10.1093/cercor/bht210

Zaborszky, L., Cullinan, W. E., and Braun, A. (1991). Afferents to basal forebrain cholinergic projection neurons: an update. *Adv. Exp. Med. Biol.* 295, 43–100. doi: 10.1007/978-1-4757-0145-6_2

Zaborszky, L., and Duque, A. (2000). Local synaptic connections of basal forebrain neurons. *Behav. Brain Res.* 115, 143–158. doi: 10.1016/s0166-4328(00)00255-2

Zaborszky, L., Gaykema, R. P., Swanson, D. J., and Cullinan, W. E. (1997). Cortical input to the basal forebrain. *Neuroscience* 79, 1051–1078. doi: 10.1016/s0306-4522(97)00049-3

Zaborszky, L., Van den, A., and Gyengesi, E. (2012). "The basal forebrain cholinergic projection system in mice," in *The Mouse Nervous System*, eds C. Watson, G. M. Paxinos, and L. Puelles (Amsterdam: Elsevier), 684–718.

Conflict of Interest Statement: The authors declare that the research was conducted in the absence of any commercial or financial relationships that could be construed as a potential conflict of interest.

Copyright © 2016 Chaves-Coira, Barros-Zulaica, Rodrigo-Angulo and Núñez. This is an open-access article distributed under the terms of the Creative Commons Attribution License (CC BY). The use, distribution and reproduction in other forums is permitted, provided the original author(s) or licensor are credited and that the original publication in this journal is cited, in accordance with accepted academic practice. No use, distribution or reproduction is permitted which does not comply with these terms.

A.4. Article 4 (published)

CONTROL OF SOMATOSENSORY CORTICAL PROCESSING BY THALAMIC POSTERIOR MEDIAL NUCLEUS: A NEW ROLE OF THALAMUS IN CORTICAL FUNCTION

PLOS ONE

RESEARCH ARTICLE

Control of Somatosensory Cortical Processing by Thalamic Posterior Medial Nucleus: A New Role of Thalamus in Cortical Function

Carlos Castejon, Natali Barros-Zulaica, Angel Nuñez*

Departamento de Anatomía, Histología y Neurociencia, Facultad de Medicina, Universidad Autónoma de Madrid, Madrid, Spain

* angel.nunez@uam.es

CrossMark
click for updates

OPEN ACCESS

Citation: Castejon C, Barros-Zulaica N, Nuñez A (2016) Control of Somatosensory Cortical Processing by Thalamic Posterior Medial Nucleus: A New Role of Thalamus in Cortical Function. PLoS ONE 11(1): e0148169. doi:10.1371/journal.pone.0148169

Editor: Miguel Maravall, University of Sussex, UNITED KINGDOM

Received: June 12, 2015

Accepted: January 13, 2016

Published: January 28, 2016

Copyright: © 2016 Castejon et al. This is an open access article distributed under the terms of the Creative Commons Attribution License, which permits unrestricted use, distribution, and reproduction in any medium, provided the original author and source are credited.

Data Availability Statement: All relevant data are within the paper.

Funding: This work was supported by a grant from Ministerio de Economia y Competitividad (BFU2012-36107).

Competing Interests: The authors have declared that no competing interests exist.

Abstract

Current knowledge of thalamocortical interaction comes mainly from studying lemniscal thalamic systems. Less is known about paralemniscal thalamic nuclei function. In the vibrissae system, the posterior medial nucleus (POm) is the corresponding paralemniscal nucleus. POm neurons project to L1 and L5A of the primary somatosensory cortex (S1) in the rat brain. It is known that L1 modifies sensory-evoked responses through control of intracortical excitability suggesting that L1 exerts an influence on whisker responses. Therefore, thalamocortical pathways targeting L1 could modulate cortical firing. Here, using a combination of electrophysiology and pharmacology *in vivo*, we have sought to determine how POm influences cortical processing. In our experiments, single unit recordings performed in urethane-anesthetized rats showed that POm imposes precise control on the magnitude and duration of supra- and infragranular barrel cortex whisker responses. Our findings demonstrated that L1 inputs from POm imposed a time and intensity dependent regulation on cortical sensory processing. Moreover, we found that blocking L1 GABAergic inhibition or blocking P/Q-type Ca2+ channels in L1 prevents POm adjustment of whisker responses in the barrel cortex. Additionally, we found that POm was also controlling the sensory processing in S2 and this regulation was modulated by corticofugal activity from L5 in S1. Taken together, our data demonstrate the determinant role exerted by the POm in the adjustment of somatosensory cortical processing and in the regulation of cortical processing between S1 and S2. We propose that this adjustment could be a thalamocortical gain regulation mechanism also present in the processing of information between cortical areas.

Introduction

Cortical functioning cannot be properly understood without taking into account the thalamic influence [1–9]. Knowledge of thalamocortical influence in sensory processing comes mainly from studying lemniscal core thalamic systems that project to granular layers of primary sensory cortices [3, 7, 10]; however, less is known about paralemniscal thalamic systems.

In the rodents, vibrissal information is conveyed to the somatosensory cortex via several parallel pathways [11–19]. In the lemniscal pathway, the ventral posterior medial nucleus of the thalamus (VPM) projects to L4, L5B and L6A in the primary somatosensory cortex (S1). In the extralemniscal pathway, the ventral tier of VPM projects mainly to L4 and L6 [67] in the secondary somatosensory cortex (S2). And in the paralemniscal pathway, the posterior medial nucleus (POm) projects to L1 and L5A in S1 and also to S2 [18–24]. It has been proposed that, whereas these ascending pathways appear to be parallel anatomically, they may not be functionally equivalent [39].

Thalamic VPM nucleus can be considered a "First order" relay station [5, 9], receiving sensory information from the principal trigeminal nucleus (PrV). POm nucleus is largely more complex to classify since it receives sensory information from the interpolar division of the spinal trigeminal nucleus (SpVi) and also from L5 of the somatosensory cortical areas [5, 15, 21, 25, 26]. There are several important differences between both nuclei: VPM is topographically well organized [19, 27–30]. In contrast, POm neuronal responses show poor spatial resolution [1, 15, 27, 31] with receptive fields composed of multiple vibrissae [12]. Recordings from both nuclei revealed different adaptation process to repetitive stimuli [1, 32, 33]. Offset latencies remained constant in POm neurons across the different stimulation frequencies [1]. In agreement with those findings, other studies found that onset and offset latencies of SPVi paralemniscal neuronal responses were not affected by deflecting the vibrissae at different frequencies [32, 34]. These properties of paralemniscal neurons render them poorly suited for coding specific stimulus content features. It has been proposed that signals conveyed by the lemniscal pathway involve high-resolution encoding of contact and texture information relayed from the vibrissae [17, 35]. The role of POm and the paralemniscal system in sensory processing is less clear. It is known that paralemniscal system processes temporal features of tactile stimuli [1, 34], and is involved in nociceptive transmission [32, 36–38]. Also, it has been suggested that POm neurons represent (temporal- to rate-code transformation by thalamocortical loops) the temporal frequency of whisker movements by latency and spike count [1, 34] and that the POm is involved in temporal processing related to sensory-motor control of whisker movement [17, 34, 35]. Other authors have reported that whisking in air, without vibrissae contacts, fails to evoke significant activity in POm neurons [32]. Actually, the nature and function of the messages that POm thalamic nucleus transfers to the cortex are still under debate.

It has been proposed that the role of the paralemniscal projection is to provide modulatory inputs to barrel cortex [39]. However, the possible mechanisms by which these projections could regulate the cortex are unknown.

Here, we have sought to determine POm influences in cortical processing by single-unit recordings in somatosensory cortex of urethane-anesthetized rats. Our findings demonstrate that POm modulates magnitude and duration of S1 cortical responses to sensory input. We found that GABAergic inhibitory transmission in L1 is implicated in the regulation of cortical excitability and sensory response magnitude and duration. Our results are consistent with a previous work that described L1 inhibitory influence on whisker responses [40]. Accordingly, we demonstrate that POm exerts its control of cortical sensory responses mainly through L1.

Additionally, it has been suggested that 'Higher order' thalamic nuclei play a key role in corticocortical communication [41, 42]. In S1, L5 corticofugal neurons send the processed information to the POm and to various subcortical regions [9, 15, 25, 26, 43]. Recently, both anatomical and physiological findings have shown that ascending inputs from the brainstem and descending inputs from L5 converge on single thalamocortical neurons in POm [25]. Both individual pathways interact functionally in a time-dependent manner [25]. From here, POm neuron projections also target other cortical areas including the primary motor cortex (M1) and higher-order somatosensory cortical regions [18, 21]. Furthermore, it is well described the

reciprocal connections between these areas. These connections are likely to play a crucial role in sensory-motor integration and sensory learning. However, both the function of that trans-thalamic pathway and the nature of the messages that are relayed through the POm from one cortical area to another remain unclear.

In this study, we propose that cortical sensory response modulation by POm could be also present in the processing of information between somatosensory cortical areas. We performed a complementary set of experiments to test this hypothesis and found that POm is also controlling the sensory processing in S2 and this regulation is modulated by corticofugal activity from L5 in S1 [25]. In sum, our findings demonstrate the determinant role exerted by the POm in the adjustment of barrel cortex sensory processing and in the regulation of cortical processing between somatosensory cortical areas.

Materials and Methods

Animal procedures and electrophysiology

All animal procedures were approved by the Ethical Committee of the Universidad Autonoma de Madrid, in accordance with European Community Council Directive 2010/63/UE. Rats were group housed with a 12-h light/dark cycle and had free access to food and water. Every effort was made to minimize the number and suffering of the animals used. Experiments were performed on 98 (36 males and 62 females) urethane-anesthetized (1.6 g/kg i.p.) adult Sprague Dawley rats weighing 200–250 g. Animals were placed in a Kopf stereotaxic frame in which surgical procedures and recordings were performed. The animals breathed freely. The body temperature was maintained at 37°C; the end-tidal CO_2 and heart rate were monitorized. Local anaesthetic (Lidocaine 1%) was applied to all skin incisions. The level of anesthesia was monitored and kept constant (absence of whisker movements and pinch withdrawal reflex) using supplemental doses of urethane. The skull was exposed and then openings were made to allow electrode penetrations to different neuronal stations in the cortex, thalamus and brainstem. Tungsten microelectrodes (2–5 MΩ) were driven using a microdrive system. Extracellular recordings were made of putative excitatory neurons in the interpolar division of the ipsilateral spinal trigeminal complex (SpVi; AP 11.5–14; L 2.5–3.5, D 8.5–9.5; in mm from Bregma; [44], contralateral posterior medial nucleus (POm; AP 2.5–4.5, L 2–2.5, D 5–6.5) of the thalamus and contralateral vibrissal region of the primary (S1; AP 0.5–4, L 5–7) and secondary (S2; AP 0–3.7; L 7–7.5) somatosensory cortices. In S1, barrel cortical neurons were recorded in supragranular (D: 200–600 μm) or infragranular (D: 900–1500 μm) layers. In S2, neurons were recorded along the cortical depth (D: 400–1300 μm). To estimate the depths of recorded neurons, we used the micromanipulator axial depth readings.

Sensory stimulation

Controlled whisker deflections were performed by brief air puffs (20–200 ms) applied to one whisker (deflected in caudal direction) at 0.5 Hz using a pneumatic pressure pump (Picospritzer) that delivers an air pulse through a 1 mm inner diameter polyethylene tube (1.2–2 kg/cm^2) avoiding skin stimulation. We choose this precise stimulus to assure the effect of our protocols and to avoid complex, likely nonphysiological responses. Vibrissae were cut 9 mm from the skin in order to allow a controlled mechanical stimulation of single vibrissae and to evoke reproducible responses. Details on train duration, pulse duration and number of consecutive deflections applied are provided in figures. We determined receptive field size of single units by deflecting individual vibrissae with a hand-held probe and monitoring the audio conversion of the amplified activity signal.

Electrical stimulation

Electrical microstimulation was carried out with single square pulses (0.5 ms, 5–80 μA; S88 Grass Stimulator). We applied these pulses at 0.5 Hz to avoid possible adaptation phenomena. Electrical stimulation (E-stimulation) was applied in POm, VPM, L5 or L1 in S1 cortex, using 120 μm diameter stainless steel bipolar electrodes. The E-stimulation parameters were digitally controlled by Spike2 software (Cambridge Electronic Design, Cambridge, UK) and transmitted to the current source via a digital-to-analog converter built in to the CED Power 1401 data acquisition unit (Cambridge Electronic Design). We tried to establish the minimal, but effective, stimulation parameters for detecting changes in cortical neural responses and to avoid possible antidromic activity [45] in order to study only orthodromic effects. Stimulation within the current range used in our study (<80 μA) is estimated to activate cells within a maximal radius of 0.5 mm [46]. At the end of each E-stimulation experiment we applied a train of 20 pulses (0.5 ms; same intensity) at high frequency (100 Hz) to check for antidromic activity. We did not find evoked spikes having the ability to follow this high frequency E-stimulation. Thus, none of the cortical recorded neurons were antidromically activated by thalamic E-stimulation at the intensities used. None of the E-stimulation parameters used here induced subtle motor effects, whisking or facial twitching.

We identify the placement of the electrodes on histological sections or according to their response pattern. Only the data from cases in which the electrode tip was unambiguously well localized inside the corresponding thalamic nucleus or cortical layer were quantitatively analyzed.

Pharmacological study

The following drugs were used: Muscimol (5-(aminomethyl)-isoxazol-3-ol; selective agonist for γ-aminobutyric acid receptor-A ($GABA_A$) receptors; 1 mM), Picrotoxin (PTX; prototypic antagonist of $GABA_A$ receptors; 1mM) and Cav2.1 (P/Q- type) voltage-gated calcium channels blocker ω-agatoxin-IVa (AGA; 0.1 μM). Drugs were injected through a cannula connected to a Hamilton syringe (1 μl). The syringe was driven using a microdrive system to inject the drug solution into the cortical surface or into the thalamic nucleus (AP 3.3 mm, L 2.5 mm to the Bregma for POm, or L 3.2 mm for VPM and D 4.8–6.8 mm from the surface of the brain; [44]). The piston of the syringe was moved manually at a slow speed (infusion speed 0.3 μl/min). A volume of 0.1 to 0.3 μl of muscimol was infused unilaterally into the corresponding thalamic nuclei. PTX or AGA was applied to the surface of the cortex (1 μl). Given the potential of $GABA_A$ receptors antagonists, PTX in our experiments, to induce seizures (e.g. [47–49]), all rats were carefully monitored for indicators of seizures after infusions. None of the PTX injections elicited tremor, motor convulsions or more subtle seizure effects such as jaw or facial twitching.

Histology

Upon completion of the experiments, animals were deeply anesthetized with sodium-pentobarbital (50 mg/kg) and then perfused transcardially with saline followed by formalin (4% in saline). Subsequently, 50 μm thick sections were prepared for Nissl staining for verification of cannula placement and to locate the stimulation and recording electrode tracks. Placements of the lesions were determined using a light microscope and mapped onto coronal sections of a rat brain stereotaxic atlas [44].

Data acquisition and analysis

Raw signal was filtered (0.3–3 kHz band pass), amplified via an AC preamplifier (DAM80; World Precision Instruments, Sarasota, USA), and fed into a computer (sampled at 10 kHz)

with the temporal references of the stimuli for off-line analysis. Single-unit activity was extracted with the aid of commercial software Spike2 (Cambridge Electronic Design, Cambridge, UK) for spike waveform identification and analysis. Furthermore, we also supervise waveforms to confirm that units were well isolated. The sorted spikes were stored at a 1-ms resolution and isolated single-units were analyzed and quantified. We defined response magnitude as the total number of spikes per stimulus occurring between response onset and offset from the peristimulus time histogram (PSTH, bin width 1 ms). Response onset was defined as the first of three consecutive bins displaying significant activity (three times higher than the mean spontaneous activity) after stimulus and response offset as the last bin of the last three consecutive bins displaying significant activity. Response duration was defined as the time elapsed from the onset to offset responses. The baseline firing rate was calculated from mean firing within a 10 s window before the first stimulus (air puff). In all figures, raster plots represent each spike as a dot for sample neuron. Spikes were aligned on stimulus presentation (Time 0 ms). In some figures, PSTHs and rasters are shown from multi-units recordings just to clarify the effects.

Statistical analysis was performed using GraphPad Prism 5 software (San Diego, CA, USA). For all experiments, data analysis was based on single unit responses. For normally distributed data (Shapiro-Wilk normality test), comparisons of activities of single units in different conditions were performed by using paired two-tailed t test, where $P<0.05$ was considered significant. Data are presented as means ± SEM. Non-normally distributed data were compared with Wilcoxon-matched pairs test (as indicated in the text).

Results

Our experiments were designed to study thalamic POm influence in somatosensory cortical processing. First, we studied and characterized the firing pattern of POm responses to whisker deflections. After that, to test whether POm activity modulates cortical tactile processing, we investigated whisker response changes in barrel cortex by electrically stimulating the POm immediately before whisker stimulus or by muscimol-induced inactivation of the POm. Finally, we pharmacologically blocked GABAergic inhibitory transmission in L1 to understand the contribution of this layer in POm regulation of cortical processing.

Additionally, to determine the possible role exerted by the POm in the adjustment of somatosensory cortical processing between S1 and S2, we performed a complementary set of experiments investigating whisker response changes in S2 by electrically stimulating S1 and by muscimol-induced inactivation of the POm.

POm responses lasted the duration of the stimulus

Performing experiments in 10 rats, we firstly characterized the firing pattern of POm neurons delivering air-puffs of different durations (20–200 ms) to one whisker, avoiding skin stimulation. We found multivibrissae receptive fields (mean receptive field size: 6.1±2.5 vibrissae; range: 3–12; n = 118) at all POm recording sites. Our recordings from POm revealed a sustained response along stimulus presence, as shown by the raster of spikes in response to 0.5 Hz periodic vibrissae deflections (Fig 1). Specifically, 72% of the recorded neurons exhibited this response pattern (85 of 118). We also found that 83% of the recorded neurons in SpVi exhibited the same pattern (85 of 102; data not shown). These findings demonstrated the presence of this sustained response pattern along the paralemniscal pathway.

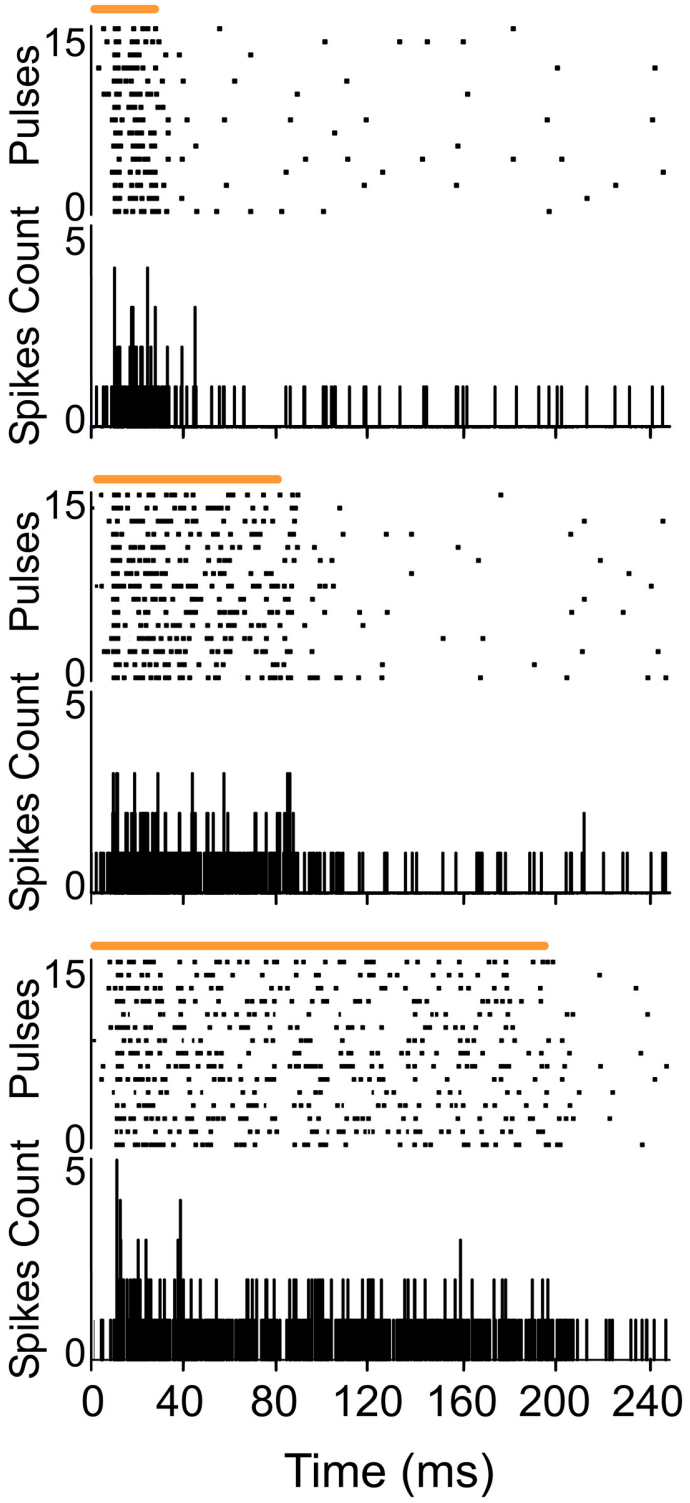

Fig 1. POm responses lasted the duration of the whisker stimulus. Raster plots and PSTHs showing sustained multiunit POm responses evoked by different stimulus duration (top: 20 ms, middle: 80 ms and bottom: 200 ms). Air puff duration is indicated by horizontal orange lines.

doi:10.1371/journal.pone.0148169.g001

POm activity modulates sensory cortical processing

To examine the influence of POm nucleus on infra- and supragranular neurons in barrel cortex, we compared whisker responses in several experimental conditions increasing or decreasing POm activity.

POm E-stimulation evokes orthodromic spikes in infra- and supragranular layers of barrel cortex. We investigated whisker response changes in barrel cortex by POm electrical stimulation (E-stimulation) immediately before whisker stimulus (air puff) application in 15 rats (Fig 2). We restricted our recordings to infra- and supragranular layers of barrel cortex (see Discussion). Cortical neurons were silent or displayed a low firing rate in spontaneous conditions (0.89±0.1 spikes/s in infragranular layers, n = 69; 0.69±0.1 in supragranular layer, n = 51). Whisker deflections caused short-latency spikes in infra- and supragranular layers of barrel cortex. All neurons displayed a contralateral response to whisker displacements. Spike shape and firing pattern (low spontaneous firing rate and reduced tactile response to the deflection) provide strong support to the notion that recordings were obtained from pyramidal cells, as has been previously reported [50–54].

First, we stimulated electrically the POm (single pulse of 0.5 ms; 15–80 μA) alone. POm E-stimulation elicited spikes (for example see Fig 2C) in infra- and supragranular layers of barrel cortex. In infragranular layers the latencies of these spikes varied in the range of 5–50 ms (mean latency: 23.67±0.9 ms; n = 69). In supragranular layers in the range of 5–50 ms (mean latency: 16.30±0.5 ms; n = 51). These findings are in agreement with recent studies suggesting that POm projections make excitatory synapses with barrel cortex pyramidal cells [20, 39, 43].

Also, in all cases, we checked for potential rebound excitation (potential delayed spikes >150 ms in infra- or >50 ms in supragranular layers after E-stimulation offset). However, after POm E-stimulation we did not find rebound excitation even at maximal intensity used in our experiments (80 μA;).

Anatomically POm receives corticothalamic inputs from infragranular layers, thus, infragranular activity elicited by thalamic POm E-stimulation could also result from antidromic activation of corticothalamic axons. This would induce cortical responses characterized by minimal response variability and failure to show neural response fatigue [55, 56]. In contrast, orthodromic stimulation would activate cortical sites through neural pathways, characterized by substantial response timing variability and decremental cortical responses with repeated electrical stimulation pulses. At the end of each E-stimulation experiment we applied a train of 20 pulses (0.5 ms; same intensity) at high frequency (100 Hz) to check for antidromic activity. We did not find evoked spikes having the ability to follow this high frequency E-stimulation. None of the cortical recorded neurons were antidromically activated by thalamic E-stimulation at the intensities used. Thus, the results obtained in our experiments were due to orthodromic cortical activation from thalamic inputs.

Increasing POm activity by E-stimulation modulates sensory response in barrel cortex. To examine the effects of POm E-stimulation on infra- and supragranular neurons, we compared cortical sensory responses before and during POm E-stimulation (500 ms before each vibrissae stimulus; Fig 2). We applied the E-stimulation protocol defined by two blocks of 30 pulses (air puff 20 ms duration) delivered to one whisker at 0.5 Hz. In the second block, we stimulated electrically the POm just before each sensory stimulus (Fig 2D). Quantitative measures of neural responses were examined to determine how paralemniscal thalamic E-stimulation affected cortical responses to vibrissae deflections. We found that POm E-stimulation was accompanied by a marked change in cortical sensory responses in a layer specific manner. Following POm E-stimulation just before whisker stimulus, cortical sensory response magnitude and duration significantly decreased. These effects were demonstrated both by the rasters and

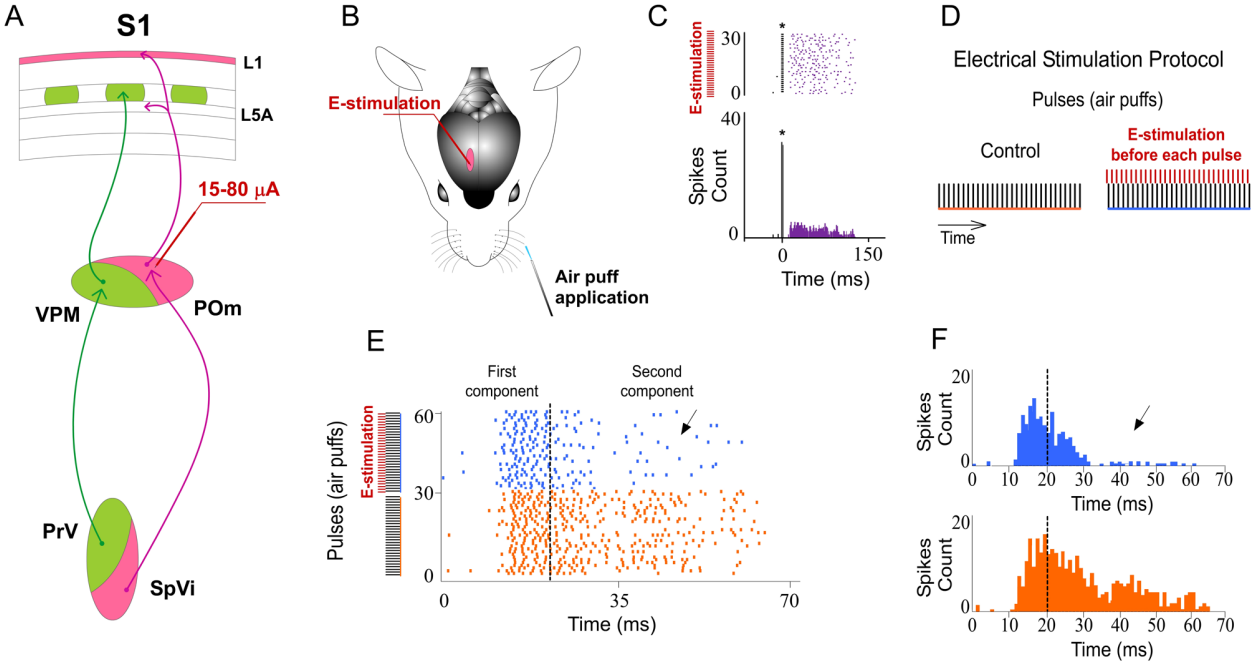

Fig 2. Increasing POm activity by POm E-stimulation just before sensory stimulus modulates whisker cortical responses. (A) Schematic diagram summarizing the main components of the lemniscal (green) and paralemniscal (pink) thalamocortical circuitry to barrel cortex. (B) Schematic diagram indicating the experimental protocol used in our study. (C) In agreement with recent studies suggesting that POm projections make excitatory synapses with barrel cortex pyramidal cells [20, 39, 43, 73], POm E-stimulation alone (single pulse of 0.5 ms; 15–80 μA) elicited orthodromic spikes in infra- and supragranular layers of barrel cortex. An example of evoked orthodromic spikes in the barrel cortex infragranular layer by POm E-stimulation is shown. * indicates stimulation artifacts. (D) Experimental protocol. The 'Electrical Stimulation Protocol' consisted of two blocks of 30 pulses (air puff 20 ms) delivered to the principal whisker at 0.5 Hz. We stimulated electrically the POm, VPM, L1 or L5 in S1 50–1000 ms before each pulse in the second block (blue) applied 60 s after the first block (orange). (E, F) POm E-stimulation 500 ms before whisker stimulus reduced sensory responses in infra- and supragranular layers of S1. Raster plots (E) and PSTHs (F) are shown for a sample multiunit infragranular response. Vertical dashed lines separate response components. POm E-stimulation shortened responses and reduced spikes mainly in the second response component (arrows). Spikes are aligned on sensory stimulus (air puff) presentation (Time 0 ms). POm E-stimulation was applied 500 ms before air puffs (31 to 60 pulses; red bars).

doi:10.1371/journal.pone.0148169.g002

by the peristimulus time histograms (PSTHs; Fig 2F). Results were consistent across all animals (n = 15).

Taken into account that POm projections target specifically L5A, we performed a preliminary analysis of single-units from different deeps. POm E-stimulation induced similar response decrease in both superficial (900–1200 μm) and deep (1200–1500 μm) infragranular units (-27%; n = 27; $P<0.001$ and -33%; n = 31; $P<0.001$, respectively). A total of 82% of superficial infragranular neurons (27 of 33) and 86% of deep infragranular neurons (31 of 36) decreased their sensory responses correlated with POm E-stimulation. Therefore, we combined all these single units across different depths into a single neuronal population termed infragranular layer. In this cortical layer, POm E-stimulation before each vibrissae stimulus induced a mean response decrease from 2.08±0.1 spikes/stimulus in control condition (before the application of the POm E-stimulation) to 1.48±0.1 spikes/stimulus during POm E-stimulation condition (-29%; n = 80; $P< 0.001$). A total of 89% of infragranular neurons (80 of 90) displayed changes in responses correlated with POm E-stimulation. The latency of the vibrissae response onset did not change while offset latencies significantly decreased during POm E-stimulation. Onset tactile responses had on average 13.20±0.12 ms latency in control and 13.09±0.10 ms after POm E-stimulation (-1%; n = 80; P = 0.41). Offset tactile responses decreased on average from

59.64±0.55 in control condition to 46.14±0.32 ms during POm E-stimulation (-23%; n = 80; P< 0.001).

In supragranular layers, POm E-stimulation applied before each whisker stimulus induced a mean response decrease from 1.95±0.1 spikes/stimulus in control condition to 1.33±0.1 spikes/stimulus in POm E-stimulation condition (-32%; n = 67; P < 0.001). A total of 90% neurons (67 of 74) displayed changes correlated with POm E-stimulation. Onset tactile responses had on average 14.92±0.22 ms latency and 14.14±0.18 ms after POm E-stimulation (-4%; n = 67; P = 0.06). Offset tactile responses had on average 41.64±0.6 ms latency and was reduced to 32.81±0.71 ms after POm E-stimulation (-21%; n = 67; P<0.001).

In both layers, POm E-stimulation before whisker stimulus resulted in decreased spike count. However, this reduction was not homogeneous along the sensory response (Fig 2E and 2F). Previous reports from our laboratory have described two different components of tactile responses and the relevant implication of N-methyl-D-aspartate (NMDA) receptors manly in the late component of the response [57, 58]. Accordingly, here we divided each PSTH in two components: the first (from onset to 20 ms) and the second (from 20 ms to offset) components. We found important differences between these components. In infragranular layers, the first component of the PSTH did not decrease (from 1.02±0.1 to 0.97±0.1 spikes/stimulus; -5%; n = 80; P = 0.44). However, spikes were suppressed abruptly in the second component of the response by POm E-stimulation (from 1.06±0.1 to 0.50±0.1 spikes/stimulus; -52%; n = 80; P<0.001). In supragranular layers, the first component decreased from 1.15±0.1 to 0.94±0.1 (-19%; n = 67; P< 0.001) and from 0.80±0.1 to 0.40±0.1 (-50%; n = 67; P<0.001) in the second component. These findings demonstrate the important differences between both components.

As a control for specificity of the POm E-stimulation site, we also stimulated electrically (single pulse of 15–80 μA, 0.5 ms) the VPM in 9 rats. We found that VPM E-stimulation alone elicited short latencies spikes in infra- and supragranular layers of barrel cortex. In infragranular layers the latencies of these spikes varied in the range of 4–38 ms (mean latency: 13.42±0.5 ms; n = 38) and in supragranular layers in the range of 4–30 ms (mean latency: 12.37±0.4 ms; n = 50). We also applied high frequency VPM E-stimulation (a train of 20 pulses at 100 Hz). Cortical spikes decreased with increasing pulse number consistent with orthodromic stimulation. Also, we test the possibility of rebound excitation. We did not find delayed rebound excitation occurring 38 ms after VPM E-stimulation (for example see Fig 3A) within the current range used in our study (<80 μA). However, applying VPM E-stimulation with a higher intensity (>130 μA) we found rebound activity in same tested cases (data not shown).

After that, we compared cortical sensory responses before and after VPM E-stimulation (500 ms before each stimulus). Cortical responses increased their magnitude in both layers (quantified in Fig 3B; P<0.001in both layers). This effect was more prevalent in the second component of the response. In infragranular layers, we found an increased number of spikes from 0.96±0.1 to 1.01±0.1 spikes/stimulus (5%; n = 38; P = 0.031) in the first component. Spikes in the second component of the response were also increased by VPM E-stimulation (from 1.09±0.2 to 1.36±0.2 spikes/stimulus; 25%; n = 38; P<0.001; Fig 3). Similarly, the number of spikes in the first component increased from 1.13±0.1 to 1.21±0.1 (7%; n = 50; P<0.001) and from 0.69±0.1 to 0.89±0.1 (29%; n = 50; P<0.001; Fig 3) in the second component of supragranular layer neurons. A total of 73% of infragranular layer neurons (38 of 52) and 76% of supragranular neurons (50 of 66) displayed increments in responses correlated with VPM E-stimulation.

These findings suggest significant differences between POm and VPM thalamic nuclei. Our results showed that VPM E-stimulation alone elicited shorter latencies orthodromic spikes in infra- and supragranular layers of barrel cortex than POm E-stimulation. VPM orthodromic spikes varied in the range of 4–38 ms in infra- and of 4–30 ms in supragranular layers.

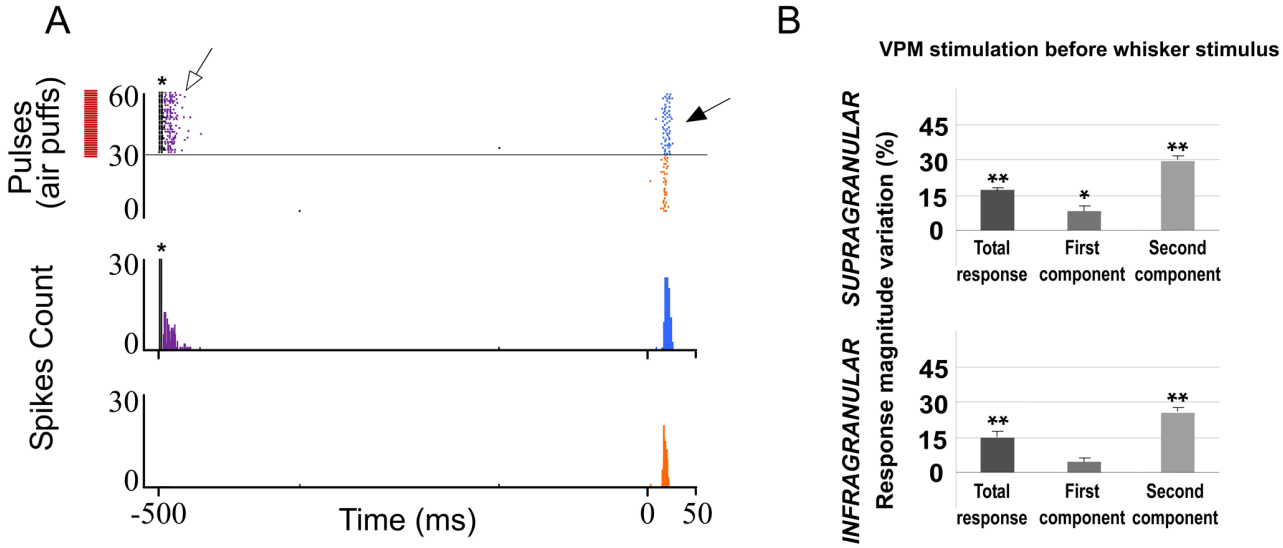

Fig 3. VPM E-stimulation just before whisker stimulus enhances sensory responses in barrel cortex. (A) Raster plots and PSTHs are shown for a sample supragranular neuron. VPM E-stimulation was applied 500 ms before pulses 31 to 60 (red bars). In contrast to POm E-stimulation, spikes mainly in the second component of the response were strongly increased by VPM E-stimulation (filled arrow). We did not find delayed rebound excitation occurring 30 ms after VPM E-stimulation within the current range used in our study (<80 μA). VPM E-stimulation evoked cortical spikes (open arrow). * indicates E-stimulation artifacts. (B) Change (%) in mean sensory response magnitude by VPM E-stimulation 500 ms before stimulus. Total response was increased in both layers by VPM E-stimulation. First component of infragranular responses was not significantly affected. Spikes in the second component were strongly increased in both layers.

doi:10.1371/journal.pone.0148169.g003

However, POm E-stimulation (same intensity) elicited evoked-spikes lasting up to 150 ms in infra- and up to 50 ms in supragranular layers. These results are in agreement with other studies showing that evoked bursts of EPSCs in neocortical neurons triggered by VPM neurons had faster decay times than those from POm neurons [20].

Moreover, in contrast to VPM E-stimulation, following POm E-stimulation just before whisker stimulus, cortical responses magnitude and duration significantly decreased. These opposite results from VPM or POm E-stimulation on whisker cortical responses suggested a different functional role of these thalamic nuclei in somatosensory processing.

POm inactivation enhances whisker response magnitude and duration in barrel cortex. To further understand the POm implication in cortical sensory processing, we pharmacologically inactivated POm neurons by infusing a small volume (0.1–0.3 μl; 1 mM) of the $GABA_A$ receptor agonist muscimol in 16 rats. Surprisingly, inactivating POm enhanced sensory responses in infra- and supragranular layers within a few minutes (<5 min) of the injection (Fig 4). We found enhanced tactile responses in 37 out of 51 neurons (67%) and 51 of 59 neurons (86%) in infra- and supragranular layer, respectively (measured at 15 min after injection). The evoked spikes in response to whisker stimulation were enhanced from 1.96±0.3 spikes/stimulus to 2.26±0.3 spikes/stimulus (15%; n = 37; P<0.001) in infragranular layers and from 1.86±0.2 spikes/stimulus to 2.16±0.3 spikes/stimulus (16%; n = 51; P<0.001) in supragranular layers (Fig 4C). The response facilitation was evident in the second response component (Fig 4C). In infragranular layers, the first component was not affected (from 1.04±0.2 to 1.03 ±0.2 spikes/stimulus; -2%; n = 37; P = 0.4). In contrast, spikes in the second component of the response were increased abruptly by POm inactivation (from 0.92 ± 0.1 to 1.23 ± 0.2 spikes/stimulus; 34%; n = 37; P<0.001). In supragranular layers, the first component was also not affected (from 1.13±0.2 to 1.17±0.2 spikes/stimulus; 3%; n = 51; P = 0.61) while the second component increased from 0.73±0.1 to 1.01±0.1 spikes/stimulus (37%; n = 51; P<0.001). The

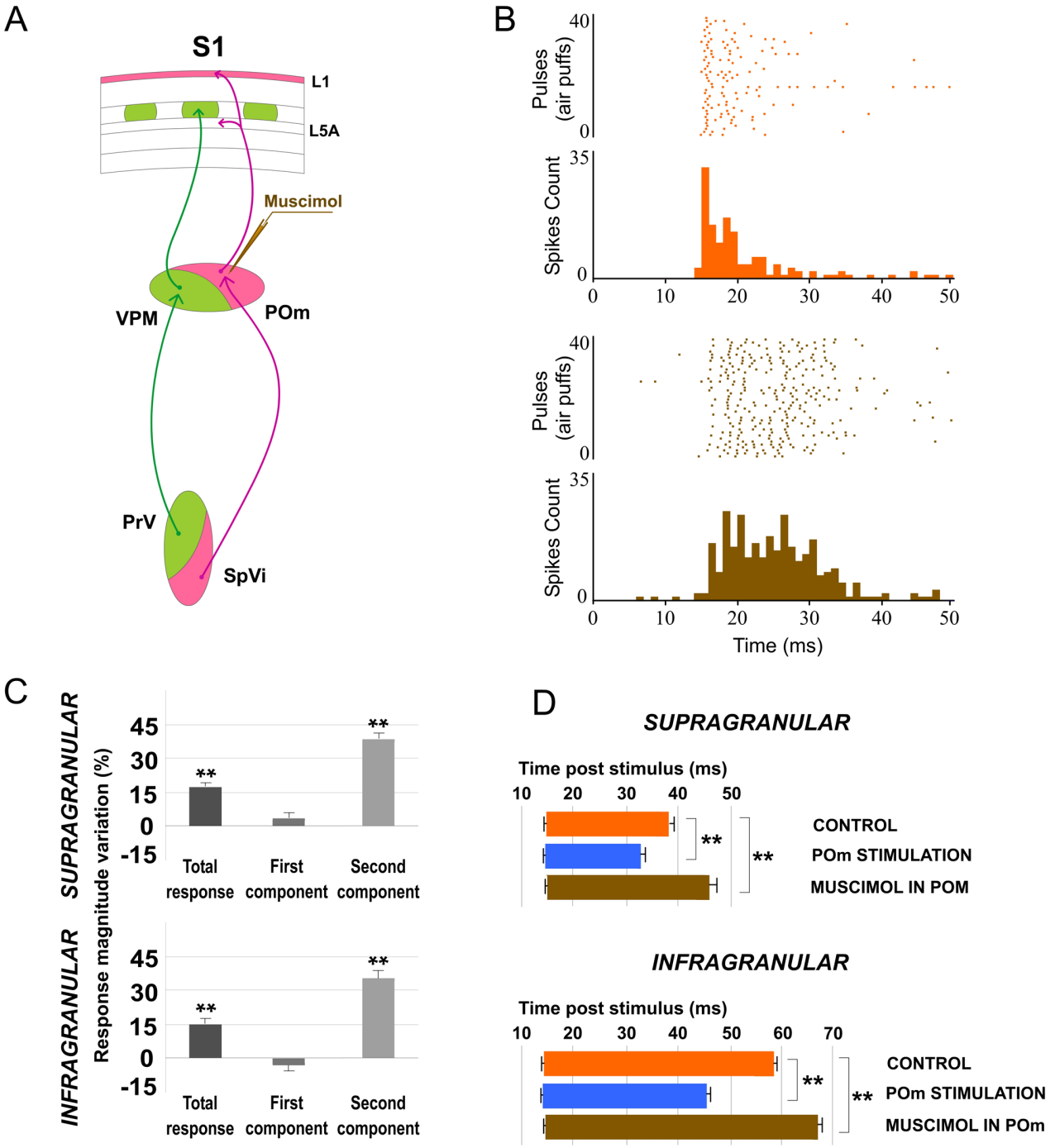

Fig 4. Muscimol-induced inactivation of the POm. (A) Schematic diagram indicating the experimental manipulation of the paralemniscal (pink) thalamocortical circuitry to barrel cortex. (B) POm inactivation enhanced responses in S1 mainly in the second component. Raster plots and PSTHs are shown for a sample supragranular neuron before (top) and after (bottom) POm inactivation. Also the pattern of spikes in the response was changed after POm inactivation suggesting that POm imposes a precise control of cortical responses. (C) Percentage change in mean response magnitude when POm was inactivated with muscimol. Spikes were strongly enhanced in the second component of the response. (D) Mean onset and offset latencies and response duration in Control (orange), in POm E-stimulation (blue) and in POm inactivation condition (brown). Response duration decreased with POm E-stimulation and increased in POm inactivation condition. We did not find differences in onset latencies but offset latencies changed significantly. Horizontal bars represent response duration.

doi:10.1371/journal.pone.0148169.g004

response onset latency was not significantly modified under muscimol application in POm (Fig 4D). However, the response offset latency was increased in infra- (12%; n = 37; P<0.001) and supragranular layers (22%; n = 51; P<0.001; Fig 4D).

Also, spontaneous activity was increased from 0.94±0.2 to 1.23±0.3 spikes/s (31%; n = 51; P<0.001) in infragranular neurons and from 0.70±0.2 to 0.95±0.2 spikes (35%; n = 37; P<0.001) in supragranular neurons. These results suggest that POm activity modulates cortical excitability of the barrel cortex.

To determine if this effect was specific of POm nucleus, we pharmacologically inactivated VPM neurons with muscimol (0.1–0.3 μl; 1 mM) in 9 rats. The magnitude of cortical responses diminished within a few minutes (<5 min) after the injection (Fig 5). A total of 82% of infragranular layer neurons (27 of 33) and 94% of supragranular layer neurons (29 of 31) displayed significant reduction in responses correlated with VPM inactivation. The evoked spikes in response to whisker sensory stimulation were reduced from 1.97±0.3 to 1.29±0.2 spikes/stimulus (-34%, P<0.001; n = 27) in infragranular layers and from 1.72±0.3 to 0.97±0.2 spikes/stimulus (-44%, P<0.001; n = 29) in supragranular layers (Fig 5B). Our results are in agreement with other studies showing that VPM lesions abolish cortical responses evoked by whisker stimulation [59].

These findings suggest more differences between POm and VPM thalamic nuclei. In contrast to VPM inactivation, following POm inactivation cortical response magnitude significantly increased. In both layers, the first component was not affected by POm inactivation. However, spikes in both components of cortical sensory responses were strongly abolished after VPM inactivation. Again, these opposite results from VPM or POm inactivation on whisker cortical responses suggest a different functional role of these thalamic nuclei in somatosensory processing.

POm regulation on cortical sensory processing is time and intensity-dependent

To further understand these effects we investigated sensory response changes according to the interval between POm E-stimulation and sensory stimulus. We found that response magnitude and duration of cortical neurons changed by POm E-stimulation intervals before sensory stimulus. The results are summarized and quantified in Fig 6. This figure also demonstrates the important differences between both cortical layers. In infragranular layers, the first component was not significantly affected at any time interval (50–1000 ms). However, spikes in the first component were strongly reduced at all intervals in supragranular layers. In addition, we found a significant reduction of spikes in the second response component in both infra- and supragranular layers. Moreover, in supragranular layers, we did not find significant response changes at longer intervals than 700 ms. In contrast, we found a significant reduction of spikes even at 1000 ms in infragranular layer. These findings implicate different dynamics between both layers, especially on the first response component.

We also found that response duration and magnitude of cortical neurons decreased with increasing E-stimulation intensity (Fig 7), indicating that POm E-stimulation effects are also intensity-dependent. Reduction in whisker response magnitude and duration by POm E-stimulation at two current intensity ranges (15–45μA and 50–80 μA) are quantified in Fig 8. We found that increasing POm E-stimulation intensity mainly reduced second component spikes, shortening the duration of sensory responses.

POm exerts its control of cortical sensory responses mainly through L1

Recent studies suggest that POm projections make excitatory synapses with barrel cortex pyramidal cells [20, 39, 43]. Accordingly, we have showed above that POm E-stimulation alone

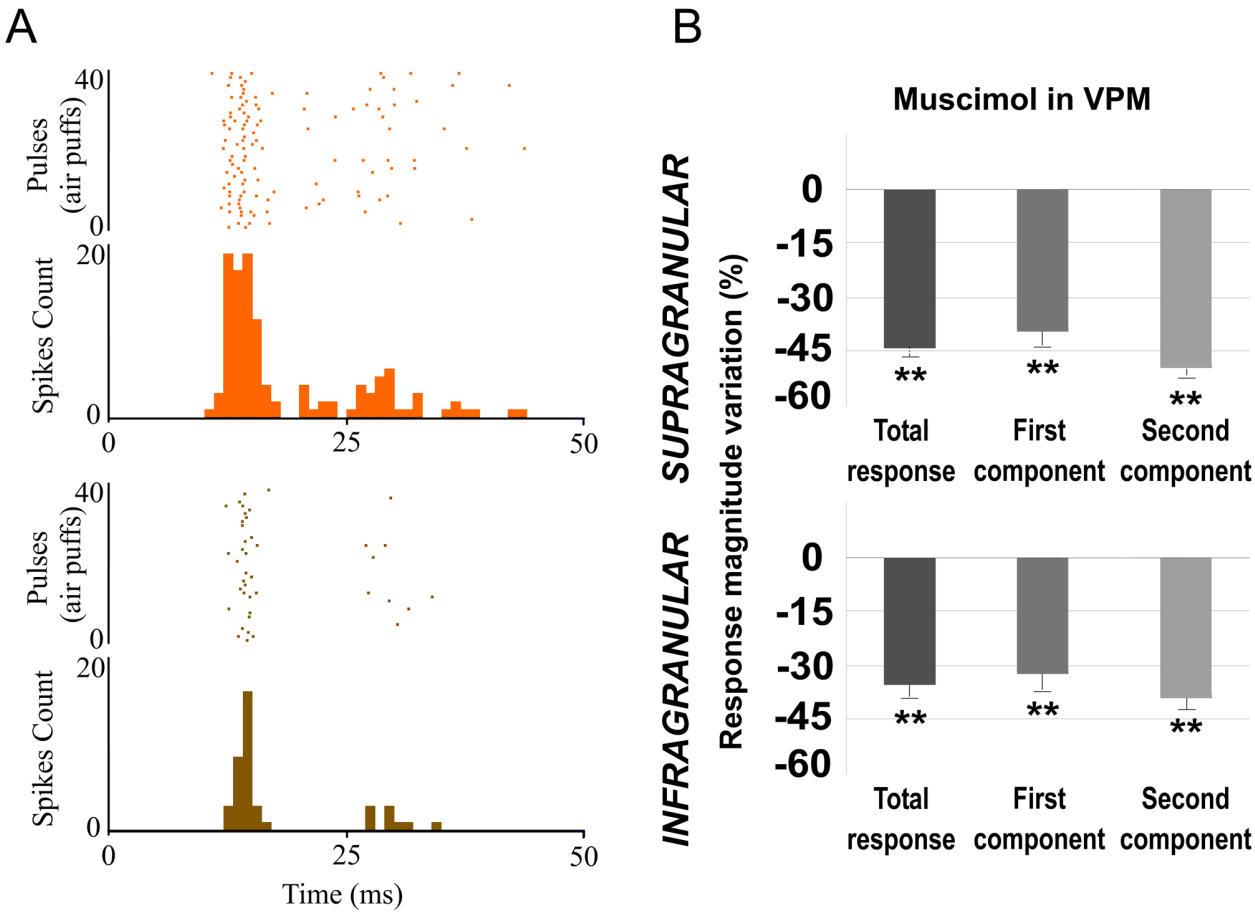

Fig 5. Muscimol-induced inactivation of the VPM. Inactivating VPM decreased responses in infra- and supragranular layers of S1. (A) Raster plots and PSTHs are shown for a supragranular sample neuron before (orange) and after (brown) VPM inactivation. (B) Mean response magnitude change (%) evoked by VPM inactivation. In both layers, spikes of sensory responses were strongly abolished after VPM inactivation by muscimol.

doi:10.1371/journal.pone.0148169.g005

elicited excitatory orthodromic spikes in infra- and supragranular layers of barrel cortex. However, our results also showed that POm E-stimulation just before sensory stimulus reduced magnitude and duration of cortical whisker responses. Moreover, POm inactivation by muscimol caused an enhancement of both sensory cortical responses and spontaneous cortical activity in the barrel cortex. How can these intriguing effects be explained? It is well described that blocking activity in L1 increases whisker-evoked responses [40], suggesting that L1 exerts an inhibitory influence on whisker responses. Since L1 receives strong inputs from POm [18, 19, 21, 23, 28], it is then possible that POm exerts its control of cortical sensory responses through L1. To test this hypothesis, we perform the following experiments.

Blocking inhibitory transmission in L1 enhances whisker response in barrel cortex. It is known that L1 inputs generate direct, rapid excitatory postsynaptic potentials in L1 interneurons [60, 85]. Accordingly, in the barrel cortex, whisker-evoked sensory information is rapidly relayed to L1 neurons, which, in turn, act to powerfully inhibit whisker-evoked responses [40, 60]. Since L1 is composed of more than 90% of GABAergic neurons [61, 62], to further understand the contribution of L1 in POm regulation of cortical sensory processing, we pharmacologically blocked GABAergic inhibitory transmission in L1 in 12 rats. Picrotoxin (PTX; antagonist of $GABA_A$ receptors; 1 mM) application (1 μl) to the cortical surface was accompanied by a

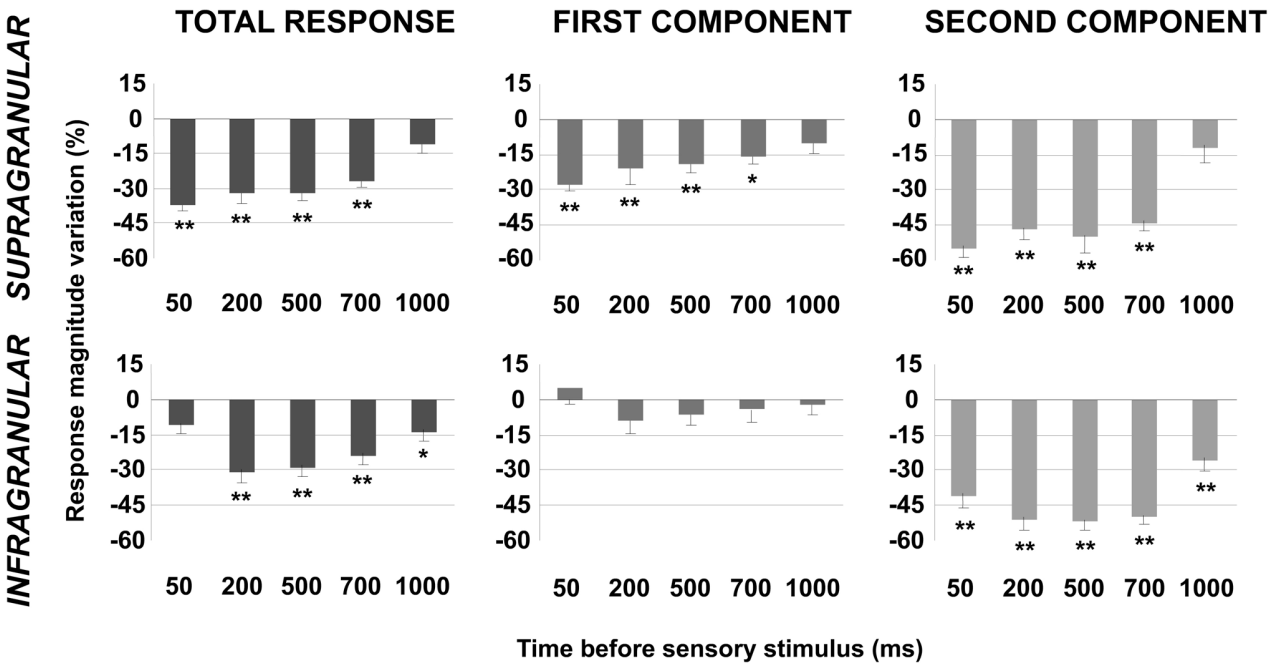

Fig 6. The effect of POm E-stimulation is time-dependent. This figure shows the change in mean sensory response magnitude by different POm E-stimulation intervals (50–1000 ms) before whisker stimulus. Supragranular total response was significantly reduced by POm E-stimulation at intervals ranged from 50 to 700 ms but not at 1000 ms. Total response of infragranular neurons was reduced at intervals from 200 to 1000 ms but not at 50 ms. In infragranular layers, the first response component (from onset to 20 ms) was not significantly affected at any time interval. In contrast, in supragranular layers, spikes in the first component were reduced at intervals <1000 ms. Spike reduction by POm E-stimulation was more prevalent in the second component of the responses in both layers (from 20 ms to offset). In supragranular neurons, spikes in the second component were decreased significantly at several time intervals from 50 to 700 ms before stimulus. The most powerful effect was found at 50 ms. Spikes in the second component of infragranular neurons were reduced significantly at time intervals from 50 to 1000 ms before sensory stimulus. In infragranular layer, the numbers of single units analyzed in each interval are: n = 38 (50 ms), n = 40 (200 ms), n = 80 (500 ms), n = 55 (700 ms) and n = 40 (1000 ms). In supragranular layer, n = 35 (50 ms), n = 33 (200 ms), n = 67 (500 ms), n = 45 (700 ms) and n = 32 (1000 ms). In all figures: * P<0.05; ** P<0.01.

doi:10.1371/journal.pone.0148169.g006

marked change in cortical sensory responses in infra- and supragranular layers. Spontaneous activity rates were significantly affected, as is depicted in Fig 9. The baseline firing rate was increased from 0.88±0.3 to 1.20±0.3 spikes/s (36%; n = 22; P<0.001; Wilcoxon-matched pairs test) in infragranular layer and from 0.59±0.2 to 0.79±0.2 spikes/s (38%; n = 21; P<0.001; Wilcoxon-matched pairs test) in supragranular layer.

It is known that Cav2.1 (P/Q- type) voltage-gated calcium channels are expressed on parvalbumin (PV) interneuron axon terminals and mediate GABA release from fast spiking interneurons to pyramidal cells [63–65]. To study in more detail the inhibitory implication in POm control of cortical processing, we applied P/Q- type voltage-gated calcium channels blocker ω-agatoxin-IVa (0.1 μM) to the cortical surface (1 μl) in 10 rats. We found that cortical sensory response magnitude and duration significantly increased 15 min after injection. A total of 88% of infragranular layer neurons (23 of 26) and 91% of supragranular neurons (21 of 23) displayed increments in sensory responses after blocking P/Q-type calcium channels in superficial cortex. Spontaneous activity rates were also significantly affected (Fig 9). The baseline firing rate was increased from 0.97±0.3 to 1.18±0.3 spikes/s (22%; n = 23; P<0.001; Wilcoxon-matched pairs test) in infragranular layer and from 0.66±0.2 to 0.86 ± 0.2 spikes/s (31%; n = 22; P<0.001; Wilcoxon-matched pairs test) in supragranular layer.

A total of 92% of infragranular layer neurons (22 of 24) and 81% of supragranular neurons (21 of 26) displayed increments in sensory responses after blocking GABAergic inhibitory

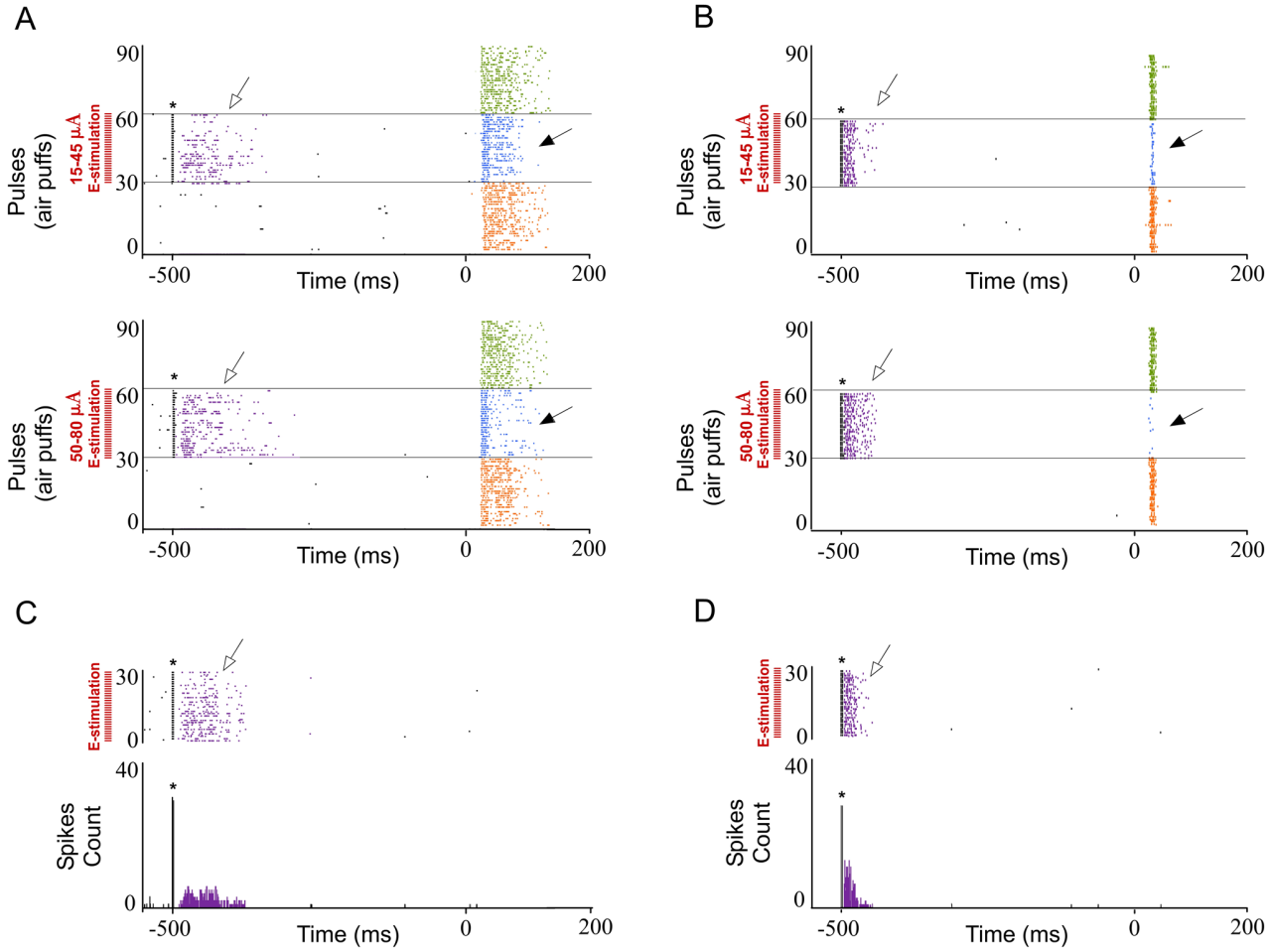

Fig 7. The effect of POm E-stimulation is intensity-dependent. Response duration and magnitude of cortical neurons decreased with increasing E-stimulation intensity. Raster plots and PSTHs are shown for a sample infragranular (A) and supragranular (B) responses after 15–45 μA (top) and 50–80 μA (bottom). Increasing POm E-stimulation intensity shortened responses more strongly, reducing spikes in the second response component (filled arrows). Control condition before (orange) and after (green) POm E-stimulation condition (blue) are shown. POm E-stimulation was applied 500 ms before pulses 31 to 60. Whisker stimulus presentation was applied at Time 0 ms. POm E-stimulation applied alone elicited orthodromic (open arrows) but not rebound activity in infra- (C) and supragranular layers (D). * indicates E-stimulation artifacts.

doi:10.1371/journal.pone.0148169.g007

transmission in L1. Cortical response magnitude (Fig 10A) and duration were significantly increased 15 min after PTX application. Again, this effect was more prevalent in the second component of the response. In infragranular layers, we found an increased number of spikes from 0.84±0.2 to 0.98±0.2 spikes/stimulus (16%; n = 22; $P<0.001$; Wilcoxon-matched pairs test) in the first component. Spikes in the second component of the response were increased from 1.12±0.2 to 1.55±0.3 spikes/stimulus (38%; n = 22; $P<0.001$; Wilcoxon-matched pairs test; Fig 10A). In supragranular layers, we found an increased number of spikes from 0.97±0.2 to 1.19±0.2 (22%; n = 21; $P<0.001$; Wilcoxon-matched pairs test) in the first component and from 0.91±0.1 to 1.20±0.2 (32%; n = 21; $P<0.001$; Wilcoxon-matched pairs test; Fig 10A) in the second component.

In infragranular layers the latency of the response onset did not change (from 14.17±0.33 to 14.38±0.32 ms; 1%; n = 22; P = 0.37; Wilcoxon-matched pairs test) while offset latency increased from 55.46±0.67 to 69.29±1.54 ms (25%; n = 22; $P<0.001$; Wilcoxon-matched pairs

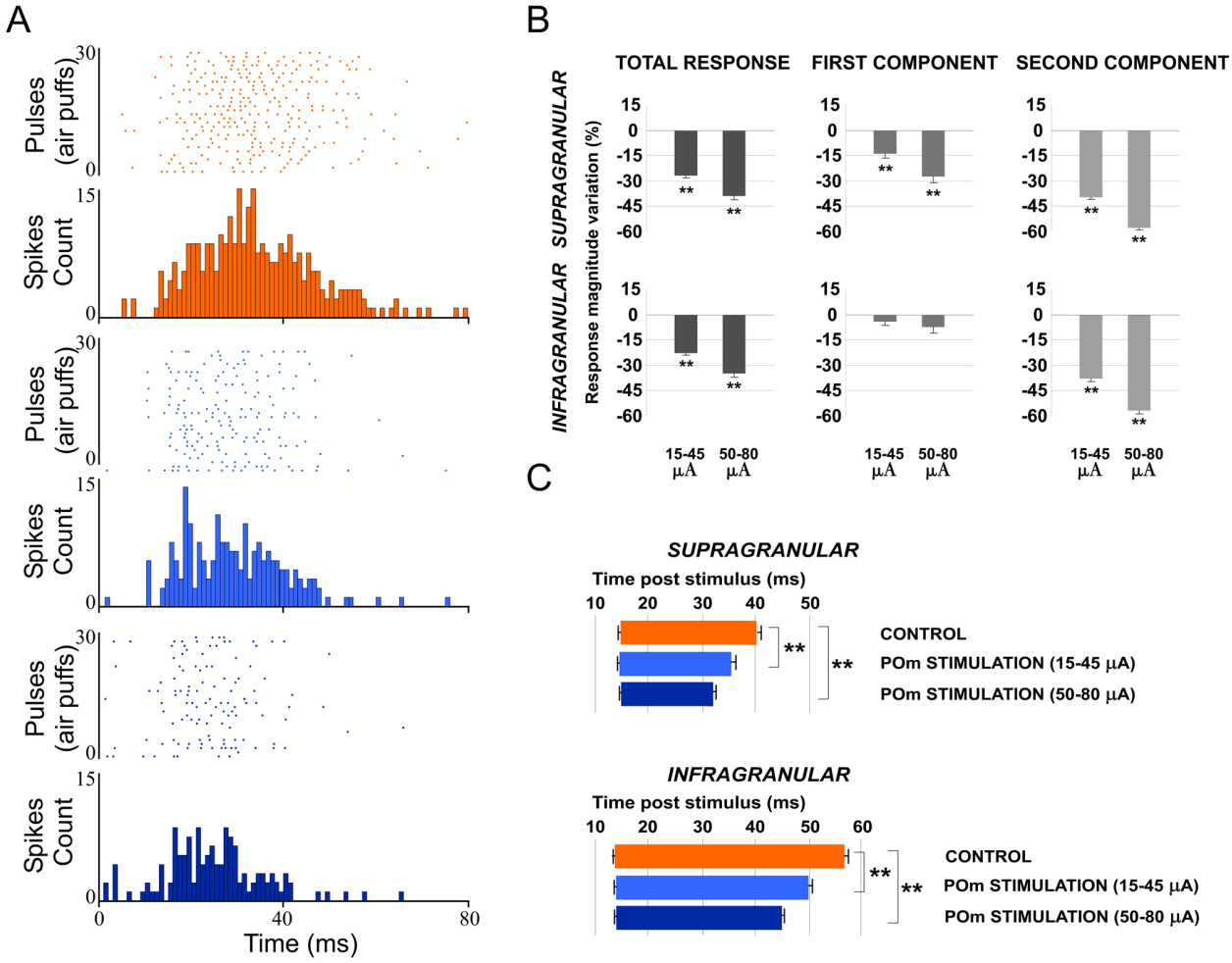

Fig 8. Increasing POm E-stimulation intensity enhances the reduction of second component spikes, shortening the duration of the sensory response. (A) Raster plots and PSTHs are shown for a supragranular whisker response change after increasing POm E-stimulation intensity before sensory stimulus. Control response (orange), 15–45μA POm E-stimulation (blue) and 50–80 μA POm E-stimulation (dark blue). (B) Response magnitude variation (%) with different POm E-stimulation intensities before sensory stimulus. (C) Increasing POm E-stimulation intensity before stimulus shortened the responses offset latencies. Horizontal bars represent response duration. In infragranular layers, the numbers of single units analyzed in B and C are: n = 57. In supragranular, n = 53.

doi:10.1371/journal.pone.0148169.g008

test;). In supragranular layers the onset latency was not modified (from 14.35±0.36 to 14.64 ±0.37 ms; 2%; n = 21; P = 0.23; Wilcoxon-matched pairs test). In contrast, offset latency increased from 38.81±1.57 to 46.96±1.02 ms (21%; n = 21; P<0.001; Wilcoxon-matched pairs test).

Whisker response magnitude and duration increased in infra- and supragranular layers (Fig 10B). In infragranular layers, the first component did not increase significantly (from 0.78±0.2 to 0.83±0.2 spikes/stimulus; 6%; n = 23; P = 0.07; Wilcoxon-matched pairs test). Spikes in the second component of the response were increased from 1.06±0.3 to 1.22±0.3 spikes/stimulus (15%; n = 23; P<0.001; Wilcoxon-matched pairs test; Fig 10B). In supragranular layers, the first component was not affected (from 0.73±0.1 to 0.79±0.1 spikes/stimulus; 8%; n = 22; P = 0.062; Wilcoxon-matched pairs test) while the second component was increased (0.68±0.1 to 0.81±0.1 spikes/stimulus; 19%; n = 22; P<0.001; Wilcoxon-matched pairs test; Fig 10B).

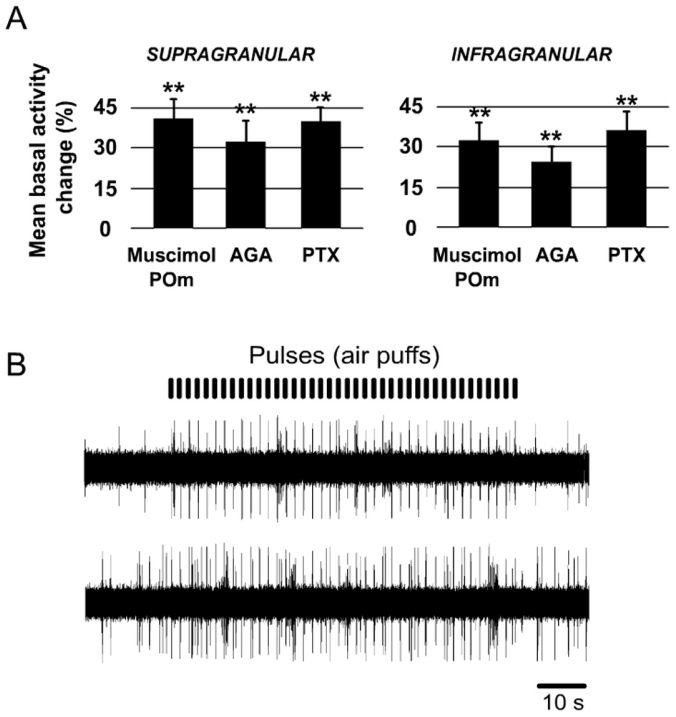

Fig 9. Cortical spontaneous activity changes in different tested conditions. (A) Mean basal activity change (%) in different conditions (muscimol in POm; AGA and PTX in cortical surface). In all conditions cortical basal activity in S1 was significantly increased after drugs applications. The baseline firing rate was calculated from mean firing within a 10 s window before the first pulse (air puff). (B) Muscimol-induced inactivation of the POm enhanced sensory responses in infra- and supragranular layers and increased cortical spontaneous activity. Raw cortical extracelular recordings are shown before (top) and after (bottom) muscimol application. These recordings show the enhancement of cortical sensory responses to whisker deflections (pulses). Cortical spontaneous activity was also increased after muscimol-induced inactivation of the POm.

doi:10.1371/journal.pone.0148169.g009

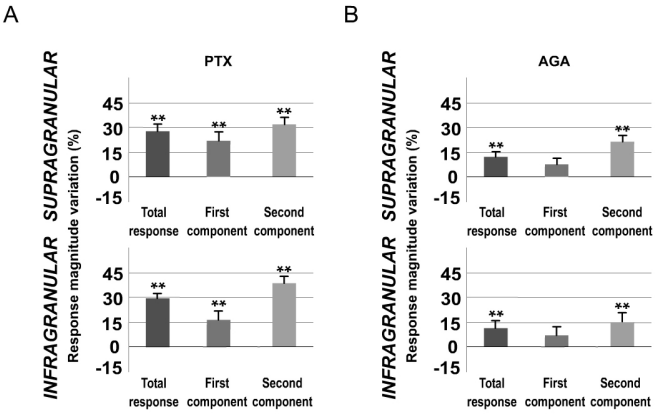

Fig 10. Blocking GABAergic inhibitory transmission in L1 enhances whisker responses. Change (%) in mean sensory response magnitude by PTX (A) or AGA (B) application in L1. Blocking GABAergic inhibitory transmission in L1 by PTX increased significantly whisker response magnitude in infra- (bottom row) and supragranular layers (top row) more strongly in the second component of the response. AGA application enhanced sensory responses in infra- and supragranular neurons. However, in both layers, AGA did not induce significant effects in the first component. * P<0.005; ** P<0.001.

doi:10.1371/journal.pone.0148169.g010

In accordance with previous studies [40], we confirm that L1 exerts an inhibitory influence on whisker responses. Our results demonstrate that GABAergic inhibitory transmission in L1 is implicated in the regulation of cortical excitability and sensory response magnitude and duration.

L1 GABAergic system is crucial in sensory cortical regulation by POm

Next, in that condition of L1 inhibitory transmission inactivation by PTX, we applied E-stimulation to the POm before (500 ms) each whisker stimulus (Fig 11). We found that response magnitude did not significantly decrease by POm E-stimulation (infragranular layers: 1%; n = 22; P = 0.67; Wilcoxon-matched pairs test; in supragranular layers: -4%; n = 21; P = 0.18; Wilcoxon-matched pairs test; Fig 12A, Total response). Response duration was also not affected by POm E-stimulation in this condition. Offset latencies were not reduced (in infragranular layer: -5%; n = 22; P = 0.098; Wilcoxon-matched pairs test; and in supragranular layer: -3%; n = 21; P = 0.9; Wilcoxon-matched pairs test; Fig 12B). Onset latencies in both layers were not significantly affected.

Blocking P/Q-type Ca2+ channels in L1 prevents POm electrical stimulation effect. When we applied POm E-stimulation before (500 ms) whisker stimulus in P/Q-type voltage-gated calcium channels blocked condition we found that cortical sensory responses did not significantly decrease. Response magnitude did not significantly decrease by POm E-stimulation in infragranular layers (-3%; n = 23; P = 0.15) and in supragranular layers (-6%; n = 22; P = 0.09; Wilcoxon-matched pairs test; Fig 13A Total response). Response duration was also not affected by POm E-stimulation in this condition. In infragranular layers, offset latencies were not reduced (-3%; n = 23; P = 0.39; Wilcoxon-matched pairs test) and the same was found in supragranular layers (-6%; n = 22; P = 0.08; Wilcoxon-matched pairs test; Fig 13B). Onset latencies in both layers were not affected.

L1 E-stimulation just before whisker stimulus modulates sensory response magnitude and duration in barrel cortex. To further confirm whether the observed POm modulation of cortical responses was mediated by L1, we investigated cortical response changes by applying L1 E-stimulation in S1 before sensory stimulus in 6 rats. Similar to POm E-stimulation, L1 E-stimulation (single pulse of 5–10 μA, 0.5 ms) before (150 ms) each whisker stimulus was accompanied by a marked change in cortical sensory responses. Magnitude and duration of cortical responses significantly decreased. Again, magnitude reduction was more prevalent in the second component of the response (Fig 14). In infragranular layers, the first component was not affected (from 1.11±0.1 to 1.08±0.1 spikes/stimulus; -3%; n = 33; P = 0.67). Evoked spikes were decreased in the second component of the response by L1 E-stimulation from 0.96 ±0.2 to 0.67±0.1 spikes/stimulus (-30%; n = 33; P< 0.001). In infragranular layers, 72% of neurons (33 of 46) displayed significant changes in responses correlated with L1 E-stimulation. In supragranular layers both response components were affected. The first component decreased from 1.02±0.1 to 0.83±0.1 spikes/stimulus (-19%; n = 39; P< 0.001) and from 0.78±0.1 to 0.48 ±0.1 spikes/stimulus (-38%; n = 39; P<0.001) in the second component. A total of 85% of supragranular layer neurons (39 of 46) displayed changes correlated with L1 E-stimulation.

The latency of the response onset did not change in infragranular neurons (13.82±0.13 ms in control and 13.68±0.1 ms after L1 E-stimulation; -1%; n = 33; P = 0.62). However, as occurred in POm E-stimulation condition, the main effect was found in offset latency (from 55.18±1.04 to 51.21±1.1 ms; -7%; n = 33; P<0.001), decreasing the duration of the response. The latency of the response onset was reduced in supragranular neurons from 14.67±0.3 to 13.93±0.25 ms (-5%; n = 39; P = 0.002) and offset latencies decreased from 40.58±1.54 to 34.33 ±1.4 ms (-15%; n = 39; P<0.001), as well.

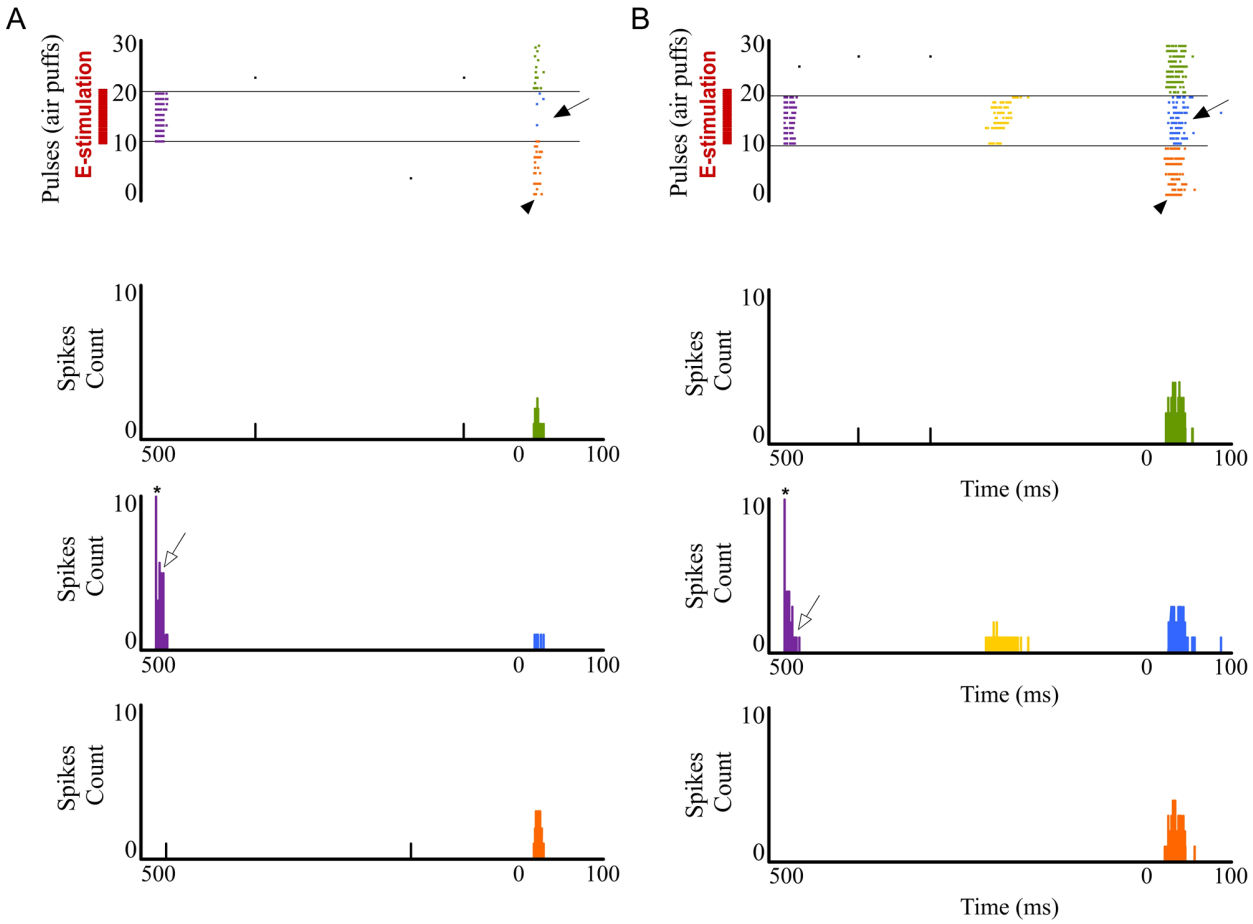

Fig 11. POm E-stimulation before whisker stimulus does not decrease cortical response magnitude and duration when PTX is applied in L1. Raster plots and PSTHs are shown for a supragranular neuron before (A) and after (B) GABAergic inhibitory inactivation in L1. Before PTX application, sensory response (filled arrows) of this example neuron was abolished by POm E-stimulation before whisker stimulus. However, POm E-stimulation did not reduce sensory response when GABAergic inhibitory transmission in L1 was inactivated (B). GABAergic inactivation in L1 allowed POm E-stimulation to cause rebound spikes (in yellow). PTX effect is also shown in the sensory response (arrowheads) enlargement after PTX application. Control condition before (orange) and after (green) POm E-stimulation condition (blue) are shown. POm E-stimulation was applied 500 ms before pulses (air puffs) 11 to 20. Open arrows indicate orthodromic spikes elicited by POm E-stimulation. * indicates stimulation artifacts.

doi:10.1371/journal.pone.0148169.g011

These results were similar to POm E-stimulation suggesting that the observed effects produced by POm E-stimulation in sensory cortical responses were mainly mediated by L1.

POm controls the sensory processing in S2 and this regulation is modulated by corticofugal activity from L5 in S1

POm neuron projections also target other cortical areas including S2 [18, 21]. It is well described the reciprocal connections between these areas. The above results demonstrate that POm modulates magnitude and duration of S1 cortical responses to sensory input. This sensory response adjustment could be also present in the processing of information between somatosensory cortical areas. Then, to determine the possible role exerted by the POm in the adjustment of somatosensory cortical processing between S1 and S2, we performed a complementary set of experiments investigating whisker response changes in S2 by electrically stimulating S1 and by muscimol-induced inactivation of the POm. The following results describe

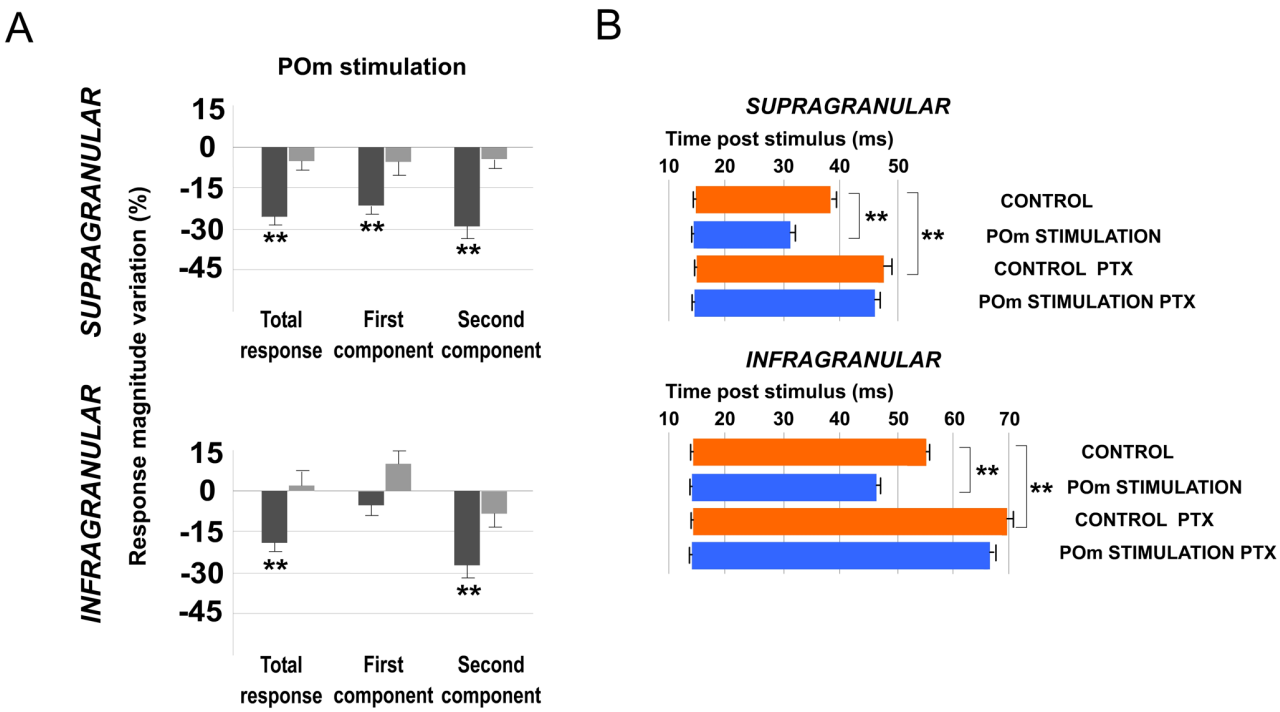

Fig 12. POm E-stimulation before whisker stimulus does not decrease cortical response magnitude and duration when PTX is applied in L1. (A) Percentage change in mean response magnitude by POm E-stimulation before (black) and after PTX application (grey). POm E-stimulation did not decrease cortical response magnitude when GABAergic inhibitory transmission in L1 was blocked. (B) PTX application in L1 increased whisker offset response latency in infra- and supragranular layers. POm E-stimulation before whisker stimulus did not decrease cortical response duration when PTX was applied in L1. Control (orange) and POm E-stimulation (blue) conditions are shown.

doi:10.1371/journal.pone.0148169.g012

below demonstrate that POm activity is also controlling the sensory processing in S2 and this regulation is modulated by corticofugal activity from L5 in S1.

L5 E-stimulation in S1 before sensory stimulus modulates whisker response in S2. It is known that L5 corticofugal neurons in S1 project to the POm (see Introduction). From here, POm neuron projections also target other cortical areas including higher-order somatosensory cortical regions.

We recorded vibrissal responses in the whisker representation area of S2 in 11 rats. We found that S2 neurons displayed a low firing rate in spontaneous conditions (0.87±0.6 spikes/s; n = 40) and displayed a contralateral response to whisker displacements. Then, we investigated sensory response changes in S2 neurons by L5 E-stimulation in S1 before whisker stimulus (150 ms). S1 L5 E-stimulation alone (single pulse of 0.5 ms; 5–30 μA) elicited strong activity in S2 (Fig 15B). The latencies of these evoked spikes varied in the range of 8–40 ms (mean latency: 21.61±0.7 ms; n = 40). When we stimulated electrically the L5 of S1 before each sensory stimulus, response magnitude decreased from 1.95± 0.3 to 1.35± 0.2 spikes/stimulus (-30%; n = 36; $P<0.001$). A total of 90% of S2 recorded units (36 of 40) displayed reduction in responses correlated with L5 E-stimulation in S1. First and second component results are described and quantified in Fig 16B. The latency of the response onset did not change (from 14.45±0.1 to 14.25±0.13 ms; -1%; n = 36; P = 0.31) but offset latency decreased by L5 E-stimulation (from 44.33±0.21 to 35.63±0.46 ms; -20%; n = 36; $P<0.001$).

Cortico-cortical sensory processing adjustment is abolished when POm is inactivated with muscimol. Next, to demonstrate that POm was implicated in the effects described

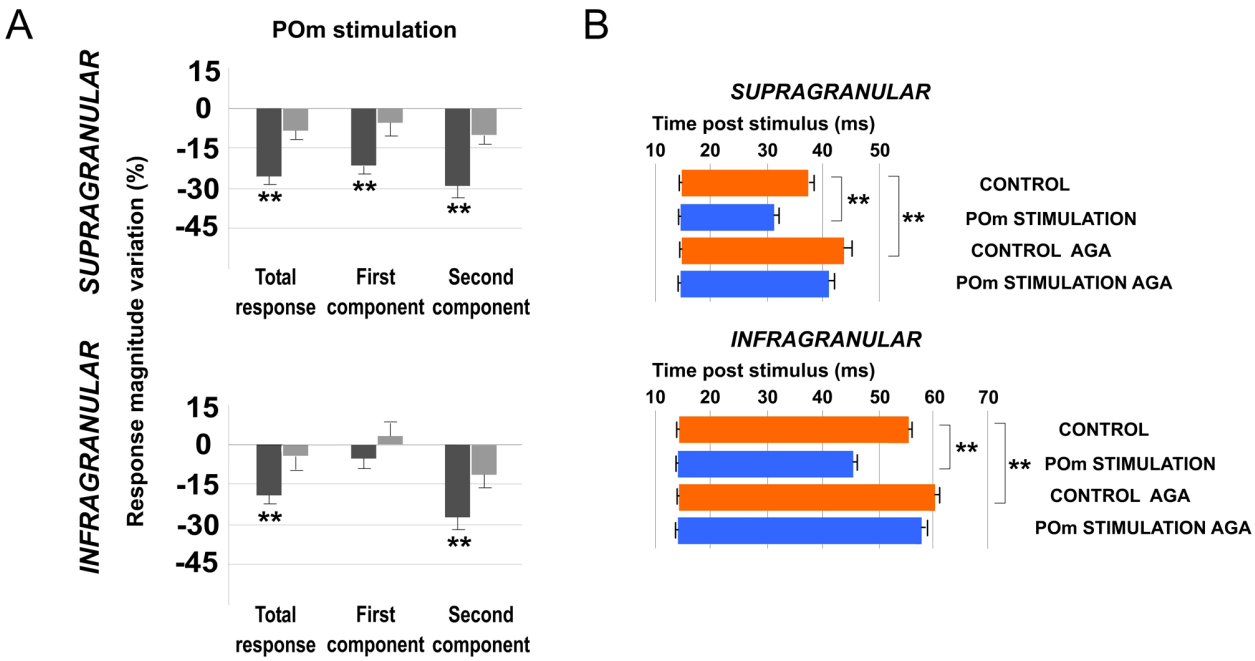

Fig 13. POm E-stimulation before whisker stimulus does not decrease cortical response magnitude and duration when AGA is applied in L1. (A) Percentage change in mean response magnitude by POm E-stimulation before (black) and after AGA application (grey). POm E-stimulation before each stimulus (500 ms) did not decrease cortical responses when P/Q-type voltage-gated calcium channels were blocked. (B) AGA application in L1 increased whisker offset response latency in infra- and supragranular layers. POm E-stimulation did not decrease cortical response duration when P/Q-type voltage-gated calcium channels were blocked. Control (orange) and POm E-stimulation (blue) conditions are shown.

doi:10.1371/journal.pone.0148169.g013

above, we inactivated the POm by infusing a small volume (0.1–0.3 μl; 1 mM) of muscimol. We found that 15 min after muscimol application, L5 E-stimulation in S1 could not reduce sensory response spikes in S2 (Fig 16). Change in mean sensory response magnitude by stimulating L5 of S1 before and after POm muscimol inactivation is quantified in Fig 16B. These findings indicate that POm activity is also controlling the sensory processing in S2 and this regulation is modulated by corticofugal activity from L5 in S1.

Furthermore, we found that S2 robust activity in response to L5 E-stimulation in S1 alone was eliminated after POm inactivation (Fig 16C and 16D white arrows) with a subsequent return after washout (data not shown). This finding is in agreement with other studies on corticothalamocortical communication implicating the POm in information transfer to higher-order cortical areas [25, 41, 42].

In sum, our results demonstrate that POm is implicated in the adjustment of information processing between somatosensory cortical areas.

Discussion

Here, using a combination of electrophysiology and pharmacology *in vivo*, we show that POm modulates magnitude and duration of supra- and infragranular barrel cortex whisker responses. Our findings demonstrate that L1 inputs from POm impose a time and intensity dependent regulation on cortical sensory processing. Moreover, we found that L1 GABAergic system mediates this process and that blocking P/Q-type Ca2+ channels in L1 prevents POm adjustment of whisker responses in the barrel cortex. Additionally, we found that POm is also controlling the sensory processing in S2 and this regulation is modulated by corticofugal activity from L5 in S1. Taken together, our data demonstrate the determinant role exerted by the

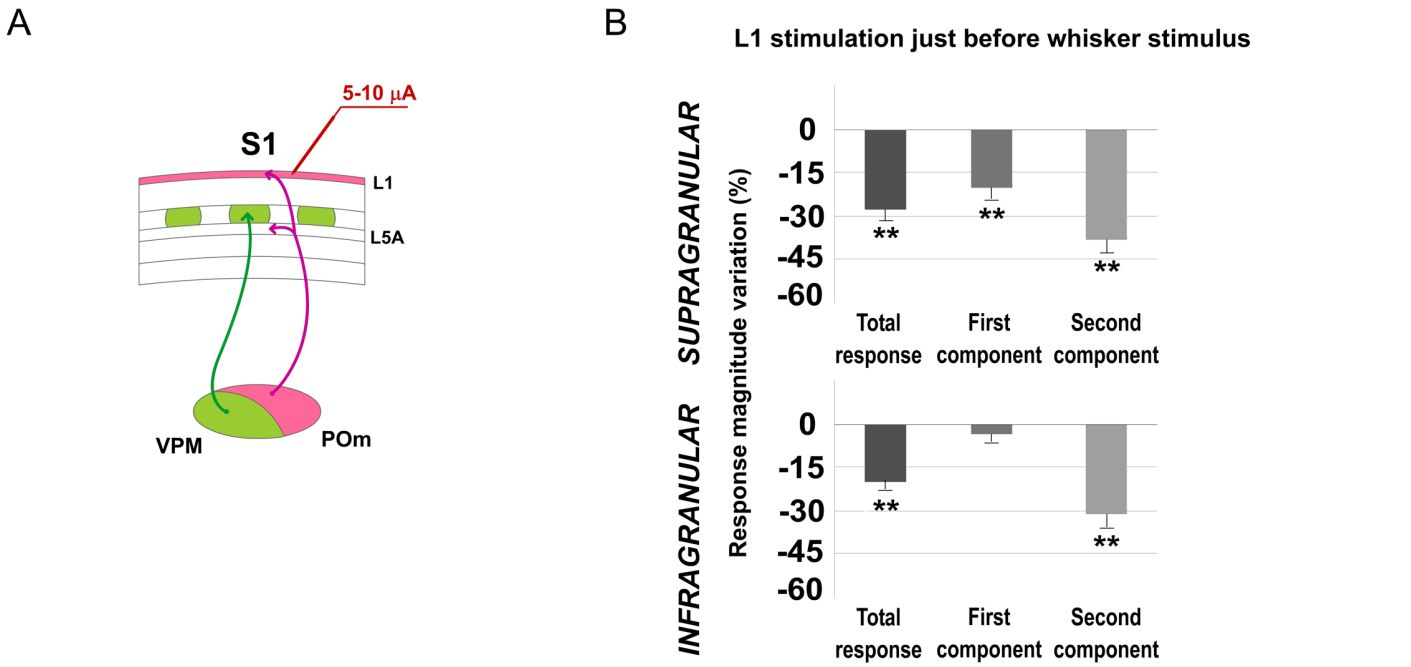

Fig 14. L1 E-stimulation before sensory stimulus modulates cortical responses. (A) Schematic diagram indicating the experimental manipulation of the barrel cortex L1. (B) Mean response magnitude variation (%) by L1 E-stimulation is quantified in this Fig Magnitude reduction was more prevalent in the second component of the response in both layers. In infragranular layers, in the first component we did not find a significant decrease of spikes. However, spikes in the second component were decreased strongly by L1 E-stimulation. In supragranular layers, in both components we found a significant reduction of spikes.

doi:10.1371/journal.pone.0148169.g014

POm in the adjustment of somatosensory cortical processing and in the regulation of cortical processing between S1 and S2. We propose that this adjustment could be a thalamocortical gain regulation mechanism also present in the processing of information between cortical areas.

Antidromic or rebound activities are not implicated in our thalamic E-stimulation effects

It is known that low intensity thalamic E-stimulation strongly activates thalamocortical neurons [45]. Yang and collaborators demonstrated that thalamic E-stimulation was capable of eliciting a cortical response that resembles the cortical activity pattern evoked by a whisker stimulus [59]. Their E-stimulation protocol (single current pulse; 10–150 μA, 100 μs duration) activated only a small region of thalamic tissue. Intensity used in our experiments (<80 μA) was estimated to activate neurons within a maximal radius that would not exceed 0.5 mm [46], suggesting that the effect induced by the E-stimulation was likely concentrated around the stimulation site. In our experiments, no cortical evoked responses were elicited when the thalamic E-stimulation was performed outside the POm or VPM. In these cases, we did not observe any detectable changes in cortical sensory responses by thalamic E-stimulation (data not shown). We assume that thalamic E-stimulation minimally affects neighbouring structures, however because POm and VPM are immediately adjacent to each other, we can not rule out possible mixed effects between VPM and POm E-stimulation. To clarify this issue we performed a set of complementary studies. Muscimol inactivation of these nuclei in separate experiments demonstrated different thalamic influence in cortical processing. VPM

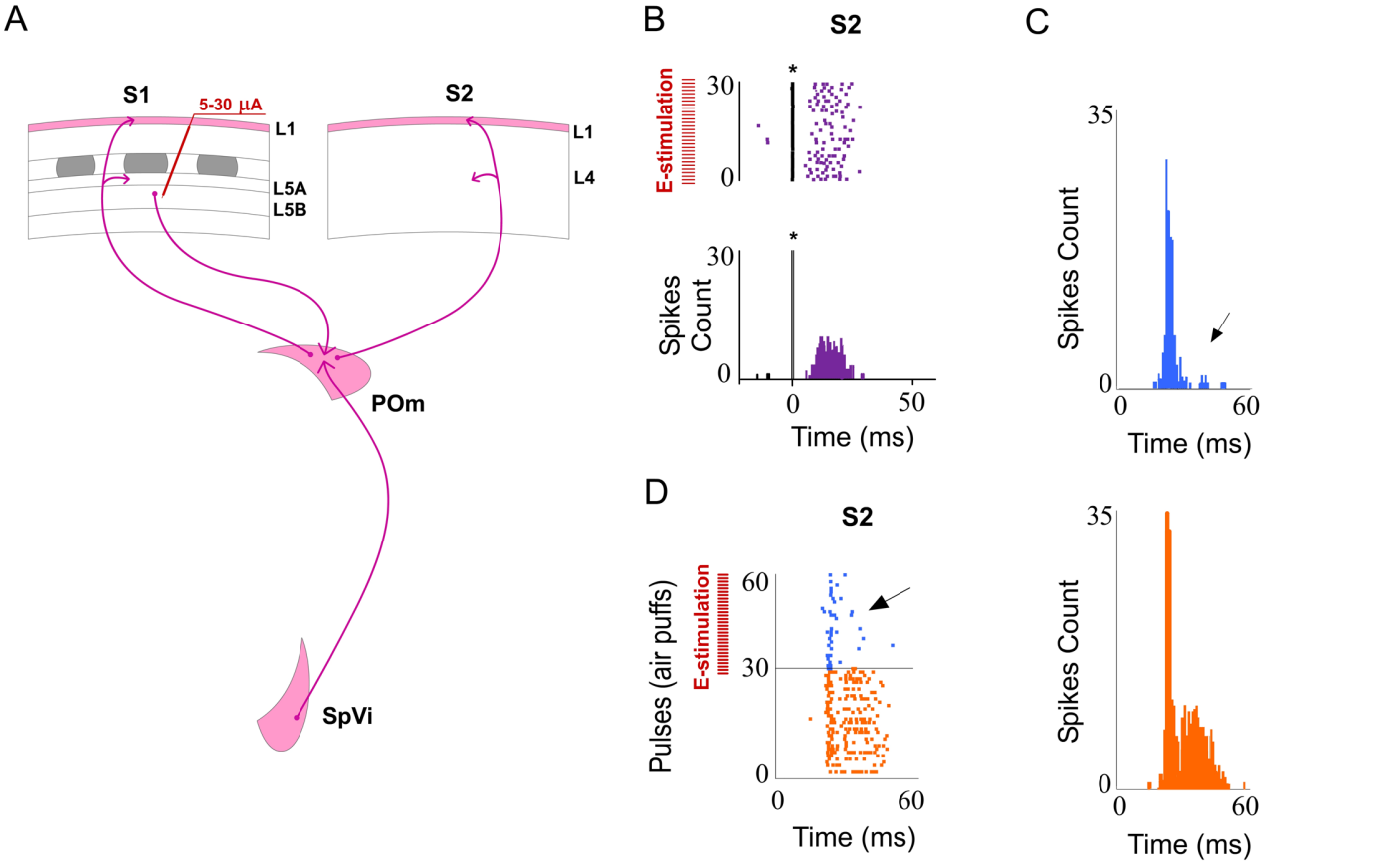

Fig 15. L5 E-stimulation in S1 before sensory stimulus modulates S2 whisker responses. (A) Schematic diagram summarizing the corticothalamocortical circuitry from S1 to S2 through the POm. The experimental manipulation of the barrel cortex is also shown. (B) An example of S2 evoked orthodromic spikes by L5 E-stimulation in barrel cortex is shown. * indicates stimulation artifacts. (C, D) L5 E-stimulation in barrel cortex just before whisker stimulus reduced responses in S2. Raster plots (D) and PSTHs (C) are shown for a sample infragranular response. L5 E-stimulation in S1 shortened responses and reduced spikes mainly in the second response component (arrows). Control (orange) and POm E-stimulation (blue) conditions are shown. Spikes are aligned on sensory stimulus (air puff) presentation (Time 0 ms). L5 E-stimulation in S1 was applied 150 ms before air puffs (31 to 60 pulses; red bars).

doi:10.1371/journal.pone.0148169.g015

inactivation by muscimol abolished whisker responses. However, POm inactivation enhanced spontaneous activity and whisker responses. Moreover, it is known that L1 receives synaptic inputs from POm but not from VPM or L4. We found that E-stimulation of L1 or POm caused similar effects in cortical sensory responses. These findings together with electrode tip position on histological sections allow us to discriminate E-stimulation effects and to understand the different function of these nuclei on cortical processing. Moreover, it is known that VPM lesions abolished the cortical responses evoked by whisker stimulation [59]. Therefore, in our POm inactivation experiments a further indication that the muscimol did not affect the VPM was the increase of cortical whisker responses.

We did not find rebound activity induced by POm or VPM E-stimulation within the current range used (<80 μA). However, we found excitatory rebound activity in some cases applying VPM E-stimulation with a higher intensity (>150 μA) (data not shown). POm E-stimulation did not elicit excitatory rebound activity even at 150 μA (data not shown). We only found excitatory rebound activity at the intensities used in our studies (<80 μA) when GABAergic inhibitory transmission in L1 was blocked by PTX. GABAergic inactivation in L1 increased

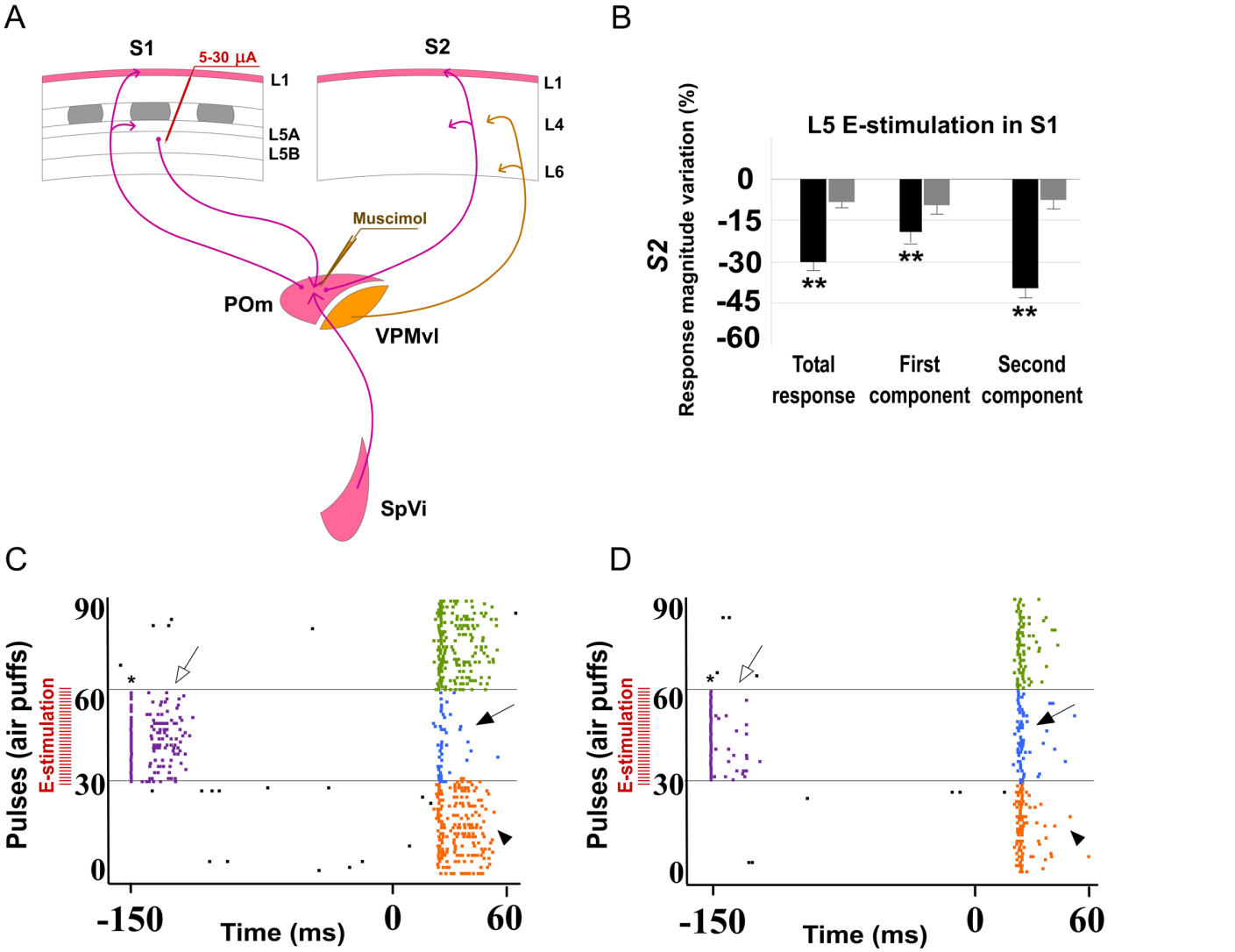

Fig 16. L5 E-stimulation in S1 does not modulate sensory responses in S2 when POm is inactivated. (A) Schematic diagram summarizing the corticothalamocortical circuitry from S1 to S2 through the POm and the extralemniscal pathway to S2 from the VPMvl thalamic nucleus. The experimental manipulation of the barrel cortex and POm is also shown. (B) Change (%) in mean S2 sensory response magnitude by stimulating L5 of S1 before (black) and after POm muscimol inactivation (gray). L5 E-stimulation in S1 did not reduce significantly sensory response spikes in S2 when POm was inactivated. ** P<0.001. (C) Sensory responses in S2 were reduced when we applied E-stimulation in L5 of S1 before each stimulus (filled arrows). This effect was abolished when the POm was inactivated with muscimol (D). Control condition before (orange) and after (green) POm E-stimulation condition (blue) are shown. E-stimulation was applied 150 ms before pulses 31 to 60. Spikes evoked in S2 by E-stimulation of L5 in S1 were eliminated by POm inactivation (open arrows). At the stimulation intensities used in this experiment, we have not observed antidromic activation in S2. Sensory responses were significantly decreased after muscimol application but not totally eliminated. Only spikes in the second component of the response were abolished (arrowheads). Spikes in the first component were not reduced by POm inactivation. * indicates stimulation artifacts.

doi:10.1371/journal.pone.0148169.g016

whisker response magnitude, increased basal activity and allowed POm E-stimulation to cause rebound spikes in some cases as shown in Fig 11B. Moreover, in our experiments we used different time intervals between POm E-stimulation and sensory stimulus ranged from 50 to 1000 ms. We consider that the time of these intervals is both, variant and long enough to allow rebound activity to be detected. However, we did not find it, ruling out rebound activity implication in our thalamic E-stimulation effects. We consider that our results support an absence

of implication of POm adaptation in our E-stimulation results. For example, sensory cortical whisker responses were strongly reduced at all intervals (1–20 Hz) in supragranular layers (Fig 6). Yet infragranular responses were not significantly reduced by POm E-stimulation at 20 Hz, a frequency high enough to cause adaptation. Furthermore, L1 E-stimulation induced similar cortical effects. In agreement with that, POm E-stimulation before whisker stimulus did not reduce cortical sensory response when GABAergic inhibitory transmission in L1 was inactivated.

Anatomically, POm receives corticothalamic inputs from L5, thus, infragranular layers activity elicited by POm E-stimulation could also result from antidromic activation of corticothalamic neurons and their axon collaterals. Thus, E-stimulation of the thalamus that is intended to activate thalamocortical afferents may also produce antidromic activation of corticothalamic neurons that subsequently contributes, via axon collaterals, to the synaptic response in the infragranular layers. Cortical studies have demonstrated that orthodromic stimulation effects are stronger than antidromic effects even between areas with strong direct projections [68–70]. Previous thalamocortical studies demonstrated that the threshold for antidromic activation was significantly higher than for orthodromic activation [45, 71]. Rose and Metherate found that mean orthodromic cortical response threshold from stimulating thalamic afferents was 28 μA. Antidromic stimulation of corticothalamic projections resulted in a mean threshold of 214 μA. This implies that low-current thalamic stimulation activates relatively few corticothalamic neurons and that it can strongly activate thalamocortical neurons. Furthermore, the threshold for evoking an antidromic spike in pyramidal neurons by L1 E-stimulation is higher than the threshold required to elicit synaptic responses in the same neuron [40]. In our experiments, we did not observe antidromic activation in infra- or supragranular recordings at stimulation intensities used in these experiments. Antidromic contribution to our findings was therefore ruled out.

L1 implication in POm control of cortical sensory responses

L1 is an important site of integration as it contains feedback corticocortical inputs from other cortical areas and TC inputs mainly from high order nuclei. In our experiments, we found that L1 inputs from POm impose precise regulation on cortical processing. In some of our experiments, we used PTX to block GABAergic transmission in L1, as was also used in other recent cortical studies *in vitro* [74] and *in vivo* [75, 76]. We also use AGA to block P/Q-type Ca2 + channels [63–65]; see below). Our results showed that POm E-stimulation before whisker stimulus did not reduce cortical sensory responses when PTX or AGA was applied over cortical surface. We did not try to determine whether these drugs reached other cortical layers, which could have directly inactivated inhibitory influence in those layers. However, we found in our experiments that POm E-stimulation did not reduce sensory responses in infra- and supragranular layers within a few minutes (<5 min) of the PTX or AGA application over the cortical surface. Taking into account that this effect was produced rapidly at the same time in both layers and since the diffusion of the drug into the infragranular layers requires more time, we consider these effects to be induced mainly by L1.

These results were similar to those resulting from POm inactivation. Furthermore, similar to POm E-stimulation, L1 E-stimulation before sensory stimulus also reduced responses in infra- and supragranular layers. It is known that L1 E-stimulation evokes two types of laminar activity in barrel cortex depending on intensity [40]. At lower intensities (<10 μA) the synaptic activation evoked by this E-stimulation was restricted to L1 and upper L2. In contrast, at higher intensities (>10 μA) L1 E-stimulation activated the entire cortical column. In our L1 E-stimulation protocol, we applied low intensities (<10 μA) to examine the effect of L1 activation on

whisker responses. We can not rule out the possibility that in our experiments L1 E-stimulation activated other cortical layers. Even L1 E-stimulation can antidromically activate vertically projecting axons of Martinotti interneurons inducing effects in other layers [40, 77]. Since, we found in our experiments similar cortical effects induced by POm E-stimulation and by L1 E-stimulation, we consider ruling out these possibilities.

In the rat barrel cortex, the border between L5 and L6 has been described at depths of 1400–1600 μm [24, 78]. In our experiments, neurons were recorded in depths from 200 to 600 μm and from 900 to 1500 μm. According to this anatomical data, we must consider that infragranular neurons recorded in our experiments were mainly from L5. Since POm strongly innervates L5A [18, 21], we considered to separate our infragranular recordings in two groups according to the depths of the recordings. A preliminary analysis of single-units from both groups (superficial and deep recordings) showed similar quantitative modulation by POm manipulations. L5A and L5B pyramidal neurons have an apical dendrite reaching L1. In accordance with that, our findings show that POm may exert its control of cortical sensory responses mainly through L1. This layer also contains a dense plexus of apical dendrites of supragranular pyramidal neurons but not of granular neurons [60, 79]. One remaining unknown is the function of L5A inputs from POm.

POm modulates the temporal integration window of cortical sensory responses

Recent studies suggest that POm projections make excitatory synapses with barrel cortex pyramidal cells [20, 39, 43, 73]. According to them, in our experiments, POm E-stimulation alone elicited orthodromic spikes in infra- and supragranular layers of barrel cortex. However, our results also showed that POm E-stimulation just before sensory stimulus reduced magnitude and duration of cortical whisker responses. Moreover, unexpectedly, we found that POm inactivation by muscimol caused an enhancement of both sensory cortical responses and spontaneous cortical activity in the barrel cortex suggesting that POm is tonically regulating cortical excitability in this region. How can these intriguing effects be explained? Our findings show that POm exerts its control of cortical sensory response magnitude and duration using the GABAergic inhibitory system in L1. Therefore, L1 inhibitory interneurons are other potential targets of POm projections. In the mouse prefrontal cortex, a recent study described that matrix thalamocortical projections terminate in outer L1, and their activation drives robust synaptic responses in L1 interneurons [80]. They found that L1 thalamocortical projections preferentially drove inhibitory interneurons of L1 and were much more effective at exciting L1 interneurons than L2/3 pyramidal cells. Accordingly, it is known that L1 inputs generate direct, rapid excitatory postsynaptic potentials in L1 interneurons [60, 85]. These interneurons could rapidly truncate afferent excitation of infra- and supragranular pyramidal neurons, limiting the temporal window during which action potentials can be generated. Our results are also in agreement with that idea. We found that POm E-stimulation or L1 E-stimulation reduced spikes mainly in the second response component. Therefore, this interplay between excitation and inhibition at the level of the barrel cortex could provide a "window of opportunity" for generating cortical responses. Our findings are consistent with that hypothesis. As our results show, the duration of the responses is regulated by POm activity. L1 inputs from POm could activate L1 GABAergic interneurons strengthening cortical inhibition, which shortens the response window. We found that increasing POm E-stimulation intensity reduced more strongly the duration of cortical responses (see Results; Fig 8). A relevant assumption supported by our data is that prolonged response duration (prolonged window) was observed when GABAergic inhibitory transmission in L1 was blocked (Fig 12B).

Accordingly, we found that response magnitude and duration of cortical neurons changed by POm E-stimulation intervals before sensory stimulus (described in Fig 6). Therefore, that interval determines the outcome of the interaction. Recently, both anatomical and physiological findings have shown that ascending inputs from the brainstem and descending inputs from L5 converge on single thalamocortical neurons in POm [25]. Both individual pathways interact functionally in a time-dependent manner and when co-activated, increase the output of thalamus supralinearly [25]. Moreover, Shlosberg et al. found that when pairing L1 E-stimulation with whisker deflection, the interval between the stimuli determined the outcome of the interaction, with facilitation of sensory responses dominating the short (<10 ms) intervals and suppression prevailing at longer (>10 ms) intervals [40]. Then, same effects could be induced by POm E-stimulation using those intervals.

We propose this mechanism could allow the temporal cortical integration of inputs from distinct pathways and could act to "reset" the network to generate the next cortical response avoiding the somatosensory cortex be captured by a single stimulus.

Since it is well described that POm is involved in temporal processing related to sensory-motor control of whisker movement [17, 34, 35], it is then possible that this mechanism could play a crucial role in sensory-motor interaction allowing the POm to control the temporal integration of the incoming tactile information during whisking exploration. The accuracy of whisking could be controlled by POm activity to optimize sensory processing. Accordingly, it has been suggested that the whisker sensory-motor system is involved in closed-loop computations [94, 95]. In particular, single unit responses from whisker sensory and motor areas show generic signatures of phase-sensitive detection and control at the level of thalamocortical and corticocortical loops [94, 95]. These loops are likely to be components within a greater closed-loop vibrissa sensory-motor system, which optimizes sensory processing. Our results are in agreement with that proposal.

Possible implication of parvalbumin interneurons in POm control of cortical responses

L1 inhibitory interneurons provide a direct source of apical dendritic inhibition to supra- and infragranular layer pyramidal neurons [80–82]; and also form inhibitory synapses onto other L1 interneurons and L2/3 interneurons [83–86]. Interneurons of L1 are heterogeneous [60, 79, 87–90]. To study in more detail the L1 inhibitory implication in POm control of cortical processing, we applied Cav2.1 (P/Q- type) voltage-gated calcium channels blocker and found that blocking P/Q-type Ca2+ channels avoided POm E-stimulation effects. It is known that these channels are expressed on parvalbumin (PV) interneuron axon terminals and mediate GABA release from fast spiking interneurons to pyramidal cells [63–65]. Consequently, it is possible that presumed PV+ interneurons were implicated in a dynamic control of sensory cortical processing by POm. Other studies have demonstrated that PV+ interneurons participate in control gain of sensory responses [86, 91, 92]. Furthermore, recent findings demonstrate that the conditional ablation of Cav 2.1 channel function from cortical PV+ interneurons alters GABA release from these cells, impairs their ability to constrain cortical pyramidal cell excitability [93].

The main effect of POm manipulation occurs in the second component of cortical response: possible NMDA receptors implication and cortical plasticity

It is known that short-latency spikes evoked by whisker stimulation in the barrel cortex are mainly mediated through non-NMDA receptors while NMDA receptors are implicated mainly

in spikes generated later after them [72]. Studies from our laboratory confirmed the implication of NMDA receptors in the late component of cortical tactile responses [57, 58]. A recent study suggest that POm associated synaptic pathways in barrel cortex are responsible for these mediating whisker-evoked NMDA receptor dependent spikes [73], in agreement with our results. Since these receptors have been directly implicated in cortical synaptic plasticity, our findings have important consequences in sensory processing implicating the POm in the control of cortical synaptic plasticity by reducing the time-window of activation in cortical neurons.

POm implication in the regulation of cortical processing between S1 and S2

Our results demonstrate the determinant role exerted by the POm in the adjustment of somatosensory cortical processing in S1 and S2. We found that vibrissal stimulus responses recorded in S1 and S2 were modulated in magnitude and duration by POm activity. These effects were abolished when we inactivated the POm with muscimol. Since our results show that POm exerts its control of barrel cortex sensory responses mainly using L1 GABAergic system, it is then possible that the same mechanism could be used by the POm to regulate sensory responses in S2 (Fig 17). Accordingly, strong POm connections to L1 in S2 have been described [18, 96].

However, in contrast to S1, it is known that L4 of S2 receives a strong projection from the POm [39, 43]. In agreement with that, in our experiment, whisker sensory responses in S2 were reduced after POm inactivation (for example see Fig 16D, arrowheads). Spikes in the second component of the response were abolished. However, spikes in the first component were not reduced by POm inactivation suggesting they come from a different pathway. Ascending whisker signals reach S2 not only through the POm. It is known that S2 receives (focally in L4 and L6; extralemniscal pathway) from thalamocortical neurons located in the ventrolateral part of the VPM [66, 67]. Since this pathway should not be affected by POm inactivation in our experiments, it is then possible that spikes in the first component of S2 whisker responses were caused by extralemniscal inputs. The short latencies of these spikes rule out the possible VPM-S1-S2 route.

We show in our experiments that vibrissal stimulus responses recorded in S2 were reduced in magnitude and duration when we applied E-stimulation in L5 of S1 before the whisker stimulus. It is possible that L6 neurons, which send feedback inputs to thalamus, were also affected by L5 E-stimulation. However, a recent study demonstrates that stimulation of L6 does not activate S2 via this circuit [43]. In our experiments, this cortical sensory processing adjustment between S1 and S2 was abolished when POm was inactivated with muscimol. L5 E-stimulation in S1 could not reduce sensory response spikes in S2 after POm inactivation (Fig 16). Furthermore, we found that S2 robust activity in response to L5 E-stimulation in S1 alone was eliminated after POm inactivation. This finding is in agreement with other studies on corticothalamocortical communication implicating the POm in information transfer to higher-order cortical areas [25, 41, 42].

POm activity modulation of cortical processing. Functional implication

There is a huge range of stimuli that reach the cortex, each with different intensities and durations. To process them the system must have the capacity to regulate itself to detect the weakest ones and not be saturated by the strongest ones. This allows the system to process a wider range of stimuli improving the ability to detect and identify tactile features. Based on our findings, we propose that control of cortical sensory processing exerted by POm could be part of a

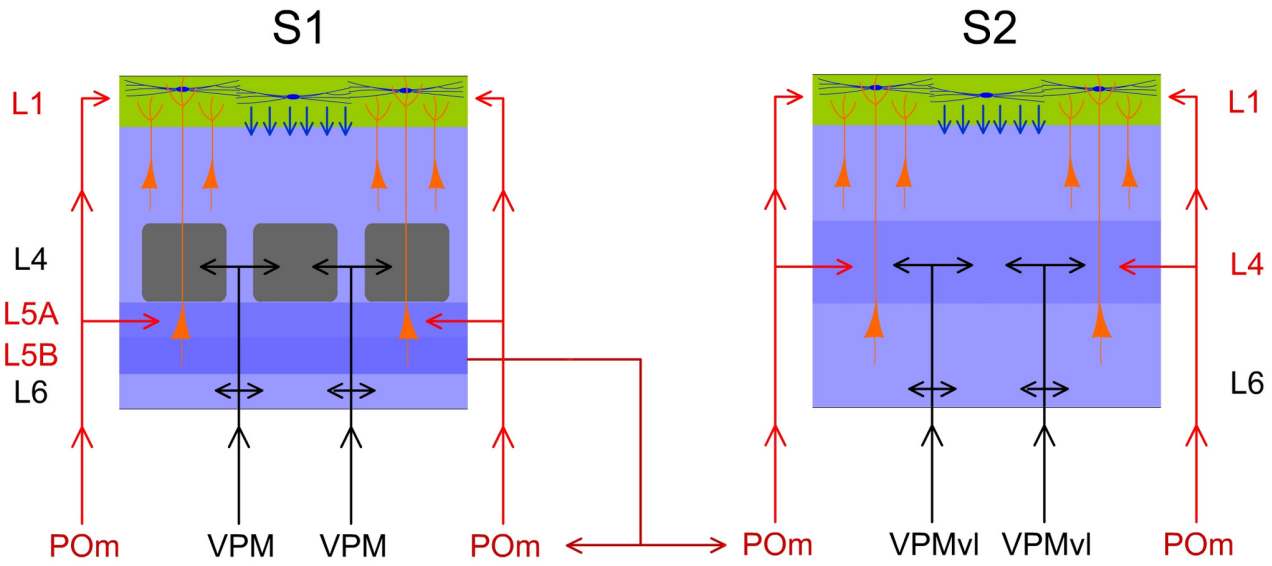

Fig 17. POm influence on somatosensory cortical response modulation. Schematic diagram summarizing the ascending thalamocortical pathways to S1 and S2. Corticothalamocortical circuitry from S1 to S2 through the POm is also shown. L5B corticofugal neurons in S1 project to the POm [9, 15, 25, 26, 43]. Ascending inputs from the brainstem and descending inputs from L5 converge on single thalamocortical neurons in POm [25]. Both individual pathways interact functionally in a time-dependent manner [25]. From here, POm neuron projections also target S2 [18, 21]. POm is also controlling the sensory processing in S2 and this regulation is modulated by corticofugal activity from L5 in S1 [25]. Whisker-evoked sensory information is rapidly relayed to L1 neurons, which, in turn, act to powerfully inhibit whisker-evoked responses [40, 60]. In accordance with previous studies [40], we confirm that L1 exerts an inhibitory influence on whisker responses.

doi:10.1371/journal.pone.0148169.g017

mechanism that has the ability to regulate the processing gain, depending on the relative intensities of stimuli across the entirety of vibrissae space. This integration of multi-whisker activity could be achieved by the POm and transmitted to the cortex to adjust the sensory processing.

Sensory activity carried by this pathway could allow the adjustment of the specific sensory content processing in the cortex. Our results show that there is a fundamental difference between the lemniscal and paralemniscal thalamic nuclei in terms of cortical influence. We must consider that these parallel pathways have a complementary function in sensory processing. Lemniscal and paralemniscal parallel ascending projection systems from the thalamus could convey specific sensory content and stimuli global sensory activity, respectively. Global activity carried by the paralemniscal pathway could allow the POm to instruct the cortex how to handle the incoming lemniscal information, which, overall, produces a precise qualitative assessment of the perceived stimulus in its specific context. Therefore, the level of activity in the POm could determine the cortical sensory processing regulation. POm could detect the changes in sensory activity (stimulus intensity and duration) and could adjust the gain and timing of cortical processing accordingly.

Our results unmask a new role of POm (and maybe other "higher-order nuclei") in cortical processing and suggest a novel framework to understand thalamocortical interaction according to which POm modulates the temporal integration window of cortical sensory responses in a POm activity-dependent manner. This could be a common feature in other sensory systems.

Acknowledgments

We thank Drs. F. Clasca and C. Porrero for their constructive comments.
We thank M. Callejo for technical assistance.

Author Contributions

Conceived and designed the experiments: CC AN. Performed the experiments: CC NBZ. Analyzed the data: CC NBZ AN. Wrote the paper: CC NBZ AN.

References

1. Ahissar E, Sosnik R, Haidarliu S. Transformation from temporal to rate coding in a somatosensory thalamocortical pathway. Nature. 2000; 406(6793):302–6. PMID: 10917531
2. Castro-Alamancos MA. Dynamics of sensory thalamocortical synaptic networks during information processing states. Prog Neurobiol. 2004; 74(4):213–47. PMID: 15556288
3. Jones EG. The thalamic matrix and thalamocortical synchrony. Trends Neurosci. 2001; 24(10):595–601. PMID: 11576674
4. McCormick DA, Bal T. Sensory gating mechanisms of the thalamus. Curr Opin Neurobiol. 1994; 4 (4):550–6. PMID: 7812144
5. Sherman SM, Guillery RW. Distinct functions for direct and transthalamic corticocortical connections. J Neurophysiol. 2011; 106(3):1068–77. doi: 10.1152/jn.00429.2011 PMID: 21676936
6. Steriade M. Synchronized activities of coupled oscillators in the cerebral cortex and thalamus at different levels of vigilance. Cereb Cortex. 1997; 7(6):583–604. PMID: 9276182
7. Jones EG. A new view of specific and nonspecific thalamocortical connections. Adv Neurol. 1998; 77:49–71; discussion 2–3. PMID: 9709817
8. Poulet JF, Fernandez LM, Crochet S, Petersen CC. Thalamic control of cortical states. Nature neuroscience. 2012; 15(3):370–2. doi: 10.1038/nn.3035 PMID: 22267163
9. Sherman SM. Thalamocortical interactions. Curr Opin Neurobiol. 2012; 22(4):575–9. doi: 10.1016/j.conb.2012.03.005 PMID: 22498715
10. Castro-Alamancos MA, Connors BW. Thalamocortical synapses. Prog Neurobiol. 1997; 51(6):581–606. PMID: 9175158
11. Castro-Alamancos MA. Properties of primary sensory (lemniscal) synapses in the ventrobasal thalamus and the relay of high-frequency sensory inputs. J Neurophysiol. 2002; 87(2):946–53. PMID: 11826059
12. Diamond ME, Armstrong-James M, Ebner FF. Somatic sensory responses in the rostral sector of the posterior group (POm) and in the ventral posterior medial nucleus (VPM) of the rat thalamus. J Comp Neurol. 1992; 318(4):462–76. PMID: 1578013
13. Feldmeyer D, Brecht M, Helmchen F, Petersen CC, Poulet JF, Staiger JF, et al. Barrel cortex function. Prog Neurobiol. 2013; 103:3–27. doi: 10.1016/j.pneurobio.2012.11.002 PMID: 23195880
14. Nicolelis MAL, Fanselow EE. Thalamcortical optimization of tactile processing according to behavioral state. Nat Neurosci. 2002; 5(6):517–23. PMID: 12037519
15. Veinante P, Jacquin MF, Deschenes M. Thalamic projections from the whisker-sensitive regions of the spinal trigeminal complex in the rat. J Comp Neurol. 2000; 420(2):233–43. PMID: 10753309
16. Woolsey TA, Van der Loos H. The structural organization of layer IV in the somatosensory region (SI) of mouse cerebral cortex. The description of a cortical field composed of discrete cytoarchitectonic units. Brain Res. 1970; 17(2):205–42. PMID: 4904874
17. Ahissar E, Zacksenhouse M. Temporal and spatial coding in the rat vibrissal system. Prog Brain Res. 2001; 130:75–87. PMID: 11480290
18. Ohno S, Kuramoto E, Furuta T, Hioki H, Tanaka YR, Fujiyama F, et al. A morphological analysis of thalamocortical axon fibers of rat posterior thalamic nuclei: a single neuron tracing study with viral vectors. Cereb Cortex. 2012; 22(12):2840–57. doi: 10.1093/cercor/bhr356 PMID: 22190433
19. Waite P. Trigeminal sensory system. In: Paxinos G, editor. The rat nervous system. 3 ed. San Diego: Academic; 2004. p. 817–51.
20. Bureau I, von Saint Paul F, Svoboda K. Interdigitated paralemniscal and lemniscal pathways in the mouse barrel cortex. PLoS Biol. 2006; 4(12):e382. PMID: 17121453
21. Clasca F, Rubio-Garrido P, Jabaudon D. Unveiling the diversity of thalamocortical neuron subtypes. Eur J Neurosci. 2012; 35(10):1524–32. doi: 10.1111/j.1460-9568.2012.08033.x PMID: 22606998
22. Herkenham M. Laminar organization of thalamic projections to the rat neocortex. Science. 1980; 207 (4430):532–5. PMID: 7352263
23. Rubio-Garrido P, Perez-de-Manzo F, Porrero C, Galazo MJ, Clasca F. Thalamic input to distal apical dendrites in neocortical layer 1 is massive and highly convergent. Cereb Cortex. 2009; 19(10):2380–95. doi: 10.1093/cercor/bhn259 PMID: 19188274

24. Wimmer VC, Bruno RM, de Kock CP, Kuner T, Sakmann B. Dimensions of a projection column and architecture of VPM and POm axons in rat vibrissal cortex. Cereb Cortex. 2010; 20(10):2265–76. doi: 10.1093/cercor/bhq068 PMID: 20453248

25. Groh A, Bokor H, Mease RA, Plattner VM, Hangya B, Stroh A, et al. Convergence of cortical and sensory driver inputs on single thalamocortical cells. Cereb Cortex. 2014; 24(12):3167–79. doi: 10.1093/cercor/bht173 PMID: 23825316

26. Killackey HP, Sherman SM. Corticothalamic projections from the rat primary somatosensory cortex. J Neurosci. 2003; 23(19):7381–4. PMID: 12917373

27. Haidarliu S, Yu C, Rubin N, Ahissar E. Lemniscal and Extralemniscal Compartments in the VPM of the Rat. Front Neuroanat. 2008; 2:4. doi: 10.3389/neuro.05.004.2008 PMID: 18958201

28. Petersen CC. The functional organization of the barrel cortex. Neuron. 2007; 56(2):339–55. PMID: 17964250

29. Simons DJ, Carvell GE. Thalamocortical response transformation in the rat vibrissa/barrel system. J Neurophysiol. 1989; 61:311–30. PMID: 2918357

30. Veinante P, Deschenes M. Single- and multi-whisker channels in the ascending projections from the principal trigeminal nucleus in the rat. J Neurosci. 1999; 19(12):5085–95. PMID: 10366641

31. Jacquin MF, Golden J, Rhoades RW. Structure-function relationships in rat brainstem subnucleus interpolaris: III. Local circuit neurons. J Comp Neurol. 1989; 282(1):24–44. PMID: 2708592

32. Masri R, Bezdudnaya T, Trageser JC, Keller A. Encoding of stimulus frequency and sensor motion in the posterior medial thalamic nucleus. J Neurophysiol. 2008; 100(2):681–9. doi: 10.1152/jn.01322.2007 PMID: 18234976

33. Sitnikova EY, Raevskii VV. The lemniscal and paralemniscal pathways of the trigeminal system in rodents are integrated at the level of the somatosensory cortex. Neurosci Behav Physiol. 2010; 40 (3):325–31. doi: 10.1007/s11055-010-9259-7 PMID: 20148310

34. Sosnik R, Haidarliu S, Ahissar E. Temporal frequency of whisker movement. I. Representations in brain stem and thalamus. J Neurophysiol. 2001; 86(1):339–53. PMID: 11431515

35. Yu C, Derdikman D, Haidarliu S, Ahissar E. Parallel thalamic pathways for whisking and touch signals in the rat. PLoS Biol. 2006; 4(5):e124. PMID: 16605304

36. Frangeul L, Porrero C, Garcia-Amado M, Maimone B, Maniglier M, Clasca F, et al. Specific activation of the paralemniscal pathway during nociception. Eur J Neurosci. 2014; 39(9):1455–64. doi: 10.1111/ejn.12524 PMID: 24580836

37. Masri R, Keller A. Chronic pain following spinal cord injury. Adv Exp Med Biol. 2012; 760:74–88. PMID: 23281514

38. Sewards TV, Sewards M. Separate, parallel sensory and hedonic pathways in the mammalian somatosensory system. Brain Res Bull. 2002; 58(3):243–60. PMID: 12128150

39. Viaene AN, Petrof I, Sherman SM. Properties of the thalamic projection from the posterior medial nucleus to primary and secondary somatosensory cortices in the mouse. Proc Natl Acad Sci USA. 2011; (108):18156–18161. doi: 10.1073/pnas.1114828108 PMID: 22025694

40. Shlosberg D, Amitai Y, Azouz R. Time-dependent, layer-specific modulation of sensory responses mediated by neocortical layer 1. J Neurophysiol. 2006; 96(6):3170–82. PMID: 17110738

41. Guillery RW. Anatomical pathways that link perception and action. Prog Brain Res. 2005; 149:235–56. PMID: 16226588

42. Guillery RW, Sherman SM. Branched thalamic afferents: what are the messages that they relay to the cortex? Brain Res Rev. 2011; 66(1–2):205–19. doi: 10.1016/j.brainresrev.2010.08.001 PMID: 20696186

43. Theyel BB, Llano DA, Sherman SM. The corticothalamocortical circuit drives higher-order cortex in the mouse. Nature Neurosci. 2010; 13(1):84–8. doi: 10.1038/nn.2449 PMID: 19966840

44. Paxinos G, Watson C. The rat brain in stereotaxic coordinates. San Diego: Academic Press; 2007.

45. Rose HJ, Metherate R. Thalamic stimulation largely elicits orthodromic, rather than antidromic, cortical activation in an auditory thalamocortical slice. Neuroscience. 2001; 106(2):331–40. PMID: 11566504

46. Ranck JB Jr. Which elements are excited in electrical stimulation of mammalian central nervous system: a review. Brain Res. 1975; 98(3):417–40. PMID: 1102064

47. Bragin A, Penttonen M, Buzsáki G. Termination of epileptic afterdischarge in the hippocampus. J Neurosci. 1997; 17(7):2567–79. PMID: 9065516

48. Castro-Alamancos MA. Neocortical synchronized oscillations induced by thalamic disinhibition in vivo. J Neurosci. 1999; 19(18).

49. Steriade M, Contreras D. Spike-wave complexes and fast components of cortically generated seizures. I. Role of neocortex and thalamus. J Neurophysiol. 1998; 80(3):1439–55. PMID: 9744951

50. Chakrabarti S, Zhang M, Alloway KD. MI neuronal responses to peripheral whisker stimulation: relationship to neuronal activity in si barrels and septa. J Neurophysiol. 2008; 100(1):50–63. doi: 10.1152/jn.90327.2008 PMID: 18450580

51. de Kock CP, Bruno RM, Spors H, Sakmann B. Layer- and cell-type-specific suprathreshold stimulus representation in rat primary somatosensory cortex. J Physiol (London). 2007; 581(Pt 1):139–54.

52. de Kock CP, Sakmann B. Spiking in primary somatosensory cortex during natural whisking in awake head-restrained rats is cell-type specific. Proc Natl Acad Sci U S A. 2009; 106(38):16446–50. doi: 10.1073/pnas.0904143106 PMID: 19805318

53. Manns ID, Sakmann B, Brecht M. Sub- and Suprathreshold Receptive Field Properties of Pyramidal Neurons in Layers 5A and 5B of Rat Somatosensory Barrel Cortex. J Physiol (London). 2004; 556 (2):601–22.

54. Wright N, Fox K. Origins of cortical layer V surround receptive fields in the rat barrel cortex. J Neurophysiol. 2010; 103(2):709–24. doi: 10.1152/jn.00560.2009 PMID: 19939962

55. Atencio CA, Shih JY, Schreiner CE, Cheung SW. Primary auditory cortical responses to electrical stimulation of the thalamus. J Neurophysiol. 2014; 111(5):1077–87. doi: 10.1152/jn.00749.2012 PMID: 24335216

56. Swadlow HA. Neocortical efferent neurons with very slowly conducting axons: strategies for reliable antidromic identification. J Neurosci Methods. 1998; 79(2):131–41. PMID: 9543479

57. Barros-Zulaica N, Castejon C, Nuñez A. Frequency-specific response facilitation of supra and infragranular barrel cortical neurons depends on NMDA receptor activation in rats. Neuroscience. 2014; 281:178–94.

58. Nuñez A, Dominguez S, Buño W, Fernandez de Sevilla D. Cholinergic-mediated response enhancement in barrel cortex layer V pyramidal neurons. J Neurophysiol. 2012; 108(6):1656–68. doi: 10.1152/jn.00156.2012 PMID: 22723675

59. Yang JW, An S, Sun JJ, Reyes-Puerta V, Kindler J, Berger T, et al. Thalamic network oscillations synchronize ontogenetic columns in the newborn rat barrel cortex. Cereb Cortex. 2013; 23(6):1299–316. doi: 10.1093/cercor/bhs103 PMID: 22593243

60. Zhu Y, Zhu JJ. Rapid arrival and integration of ascending sensory information in layer 1 nonpyramidal neurons and tuft dendrites of layer 5 pyramidal neurons of the neocortex. J Neurosci. 2004; 24 (6):1272–9. PMID: 14960597

61. Prieto JJ, Peterson BA, Winer JA. Morphology and spatial distribution of GABAergic neurons in cat primary auditory cortex (AI). J Comp Neurol. 1994; 344(3):349–82. PMID: 7914896

62. Winer JA, Larue DT. Populations of GABAergic neurons and axons in layer I of rat auditory cortex. Neuroscience. 1989; 33(3):499–515. PMID: 2636704

63. Hefft S, Jonas P. Asynchronous GABA release generates long-lasting inhibition at a hippocampal interneuron-principal neuron synapse. Nature Neurosci. 2005; 8(10):1319–28. PMID: 16158066

64. Toledo-Rodriguez M, Blumenfeld B, Wu C, Luo J, Attali B, Goodman P, et al. Correlation maps allow neuronal electrical properties to be predicted from single-cell gene expression profiles in rat neocortex. Cereb Cortex. 2004; 14(12):1310–27. PMID: 15192011

65. Zaitsev AV, Povysheva NV, Lewis DA, Krimer LS. P/Q-type, but not N-type, calcium channels mediate GABA release from fast-spiking interneurons to pyramidal cells in rat prefrontal cortex. J Neurophysiol. 2007; 97(5):3567–73. PMID: 17329622

66. Bokor H, Acsady L, Deschenes M. Vibrissal responses of thalamic cells that project to the septal columns of the barrel cortex and to the second somatosensory area. J Neurosci. 2008; 28(20):5169–77. doi: 10.1523/JNEUROSCI.0490-08.2008 PMID: 18480273

67. Pierret T, Lavallee P, Deschenes M. Parallel streams for the relay of vibrissal information through thalamic barreloids. J Neurosci. 2000; 20(19):7455–62. PMID: 11007905

68. Bullier J, McCourt ME, Henry GH. Physiological studies on the feedback connection to the striate cortex from cortical areas 18 and 19 of the cat. Exp Brain Res. 1988; 70(1):90–8. PMID: 3402571

69. Girard P, Hupe JM, Bullier J. Feedforward and feedback connections between areas V1 and V2 of the monkey have similar rapid conduction velocities. J Neurophysiol. 2001; 85(3):1328–31. PMID: 11248002

70. Movshon JA, Newsome WT. Visual response properties of striate cortical neurons projecting to area MT in macaque monkeys. J Neurosci. 1996; 16(23):7733–41. PMID: 8922429

71. Beierlein M, Connors BW. Short-term dynamics of thalamocortical and intracortical synapses onto layer 6 neurons in neocortex. J Neurophysiol. 2002; 88(4):1924–32. PMID: 12364518

72. Armstrong-James M, Welker E, Callahan CA. The contribution of NMDA and Non-NMDA receptors to fast and slow transmission of sensory information in the rat SI barrel cortex. J Neurosci. 1993; 13 (5):2149–60. PMID: 8097531

73. Gambino F, Pages S, Kehayas V, Baptista D, Tatti R, Carleton A, et al. Sensory-evoked LTP driven by dendritic plateau potentials in vivo. Nature. 2014; 515(7525):116–9. doi: 10.1038/nature13664 PMID: 25174710

74. Salling MC, Harrison NL. Strychnine-sensitive glycine receptors on pyramidal neurons in layers II/III of the mouse prefrontal cortex are tonically activated. J Neurophysiol. 2014; 112(5):1169–78. doi: 10.1152/jn.00714.2013 PMID: 24872538

75. Dilgen J, Tejeda HA, O'Donnell P. Amygdala inputs drive feedforward inhibition in the medial prefrontal cortex. J Neurophysiol. 2013; 110(1):221–9. doi: 10.1152/jn.00531.2012 PMID: 23657281

76. Pezze M, McGarrity S, Mason R, Fone KC, Bast T. Too little and too much: hypoactivation and disinhibition of medial prefrontal cortex cause attentional deficits. J Neurosci. 2014; 34(23):7931–46. doi: 10.1523/JNEUROSCI.3450-13.2014 PMID: 24899715

77. Cottam JC. Identifying the functional role of Martinotti cells in cortical sensory processing. J Neurophysiol. 2009; 102(1):9–11. doi: 10.1152/jn.00290.2009 PMID: 19420125

78. Oberlaender M, de Kock CP, Bruno RM, Ramirez A, Meyer HS, Dercksen VJ, et al. Cell type-specific three-dimensional structure of thalamocortical circuits in a column of rat vibrissal cortex. Cereb Cortex. 2012; 22(10):2375–91. doi: 10.1093/cercor/bhr317 PMID: 22089425

79. Chu Z, Galarreta M, Hestrin S. Synaptic interactions of late-spiking neocortical neurons in layer 1. J Neurosci. 2003; 23(1):96–102. PMID: 12514205

80. Cruikshank SJ, Ahmed OJ, Stevens TR, Patrick SL, Gonzalez AN, Elmaleh M, et al. Thalamic control of layer 1 circuits in prefrontal cortex. J Neurosci. 2012; 32(49):17813–23. doi: 10.1523/JNEUROSCI.3231-12.2012 PMID: 23223300

81. Larkum ME, Nevian T, Sandler M, Polsky A, Schiller J. Synaptic integration in tuft dendrites of layer 5 pyramidal neurons: a new unifying principle. Science. 2009; 325(5941):756–60. doi: 10.1126/science.1171958 PMID: 19661433

82. Williams SR, Stuart GJ. Dependence of EPSP efficacy on synapse location in neocortical pyramidal neurons. Science. 2002; 295:1907–10. PMID: 11884759

83. Christophe E, Roebuck A, Staiger JF, Lavery DJ, Charpak S, Audinat E. Two types of nicotinic receptors mediate an excitation of neocortical layer I interneurons. J Neurophysiol. 2002; 88(3):1318–27. PMID: 12205153

84. Letzkus JJ, Kampa BM, Stuart GJ. Learning rules for spike timing-dependent plasticity depend on dendritic synapse location. J Neurosci. 2006; 26(41):10420–9. PMID: 17035526

85. Jiang X, Wang G, Lee AJ, Stornetta RL, Zhu JJ. The organization of two new cortical interneuronal circuits. Nature Neurosci. 2013; 16(2):210–8. doi: 10.1038/nn.3305 PMID: 23313910

86. Lee AJ, Wang G, Jiang X, Johnson SM, Hoang ET, Lante F, et al. Canonical Organization of Layer 1 Neuron-Led Cortical Inhibitory and Disinhibitory Interneuronal Circuits. Cereb Cortex. 2014.

87. Markram H, Toledo-Rodriguez M, Wang Y, Gupta A, Silberberg G, Wu C. Interneurons of the neocortical inhibitory system. Nat Rev Neurosci. 2004; 5(10):793–807. PMID: 15378039

88. Zhou FM, Hablitz JJ. Layer I neurons of rat neocortex .1. Action potential and repetitive firing properties. J Neurophysiol. 1996; 76(2):651–67. PMID: 8871189

89. Kubota Y. Untangling GABAergic wiring in the cortical microcircuit. Curr Opin Neurobiol. 2014; 26:7–14. PMID: 24650498

90. Wozny C, Williams SR. Specificity of synaptic connectivity between layer 1 inhibitory interneurons and layer 2/3 pyramidal neurons in the rat neocortex. Cereb Cortex. 2011; 21(8):1818–26. doi: 10.1093/cercor/bhq257 PMID: 21220765

91. Atallah BV, Bruns W, Carandini M, Scanziani M. Parvalbumin-expressing interneurons linearly transform cortical responses to visual stimuli. Neuron. 2012; 73(1):159–70. doi: 10.1016/j.neuron.2011.12.013 PMID: 22243754

92. Wilson NR, Runyan CA, Wang FL, Sur M. Division and subtraction by distinct cortical inhibitory networks in vivo. Nature. 2012; 488(7411):343–8. doi: 10.1038/nature11347 PMID: 22878717

93. Rossignol E, Kruglikov I, van den Maagdenberg AM, Rudy B, Fishell G. CaV 2.1 ablation in cortical interneurons selectively impairs fast-spiking basket cells and causes generalized seizures. Ann Neurol. 2013; 74(2):209–22. doi: 10.1002/ana.23913 PMID: 23595603

94. Ahissar E, Kleinfeld D. Closed-loop neuronal computations: focus on vibrissa somatosensation in rat. Cereb Cortex. 2003; 13:53–62. PMID: 12466215

95. Ahissar E, Oram T. Thalamic Relay or Cortico-Thalamic Processing? Old Question, New Answers Cereb. Cortex. 2015; 25(4):845–848.

96. Herkenham M (1980) Laminar organization of thalamic projections of the rat neocortex. Science 207:532–534. PMID: 7352263

A.5. Article 5 (published)

BIDIRECTIONAL HEBBIAN PLASTICITY INDUCED BY LOW-FREQUENCY STIMULATION IN BASAL DENDRITES OF RAT BARREL CORTEX LAYER 5 PYRAMIDAL NEURONS

frontiers in Cellular Neuroscience

ORIGINAL RESEARCH
published: 01 February 2017
doi: 10.3389/fncel.2017.00008

Bidirectional Hebbian Plasticity Induced by Low-Frequency Stimulation in Basal Dendrites of Rat Barrel Cortex Layer 5 Pyramidal Neurons

Andrea Díez-García[1], *Natali Barros-Zulaica*[1], *Ángel Núñez*[1], *Washington Buño*[2] *and David Fernández de Sevilla*[1,2]*

[1] *Departamento de Anatomía, Histología y Neurociencia, Facultad de Medicina, Universidad Autónoma de Madrid, Madrid, Spain,* [2] *Instituto Cajal, Consejo Superior de Investigaciones Científicas (CSIC), Madrid, Spain*

According to Hebb's original hypothesis (Hebb, 1949), synapses are reinforced when presynaptic activity triggers postsynaptic firing, resulting in long-term potentiation (LTP) of synaptic efficacy. Long-term depression (LTD) is a use-dependent decrease in synaptic strength that is thought to be due to synaptic input causing a weak postsynaptic effect. Although the mechanisms that mediate long-term synaptic plasticity have been investigated for at least three decades not all question have as yet been answered. Therefore, we aimed at determining the mechanisms that generate LTP or LTD with the simplest possible protocol. Low-frequency stimulation of basal dendrite inputs in Layer 5 pyramidal neurons of the rat barrel cortex induces LTP. This stimulation triggered an EPSP, an action potential (AP) burst, and a Ca^{2+} spike. The same stimulation induced LTD following manipulations that reduced the Ca^{2+} spike and Ca^{2+} signal or the AP burst. Low-frequency whisker deflections induced similar bidirectional plasticity of action potential evoked responses in anesthetized rats. These results suggest that both *in vitro* and *in vivo* similar mechanisms regulate the balance between LTP and LTD. This simple induction form of bidirectional hebbian plasticity could be present in the natural conditions to regulate the detection, flow, and storage of sensorimotor information.

Keywords: Ca^{2+}spikes, NMDARs, L-type VGCC, dentritic excitabilty, STDP

OPEN ACCESS

Edited by:
Enrico Cherubini, International School for Advanced Studies, Italy

Reviewed by:
Nicola Berretta, Fondazione Santa Lucia (IRCCS), Italy
Robert Nistico, University of Calabria, Italy

***Correspondence:**
David Fernández de Sevilla
david.fernandezdesevilla@uam.es

Received: *04 November 2016*
Accepted: *12 January 2017*
Published: *01 February 2017*

Citation:
Díez-García A, Barros-Zulaica N, Núñez Á, Buño W and Fernández de Sevilla D (2017) Bidirectional Hebbian Plasticity Induced by Low-Frequency Stimulation in Basal Dendrites of Rat Barrel Cortex Layer 5 Pyramidal Neurons. Front. Cell. Neurosci. 11:8. doi: 10.3389/fncel.2017.00008

INTRODUCTION

The rat somatosensory barrel field cortex ("barrel cortex") processes sensorimotor information from the whiskers mainly through the thalamocortical inputs in Layers 4 and 5. Layer 5 (L5) pyramidal neurons (PNs), receiving a robust thalamocortical input at their basal dendrites that is weaker at their apical dendrites, produce the main output of the barrel cortex (Ramaswamy and Markram, 2015). The Ca^{2+}-mediated dendritic spikes in L5 PNs are markedly reduced by inhibition of NMDA receptors (NMDAR) and L-type voltage gated Ca^{2+} channels (VGCCs) and have been called NMDA-spikes (Schiller et al., 2000; Polsky et al., 2009). Dendritic Ca^{2+} spikes play a leading role in the genesis of long-term potentiation (LTP) allowing a robust Ca^{2+} influx into PN spines (London and Hausser, 2005; Remy and Spruston, 2007). Under blockade of γ-aminobutyric

acid type A receptors ($GABA_A$Rs), regular spiking L5 PNs in the immature rat barrel cortex can trigger NMDA-spikes that cause a robust Ca^{2+} influx (Schiller and Schiller, 2001; Gordon et al., 2006; Polsky et al., 2009; Nuñez et al., 2012). An opposing form of synaptic plasticity is long-term depression (LTD) that is caused by a repeated synaptic input leading a small or local postsynaptic Ca^{2+} rise (Artola et al., 1990; Bliss and Collingridge, 1993; Neveu and Zucker, 1996; Dan and Poo, 2004; Holthoff et al., 2004; Kampa et al., 2007).

Importantly, long-term modifications in synaptic efficacy have been widely proposed to be the cellular basis of the learning machinery of the brain (Nabavi et al., 2014; Gruart et al., 2015). A physiologically relevant protocol for inducing "hebbian LTP" is spike-timing-dependent plasticity (STDP), which consists in repeatedly pairing at low-frequency an EPSP with postsynaptic action potentials (APs) induced by depolarizing current injection (Bi and Poo, 1998; Fuenzalida et al., 2007, 2010; Caporale and Dan, 2008; Feldman, 2012; Ramaswamy and Markram, 2015). However, Hebb's original postulate holds that synapses are potentiated when presynaptic activity triggers postsynaptic firing (Hebb, 1949) and it does not predict the necessity of pairing presynaptic and postsynaptic stimulation. Nevertheless, the underlying cellular and network mechanisms required to trigger either LTP or LTD with this simpler form of "unpaired" low-frequency presynaptic stimulation remain unclear. The term unpaired is used to indicate that under current-clamp we stimulate the afferent pathway without manipulating the postsynaptic neuron. A different form of long term response enhancement induced by unpaired low-frequency stimulation of tuft dendrite inputs that is only expressed in L5 PN tuft dendrites in disinhibited slices has recently been reported (Sandler et al., 2016). In addition, we have shown that acetylcholine can facilitate long-term response enhancement induced by low frequency stimulation of basal inputs in L5 PNs (Nuñez et al., 2012).

Therefore, we analyzed *in vitro* the underlying cellular and network mechanisms required to trigger either LTP or LTD with the simpler form of unpaired low-frequency presynaptic stimulation. We show that *in vitro* under $GABA_A$R blockade, a robust LTP could be induced by low-frequency stimulation of L5 PN basal synaptic inputs (termed hereafter "basal stimulation") evoking an EPSP followed by an AP burst and a Ca^{2+} spike (termed hereafter "EPSP-Ca^{2+} spike"). The resulting LTP required Ca^{2+} influx through NMDARs and L-type VGCC, Ca^{2+} release from intracellular stores and activation of glutamatergic subtype I, muscarinic subtype 3, and nicotinic ACh receptors. The contribution of Ca^{2+}/calmodulin-dependent protein kinase II (CaMKII), phospholipase C (PLC), and protein kinase A (PKA) were also necessary. Inhibition of NMDARs, L-type VGCCs, or membrane hyperpolarization could reduce the EPSP-Ca^{2+} spikes and the associated Ca^{2+} signal and induce LTD instead of LTP. Blockade of voltage gated Na^+ channels also induced LTD in place of LTP. Consequently, it was possible to regulate the sign of the induced change in synaptic plasticity using the level of membrane depolarization attained during the Ca^{2+} spike. Importantly, basal stimulation could trigger APs despite intact inhibition but failed to evoke Ca^{2+} spikes and plasticity. We also show *in vivo* in anesthetized rats that repeated low-frequency whisker deflections can induce a similar NMDAR-dependent bidirectional plasticity, suggesting a causal relationship between network function and sensory detection.

Overall, low-frequency stimulation of basal inputs and whisker deflections can induce forms of bidirectional plasticity, possibly through the regulation of dendritic excitability in L5 barrel cortex neurons, caused by a reduced $GABA_A$ inhibition that could be functional in the natural situation and regulate both the flow and storage of novel input characteristics and the balance between LTP and LTD.

MATERIALS AND METHODS

Ethical Approval and Animal Handling

Procedures of animal care and slice preparation approved by the "Universidad Autónoma de Madrid" and "Consejo Superior de Investigaciones Científicas" follow the guidelines laid down by the European Council on the ethical use of animals (Directive 2010/63/EU) and every effort was made to minimize animal suffering and number. The procedures have been described in detail elsewhere (Nuñez et al., 2012).

In Vitro Experiments

Slice Preparation and Drug Applications

Young Sprague Dawley rats (12–19 days old) of either sex were decapitated, and their brains were removed and submerged in cold ($\approx 4^\circ$ C) solution (in mM): Choline-Cl 120.00; KCl 2.50; KH_2PO_4 1.25; Mg_2SO_4 2.00; $NaHCO_3$ 26.00; $CaCl_2$ 2.00; Na^+ aspartate 3.00; and Ascorbic acid 0.40. pH was stabilized at 7.4 by bubbling the solution with carbogen (95% O_2, 5% CO_2). Transverse slices (400 μm) containing the barrel cortex were cut with a Vibratome (Pelco 3000, St Louis, USA or Leica VT 1200S) and incubated >1 h in control artificial cerebro-spinal fluid (ACSF) at a room temperature of 20–22°C. The ACSF contained (in mM): 124.00 NaCl, 2.69 KCl, 1.25 KH_2PO_4, 2.00 Mg_2SO_4, 26.00 $NaHCO_3$, 2.00 $CaCl_2$, and 10.00 glucose. Slices were placed in a 2 ml chamber fixed to an upright microscope stage (BX51WI; Olympus, Tokyo, Japan) equipped with infrared differential interference contrast video (DIC) microscopy and a 40X water-immersion objective (**Figure 1A**). Slices were superfused with carbogen-bubbled ACSF (2 ml/min) and maintained at room temperature. Picrotoxin (P_ITX, 50 μM), D-2-amino-5 phosphonovaleric acid (D-AP5; 50 μM) and 7-nitro-2,3-dioxo-1,4-dihydroquinoxaline-6-carbonitrile (CNQX; 20 μM) were used to isolate the EPSCs. (S)-α-Methyl-4-carboxyphenylglycine(+)-alpha-methyl-4-carboxyphenylglycine (MCPG; 1.0 mM); 2-Methyl-6-(phenylethynyl) pyridine hydrochloride (MPEP; 5.0 μM); (S)-(+)-α-Amino-4-carboxy-2-methylbenzeneacetic acid (LY367385; 50 μM) were used as required. Atropine (0.3 μM), pirenzepine (75 nM), methoctramine (1 μM), Mecamylamine (MMA) (10 μM), methyllycaconitine (MLA, 50 μM), and α7-containing neuronal nAChR antagonist were also used. Nifedipine (20 μM), DAU5884 hydrochloride (1 μM), U73122 (5 μM) and H89 dihydrochloride (10 μM) were dissolved in DMSO (0.01%) and added to the ACSF as needed. Chemicals were purchased from Sigma-Aldrich Quimica (Madrid, Spain), Tocris Bioscience

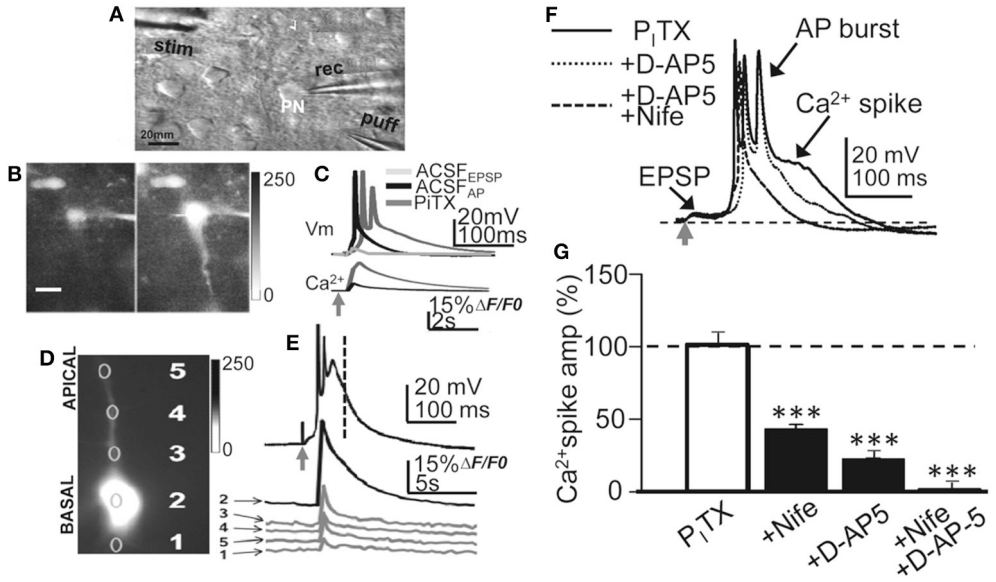

FIGURE 1 | Experimental setup, current-clamp responses and Ca^{2+} signals. (A) DIC image of a slice showing a L5 PN and placement of recording (rec) stimulation (stim) and glutamate (puff) pipettes. **(B)** left. Representative image (gray scale) showing a small somatic Ca^{2+} elevation evoked by basal stimulation that triggered an EPSP and a single AP in control ACSF. **(B)** right. Same as left but a larger Ca^{2+} signal in the soma and dendrites under the P_iTX (50 μM) that triggered an EPSP-Ca^{2+} spike (**A** and **B**, same PN). **(C)**, upper. Representative superimposed records showing EPSP, EPSP+AP in control ACSF and the EPSP-Ca^{2+} spike under P_iTX. **(C)**, lower. Time course of somatic cytosolic Ca^{2+} variations during EPSC+AP and EPSP-Ca^{2+} spike in **(B)**, left. **(D)** Somatic (2), basal (1) and apical (3-5) dendritic cytosolic Ca^{2+} variations associated with the averaged EPSP-Ca^2 spike in **(E)**. **(E)** Current-clamp response under P_iTX (upper) and Ca^{2+} signals obtained from specified regions of interest (1–5 in **D**). **(F)** Representative superimposed records obtained under P_iTX and after adding D-AP5 and D-AP5+Nifedipine. **(G)**. Bar plot showing the effects of nifedipine (20 μM, $N = 10$, $P < 0.001$), D-AP5 (50 μM, $N = 6$, $P < 0.001$) and nifedipine+D-AP5 ($N = 9$, $P < 0.001$) on the amplitude of the Ca^{2+} spike measured at delays indicated by the vertical interrupted line in **(E)**.

(Ellisville, MO; distributed by Biogen Cientıfica, Madrid, Spain), and Alomone Labs (Jerusalem, Israel). Brief localized "puffs" of glutamate (1 mM, 100–300 ms duration 2.0–2.5 *psi*) were applied through a pipette (tip diameter ≈ 5 μm) connected to a Picospritzer II (General Valve, Fairfield, NJ) and placed near the basal dendrites (50–100 μm) of the recorded L5 PN with a hydraulic micromanipulator (Narishige, Tokyo, Japan).

Electrophysiology

Whole-cell patch-clamp recordings were obtained from the soma of L5 PNs using patch pipettes (4–8 MΩ) filled with a solution that contained (in mM): 135 K-gluconate, 10.0 HEPES, 0.2 EGTA, 2.0 Na_2-ATP, and 0.4 Na_3-GTP, buffered to pH 7.2–7.3 with KOH. Intracellular solutions could also contain either 1,2-Bis (2-aminophenoxy) ethane-N,N,N, N'-tetraacetic acid (BAPTA; 40 mM), heparin sodium salt (5.0 mg/ml), ruthenium red (Ru-Red; 400 μM), AIP (Autocamtide 2-related inhibitor peptide; 5 mg/ml), GDPβS (1 mM), the quaternary lidocaine derivative QX-314 (5 mM), or chelerytrine (5 mM). Recordings were performed in current- or voltage-clamp modes using a Cornerstone PC-ONE amplifier (DAGAN, Minneapolis, MN). Pipettes were set in place with a mechanical micromanipulator (Narishige). The holding potential was adjusted to −60 mV, and the series resistance was compensated to ≈ 80%. L5 PNs located beneath the barrels were only accepted if the seal resistance was >1 GΩ before breaking into whole cell and the series resistance (7–14 MΩ) did not change >15%, and the holding current did not exceed 300 pA at −75 mV during the experiment. The junction potential (≈6 mV) was not corrected. Data were low-pass filtered at 3.0 kHz and sampled at 10.0 kHz, through a Digidata 1322A (Molecular Devices, Sunnyvale, CA) with the pClamp programs (Molecular Devices).

Synaptic Stimulation

Bipolar stimulation used either a concentric electrode (OP 200 μm, IP 50 μm, FHC) or a pipette pulled from theta glass capillary (Ø of the tip ≈ 20–40 μm), filled with ACSF and connected though two silver-chloride wires. A Grass S88 stimulator and stimulus isolation unit (Quincy, USA) was used and no significantly different results were observed with the two electrodes. Electrodes were placed 50–100 μm below the soma of the patched PN. Single pulses were continuously delivered at 0.3 Hz. After a 5 min control recording of EPSCs, the recording was switched to current-clamp, and stimulation intensity was increased to values in which the EPSP triggered APs and Ca^{2+} spikes. This stimulation was applied 60 times at 0.2 Hz, the recording was then switched back to voltage-clamp and stimulation intensity and frequency restored to the initial control values. We decided to stimulate at 0.2 Hz because frequencies >0.5 Hz caused frequent Ca^{2+} spike failures and did not induce LTP; frequencies <0.1 Hz were less effective in inducing LTP. However, the precise stimulation frequency

requirements for the induction of this LTP still remain to be determined. The pre- or postsynaptic origin of EPSC amplitude change was investigated by computing the PPR and the EPSC variance that parallels the changes in EPSC amplitude. Paired pulses (100 ms interval) were used in a group of experiments to determine changes in presynaptic release probability by computing a paired-pulse response ratio (PPR) as the quotient of the second EPSC of the pair over the first EPSC (R2/R1). PPRs above and below one respectively corresponded to paired-pulse facilitation (PPF) or paired-pulse depression (PPD), indicating the respective low and high release probabilities. To estimate the EPSC variance modifications, we first calculated the noise-free coefficient of variation (CV_{NF}) of the synaptic responses in control conditions and then $\approx$ 30 min after the induction of the Ca^{2+} spikes. We used the formula $CV_{NF} = \sqrt{(\delta^2_{EPSC} - \delta^2_{noise})/m}$, where δ^2_{EPSC} and δ^2_{noise} are the variances of the peak EPSC and the baseline, respectively, and m is the mean EPSC peak amplitude. The ratio of the CV (CVR) measured at $\approx$ 30 min over that in control conditions was obtained for each neuron as $CV_{afterCaSpikes}/CV_{control}$ (Fernández de Sevilla et al., 2002). Finally, we constructed plots comparing variation in average EPSC amplitude (M) with the change in response variance of the EPSC amplitude ($1/CVR^2$) in each cell (Fernández de Sevilla et al., 2002). Values, in these plots, should follow the diagonal if the EPSC potentiation has a presynaptic origin. This method requires a binomial EPSC amplitude distribution but we could not directly test whether our data fitted the binomial distribution. Nevertheless, synaptic fluctuations were always evident and we assumed that synaptic release followed a binomial distribution.

Calcium Imaging

Simultaneous electrophysiology and cytosolic Ca^{2+} imaging were obtained by filling patch pipettes with a solution containing 50–100 μM fluo-3 (Molecular Probes, Eugene, OR, USA). Imaging experiments were performed after a 10–15 min stabilization period that allowed equilibration of the dye. Slices were illuminated for 40 ms every 200 ms at 490 nm with a monochromator (Polychrome IV; TILL Photonics) and successive images were obtained at 5 s^{-1} with a cooled monochrome CCD camera (Luca, Andor Technologies) attached to the Olympus microscope equipped with a filter cube optimized for fluo-3. Camera control, synchronization with electrophysiological measurements and quantitative epifluorescence measurements were made with the ImagingWorkbench software (INDEC-BioSystems, Santa Clara, CA, USA). Fluctuations in fluorescence were expressed as the proportion (%) of relative change in fluorescence ($\Delta F/F_0$) where F_0 is the pre-stimulus fluorescence level when the cell is at rest and ΔF is the change in fluorescence during activity. Plots of Ca^{2+} signal variations vs. time were obtained "off-line" at specified regions of interest from stored image stacks and expressed as $\Delta F/F_0$. Corrections were made for indicator bleaching during trials by subtracting the signal measured under the same conditions when cells were not stimulated. Although, we could record the strong calcium signal associated to the Ca^{2+} spikes (**Figures 1B,C**), the low temporal resolution of our Ca^{2+} recordings did not allow us to resolve the site of initiation of the Ca^{2+} signal (**Figures 1D,E**), although it probably originated at the basal dendrites and propagated rapidly to the soma and apical dendrite.

Data Analysis

Data were analyzed with the pClamp programs (Molecular Devices, Chicago, USA) and Excel (Microsoft, Redmond, USA) and responses were averaged (n = 10 or 20), except when indicated otherwise. The magnitude of the change in peak amplitude of EPSCs was expressed as a proportion (%) of the baseline control amplitude and plotted in function of time. The amplitude and duration of the Ca^{2+} spikes was measured after the AP burst had ended (50 ms) and when the membrane potential reached pre-stimulation values (300 ms). Results are given as average ± SEM (N = number of cells), and presented as percentage of controls. Statistical analyses were calculated with Student's two-tailed t-tests for unpaired or paired data as required. The threshold for statistical significance was $P < 0.05$ (*); $P < 0.01$ (**); and $P < 0.001$(***) are also indicated. Gender related differences were not detected in our sample.

In vivo Experiments

Electrophysiological Recordings

Experiments were performed on 18 urethane-anesthetized (1.6 g/kg i.p.) Sprague Dawley rats weighing 200–250 g. Animals were placed in a Kopf stereotaxic device, the body temperature was maintained at 37°C, and the end-tidal CO_2 and heart rate were monitored. Lidocaine (1%) was applied to all skin incisions and additional doses of anesthetic were delivered to maintain areflexia. An incision was made exposing the skull and a small hole was drilled in the bone over the barrel cortex (A 1–3 mm, L 5–7 mm from bregma). Single-unit recordings in L5 barrel cortex were made 900–1200 μm below the surface with tungsten microelectrodes (2–5 MΩ). Recordings were filtered (0.3–3.0 kHz), amplified *via* an AC preamplifier (DAM80; World Precision Instruments), and fed into a personal computer (sample rate 10.0 kHz) together with the temporal references of the stimuli for off-line analysis with Spike 2 software (Cambridge Electronic Design, Cambridge, UK).

Whisker Stimulation and Induction of Plasticity

Whisker deflections were generated by brief 20 ms air puffs using a pneumatic pressure pump (Picospritzer) delivered through a 1-mm-inner diameter polyethylene tube (**Figure 8A**). The air pressure was set at 1–2 kg/cm^2, resulting in whisker deflections of $\approx$ 15°. When a single neuron was isolated, its cutaneous receptive field was carefully mapped with a small hand-held brush and the response of the principal whisker was confirmed. The protocol used to investigate plasticity consisted of 30 air pulses delivered to the principal whisker at 0.5 Hz (CONTROL), followed by a train of 40 pulses at 1.0 Hz (INDUCTION) delivered to the same whisker. Thirty pulses at 0.5 Hz were then delivered to the same whisker 1, 5, 15, and 30 min after (POST-INDUCTION). This stimulation protocol could either induce LTP or depression (LTD) of whisker-evoked AP responses (see below). In some experiments NMDARs were inhibited with D-AP5 (50 μM; 0.1 μl) injected through a cannula connected to a

5 μl Hamilton syringe and targeted on L5. Five minutes after the injection the complete experimental protocol began: control, induction train, and post-induction whisker stimulations during 30 min.

Data Analysis

Peristimulus time histograms (PSTH; 1 ms bin width; 30 successive stimuli) were computed during the CONTROL, INDUCTION, and POST-INDUCTION periods. Whisker-evoked responses were estimated from the total number of spikes evoked over a 100 ms post-stimulation time window, divided by the number of stimuli. To determine differences in whisker-evoked responses induced by the experimental manipulations, cumulative spike plots (CSPs) were constructed by adding successive PSTH bins. A grand average of all PSTHs computed over a given experimental condition was also constructed, and the corresponding averaged CSPs were computed.

RESULTS

Basal Stimulation Triggered EPSP-Ca^{2+} Spikes in Disinhibited Slices

Recordings were obtained from slender tufted L5A PNs ($N = 244$) and confirmed by intracellular biocytin staining (Nuñez et al., 2012). In control ACSF, basal stimulation induced an EPSP that above a threshold depolarization level triggered a single AP (**Figure 1C**). Increasing stimulation intensity could increase the number of APs (1–3 APs, with frequent failures) without further modifying the response. In contrast, under P_ITX (50 μM) blockade of $GABA_A$ inhibition, the EPSP could trigger at short delays of 5 ± 3 ms 1 AP or a brief high frequency burst of 2 and occasionally 3 APs with failures, that lasted 20 ± 8 ms ($N = 14$). The AP burst rode on a slow high amplitude depolarization wave (peak amplitude 53 ± 6 mV; duration 375 ± 60 ms; same cells; **Figures 1C–F**, **2A–C**). The slow depolarization wave was not modified when stimulation intensity was further increased, displaying an all-or-none behavior.

The amplitude and duration of the slow depolarization wave was markedly reduced when either nifedipine (20 μM; reaching values of 47 ± 7% of the controls; $P < 0.001$; $N = 10$) or D-AP5 were superfused (50 μM; reaching values of 28 ± 5% of the controls; $P < 0.001$; $N = 6$) (Schiller and Schiller, 2001; Nuñez et al., 2012). When both D-AP5 and nifedipine were superfused the slow depolarization wave was totally suppressed ($P < 0.001$; $N = 9$; **Figures 1F,G**). In addition, a robust cytosolic Ca^{2+} signal that could be recorded in the soma, where the $\Delta F/F_0$ reached values that were 52 ± 9% of the controls ($P < 0.001$; $N = 6$), while in basal and apical dendrites, the $\Delta F/F_0$ attained values that were 19 ± 9% of the controls ($P < 0.001$; same cells; **Figures 1B–E**). Much smaller Ca^{2+} signals (8 ± 1% of controls, $P < 0.01$; same cells) were induced when a single AP was triggered in the absence of Ca^{2+} spikes (**Figures 1B,C**). The all-or-none behavior of the slow depolarization wave following EPSPs and the robust dendritic Ca^{2+} signals suggests that the slow depolarizations were Ca^{2+} spikes.

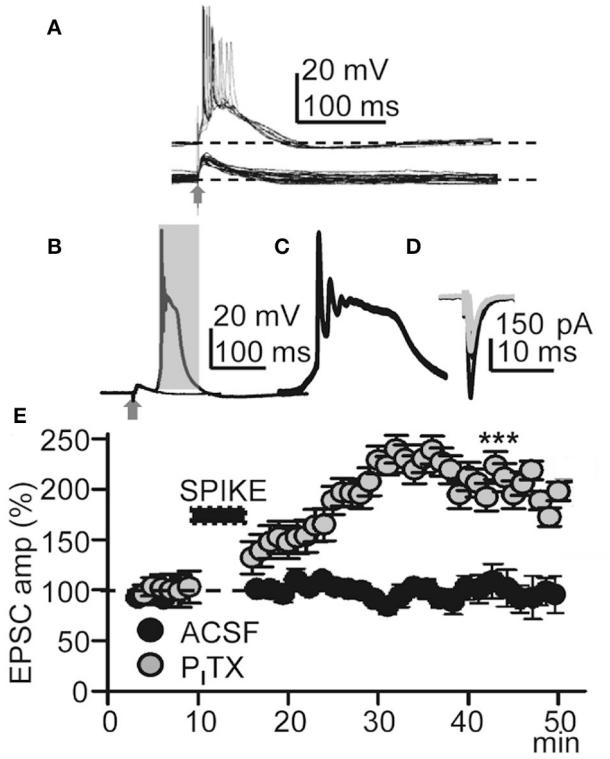

FIGURE 2 | Repeated Ca^{2+} spikes induce LTP. (A) Representative superimposed EPSPs recorded in control ACSF (bottom) and superimposed EPSP-Ca^{2+} spikes ($n = 20$) recorded under P_ITX (50 μM) (top); note AP bursts. **(B)** Superimposed averaged EPSP and EPSP-Ca^{2+} spike ($n = 20$ as in all other Figures) recorded under P_ITX. **(C)** Expanded time record taken from the shaded area in **(B)**. **(D)** Representative superimposed averaged EPSCs recorded before and ≈30 min after LTP induction (gray and black records, respectively). **(E)** Time course of the peak EPSC amplitude (% of controls, as in all other Figs.) in ACSF (black circles, $N = 8$, $P > 0.05$) and under P_ITX (gray circles, $N = 10$, $P < 0.001$).

EPSP-Ca^{2+} Spikes Triggered by Low-Frequency Stimulation Induced LTP

We first tested if EPSP-Ca^{2+} spikes triggered by low-frequency basal stimulation could induce LTP. Under blockade of $GABA_A$Rs with P_ITX (50 μM), basal stimulation induced inward EPSCs at −65 mV with mean peak amplitudes of −160 ± 9 pA ($P < 0.001$; $N = 6$). After a 5–10 min control recording of EPSCs under voltage-clamp with stimulation at 0.3 Hz, the recording was switched to current-clamp and stimulation intensity was increased until EPSP-Ca^{2+} spikes were evoked without failure. In these conditions the delay between the EPSP and the AP burst-Ca^{2+} spike was fixed for a given experiment although it could fluctuate between ≈ 2 and ≈ 20 ms in different experiments. EPSP-Ca^{2+} spikes were applied 60 times at 0.2 Hz, the recording was switched back to voltage-clamp, and stimulation intensity and frequency restored to the initial control conditions. The repeated EPSP-Ca^{2+} spikes induced a robust LTP typified by an increase in the mean peak EPSC amplitude that in ≈ 30 min reached values that were 210 ± 45% of the control ($P < 0.001$; $N = 23$; **Figures 2D,E**).

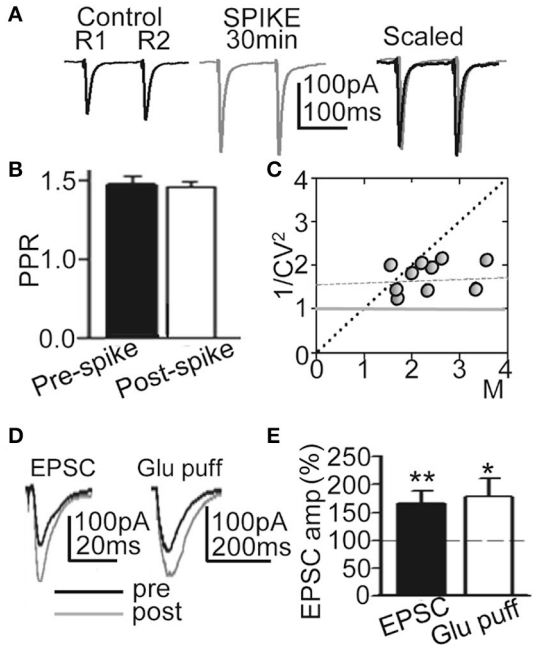

FIGURE 3 | LTP was induced without changes in Glu release probability. (A) Representative averaged EPSCs ($n = 20$) evoked by paired pulse stimulation (100 ms delay) before (Control R1, R2), at ≈30 min after 60 EPSP-Ca^{2+} spikes (SPIKE, 30 min) and superimposed and scaled to the amplitude of the first ESPC (Scaled). **(B)** Summary data showing the unchanged PPR (% of control, $N = 15$, $P > 0.05$) before (Pre-spike) and ≈30 min after induction with 60 EPSP-Ca^{2+} spikes (Post-spike). **(C)** Plot of the variance ($1/CV^2$) in function of the mean peak EPSC amplitude normalized to controls (M) measured ≈30 min after 60 EPSP-Ca^{2+} spikes were applied ($N = 10$). **(D)** left. Representative superimposed EPSCs recorded before and at ≈30 min after LTP induction. **(D)** right. Same as left, but currents evoked by Glu puffs. **(E)** Summary data showing changes in peak EPSC ($N = 6$, $P < 0.01$) and Glu puff current amplitudes (same cells, $P < 0.05$) 30 min after LTP induction, relative to control (100%).

We also tested if the same basal stimulation protocol could induce plasticity when synaptic inhibition was active in control ACSF. In control ACSF Ca^{2+} spikes were never evoked by repeated basal stimulation and EPSC amplitudes were essentially identical to the controls, reaching values that were 97 ± 2% of the control ($P > 0.05$; $N = 8$; **Figure 2E**) in ≈ 30 min. The above results suggest that this LTP was intimately dependent on active dendritic mechanisms under close control by $GABA_A$ inhibition (Wigström and Gustafsson, 1983; Kampa et al., 2007; Marlin and Carter, 2014).

To verify the pre- or postsynaptic origin of this LTP we first tested for possible increases in release probability at excitatory synapses. There were no modifications in PPR or the $1/CV^2$ ratio (**Figures 3A–C**), suggesting that this LTP was not associated with changes in the probability of glutamate (Glu) release, and that there was no presynaptic contribution to it. In addition, both EPSCs and currents evoked by Glu puffs (that bypass the presynaptic components of Glu transmission) were potentiated to similar values (166.5 ± 22.3%; $P < 0.01$; $N = 6$ and 169.2 ± 23.7, $P < 0.05$; same cells, for the EPSCs and Glu currents, respectively) following the induction of LTP (**Figures 3D,E**).

Both the Action Potential Burst And Ca^{2+} Spike were Required to Induce This LTP

To determine the contribution of the Ca^{2+} spike to the induction of this LTP under P_ITX (50 μM), we inhibited Ca^{2+} spikes through a blockade of NMDARs with D-AP5 (50 μM), and of L-type VGCCs with nifedipine (20 μM). Basal stimulation was increased well above the intensity (x2) at which the EPSP triggered APs to compensate for the EPSP amplitude reduction caused by the blockade of the NMDA component. In these conditions the Ca^{2+} spike was blocked (**Figures 1F,G**) and basal stimulation (60 times at 0.2 Hz) was unsuccessful in inducing LTP (EPSCs reached values that were 98 ± 9% of the controls, $P > 0.05$; $N = 6$; **Figure 4B**).

In L5 PNs STDP requires pairing an EPSP with an AP burst induced by depolarizing current injection to rescue AP back-propagation through the generation of a Ca^{2+} spike (Larkum et al., 1999b; Kampa et al., 2004). Accordingly, we tested the effects of avoiding the AP burst by antagonizing voltage-gated Na^+ channels with intracellular QX-314 under PITX (50 μM). Under QX-314-loading (5 mM in the pipette solution) APs were inhibited and the EPSP and Ca^{2+} spike remained (see below). In addition, under QX-314 the peak amplitude of Ca^{2+} spikes (58 ± 5 mV, $N = 6$) were even larger than those linked with the induction of LTP (53 ± 6 mV, see above), likely indicating that what was required for LTP was not just the Ca^{2+} rise, but that Na^+-mediated back-propagating APs played a key role. In these conditions, repeated basal stimulation (60 times at 0.2 Hz) induced a robust LTD instead of LTP, and EPSCs reached values that were 48 ± 6% of the controls ($P < 0.01$; $N = 6$) ≈ 30 min after the onset of stimulation (**Figure 4B**). These results suggest that the AP burst and Ca^{2+} spike were essential to the induction of this LTP.

A Cytosolic Ca^{2+} Rise Is a Prerequisite for the Induction of This LTP

To determinate the contribution of the cytosolic Ca^{2+} rise in the LTP induction, we tested the effects of BAPTA-loading, which chelates Ca^{2+}, preventing a rise of Ca^{2+} in the cytosol. BAPTA-loading (40 mM in the pipette solution) did not modify the EPSP-Ca^{2+} spike (**Figure 4C**), and repeated basal stimulation (60 times at 0.2 Hz) was unable to induce LTP while EPSCs reached values that were 103 ± 6% of the controls ($P > 0.05$; $N = 6$) ≈ 30 min after the induction process (**Figures 4B,C**).

Because Ca^{2+} release from IP3-sensitive stores and Ca^{2+} induced-Ca^{2+} release (CICR) through ryanodine receptors can contribute to the cytosolic Ca^{2+} rise we tested the effects of blocking the ryanodine receptors with intracellular ruthenium red (Ru-Red 400 μM in the pipette solution). Ru-Red blocked the LTP without modifying the EPSP-Ca^{2+} spike, while EPSCs reached values that were 99 ± 11% of the controls ($P > 0.05$; $N = 6$; **Figure 4C**) ≈ 30 min after the induction process. We next examined the effects of blocking IP_3Rs with intracellular heparin (5 mg/ml in the pipette solution). In these conditions the LTP was inhibited without modification of the EPSP-Ca^{2+} spike and the EPSCs reached amplitudes that were 86 ± 8% of the controls ($P > 0.05$ $N = 6$) ≈ 30 min after 60 basal stimulations at 0.2 Hz

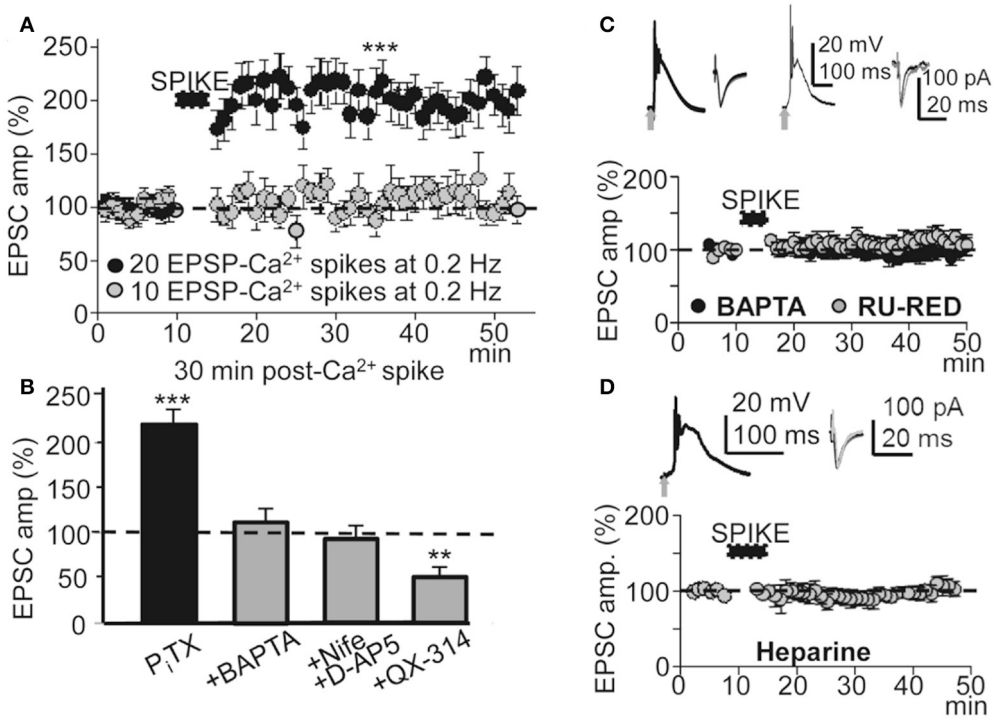

FIGURE 4 | A threshold number of EPSP-Ca^{2+} spikes was required to induce this LTP. Effects of blocking the Ca^{2+} spike, AP burst and Ca^{2+} release. **(A)** Time course of the peak EPSC amplitude showing the effects of 10 (gray circles, $N = 8$, $P > 0.05$) and 20 successive EPSP-Ca^{2+} spikes (black circles, $N = 6$, $P > 0.001$), both at 0.2 Hz. **(B)** Bar plot showing average peak EPSC amplitudes relative to pre-induction controls (100%) under P_iTX (50 μM, $N = 10$, $P < 0.001$) and the effects of antagonizing the cytosolic Ca^{2+} rise by chelation with +BAPTA-loading (40 mM in the pipette solution, $N = 6$, $P > 0.05$), of inhibition of the Ca^{2+} spike by superfusing with nifedipine (20 μM) + D-AP5 (50 μM) (+Nife+D-AP5, $N = 9$, $P > 0.05$) and of blocking voltage dependent Na^{+} currents with intracellular +QX-314 (5 mM in the pipette solution, $N = 6$, $P > 0.05$). **(C)** upper left. Representative averaged EPSP-Ca^{2+} spike recorded in a BAPTA-loaded PN (40 mM in the intracellular solution) and superimposed EPSCs recorded before and ≈30 min after LTP induction. **(C)** upper right. Same as left, but in a RU-RED-loaded cell (400 μM in the intracellular solution). **(C)** bottom. Time course of the peak EPSC amplitude in BAPTA-loaded (black circles, $N = 6$, $P > 0.05$) and RU-RED-loaded (gray circles, $N = 6$, $P > 0.05$) PNs. **(D)** same as **(A)**, but in Heparin-loaded PNs (5 mg/ml, $N = 6$, $P > 0.05$).

(**Figure 4D**). Therefore, a rise in cytosolic Ca^{2+} was required for the induction of this LTP and was produced by influx through NMDARs, L-type VGCC and release from intracellular stores.

This LTP Required G-Proteins, Activation of Metabotropic Glu Receptors, and Muscarinic and Nicotinic AChRs

Synaptic plasticity is controlled by intracellular cascades in which G-protein coupled receptors (GPCRs) play key roles (Mukherjee and Manahan-Vaughan, 2013). Therefore, we first tested the effects of blocking G-proteins by loading the PN with GDPβS. With intracellular GDPβs (1 mM in the pipette solution) EPSP-Ca^{2+} spikes continued but failed to induce LTP. Thirty min after the induction protocol, EPSCs reached values that were 101 ± 6% of the controls ($P > 0.05$; $N = 6$; **Figures 5A,D**). Since metabotropic receptors are coupled to G-proteins we checked whether metabotropic Glu receptors (mGluRs) were involved in LTP induction. Superfusion with MCPG (1.0 mM), a group I/II mGluR antagonist, prevented LTP and, ≈ 30 min after induction, EPSCs reached values that were 92 ± 25% of the controls ($P > 0.05$; $N = 4$, **Figure 5D**). Although there was a small but not significant increase in EPSC amplitude, there was no LTP with the selective mGluR1 antagonist LY367385 (50 μM) and EPSC amplitudes reached values that were 109 ± 25% of the controls ($P > 0.05$; $N = 5$; **Figures 5C,D**). In contrast, a robust LTP was induced ≈30 min after the EPSP-Ca^{2+} spike in the presence of the mGluR5 selective antagonist MPEP (5.0 μM), with EPSC amplitudes that reached 196 ± 32% of the controls ($P < 0.01$; $N = 6$; **Figures 5C,D**). Therefore, mGLuR1 activation was required to induce the LTP.

Muscarinic AChRs (mAChRs) play a key role in certain forms of long-term enhancement of excitatory synaptic transmission (Fernández de Sevilla et al., 2008; Buchanan et al., 2010; Fernández de Sevilla and Buño, 2010; Nuñez et al., 2012; Dennis et al., 2016). Accordingly, we tested the effects of the non-selective mAChR antagonist atropine (0.3 μM), which prevented LTP induction. Under atropine EPSCs reached values that were 101 ± 2% of the controls ($P > 0.05$; $N = 5$) ≈ 30 min after the induction process (**Figure 5D**). DAU5884 (1 μM), a selective subtype 3 mAChR antagonist, blocked the LTP and EPSCs reached values of 103 ± 4% of the controls ($P > 0.05$; $N = 5$) ≈ 30 min after induction (**Figures 5B,D**). Pirenzepine (75 nM), a selective M1 mAChR antagonist, did not prevent the LTP and EPSCs reached

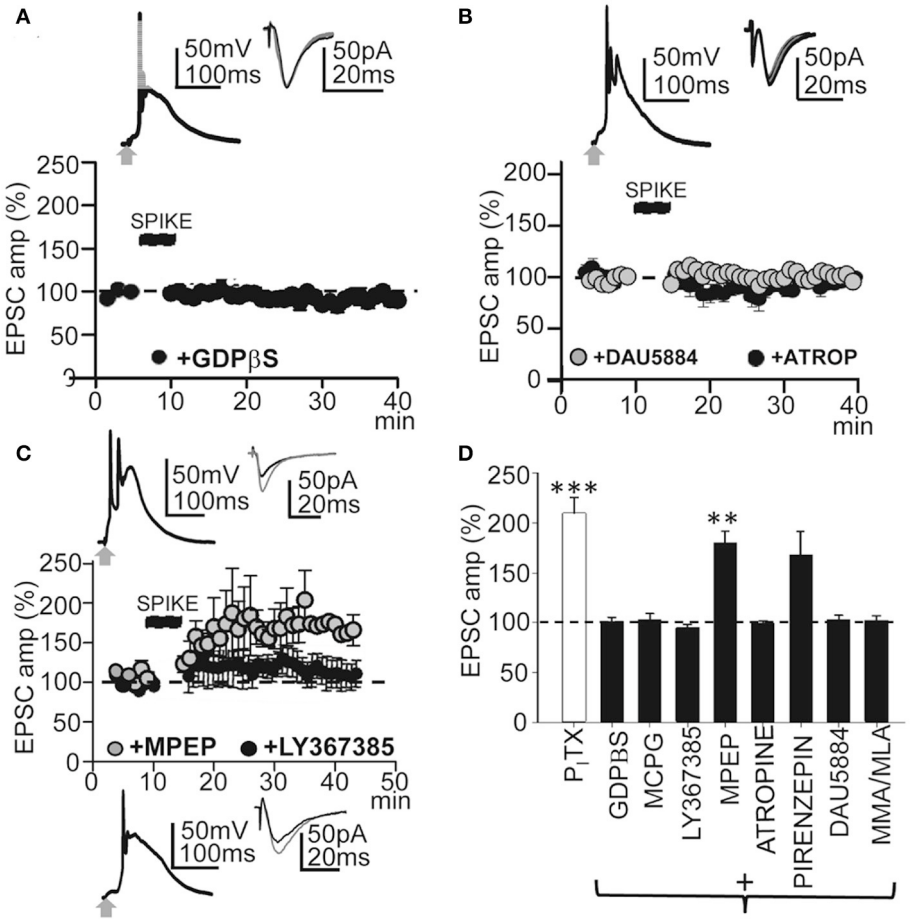

FIGURE 5 | GPCRs and metabotropic receptors participate in the induction of this LTP. (A) upper. Averaged EPSP-Ca^{2+} spike and superimposed EPSCs recorded with intracellular GDPβS (1 mM in the pipette solution). **(A)** lower. Time course of the peak EPSC amplitude showing the effects of intracellular GDPβS ($N = 6$, $P > 0.05$). **(B)** Same as in **(A)**, but effects of superfusion with atropine (ATRO, 0.3 μM; filled circles, $N = 5$, $P > 0.05$) and DAU5884 (1 μM, gray circles, $N = 6$, $P > 0.05$). **(C)** Same as in **(A)**, but effects of superfusion with LY367385 (50 μM, top insets and black circles, $N = 5$, $P > 0.05$) and with MPEP (5.0 μM, gray circles and bottom insets, $N = 6$, $P < 0.001$). **(D)** Summary data showing the effect of P_ITX ($N = 10$, $P < 0.001$), GDPβS ($N = 6$, $P > 0.05$), MCPG (1.0 mM, $N = 4$, $P > 0.05$), LY367385 ($N = 5$, $P > 0.05$), MPEP ($N = 6$, $P < 0.01$), atropine ($N = 5$, $P > 0.05$), Pirenzepine (75 nM, $N = 5$, $P < 0.01$), DAU5884 ($N = 6$, $P > 0.05$) and MMA/MLA (10/50 μM, $N = 5$, $P > 0.05$), relative to EPSCs in control ACSF (100%). 60 EPSP-Ca^{2+} spikes were used in **(A–D)**.

values of 168 ± 5% of the controls ($P < 0.01$; $N = 5$) ≈30 min after induction (**Figure 5D**). Nicotinic AChRs (nAChRs) have also been involved in the regulation of transmitter release and synaptic plasticity. Therefore, we tested the effects of blockade of α4β2-containing and α7-containing nAChRs using MMA (10 μM) plus MLA (50 μM). This prevented LTP induction and EPSC reached values that were 102 ± 4% of the controls ($P > 0.05$; $N = 5$; **Figure 5D**). Taken together these results suggest that this LTP required the participation of GPCRs and activation of mGluR R1 and subtype M3 mAChRs, as well as nAChRs. Note that none of these treatments modified the EPSP-Ca^{2+} spikes, suggesting that the inhibition of LTP occurred downstream of the cytosolic Ca^{2+} rise.

LTP Induction Required Kinase Activation

Cytosolic Ca^{2+}-mediated activation of intracellular kinases can induce LTP through an increase in the number of functional AMPARs in dendritic spines (Fernández de Sevilla et al., 2008). Kinases can also enhance NMDAR-mediated responses by changing the biophysical properties of NMDARs (Fernández de Sevilla and Buño, 2010). We therefore tested whether activation of the CaMKII was required to induce the LTP. Blockade of CaMKII with the peptide inhibitor AIP (5 μM in the pipette solution) suppressed LTP without preventing the EPSP-Ca^{2+} spike and ≈30 min after the induction process EPSCs reached values that were 93 ± 10% of the controls ($P > 0.05$; $N = 4$; **Figures 6A,C**).

We have shown that Ca^{2+} release from endoplasmic reticulum stores by activation of IP_3Rs plays a key role in the cholinergic LTP in CA1 PNs (Fernández de Sevilla and Buño, 2010). The Ca^{2+} released plays a key role in long-term enhancement excitatory synaptic transmission (see above). Accordingly, we tested the effects of inhibiting the production of IP3 by blocking the PLC translocation with intracellular U73122. U73122 (2 mM

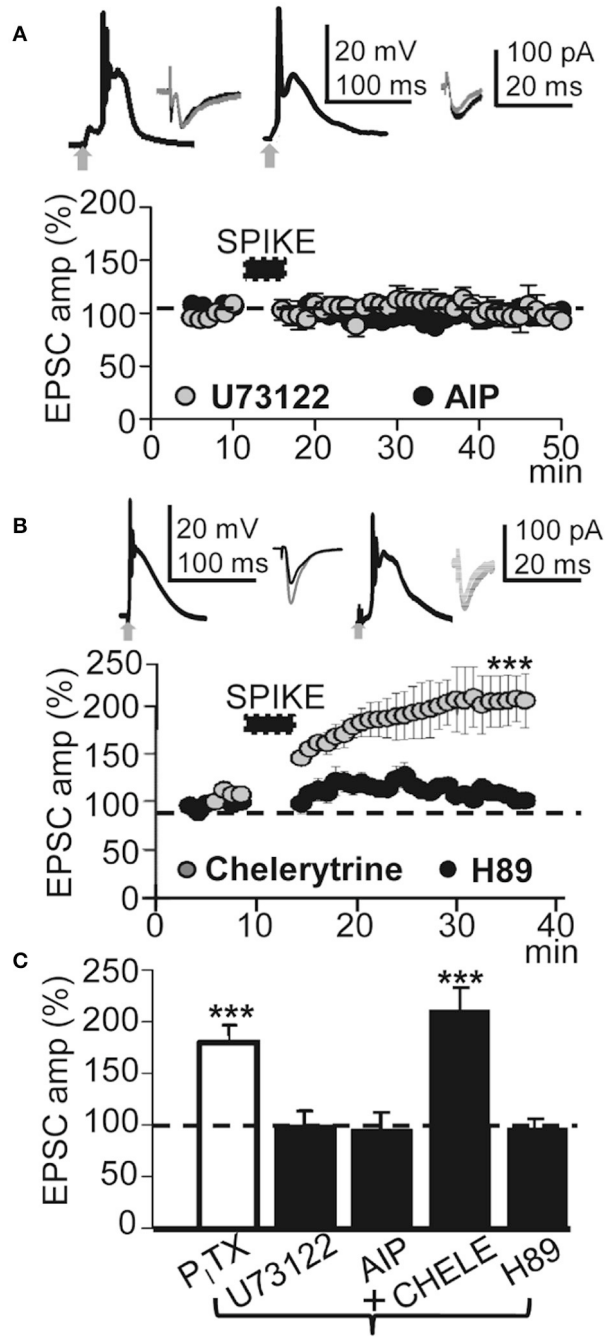

FIGURE 6 | This LTP required activation of PLC and PKA. (A) , upper left. Averaged EPSP-Ca^{2+} spike recorded with intracellular U73122 (2 mM in the pipette solution). **(A)**, upper right**.** Same as left but intracellular AIP. **(A)**, lower. Time course of the peak EPSC amplitude showing the effects of intracellular U73122 (gray circles, $N = 6$, $P > 0.05$) and AIP (black circles, $N = 4$, $P > 0.05$). **(B)** Same as **(A)**, but PNs were loaded with chelerytrine (5 μM in the pipette solution, left insets and gray circles, $N = 5$, P<0.001) or H89 (10 μM, right insets and black circles, $N = 5$, P>0.05). **(C)** Summary data showing the EPSC peak amplitude under P_ITX (50 μM, $N = 10$, $P < 0.001$) and effects of loading the PN with U73122 (5 μM, $N = 6$, $P > 0.05$), AIP (5 mg/ml, $N = 4$, $P > 0.05$), Chelerytine (5 μM, $N = 5$, $P < 0.001$) and H89 (10 μM, $N = 6$, $P > 0.05$), relative to EPSCs in control ACSF (100%). 60 EPSP-Ca^{2+} spikes were used in **(A–C)**.

in the pipette solution) inhibited the LTP without preventing the EPSP-Ca^{2+} spike and EPSCs reached values that were 97 ± 18% of the controls ($P > 0.05$; $N = 6$; **Figures 6A,C**). We next investigated the effects of inhibiting PKC with intracellular chelerytrine (5 μM); there was no effect on LTP and EPSCs reached values that were 191.47 ± 30% ($P < 0.001$; $N = 5$) of the controls ≈30 min after induction. In contrast, PKA blockade with H89 dihydrochloridre (10 μM in the pipette solution) had no effect on the EPSP-Ca^{2+} spike but did inhibit the LTP and ≈30 min after induction, EPSCs reached values that were 92.4 ± 4% of the controls ($P > 0.05$; $N = 6$; **Figures 6B,C**). The above results suggest that this LTP requires CaMKII, PLC, and PKA activation.

Reducing the Ca^{2+} Spike and the Associated Ca^{2+} Signal or the AP Burst Induced LTD Instead of LTP

Protocols that produce strong membrane depolarization induce LTP while those that cause modest or local depolarization generate LTD (Holthoff et al., 2004). This bidirectional behavior is thought to be caused by the level of Ca^{2+} influx during dendritic depolarization (Artola et al., 1990; Bliss and Collingridge, 1993; Neveu and Zucker, 1996; Dan and Poo, 2004; Kampa et al., 2007). Accordingly, we analyzed the effects of membrane hyperpolarization during the induction process. Hyperpolarization to −100 mV decreased the amplitude and duration of averaged EPSP-Ca^{2+} spike to 27 ± 2 mV and 50 ± 8 ms ($P < 0.01$; $N = 5$). In these conditions repeated basal stimulation (60 times at 0.2 Hz) induced an LTD that rapidly reached values of 63 ± 1% of the controls ($P < 0.001$; $N = 5$; **Figure 7A**). A NMDAR blockade with D-AP5 (50 μM) reduced the average amplitude and duration of Ca^{2+} spikes to 25 ± 4 mV and 55 ± 13 ms ($P < 0.01$; $N = 5$). In these conditions, basal stimulation (as above) produced a potent LTD that reached values that were 56 ± 3% of the controls ($P < 0.01$; $N = 6$) (**Figure 7B**). Nifedipine (20 μM) blockade of L-type VGCC also reduced the amplitude and duration of the Ca^{2+} spikes to 21 ± 1 mV and 100 ± 9 ms ($P < 0.01$; $N = 5$). Thirty min after induction, repeated basal stimulation (as above) induced a slowly declining LTD that reached values of 77 ± 5% of the controls ($P < 0.05$; $N = 5$; **Figure 7C**). A single or a pair of AP and Ca^{2+} spikes was followed by hyperpolarization in **Figures 7A–C**.

Moreover, a robust LTD that reached values of 48 ± 6% of the controls ($P < 0.01$; $N = 6$; **Figures 7D**, **4B**) was induced when APs were inhibited by QX-314. Under QX-314 Ca^{2+} spikes were larger than those linked with the LTP (see above). These results suggest that what was required for LTP was not just the Ca^{2+} rise, but that Na^{+}-mediated back-propagating APs played a role. In contrast, with the LTP that increased gradually in amplitude following induction, the LTD in these circumstances was fully developed at the end of the induction process.

The Ca^{2+} spike is strongly linked with Ca^{2+} influx, consequently an analysis of the relationship between the Ca^{2+} spike and the cytosolic Ca^{2+} signal could provide a direct estimate of the conditions that induce the bidirectional synaptic

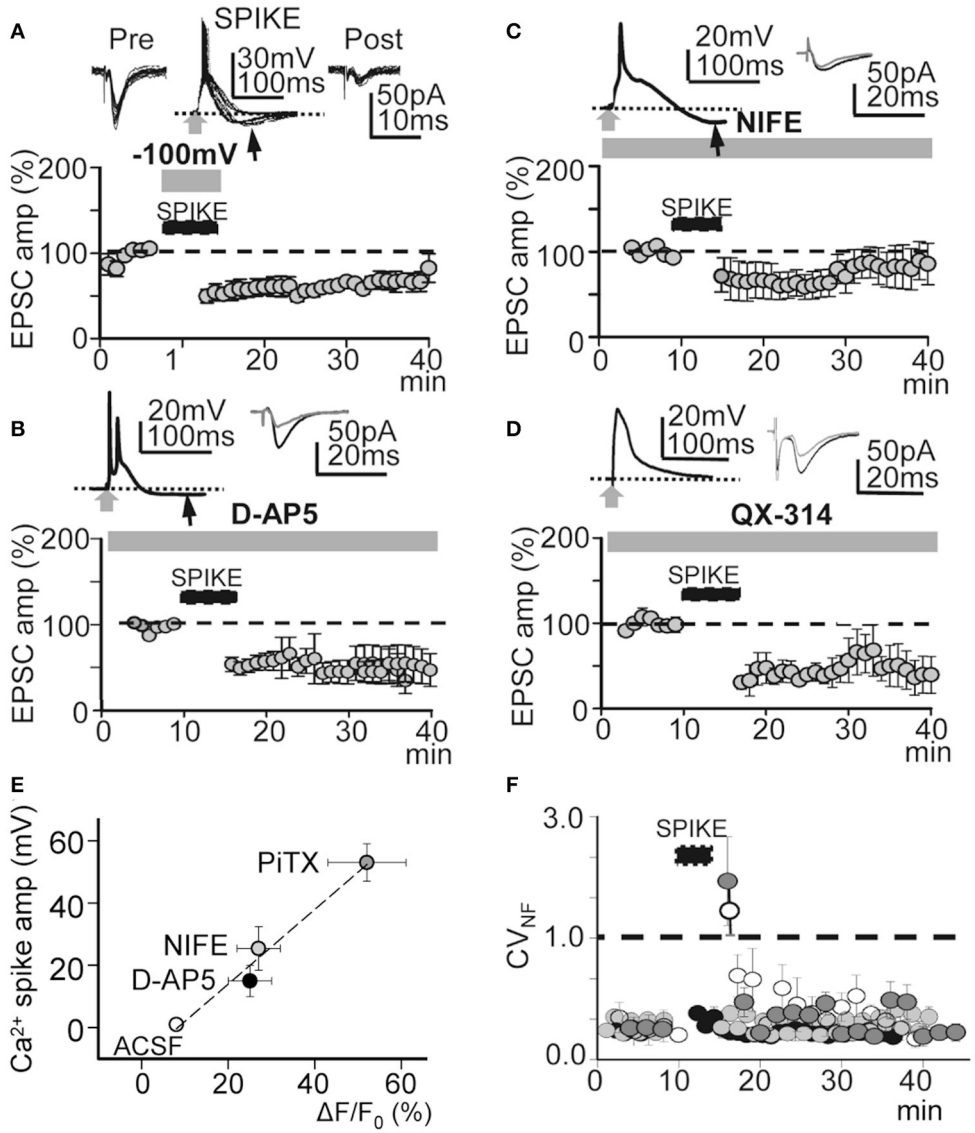

FIGURE 7 | Effects of hyperpolarization and NMDAR, L-type VGCC, and voltage-gated Na^+ conductance blockade. (A), upper. Superimposed records of pre-induction EPSCs ($n = 20$), Ca^{2+} spikes during hyperpolarization to −100 mV ($n = 20$) and post-induction EPSCs ($n = 10$). **(A)**, lower. Same as **Figure 4A**, but LTD was induced with hyperpolarization to -100 mV during the INDUCTION process ($N = 5$, $P < 0.001$). **(B)** Same as **(A)**, but the LTD was induced under inhibition of NMDARs with D-AP5 (50 μM, $N = 6$, $P < 0.001$). **(C)** Same as **(A)**, but LTD induced under nifedipine (20 μM) inhibition of L-type VGCC ($N = 5$, $P < 0.001$). **(D)** Same as **(A)**, but the LTD was induced by intracellular QX-314 (5 mM in the pipette solution) inhibition of voltage gated Na^+ conductance ($N = 6$, $P < 0.001$). **(E)** Plot of the Ca^{2+} spike amplitude in function of the cytosolic peak somatic Ca^{2+} signal recorded in control ACSF (open circle) and when PiTX (dark gray circle), nifedipine (gray circle) and D-AP5 (black circle) were added. Note the linear correlation ($r^2 = 0.98$) indicating a close association between the amplitude of Ca^{2+} spikes the cytosolic Ca^{2+} signal. **(F)** Time course of the noise free coefficient of variation (CV_{NF}) calculated form the experiments under intracellular QX-314 (white circles), nifedipine (dark gray circles), D-AP5 (light gray circles) and during hyperpolarization to −100 mV (black circles). Note the lack of long term modifications of the CV_{NF} in all conditions tested. Black arrows in **(A–C)** indicate hyperpolarizations following Ca^{2+} spikes.

plasticity. Therefore, we recorded the somatic Ca^{2+} signals associated with the Ca^{2+} spike in control ACSF and under PiTX, PiTX + D-AP5, and PiTX + nifedipine. In control ACSF small Ca^{2+} signals with $\Delta F/F_0$ values of 8 ± 1% of the controls ($P < 0.01$; $N = 6$) were induced when APs were triggered in the absence of Ca^{2+} spikes. Under PiTX (50 μM) the $\Delta F/F_0$ reached much higher values that were 52 ± 9% of the controls ($P < 0.001$; $N = 6$), whereas lower values of 25 ± 5% ($P < 0.00$; same cells) were attained when D-AP5 (50 μM) was added to block NMDARs. Under nifedipine (50 mM) added to inhibit L-type VGCC, $\Delta F/F_0$ achieved values of 27 ± 5% from the controls ($P < 0.001$; $N = 5$) (**Figure 7E**). Taken together the above results suggest that the direction of the induced change in synaptic plasticity could be regulated by the degree of membrane

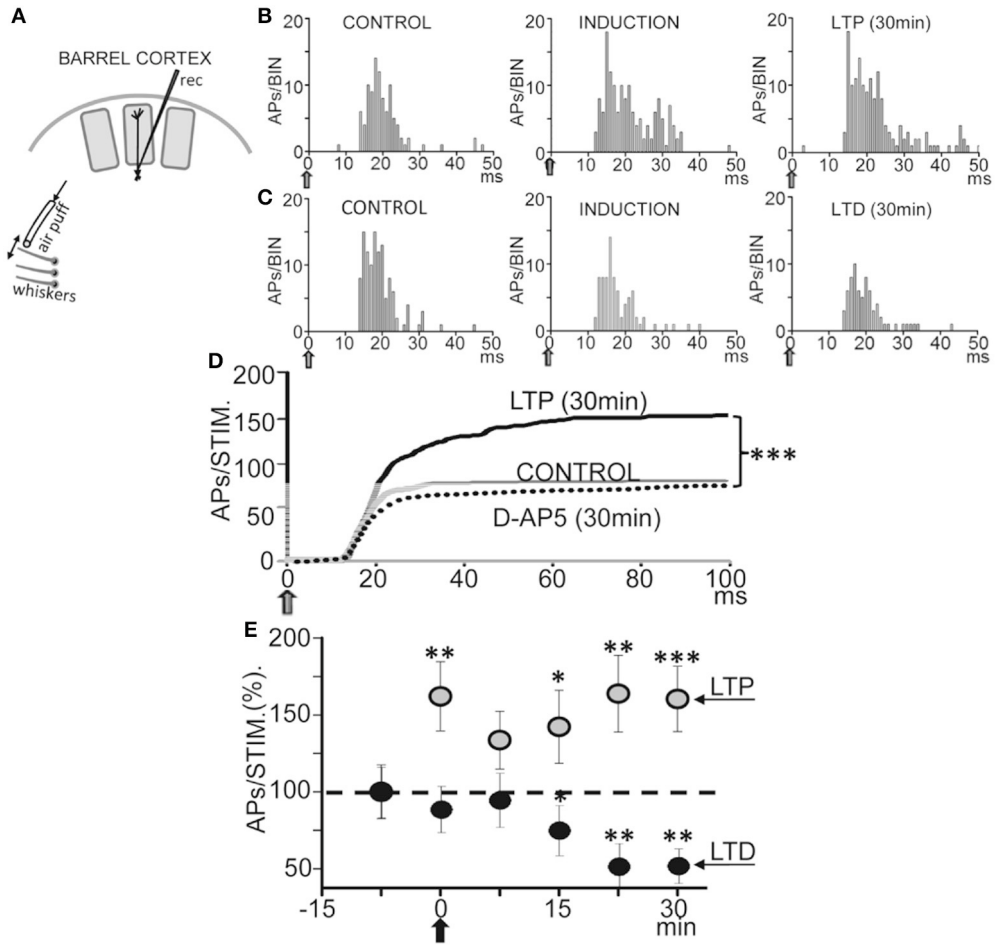

FIGURE 8 | Bidirectional plasticity evoked by whisker deflections in anesthetized rats. (A) Schematic diagram of experimental setup. **(B)** Representative PSTHs computed during whisker deflections (gray arrows) in CONTROL (0.5 Hz), INDUCTION (1.0 Hz), and LTP (0.5 Hz) conditions. Note the increase in the number of APs during induction and the LTP 30 min after. **(C)** Same as **(B)**, but the number of APs was reduced 30 min after INDUCTION, or LTD, and APs did not increase during induction. **(D)** Cumulative spike plots (CSP) computed by averaging all PSTHs (see Materials and Methods) in CONTROL, LTP ($N = 16$, $P < 0.001$) and under an injection of D-AP5 (50 μM; 0.1 μl, $N = 14$, $P < 0.001$) in L5 (see Materials and Methods). Note the enhanced whisker-evoked response during LTP and the reduced response with D-AP5. Blockade of NMDARs by injections of D-AP5 inhibited plasticity. **(E)** Plot showing averaged responses vs. time before and after induction (black arrow). Data points represent the mean area of PSTHs (CSPs;% of controls) computed over 5 min showing LTP (gray circles, $N = 16$, $P < 0.001$) and LTD (black circles, $N = 5$, $P < 0.01$).

depolarization and the cytosolic Ca^{2+} level attained during the EPSP-Ca^{2+} spike.

To verify the pre- or postsynaptic origin of this LTD we first tested for possible decreases in release probability at excitatory synapses. We plotted the noise-free coefficient of variation (CV_{NF}) vs. time. Under all LTD-inducing manipulations, the CV_{NF} values remained below 1.0 (**Figure 7F**), suggesting the absence of significant changes in Glu release probability during an LTD and meaning that the synaptic depression originated postsynaptically.

Bidirectional Plasticity of Whisker-Evoked Responses in Anesthetized Rats

We first tested if repetitive low-frequency deflections delivered at the principal whisker (**Figure 8A**) could induce long-term response changes resembling those that occur *in vitro*. The 37 L5 neurons recorded were either silent or displayed a low spontaneous firing rate (0.5–2 APs/s), and responded to contralateral displacements of the principal whisker. Control whisker-evoked responses had on average 3.5 ± 0.5 APs/stimulus (measured from 0 to 100 ms after the stimulus onset). The low spontaneous AP firing rate and the activation by deflection of the principal whisker provide strong support to the notion that recordings were obtained from L5A PNs, as has been described previously (Manns et al., 2004; de Kock and Sakmann, 2009).

Following a 60 s control stimulation at 0.5 Hz a train of 40 stimuli at 1.0 Hz induced a long-lasting enhancement of the response (or LTP) from 3.9 ± 0.4 APs/stimulus in control to 5.3 ± 0.6 APs/stimulus, measured 30 min after induction in 16 neurons out of 23 (or 66%; $P < 0.001$; **Figures 8B,D,E**), while 5 neurons (22%) reduced their response (or LTD; from 3.5 ± 0.5 APs/stimulus in the control to 2.4 ± 0.1 APs/stimulus; $P < 0.01$;

Figures 8C–E) and 2 neurons (9%) were not affected (from 3.2 ± 0.6 APs/stimulus in the control to 3.4 ± 0.4 APs/stimulus after induction; $P > 0.05$). **Figure 8E** shows the time course of the AP response plasticity.

Different Responses during Induction Typified Cells That Showed LTP or LTD

Interestingly, the whisker-evoked response was enhanced during the 1 Hz induction from 3.9 ± 0.41 APs/stimulus in the control to 5.5 ± 0.58 APs/stimulus ($P < 0.01$; $N = 5$) in neurons that showed LTP (**Figure 8B**). In contrast, in neurons that showed LTD whisker-evoked responses were not altered during induction (from 3.5 ± 0.48 APs/stimulus in control to 2.9 ± 0.37 APs/stimulus; $P > 0.05$; $N = 5$; **Figure 8C**).

Bidirectional Plasticity Required NMDAR Activation

We next tested if blockade of NMDARs by injection of D-AP5 (50 μM; 0.1 μl) in L5 (see Section Materials and Methods) prevented plasticity. To exclude possible artifacts caused by this manipulation we checked that the D-AP5 injection did not modify AP amplitudes. Under the effects of D-AP5 the whisker-evoked response measured ≈30 min after the 1 Hz induction stimulation train was essentially identically to the control response and plasticity was absent (from 2.6 ± 0.38 in control to 2.5 ± 0.36 APs/stimulus after induction; $P > 0.05$; $N = 14$; **Figure 8D**). Therefore, the above results suggest that the activation of NMDA receptors in L5 play a key role in the genesis of the bidirectional synaptic plasticity.

DISCUSSION

Here, we describe a form of bidirectional plasticity induced by unpaired low-frequency stimulation of basal inputs in regular spiking L5 PNs of the rat barrel cortex. This stimulation can trigger an EPSP closely followed by an AP burst and Ca^{2+} spike that were present when the $GABA_A$Rs were blocked with P_ITX. In contrast, Ca^{2+} spikes and LTP were absent when synaptic inhibition was active, revealing a powerful $GABA_A$ inhibitory control of excitability and synaptic plasticity (Kampa et al., 2007; Caporale and Dan, 2008; Sjöström et al., 2008; Feldman, 2012; Hao and Oertner, 2012; Chiu et al., 2013; Hsieh and Levine, 2013).

This LTP (present Results) has all the attributes of an activity-dependent hebbian LTP. Indeed, it required: (*i*) activation of NMDARs; (*ii*) depolarization to facilitate Ca^{2+} influx through NMDARs; and (*iii*) AP backpropagation facilitated by the a dendritic Ca^{2+} spike. NMDARs are thought to represent the "coincidence detector" that links synaptic input with postsynaptic depolarization. Depolarization is required to relieve the extracellular voltage-dependent Mg^{2+} block of the NMDA channel and allow Ca^{2+} influx (Schiller and Schiller, 2001; Kampa et al., 2004, 2007; Fuenzalida et al., 2010). Therefore, the EPSP-Ca^{2+} spike fulfills the attributes of a coincidence detector because it associates the EPSP with the Ca^{2+} influx through NMDARs, a Ca^{2+} influx that is facilitated by the depolarization contributed by the activation of L-type VGCC. In addition, the resulting depolarization triggers backpropagation of the AP burst that is a prerequisite for the induction of LTP in L5 PNs (Larkum et al., 1999a; Kampa et al., 2004).

The EPSP-Ca^{2+} spike fulfills the components that define STDP and represents a simple form of the hebbian LTP induction protocol, one that obeys the original hebbian rule (Hebb, 1949). We also show that the same presynaptic stimulation can induce LTD when the Ca^{2+} spike and the associated cytosolic Ca^{2+} signal were reduced or when the AP burst is inhibited. The EPSP-AP STDP protocol is ineffective in L5 PNs because single APs are not back-propagated (Stuart et al., 1997; Kampa and Stuart, 2006). However, AP bursts evoked by depolarizing current injection can trigger Ca^{2+} spikes that boost AP backpropagation and induce LTP by STDP in L5 PNs (Larkum et al., 1999a; Kampa et al., 2004). The AP burst associated with Ca^{2+} spikes, (present Results) and the EPSP-AP burst triggered by the postsynaptic current injection of Larkum et al. (1999b) and Kampa and Stuart (2006), can be considered to accomplish an essentially identical operational role that facilitates AP backpropagation and produces a robust dendritic Ca^{2+} signal that induces LTP (present Results). In addition, we show that in anesthetized rats equivalent bidirectional plasticity is induced in L5 neurons when whiskers are repeatedly deflected.

We used higher stimulation intensities to trigger EPSP-Ca^{2+} spikes during the induction process than the intensities used to evoke control EPSCs. The larger EPSPs evoked by the additional Glu released by presynaptic fibers recruited by the higher stimulation intensity was able to relieve the Mg^{2+} blockade of NMDA receptors at the weakly-stimulated synapses and potentiate those synapses. However, heterosynaptic input did not appear to contribute to this LTP because high intensity induction protocols were ineffective when the AP bursts or the Ca^{2+} spikes were blocked.

Inducing the LTP required stimulation within a narrow repetition rate. The stimulation rate used here (0.2–0.3 Hz) approximately matches the slow firing frequencies of cortico-thalamic circuits (Steriade et al., 1993) and of a subset of L5 PNs (Lorincz et al., 2015) during specific behavioral states. Therefore, this LTP could be facilitated during these states.

With classic STDP protocols the degree and sign of the synaptic change is critically dependent on the timing between the EPSP and the postsynaptic spikes (Bi and Poo, 1998; Fuenzalida et al., 2007). Although the time window is fixed by the EPSP-Ca^{2+} spike, the direction of the synaptic modification can be changed since LTD is induced when the Ca^{2+} spike and the associated cytosolic Ca^{2+} signal was reduced by hyperpolarization and when NMDARs or L-type VGCCs are blocked (present Results). Different levels of cytosolic Ca^{2+} are thought to control the magnitude and nature of the induced synaptic change by activating different molecular cascades (Lisman, 1989; Artola et al., 1990; Bliss and Collingridge, 1993; Cho et al., 2001; Kampa et al., 2007). STDP-induced LTP requires the sequential activation of NMDARs and VGCC within dendritic spines (Tigaret et al., 2016), as is likely to occur in these experiments.

Our present results show that the simple induction form of LTP studied here requires an EPSP followed by an AP burst and a robust dendritic Ca^{2+} spike mediated by activation of both NMDA and L-Type VGCC, and agrees with a previous report (Tigaret et al., 2016). Consequently, the degree of inhibition can control the type of synaptic change by regulating the magnitude of the Ca^{2+} spike. We showed that, with intact inhibition under superfusion with acetylcholine (ACh), low-frequency basal stimulation can evoke the EPSP-Ca^{2+} spike and LTP in L5 PNs by enhancing EPSPs and reducing IPSPs through activation of AChRs (Nuñez et al., 2012). Consequently, low-frequency stimulation of basal inputs could theoretically induce LTP under natural physiological conditions when mAChRs are activated or the activity of inhibitory interneurons is decreased or GABA release probability is reduced through activation of type 1 endocannabinoid receptors (CB_1Rs); these attractive possibilities remain to be investigated. A novel form of plasticity has recently been reported in tuft dendrites of L5 PNs (Sandler et al., 2016). This plasticity is induced by unpaired low-frequency (0.1 Hz) stimulation of the tuft inputs and requires Kv4.2 channels, NMDARs, membrane internalization and AMPAR insertion. It is different from the plasticity reported here, but nevertheless it also required $GABA_A$R blockade. These two forms of plasticity at separate processing and storing compartments in L5 PNs can possibly be coupled or uncoupled by the dynamic regulation of dendritic excitability. Therefore, they could either function in site-specific or in a cooperative manner depending on system demands.

The LTP reported here required activation of mGluR1, CaMKII, G-proteins, PLC and PKA. Postsynaptic group I mGluRs are crucial for the induction of LTP because they lead to depolarization, increased excitability and LTP at glutamatergic synapses (Lisman et al., 2002; Lamsa et al., 2007). Neocortical expression of hebbian LTP requires CaMKII activation (Otmakhov et al., 1997; Malenka and Nicoll, 1999; Fukunaga and Miyamoto, 2000). In addition, mAChR activation can induce LTP in both the hippocampus and the barrel cortex where release from IP_3-sensitive intracellular Ca^{2+}stores plays a key role (Rose and Konnerth, 2001; Fitzjohn and Collingridge, 2002; Fernández de Sevilla et al., 2008; Fernández de Sevilla and Buño, 2010; Baker et al., 2013; Domínguez et al., 2014). Moreover, nAChRs can enhance excitatory and reduce inhibitory synaptic transmission (Buccafusco et al., 2005; Nuñez et al., 2012; Udakis et al., 2016). Thus, equivalent signaling cascades activated through different mechanisms can lead to similar long-term synaptic modifications.

We show that equivalent bidirectional plasticity is induced in L5 neurons when whiskers are repeatedly deflected at 1.0 Hz. Interestingly, this plasticity mainly consists in a modification of the late component of the whisker-evoked response and is dependent on the activation of NMDARs. Rats exploring the environment move their whiskers on objects or surfaces in repeated rhythmic sweeps at frequencies of 4–12 Hz (Carvell and Simons, 1990; Fanselow and Nicolelis, 1999). In contrast, resting rats either do not move their whiskers or do so at low-frequencies <1 Hz. It has been shown that repetitive whisker deflections at the frequency used to explore the environment induce a long-lasting response facilitation of cortical neurons by activation of NMDA receptors (Barros-Zulaica et al., 2014). We now show that low-frequency stimulation can induce bidirectional plasticity of cortical barrel neurons through activation of NMDARs. Spontaneous ACh release is lower under urethane anesthesia than in freely moving animals (Bertorelli et al., 1991), but basal ACh release is sustained in both conditions (Rasmusson et al., 1992; Jiménez-Capdeville et al., 1997). Cortical ACh reduces GABAergic transmission (Nuñez et al., 2012), this may explain why LTP is induced *in vivo,* while LTP required $GABA_A$R blockade *in vitro*. Therefore, it is likely that this form of bidirectional plasticity that is present both *in vivo* and *in vitro* under the inhibitory regulation of dendritic excitability could control the flow and storage of select input characteristics and regulate behavior and the flow of sensorimotor information in natural conditions. Importantly, Ca^{2+} activity in the apical dendrites and AP bursts in L5 PNs in mice are correlated with the threshold for perceptual detection of whisker deflections (Takahashi et al., 2016), demonstrating that active dendritic mechanisms are causally linked to perceptual detection and behavior.

AUTHOR CONTRIBUTIONS

AD, DF, and NB performed the experiments; DF, AN, and WB designed the experiments; AD, NB, DF, AN, and WB analyzed data; AD, NB, DF, AN, and WB wrote the manuscript and edited and approved the final version.

ACKNOWLEDGMENTS

Work supported by "*Ministerio de Ciencia y Tecnología* y *Ministerio de Ciencia e Innovación"* grants (BFU2005-07486, BFU2008-03488, SAF2009-10339, BFU2011-23522, BFU2012-36107, BFU2013-43668-P and BFU2016-80802-P) and a "*Comunidad Autónoma de Madrid*" (GR/SAL/0877/2004) grant. Dr. D. Fernández de Sevilla was a postdoctoral fellow at the "*Instituto Cajal,"* funded by GR/SAL/0877/2004 and a "*Ministerio de Ciencia and Tecnología*" grant (BFU2005-07486). He was subsequently supported by a Ramón y Cajal Contract and is now a Professor at the "*Departamento de Anatomía, Histología y Neurociencia, Facultad de Medicina, Universidad Autónoma de Madrid."* Dr. Andrea Diez was a doctoral fellow funded by the BFU2011-23522 grant and is now a postdoctoral fellow funded by "*Ministerio de Ciencia e Innovación*" grant (BFU2013-43741-P) at the "*Departamento de Anatomía, Histología y Neurociencia, Facultad de Medicina, Universidad Autónoma de Madrid."* N. Barros-Zulaica was a doctoral fellow funded by the BFU2012-36107 grant. We thank Carol Fox Warren for correcting the English.

REFERENCES

Artola, A., Bröcher, S., and Singer, W. (1990). Different voltage-dependent thresholds for inducing long-term depression and long-term potentiation in slices of rat visual cortex. *Nature* 347, 69–72. doi: 10.1038/347069a0

Baker, K. D., Edwards, T. M., and Rickard, N. S. (2013). The role of intracellular calcium stores in synaptic plasticity and memory consolidation. *Neurosci. Biobehav. Rev.* 37, 1211–1239. doi: 10.1016/j.neubiorev.2013.04.011

Barros-Zulaica, N., Castejon, C., and Nunez, A. (2014). Frequency-specific response facilitation of supra and infragranular barrel cortical neurons depends on NMDA receptor activation in rats. *Neuroscience* 281, 178–194. doi: 10.1016/j.neuroscience.2014.09.057

Bertorelli, R., Forloni, G., and Consolo, S. (1991). Modulation of cortical *in vivo* acetylcholine release by the basal nuclear complex: role of the pontomesencephalic tegmental area. *Brain Res.* 563, 353–356.

Bi, G. Q., and Poo, M. M. (1998). Synaptic modifications in cultured hippocampal neurons: dependence on spike timing, synaptic strength, and postsynaptic cell type. *J. Neurosci.* 18, 10464–10472.

Bliss, T. V., and Collingridge, G. L. (1993). A synaptic model of memory: long-term potentiation in the hippocampus. *Nature* 361, 31–39. doi: 10.1038/361031a0

Buccafusco, J. J., Letchworth, S. R., Bencherif, M., and Lippiello, P. M. (2005). Long-lasting cognitive improvement with nicotinic receptor agonists: mechanisms of pharmacokinetic-pharmacodynamic discordance. *Trends Pharmacol. Sci.* 26, 352–360. doi: 10.1016/j.tips.2005.05.007

Buchanan, K. A., Petrovic, M. M., Chamberlain, S. E., Marrion, N. V., and Mellor, J. R. (2010). Facilitation of long-term potentiation by muscarinic M(1) receptors is mediated by inhibition of SK channels. *Neuron* 68, 948–963. doi: 10.1016/j.neuron.2010.11.018

Caporale, N., and Dan, Y. (2008). Spike timing-dependent plasticity: a Hebbian learning rule. *Annu. Rev. Neurosci.* 31, 25–46. doi: 10.1146/annurev.neuro.31.060407.125639

Carvell, G. E., and Simons, D. J. (1990). Biometric analyses of vibrissal tactile discrimination in the rat. *J. Neurosci.* 10, 2638–2648.

Chiu, C. Q., Lur, G., Morse, T. M., Carnevale, N. T., Ellis-Davies, G. C., and Higley, M. J. (2013). Compartmentalization of GABAergic inhibition by dendritic spines. *Science* 340, 759–762. doi: 10.1126/science.1234274

Cho, K., Aggleton, J. P., Brown, M. W., and Bashir, Z. I. (2001). An experimental test of the role of postsynaptic calcium levels in determining synaptic strength using perirhinal cortex of rat. *J. Physiol.* 532(Pt 2), 459–466. doi: 10.1111/j.1469-7793.2001.0459f.x

Dan, Y., and Poo, M. M. (2004). Spike timing-dependent plasticity of neural circuits. *Neuron* 44, 23–30. doi: 10.1016/j.neuron.2004.09.007

de Kock, C. P., and Sakmann, B. (2009). Spiking in primary somatosensory cortex during natural whisking in awake head-restrained rats is cell-type specific. *Proc. Natl. Acad. Sci. U.S.A.* 106, 16446–16450. doi: 10.1073/pnas.0904143106

Dennis, S. H., Pasqui, F., Colvin, E. M., Sanger, H., Mogg, A. J., Felder, C. C., et al. (2016). Activation of muscarinic M1 acetylcholine receptors induces long-term potentiation in the hippocampus. *Cereb. Cortex* 26, 414–426. doi: 10.1093/cercor/bhv227

Domínguez, S., Fernández de Sevilla, D., and Buño, W. (2014). Postsynaptic activity reverses the sign of the acetylcholine-induced long-term plasticity of GABAA inhibition. *Proc. Natl. Acad. Sci. U.S.A.* 111, E2741–E2750. doi: 10.1073/pnas.1321777111

Fanselow, E. E., and Nicolelis, M. A. (1999). Behavioral modulation of tactile responses in the rat somatosensory system. *J. Neurosci.* 19, 7603–7616.

Feldman, D. E. (2012). The spike-timing dependence of plasticity. *Neuron* 75, 556–571. doi: 10.1016/j.neuron.2012.08.001

Fernández de Sevilla, D., and Buño, W. (2010). The muscarinic long-term enhancement of NMDA and AMPA receptor-mediated transmission at Schaffer collateral synapses develop through different intracellular mechanisms. *J. Neurosci.* 30, 11032–11042. doi: 10.1523/JNEUROSCI.1848-10.2010

Fernández de Sevilla, D., Cabezas, C., de Prada, A. N., Sanchez-Jiménez, A., and Buño, W. (2002). Selective muscarinic regulation of functional glutamatergic Schaffer collateral synapses in rat CA1 pyramidal neurons. *J. Physiol.* 545(Pt 1), 51–63. doi: 10.1113/jphysiol.2002.029165

Fernández de Sevilla, D., Nuñez, A., Borde, M., Malinow, R., and Buño, W. (2008). Cholinergic-mediated IP3-receptor activation induces long-lasting synaptic enhancement in CA1 pyramidal neurons. *J. Neurosci.* 28, 1469–1478. doi: 10.1523/JNEUROSCI.2723-07.2008

Fitzjohn, S. M., and Collingridge, G. L. (2002). Calcium stores and synaptic plasticity. *Cell Calcium* 32, 405–411. doi: 10.1016/S0143416002001999

Fuenzalida, M., Fernández de Sevilla, D., and Buño, W. (2007). Changes of the EPSP waveform regulate the temporal window for spike-timing-dependent plasticity. *J. Neurosci.* 27, 11940–11948. doi: 10.1523/JNEUROSCI.0900-07.2007

Fuenzalida, M., Fernández de Sevilla, D., Couve, A., and Buño, W. (2010). Role of AMPA and NMDA receptors and back-propagating action potentials in spike timing-dependent plasticity. *J. Neurophysiol.* 103, 47–54. doi: 10.1152/jn.00416.2009

Fukunaga, K., and Miyamoto, E. (2000). A working model of CaM kinase II activity in hippocampal long-term potentiation and memory. *Neurosci. Res.* 38, 3–17. doi: 10.1016/S0168-0102(00)00139-5

Gordon, U., Polsky, A., and Schiller, J. (2006). Plasticity compartments in basal dendrites of neocortical pyramidal neurons. *J. Neurosci.* 26, 12717–12726. doi: 10.1523/JNEUROSCI.3502-06.2006

Gruart, A., Leal-Campanario, R., Lopez-Ramos, J. C., and Delgado-Garcia, J. M. (2015). Functional basis of associative learning and their relationships with long-term potentiation evoked in the involved neural circuits: lessons from studies in behaving mammals. *Neurobiol. Learn. Mem.* 124, 3–18. doi: 10.1016/j.nlm.2015.04.006

Hao, J., and Oertner, T. G. (2012). Depolarization gates spine calcium transients and spike-timing-dependent potentiation. *Curr. Opin. Neurobiol.* 22, 509–515. doi: 10.1016/j.conb.2011.10.004

Hebb, D. O. (1949). *The Organization of Behavior*. New York, NY: Wiley.

Holthoff, K., Kovalchuk, Y., Yuste, R., and Konnerth, A. (2004). Single-shock LTD by local dendritic spikes in pyramidal neurons of mouse visual cortex. *J. Physiol.* 560(Pt 1), 27–36. doi: 10.1113/jphysiol.2004.072678

Hsieh, L. S., and Levine, E. S. (2013). Cannabinoid modulation of backpropagating action potential-induced calcium transients in layer 2/3 pyramidal neurons. *Cereb. Cortex* 23, 1731–1741. doi: 10.1093/cercor/bhs168

Jiménez-Capdeville, M. E., Dykes, R. W., and Myasnikov, A. A. (1997). Differential control of cortical activity by the basal forebrain in rats: a role for both cholinergic and inhibitory influences. *J. Comp. Neurol.* 381, 53–67.

Kampa, B. M., Clements, J., Jonas, P., and Stuart, G. J. (2004). Kinetics of Mg2+ unblock of NMDA receptors: implications for spike-timing dependent synaptic plasticity. *J. Physiol.* 556(Pt 2), 337–345. doi: 10.1113/jphysiol.2003.058842

Kampa, B. M., Letzkus, J. J., and Stuart, G. J. (2007). Dendritic mechanisms controlling spike-timing-dependent synaptic plasticity. *Trends Neurosci.* 30, 456–463. doi: 10.1016/j.tins.2007.06.010

Kampa, B. M., and Stuart, G. J. (2006). Calcium spikes in basal dendrites of layer 5 pyramidal neurons during action potential bursts. *J. Neurosci.* 26, 7424–7432. doi: 10.1523/JNEUROSCI.3062-05.2006

Lamsa, K., Irvine, E. E., Giese, K. P., and Kullmann, D. M. (2007). NMDA receptor-dependent long-term potentiation in mouse hippocampal interneurons shows a unique dependence on Ca(2+)/calmodulin-dependent kinases. *J. Physiol.* 584(Pt 3), 885–894. doi: 10.1113/jphysiol.2007.137380

Larkum, M. E., Kaiser, K. M., and Sakmann, B. (1999a). Calcium electrogenesis in distal apical dendrites of layer 5 pyramidal cells at a critical frequency of back-propagating action potentials. *Proc. Natl. Acad. Sci. U.S.A.* 96, 14600–14604.

Larkum, M. E., Zhu, J. J., and Sakmann, B. (1999b). A new cellular mechanism for coupling inputs arriving at different cortical layers. *Nature* 398, 338–341. doi: 10.1038/18686

Lisman, J. (1989). A mechanism for the Hebb and the anti-Hebb processes underlying learning and memory. *Proc. Natl. Acad. Sci. U.S.A.* 86, 9574–9578.

Lisman, J., Schulman, H., and Cline, H. (2002). The molecular basis of CaMKII function in synaptic and behavioural memory. *Nat. Rev. Neurosci.* 3, 175–190. doi: 10.1038/nrn753

London, M., and Hausser, M. (2005). Dendritic computation. *Annu. Rev. Neurosci.* 28, 503–532. doi: 10.1146/annurev.neuro.28.061604.135703

Lorincz, M. L., Gunner, D., Bao, Y., Connelly, W. M., Isaac, J. T., Hughes, S. W., et al. (2015). A distinct class of slow (~0.2-2 Hz) intrinsically bursting layer 5 pyramidal neurons determines UP/DOWN state dynamics in the neocortex. *J. Neurosci.* 35, 5442–5458. doi: 10.1523/JNEUROSCI.3603-14.2015

Malenka, R. C., and Nicoll, R. A. (1999). Long-term potentiation–a decade of progress? *Science* 285, 1870–1874.

Manns, I. D., Sakmann, B., and Brecht, M. (2004). Sub- and suprathreshold receptive field properties of pyramidal neurones in layers 5A and 5B of rat somatosensory barrel cortex. *J. Physiol.* 556(Pt 2), 601–622. doi: 10.1113/jphysiol.2003.053132

Marlin, J. J., and Carter, A. G. (2014). GABA-A receptor inhibition of local calcium signaling in spines and dendrites. *J. Neurosci.* 34, 15898–15911. doi: 10.1523/JNEUROSCI.0869-13.2014

Mukherjee, S., and Manahan-Vaughan, D. (2013). Role of metabotropic glutamate receptors in persistent forms of hippocampal plasticity and learning. *Neuropharmacology* 66, 65–81. doi: 10.1016/j.neuropharm.2012.06.005

Nabavi, S., Fox, R., Proulx, C. D., Lin, J. Y., Tsien, R. Y., and Malinow, R. (2014). Engineering a memory with LTD and LTP. *Nature* 511, 348–352. doi: 10.1038/nature13294

Neveu, D., and Zucker, R. S. (1996). Postsynaptic levels of [Ca2+]i needed to trigger LTD and LTP. *Neuron* 16, 619–629.

Nuñez, A., Domínguez, S., Buño, W., and Fernández de Sevilla, D. (2012). Cholinergic-mediated response enhancement in barrel cortex layer V pyramidal neurons. *J. Neurophysiol.* 108, 1656–1668. doi: 10.1152/jn.00156.2012

Otmakhov, N., Griffith, L. C., and Lisman, J. E. (1997). Postsynaptic inhibitors of calcium/calmodulin-dependent protein kinase type II block induction but not maintenance of pairing-induced long-term potentiation. *J. Neurosci.* 17, 5357–5365.

Polsky, A., Mel, B., and Schiller, J. (2009). Encoding and decoding bursts by NMDA spikes in basal dendrites of layer 5 pyramidal neurons. *J. Neurosci.* 29, 11891–11903. doi: 10.1523/JNEUROSCI.5250-08.2009

Ramaswamy, S., and Markram, H. (2015). Anatomy and physiology of the thick-tufted layer 5 pyramidal neuron. *Front. Cell. Neurosci.* 9:233. doi: 10.3389/fncel.2015.00233

Rasmusson, D. D., Clow, K., and Szerb, J. C. (1992). Frequency-dependent increase in cortical acetylcholine release evoked by stimulation of the nucleus basalis magnocellularis in the rat. *Brain Res.* 594, 150–154.

Remy, S., and Spruston, N. (2007). Dendritic spikes induce single-burst long-term potentiation. *Proc. Natl. Acad. Sci. U.S.A.* 104, 17192–17197. doi: 10.1073/pnas.0707919104

Rose, C. R., and Konnerth, A. (2001). Stores not just for storage. intracellular calcium release and synaptic plasticity. *Neuron* 31, 519–522. doi: 10.1016/S0896-6273(01)00402-0

Sandler, M., Shulman, Y., and Schiller, J. (2016). A novel form of local plasticity in tuft dendrites of neocortical somatosensory layer 5 pyramidal neurons. *Neuron* 90, 1028–1042. doi: 10.1016/j.neuron.2016.04.032

Schiller, J., Major, G., Koester, H. J., and Schiller, Y. (2000). NMDA spikes in basal dendrites of cortical pyramidal neurons. *Nature* 404, 285–289. doi: 10.1038/35005094

Schiller, J., and Schiller, Y. (2001). NMDA receptor-mediated dendritic spikes and coincident signal amplification. *Curr. Opin. Neurobiol.* 11, 343–348. doi: 10.1016/S0959-4388(00)00217-8

Sjöström, P. J., Rancz, E. A., Roth, A., and Hausser, M. (2008). Dendritic excitability and synaptic plasticity. *Physiol. Rev.* 88, 769–840. doi: 10.1152/physrev.00016.2007

Steriade, M., Amzica, F., and Nuñez, A. (1993). Cholinergic and noradrenergic modulation of the slow (approximately 0.3 Hz) oscillation in neocortical cells. *J. Neurophysiol.* 70, 1385–1400.

Stuart, G., Spruston, N., Sakmann, B., and Hausser, M. (1997). Action potential initiation and backpropagation in neurons of the mammalian CNS. *Trends Neurosci.* 20, 125–131.

Takahashi, N., Oertner, T. G., Hegemann, P., and Larkum, M. E. (2016). Active cortical dendrites modulate perception. *Science* 354, 1587–1590. doi: 10.1126/science.aah6066

Tigaret, C. M., Olivo, V., Sadowski, J. H., Ashby, M. C., and Mellor, J. R. (2016). Coordinated activation of distinct Ca(2+) sources and metabotropic glutamate receptors encodes Hebbian synaptic plasticity. *Nat. Commun.* 7:10289. doi: 10.1038/ncomms10289

Udakis, M., Wright, V. L., Wonnacott, S., and Bailey, C. P. (2016). Integration of inhibitory and excitatory effects of a7 nicotinic acetylcholine receptor activation in the prelimbic cortex regulates network activity and plasticity. *Neuropharmacology* 105, 618–629. doi: 10.1016/j.neuropharm.2016.02.028

Wigström, H., and Gustafsson, B. (1983). Facilitated induction of hippocampal long-lasting potentiation during blockade of inhibition. *Nature* 301, 603–604.

Conflict of Interest Statement: The authors declare that the research was conducted in the absence of any commercial or financial relationships that could be construed as a potential conflict of interest.

Copyright © 2017 Díez-García, Barros-Zulaica, Núñez, Buño and Fernández de Sevilla. This is an open-access article distributed under the terms of the Creative Commons Attribution License (CC BY). The use, distribution or reproduction in other forums is permitted, provided the original author(s) or licensor are credited and that the original publication in this journal is cited, in accordance with accepted academic practice. No use, distribution or reproduction is permitted which does not comply with these terms.

A.6. Article 6 (under construction)

DISCHARGE PROPERTIES OF NEURONS RECORDED IN THE SOMATOSENSORY CORTEX OF THE MOUSE

Discharge Properties of Neurons Recorded in the Somatosensory Cortex of the Mouse

Natalí Barros-Zulaica[1,b], Ángel Nuñez[b], Alessandro E.P. Villa[1,*]

[a]*Neuroheuristic Research Group, HEC Lausanne, University of Lausanne, Switzerland*
[b]*Departamento de Anatomía, Histología y Neurociencia, Facultad de Medicina, Universidad Autónoma de Madrid, Madrid, Spain*

Abstract

Here we present a study of the firing pattern distribution in the barrel cortex not only along the different layers, but also along the antero-posterior and medio-lateral directions. Performing extracellular recordings in the barrel cortex with a multi-electrode array with four recording points and in Urethane anesthetized mice. We found significant differences between antero-posterior and medio-lateral firing pattern distribution of four types of firing patterns according to their autocorrelogram. Bursting cells where placed mostly in the more posterior and lateral part of the barrel cortex, while regular firing neurons where placed mostly in the middle of the medio-lateral direction and in the infra-granular layer. No significant difference was found in the distribution in the dorso-ventral direction. These findings set the idea for the first time that processing of information in the barrel cortex is not uniform, neither inside the column nor in the whole volume of the barrel cortex.

Keywords: Barrel cortex, Spontaneous firing pattern, Autocorrelograms, Fano Factor,

1. Introduction

Rodents use the whiskers on their snouts for exploring the environment seeking for objects, making maps of the surroundings and even performing fine-grain texture discrimination. In order to transmit all this important information to the subsequent brain nuclei the sensory innervation of each whisker follicle is quite high.

Sensory information from whiskers is sent from the whisker follicle to the contralateral area of the thalamus through two different pathways: the lemniscal and the paralemniscal pathways. In the lemniscal pathways, receptors are connected with the sensory principal trigeminal nucleus into the brain stem and send projections to the ventro-postero-medial thalamus nucleus (VPM). On the contrary, paralemniscal pathway source from the interpolar section of the rostral area in the spinal trigeminal nucleus at the brain stem level and send projections to the medial area of the posterior thalamus nucleus (POm) and to a little area of the VPM [1].

These projections from thalamus target the primary somatosensory cortex (SI), mainly in layer IV, which is conformed to clusters of neurons (barrel). Each cluster is related to one whisker and this area is called the barrel cortex [2].

It is known that the somatosensory barrel cortex is composed of local circuits heavily interconnected by vertical and horizontal projections [3, 4, 5]. In the lemniscal pathway, the barrel cortex receive a strong innervation from VPM mainly to layer IV and also to layers III and VIa, while in paralemniscal pathway the POm sends projections to layers I and Va [1, 2, 3, 4, 5, 6, 7]. This vertical organization is linked horizontally by prominent projections within layer II/III and layer V [8, 9, 10, 11, 12].Sensory cortices have a laminar architecture with specific functions of each layer in information processing. In rat, sensory processing is performed by means of different response properties that differ according to the cortical layer and the cell type [13, 14].

It is known that in the neocortex there are three principal types of firing patterns: regular spiking (RS), intrinsically bursting (IB) and fast spiking (FS) [15, 16]. RS cells are pyramidal and stellate cells that trigger sodium action potentials in a sustained manner during the application of a depolarizing current pulse. They are placed in all cortical layers except in layer I. IB cells are pyramidal cells principally from layer V that surprisingly do not receive direct thalamo-cortical inputs. They possess unusually thick apical dendrites that rise to layer I. They generate a burst of 3-5 action potentials riding on a calcium spike in response to an intracellular depolarization. FS cells are characterized by short duration action potentials, an ability to fire tonically at high frequency (>250 Hz) and a relative lack of spike frequency adaptation when long-lasting depolarizing current pulses are applied to these neurons; they are GABAergic interneurons [17]. Although the laminar distribution of the functional firing pattern has been little described, nothing is known about the superficial functional distribution.

The complexity of connectivity pattern and the variety of numerous types of neurons that built the somatosensory cortex makes it difficult to study. This is why despite of all the researches made in the lasts years about the mouse barrel cortex[18, 19, 20, 21, 22, 23], little is known about the basis of the functional activity of neurons in this area. In our study we recorded the activity of neurons during spontaneous periods in four different layers simultaneously with extracellular record-

*University of Lausanne, Tel. +41-21-6923594, Internef 138.1, CH-1015 Lausanne, Switzerland

Email address: alessandro.villa@unil.ch (Alessandro E.P. Villa)

ings *in vivo*. Our main objective was to describe a functional map of the firing characteristics of the neurons along the mouse barrel cortex.

2. Material and Methods

2.1. Animals

All animal procedures were performed in accordance with the Ethics Committee of the Universidad Autonoma de Madrid, and with Council Directive 86/609/EEC of the European Community. Mice were group housed with a 12 h light/dark cycle and had free access to food and water. Every effort was made to minimize the number, and suffering, of the animals used.

2.2. Electrophysiological recordings

Experiments were performed on 9 urethane-anesthetized (1.2 g/kg i.p.) adult C57BL/6 WT mice (3 - 6 months old) weighing 25 - 30g. Animals were placed in a Kopf stereotaxic device in which surgical procedures and recordings were performed. The body temperature was maintained at 37 C. An incision was made exposing the skull and a small hole was drilled in the bone over the barrel cortex. Single-unit recordings in the BC (A 0 - 2 mm, L 3 - 4 mm from bregma and V 0.3 - 1.2 mm from dura) [24] were made through a multielectrode Neuronexus or MicroLIQUID longitudinal array of four Iridium Oxid electrodes (15 μm electrodes diameter; 200 μm separation between electrodes; 1.5 - 2 MΩ impedance). Unit firing was filtered (0.3 - 5 kHz), amplified via an AC preamplifier (DAM80; World Precision Instruments, Sarasota, USA), visualized on an oscilloscope, digitally recorded in WAV format (44,100 Hz sampling rate, 16 bit), and stored for post hoc analysis. The files were analyzed offline using a spike-sorting program [25, 26]. From one to five cells were detected from each single electrode. The spike trains were digitally stored for time series analysis.

2.3. Statistical analysis

Spike trains were analyzed by time series renewal density plots scaled in rate units (spikes/s) to evaluate statistical properties of single-unit discharges during spontaneous activity. For each histogram, the 99% confidence limits were calculated, assuming that spikes occurred following a Poisson distribution. The Fano factor (equal to 1 if data follow Poisson process) was used to characterized the variability of the spike train. The busting index indicates the grade of bursting of the cell, if the value is between [0, 1] it means that the cell fires more "bursting". We also computed the Intra-burst frequency (IBF) and the average burst duration (ABD) (Table 1) [**?**]. We calculated the Fisher stadistic test in order to determine if the functional distribution of the different firing patterns was significant respect to the others. This test was performed with R Project of Statistical Computing (http://www.r-project.org/)

2.4. Histological analysis

Following the recording session (2 - 3 h), electrolytic lesions using five pulses of 5 μA for 10 s at intervals of 10 s were induced at the top and at the bottom of the electrode array. Mice were given a sublethal dose of 8 μl/g ketamine/xylazine and perfused with 100 ml of 0.9% NaCl, followed by 100 ml 4% paraformaldehyde in 0.1 M phosphate buffer. Brains were removed after perfusion and cut of coronal sections at 50 μm thickness with a Leica freezing microtome. Sections were mounted on two parallel slide series for cresyl violet staining [Figure 1].

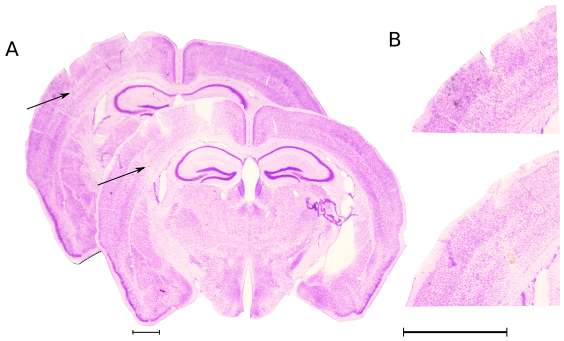

Figure 1: Histological analysis. **A**: Microphotographs of coronal sections of the superficial and deep recordings areas stained with cresyl violet showing a representative electrode penetration in the barrel cortex. **B**: Enlargement of the previous panel emphasizing the electrolytic lesions within the barrel cortex at the supragranular (top) and infragranular (down) layers. Scale bar is 1 mm.

3. Results

In this study of spontaneous activity in the mouse barrel cortex under Urethane anesthetized condition we found four different types of firing patterns according to their autocorrelograms: irregular (IRR) or type I, bursting cell (BC) or type II, large bursting cell (LBC) or type III and regular (REG) or type IV (Fig. 2A, B, C and D) (Table 1). Most of the recording cells (48%, n=50) showed a REG activity, which is characterized by a constant probability to spike, showing a flat autocorrelogram (Fig. 2D), a median firing rate of 1.3 spikes/s and a median Fano factor close to 1 (0.7), meaning that the spikes distribution for this type of firing pattern is almost Poissonian. The second more abundant (25%, n=26) type of firing is BC that is characterized by an autocorrelogram with a hump close to time zero (Fig. 2B) with a median firing rate of 1.8 spikes/s. We also found that the 14% (n=15) of cells showed a LBC type of firing pattern characterized by an autocorrelogram with big hump close to time zero (Fig. 2C) and a median firing rate of 1.6 spikes/s. The rest of the recorded cells (13%, n=14) presented an IRR type of firing pattern with an autocorrelogram characterized by a narrow peak very close to time zero that decay fast to a flat form (Fig. 2A) and a median firing rate of 1.1 spikes/s.

A study of all recorded cells distribution in the different stereotaxic directions is shown in Figure 2 E, F and G. In the antero-posterior versus dorso-ventral distribution (Fig. 2E) an

Cell Type	IRR1 (TYPE I)	BC2 (TYPE II)	LBC3 (TYPE III)	REG4 (TYPE IV)
N = 105 (100%)	14 (13%)	26 (25%)	15 (14%)	50 (48%)
Firing rate (spikes/s)	1.1 (1.3±0.2)	1.8 (1.2±0.1)	1.6 (1.8±0.2)	1.3 (1.5±0.1)
Fano factor	1.1 (1.0±0.1)	1.6 (1.8±0.1)	2.1 (3.3±0.7)	0.7 (0.8±0.1)
Bursting index	10.5 (11.6±1.6)	1.9 (1.6±0.1)	0.7 (0.6±0.1)	-
IBF	43 (38±4)	20 (22±5)	41 (47±5)	-
ABD	29 (36±5)	115 (111±5)	160 (170±12)	-

Table 1: Discharge properties of spike trains recorded in the somatosensory cortex of the mouse. Statistics are described in the text. In this table is possible to see the median and the mean (± standard desviation) values of the firing rates, the Fano factor, the busrting index, the IBF and the ABD of all the recorded neurons

analysis of Fisher exact test showed significant differences (p-value < 0.05) between all the sectioned areas (p-value=1.44e-05). A pair wise post hoc analysis showed that mostly significant differences could be found within each layer between the different antero-posterior areas. Is possible to observe that most of the cells with a BC or LBC firing pattern are placed more posterior. IRR cells are placed almost all of them, in the third antero-posterior subdivision, while REG cells seems to be uniformly distributed along the antero-posterior direction, however the number of REG neurons increase in the infra-granular layer.

For the distribution along medio-lateral and dorso-ventral directions (Fig. 2F) the Fisher exact test showed that the cell firing pattern distribution was significantly different between segmented areas (p-value=0.00624). The post hoc analysis revealed that again the main differences could be found within layers along the medio-lateral direction. Is also possible to see that most of the BC and LBC are located in more medial than lateral. IRR cells are placed mostly in the middle section along the medio-lateral direction. REG cells are mostly placed in the middle of the medio-lateral direction but specially in the infra-granular layer, as we saw previously.

In the figure of the antero-posterior versus medio-lateral directions (Fig. 2G) the Fisher exact test showed again a big significance between the different distribution groups (p-value=2.941e-06). The post hoc analysis revealed that the main differences could be found in the antero-posterior direction. According with the previous distribution diagrams BC and LBC could be found in the more posterior and more lateral area of the barrel cortex. IRR cells are localized in the middle area of the barrel cortex with some preference of being more posterior and medial. REG cells are mostly localized in the middle section of the medio-lateral direction with a tendency of being distributed medial and posterior. Notice that the medio-lateral coordinate is measured from 3.65 to 2.5 mm, while in the Figure 2F it is set from 3.65 to 2.2 mm. Electrophysiological recordings were performed from 3.65 to 2.2 mm, however recordings from 2.2 to 2.5 mm where placed deeper and they are not represented in the diagram. Consequently, to fix these recordings points into the diagram we projected them into the picture.

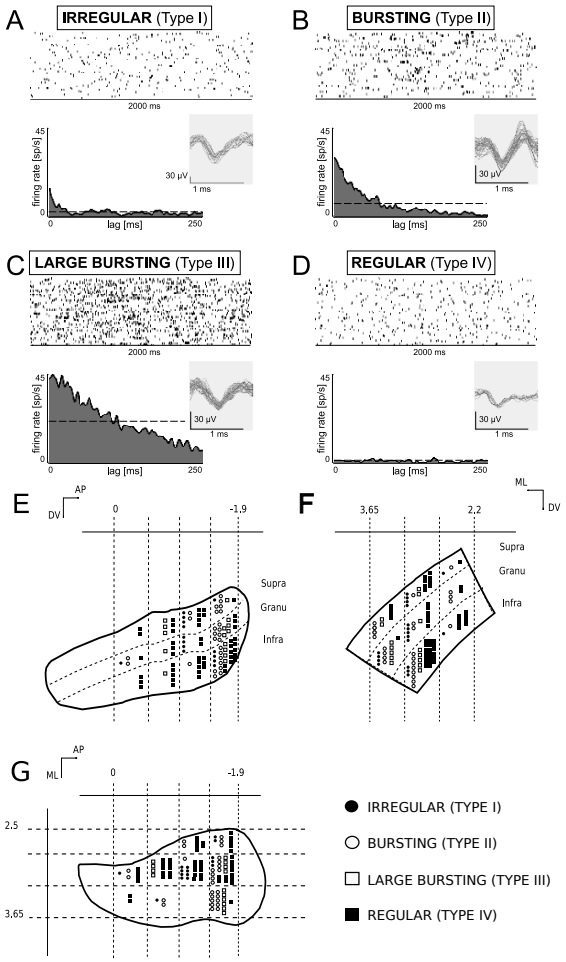

Figure 2: Firing patterns according to their raster plots, autocorrelograms and one example of a spike form (A, B, C, D) and their dictribution in the barrel cortex (E, F G). **A**: Irregular firing pattern or Type I. **B**: Busrt firing pattern or Type II. **C**: Large Burst firing pattern or Type III. **D**: Regular firing pattern or Type IV. **E**: Cell type distribution according to antero-posterior and dorso-ventral recoording coordinades. **F**: Cell type distribution according to medio-lateral and dorso-ventral recoording coordinades. **G**: Cell type distribution according to antero-posterior and medio-lateral recoording coordinades. The shapes of barrel cortex S1 were selected according to Kirkcaldie 2012 [27] (E, G) and Paxinos and Franklin 2001 (F) [24]

4. Discussion

The main finding of this study is that is possible to describe a functional distribution of cells according to their autocorrelogram and that this distribution is not homogeneous in the barrel cortex. We found that most of the cells fired in a regular manner with a median firing rate of 1.3 spikes/s and with a Fano factor close to 1 which means that these cells fired following a Poisson distribution or randomly. These type IV or REG cells are mainly located in the middle area of the barrel cortex and most of them are placed in the infra-granular layer. Another important finding was that most of the type II and type III cells, the ones that fired in bursts, are placed mostly in the more posterior and lateral zone of the barrel cortex.

Probably these type IV REG neurons are the same RS pyramidal and stellate neurons described in many studies that are

placed in all cortical layers except in layer I [28]. May be the fact that is easier to find them in infra-granular layer has to do with thalamo-cortical projections, because it is known that these neurons receive a lot of projections from the thalamus [17] while REG neurons in supra-granular layer do not receive any thalamic projection [15]. BC and LBC are placed mostly in infra-granular and more posterior, these neurons seems to match the previously described IB pyramidal neurons that are mainly placed in layer V and VI and that do not receive direct thalamic projections. For sure they have an specific work in processing sensory information and connecting infra-granular layer with layer I [29]. It is interesting to observe how type I IRR cells are located in a very specific area practically distributed only in the middle of the barrel cortex. It is possible to hypothesize that type II and III neurons role is mainly to syncronized neuronal cortical activity through thalamo-cortical inputs [30] keeping some reverberant base activity, while REG and IRR cells maybe process the information by their own and after processing they share the process with the adjacent cells.

The fact that there are no significat differences between cell distribution in the layers means that inside the cortical column the process of information does not depend on the cell distribution. However, the different distribution along the directions, antero-posterior and medio-lateral give the idea that probably the different functional firing rates not only have a processing function but also a trasnmission function [31]. One possibility is that the neuronal distribution change according to the projection pattern. For example, posterior barrel cortex areas project to other cortical areas that need to send the information differently than more anterior barrel cortex areas [32]. On the other hand, it is well known that there is a cortical representation of the whiskers on the barrel cortex [1]. Our data indicate that the different cortical cell types described here are not homogeneous distributed on the barrel cortex that may means that according to the sensory input, barrel cortex uses different neuronal types to processes sensory information. This point is crucial for sensory plasticity because single spikes or bursting discharges may induce long-term facilitation [33].

5. Conclusions

Our findings suggest that there is a cell distribution in the barrel cortex depending on the firing pattern of the neurons. This distribution is significantly different in the antero-posterior and medio-lateral directions giving the idea that the spreading of the processed information depends on the way neurons fired. As this is the first study performed in this issue of cell distribution according to their firing pattern in the barrel cortex we suggest that more research should be done in order to better understand the problem.

References

[1] C. Petersen, The functional organization of the barrel cortex, Neuron 56 (2007) 339–355.

[2] T. A. Woolsey, H. V. D. Loos, The structural organization of layer iv in the somatosensory region (si) of mause cerebral cortex, Brain research 17 (1969) 205–242.

[3] C. Welker, Receptive fields of barrels in the somatosensory neocortex of the rat, Journal of Comparative Neurology 166 (1976) 173–189.

[4] K. Alloway, Information processing streams in rodent barrel cortex: the differential functions of barrel and septal circuits, Cerebral Cortex 18 (2007) 979–989.

[5] D. Feldmeyer, Excitatory neuronal connectivity in the barrel cortex, Frontiers in Neuroanatomy eCollection 2012 (2012) 6–24.

[6] I. Bureau, Interdigitated paralemniscal and lemniscal pathways in the mouse barrel cortex, PLOS Biology 4 (2006) e382.

[7] R. Aronoff, F. Matyas, C. Mateo, C. Ciron, B. Schneider, C. Petersen, Long-range connectivity of mouse primary somatosensory barrel cortex, European Journal of Neuroscience 12 (2010) 2221–2233.

[8] K. A. Koralek, K. F. Jensen, H. P. Killackey, Evidence for two complementary patterns of thalamic input to the rat somatosensory cortex, Brain Res 463 (2) (1988) 346–51.

[9] S. M. Lu, R. C. Lin, Thalamic afferents of the rat barrel cortex: a light- and electron-microscopic study using phaseolus vulgaris leucoagglutinin as an anterograde tracer, Somatosens Mot Res 10 (1) (1993) 1–16.

[10] R. Douglas, K. Martin, Long-range connectivity of mouse primary somatosensory barrel cortex, Annual reviews Neuroscience 27 (2004) 419–452.

[11] H. S. Meyer, V. C. Wimmer, M. Oberlaender, C. P. J. de Kock, B. Sakmann, M. Helmstaedter, Number and laminar distribution of neurons in a thalamocortical projection column of rat vibrissal cortex, Cereb Cortex 20 (10) (2010) 2277–86. doi:10.1093/cercor/bhq067.

[12] J. Wester, D. Contreras, Columnar interactions determine horizontal propagation of recurrent network activity in neocortex, Journal Neuroscience 32 (2012) 5454–5471.

[13] I. D. Manns, B. Sakmann, M. Brecht, Sub- and suprathreshold receptive field properties of pyramidal neurones in layers 5a and 5b of rat somatosensory barrel cortex, J Physiol 556 (Pt 2) (2004) 601–22. doi:10.1113/jphysiol.2003.053132.

[14] C. P. J. de Kock, R. M. Bruno, H. Spors, B. Sakmann, Layer- and cell-type-specific suprathreshold stimulus representation in rat primary somatosensory cortex, J Physiol 581 (Pt 1) (2007) 139–54. doi:10.1113/jphysiol.2006.124321.

[15] A. Agmon, B. W. Connors, Correlation between intrinsic firing patterns and thalamocortical synaptic responses of neurons in mouse barrel cortex, J Neurosci 12 (1) (1992) 319–29.

[16] A. E. Villa, I. V. Tetko, B. Hyland, A. Najem, Spatiotemporal activity patterns of rat cortical neurons predict responses in a conditioned task, Proc Natl Acad Sci U S A 96 (3) (1999) 1106–11.

[17] D. A. McCormick, B. W. Connors, J. W. Lighthall, D. A. Prince, Comparative electrophysiology of pyramidal and sparsely spiny stellate neurons of the neocortex, J Neurophysiol 54 (4) (1985) 782–806.

[18] T. R. Sato, N. W. Gray, Z. F. Mainen, K. Svoboda, The functional microarchitecture of the mouse barrel cortex, PLoS Biol 5 (7) (2007) e189. doi:10.1371/journal.pbio.0050189.

[19] D. Feldmeyer, M. Brecht, F. Helmchen, C. C. H. Petersen, J. F. A. Poulet, J. F. Staiger, H. J. Luhmann, C. Schwarz, Barrel cortex function, Prog Neurobiol 103 (2013) 3–27. doi:10.1016/j.pneurobio.2012.11.002.

[20] K. B. Clancy, P. Schnepel, A. T. Rao, D. E. Feldman, Structure of a single whisker representation in layer 2 of mouse somatosensory cortex, J Neurosci 35 (9) (2015) 3946–58. doi:10.1523/JNEUROSCI.3887-14.2015.

[21] S. Hires, D. Gutnisky, J. Yu, D. O'Connor, K. Svoboda, Low-noise encoding of active touch by layer 4 in the somatosensory cortex, Elife 4 (2015) e06619.

[22] L. DeNardo, D. Berns, K. DeLoach, L. Luo, Connectivity of mouse somatosensory and prefrontal cortex examined with trans-synaptic tracing, Nature Neuroscience 18 (2015) 1687–1697.

[23] J. Yu, D. Gutnisky, S. Hires, K. Svoboda, Layer 4 fast-spiking interneurons filter thalamocortical signals during active somatosensation, Nature Neuroscience 19 (2016) 1647–1657.

[24] G. Paxinos, K. Franklin., The mouse brain in stereotaxic coordinates, Academic Press.

[25] T. Aksenova, O. Chibirova, O. Dryga, I. Tetko, A. Benabid, A. Villa, An unsupervised automatic method for sorting neuronal spike waveforms in awake and freely moving animals, Methods 30 (2003) 178–187.

[26] Y. Asai, T. Aksenova, A. Villa, Unsupervised recognition of neuronal discharge waveforms for on-line real-time operation, Lecture Notes in Computer Science 3704 (2005) 29–38.

[27] M. Kirkcaldie, C. Watson, G. Paxinos, K. Franklin, Stereotaxic map of the mouse neocortex, Proceedings of the Australian Neuroscience Society.
[28] K. Fox, The barrel cortex, Cambridge University Press.
[29] J. F. Staiger, A. J. C. Loucif, D. Schubert, M. Möck, Morphological characteristics of electrophysiologically characterized layer vb pyramidal cells in rat barrel cortex, PLoS One 11 (10) (2016) e0164004. doi:10.1371/journal.pone.0164004.
[30] J. J. Zhu, B. W. Connors, Intrinsic firing patterns and whisker-evoked synaptic responses of neurons in the rat barrel cortex, J Neurophysiol 81 (3) (1999) 1171–83.
[31] C. C. H. Petersen, S. Crochet, Synaptic computation and sensory processing in neocortical layer 2/3, Neuron 78 (1) (2013) 28–48. doi:10.1016/j.neuron.2013.03.020.
[32] M. M. Sabri, M. Adibi, E. Arabzadeh, Dynamics of population activity in rat sensory cortex: Network correlations predict anatomical arrangement and information content, Front Neural Circuits 10 (2016) 49. doi:10.3389/fncir.2016.00049.
[33] A. Díez-García, N. Barros-Zulaica, Á. Núñez, W. Buño, D. Fernández de Sevilla, Bidirectional hebbian plasticity induced by low-frequency stimulation in basal dendrites of rat barrel cortex layer 5 pyramidal neurons, Front Cell Neurosci 11 (2017) 8. doi:10.3389/fncel.2017.00008.